

This file is part of the following work:

Shephard, Angus C. G. (2022) *Explorations into the rare earth chemistry of biphenolates and superbulky cyclopentadienyl ligands, and a study of C-F activation by rare earth metals*. PhD Thesis, James Cook University.

Access to this file is available from:

<https://doi.org/10.25903/f5yv%2D0v76>

Copyright © 2022 Angus C. G. Shephard.

The author has certified to JCU that they have made a reasonable effort to gain permission and acknowledge the owners of any third party copyright material included in this document. If you believe that this is not the case, please email

researchonline@jcu.edu.au

**Explorations into the Rare Earth Chemistry of
Biphenolates and Superbulky Cyclopentadienyl
Ligands, and a Study of C-F Activation by Rare
Earth Metals**

A thesis submitted for the degree of

Doctor of Philosophy

by

Angus C. G. Shephard

BSc(Hons)

College of Science and Engineering

James Cook University

August 2022



Declaration

I declare that this thesis is my own work and contains no material which has been accepted for the award of any other degree or diploma at any university or other institution, and contains no material previously published or written by another person except where due reference is made in the text.

Every reasonable effort has been made to gain permission and acknowledge the owners of copyright material. I would be pleased to hear from any copyright owner who has been omitted or incorrectly acknowledged.

Angus Charles Gordon Shephard

College of Science and Engineering

James Cook University

August 2022

Acknowledgements

Firstly, I would like to express my immense gratitude to my two supervisors, Professor Peter Junk, and Dr. Murray Davies. Peter, your unwavering support, trust, and encouragement throughout my studies has been more than I could ever ask for, and I am extremely grateful for all you have done for me as a supervisor, and the countless opportunities you've provided me with. And Murray, I'm incredibly appreciative of the continued guidance you've offered me, ensuring I stay sufficiently caffeinated, and being a key component of the most formidable trivia team the Riverview Tavern has seen in some time. You have both been absolutely paramount to my growth as a chemist.

I would also like to offer my thanks to my two unofficial supervisors, Professor Glen Deacon, and Dr. Florian Jaroschik. Glen, I thank for you for all of the detailed discussions we have had that have allowed me to learn so much about lanthanoid chemistry from you, alongside the countless hours you have put into providing feedback on manuscripts for me. And Florian, I can't thank you enough for the guidance you've provided me with. What started out as one small project in Montpellier quickly turned into the majority of this thesis, and your expertise, patience, and mentorship (even from the other side of the world) has made my PhD experience that much easier to manage. It has been an absolute pleasure to work alongside you both, and I can't express how much I appreciate the time you have invested in me.

My thanks are also extended to the chemistry staff, in particular the efforts of Dr. Mark Robertson, for all of your support and assistance with NMR spectroscopy, HPLC/MS and advice on organic synthesis. I would also like to thank Dr. Dana Roberts, Dr. Winnie Lee and Shiyoh Nobile, for having an open door for me to come and chat about anything, and seemingly endless patience when I needed obscure chemicals, or last minute help preparing for a school

visit. Some of the fondest memories I have made at JCU have been in the teaching labs and the prep room with you all.

I would also like to thank both Junk and Deacon group members, past and present. Each of you have made coming into the lab each day such a pleasure, and I am grateful for the lifelong friendships I have made. A very special mention goes to Dr. Zhifang Guo. You've provided me with an unparalleled amount of support through my PhD, and I can't thank you enough for that. My thanks also go to the Taillefer group, in particular to Lucas Pagès and Maxime Bouquin. You both made me feel incredibly welcome during my two trips to Montpellier, and I truly appreciate it.

To all of my good friends, with special mentions to Hans Dirks, Grace Derrick, Joseph Connell, Bronte Davey, Michaela Padayachee, Alexandra Gulizia, Emily Olditch, Joelle Blucher, Malcolm Burt, Peter Cameron, Aymeric Delon and Marie-Lou Lorenzato, thanks for the many different ways that you have supported me across our friendship and during my studies, whether it be in the form of a place to stay when I visit, a cold beer, or a piece of advice, I'm grateful for you all, and all you've done for me.

And lastly to my family, I could not have asked for a more supportive, kind and encouraging group of people, and you inspire me to be my best each and every day. Thanks so much for supporting me through "just a few more years of study".

Statement of the contribution of others

Outside of personal contributions outlined in the acknowledgements, there have been several key bodies who have provided contributions in direct support of this thesis:

Financial Support

The Australian Government has provided support for this research through the Research Training Program Scholarship scheme, providing both tuition fee offset and a stipend, supporting me through my postgraduate study. The Australian Government has also provided generous financial support for the research projects undertaken through two Australian Research Council Discovery Project grants.

James Cook University has also provided financial assistance in the form of funding for attending conferences, travel for my studies, and the purchase of necessary research materials.

Intellectual Support

The completion of this thesis has been a result of the extraordinary supervision I have received, by both of my supervisors, Professor Peter Junk and Dr. Murray Davies, and my external collaborators, Professor Glen Deacon and Dr. Florian Jaroschik. They have each provided many ideas, suggestions, and editorial contributions towards this thesis.

I also acknowledge the contributions of Dr. Zhifang Guo, Dr. Dominique Granier and Owen Beaumont, for their assistance in both data collection and processing for all of the crystal structures presented in this thesis.

Abstract

This thesis is comprised of three distinct, yet interrelated areas of synthetic organometallic chemistry of the rare earth elements. The first being the synthesis of rare earth biphenolate complexes by redox transmetallation/protolysis, a previously unused method of accessing them. The second being the synthesis of superbulky polyarylcyclopentadienyl complexes of both rare, and alkaline earth metals, by selective carbon-phosphorus bond cleavage, and reductive dimerisation. And the third area discussing carbon-fluorine bond activation of pentafluorobenzene by rare earth metals, and applications in organometallic chemistry.

Chapter 1 of the thesis gives an overview of the rare earth elements, including their properties, separation methods, and their applications in everyday life. Further details are then provided on the syntheses of organometallic complexes, as well as specific information on rare earth biphenolate and cyclopentadienyl chemistry, alongside carbon-fluorine bond activation by rare earth metals.

Chapter 2 explores the application of redox transmetallation/protolysis as a means of synthesising rare earth biphenolate complexes with the 2,2'-methylenebis(6-*tert*-butyl-4-methylphenol) (mbmpH₂) ligand to form complexes of the general form [Ln(mbmp)(mbmpH)(thf)₃]. Assessment of the reactivity of these complexes towards trimethylaluminium is described, as well as assessment of their efficacy as catalysts for the ring opening polymerisation of *rac*-lactide.

Chapter 3 details the synthesis of superbulky divalent polyarylcyclopentadienyl complexes of samarium, europium, and ytterbium, by the previously undescribed route of carbon-phosphorus bond cleavage. Both octaphenyl, and decaphenyl lanthanocenes were synthesised directly by treatment of the pro-ligands C₅Ph₄HPPH₂ or C₅Ph₅PPh₂ with activated metal. Insight into the

carbon-phosphorus bond cleavage mechanism was gained by ^{31}P NMR studies, alongside trapping studies with pentafluorobenzene.

Chapter 4 continues the discussion of superbulky polyarylcyclopentadienyl complexes with a tethering moiety between the two cyclopentadienyl rings, also known as *ansa* metallocene complexes. Ethano bridged *ansa* metallocene complexes of calcium, magnesium, strontium, barium, samarium, europium, and ytterbium were synthesised by the reductive dimerisation of 1,2,3,4-tetraphenylfulvene by direct treatment with the activated metal. Luminescence properties of the europium *ansa* metallocene complex were analysed and compared with that of the untethered analogue.

Chapter 5 outlines the carbon-fluorine bond activation of pentafluorobenzene by rare earth metals, as well as applications of this process in the synthesis of organolanthanoid complexes. ^{19}F NMR studies were undertaken on reactions of pentafluorobenzene with activated samarium, europium, and ytterbium metals to determine the selectivity of carbon-fluorine bond activation, and to gain insight into the mechanism. A pseudo-Grignard mechanism was proposed based on the products observed in the ^{19}F NMR spectra. This mechanism was exploited to synthesise both sandwich, and fluoride half sandwich lanthanoid complexes of tetraphenyl- and pentaphenyl-cyclopentadienyl complexes which have otherwise proven difficult to synthesise, alongside the synthesis of divalent lanthanoid formamidinate, and pyrazolate complexes.

Overall, this thesis presents a range of alternative and new synthetic methods for accessing interesting divalent and trivalent lanthanoid complexes. The redox transmetallation/protolysis reaction has opened doors to a wide variety of new, simple biphenolate complexes, which can be used to synthesise bimetallic species. The selective carbon-phosphorus cleavage of phosphinated pro-ligands offers a wealth of potential synthetic pathways to well-known

lanthanoid complexes, by a facile, one-pot synthesis. The reductive dimerisation of fulvenes has also proven to be a convenient method of synthesising bulky lanthanoid and group 2 *ansa* metallocene complexes, whilst the carbon-fluorine bond activation of pentafluorobenzene has exhibited potential to synthesise a range of hetero- and homo-leptic divalent lanthanoid complexes, as well as harbouring potential applications in organic chemistry.

Abbreviations

ALD	Atomic layer deposition
APCI	Atmospheric-pressure chemical ionisation
Ar	Aryl
bipy	2,2'-Bipyridine
Bn	Benzyl
Cn	Centroid
Cp	Cyclopentadienyl (C ₅ H ₅ ⁻)
Cp*	Pentamethylcyclopentadienyl (C ₅ Me ₅ ⁻)
Cp ^{BIG}	C ₅ (4- <i>n</i> BuC ₆ H ₄) ₅ ⁻
d	Day
DippFormH	N,N'-Bis(2,6-diisopropylphenyl)formamidine
dme	1,2-Dimethoxyethane
edbpH ₂	6,6'-(Ethane-1,1-diyl)bis(2,4-di- <i>tert</i> -butylphenol)
EDTA	Ethylenediaminetetraacetic acid
e.s.d.	Estimated standard deviation
Et	Ethyl
Et ₂ O	Diethyl ether
GC/MS	Gas chromatography/mass spectrometry
GPC	Gel permeation chromatography
h	Hour
HMPA	Hexamethylphosphoramide
HPLC	High performance liquid chromatography
<i>i</i> Pr	Isopropyl
IR	Infrared

IUPAC	International Union of Pure and Applied Chemistry
Ln	Lanthanoid
mbbpaH ₂	6,6'-((2-Methoxyphenyl)methylene)bis(2,4-di- <i>tert</i> -butylphenol)
mbbpH ₂	6,6'-Methylenebis(2,4-di- <i>tert</i> -butylphenol)
mbmpaH ₂	6,6'-((2-Methoxyphenyl)methylene)bis(2-(<i>tert</i> -butyl)-4-methylphenol)
mbmpH ₂	2,2'-Methylenebis(6- <i>tert</i> -butyl-4-methylphenol)
mCPBA	<i>meta</i> -Chloroperoxybenzoic acid
Me	Methyl
min	Minute
M _n	Number average molecular weight
MOCVD	Metal organic chemical vapour deposition
MRI	Magnetic resonance imaging
MS	Mass spectrometry
<i>n</i> Bu	<i>n</i> -Butyl
nm	Nanometre
NMR	Nuclear magnetic resonance
OTf	Triflate (CF ₃ SO ₃ ⁻)
PDI	Polydispersity index
PFAS	Polyfluoroalkylated substances
Ph	Phenyl
Ph ₂ PzH	3,5-Diphenylpyrazole
PhMe	Toluene
ppm	Parts per million
Pz	Pyrazolate
r.t.	Room temperature
REE	Rare earth element

ROP	Ring opening polymerisation
RT	Redox transmetallation
RTP	Redox transmetallation/protolysis
SIR	Sterically induced reduction
solv	Solvent
SSIP	Solvent separated ion pair
<i>t</i> Bu	<i>tert</i> -Butyl
TEMPO	2,2,6,6-Tetramethylpiperidine 1-oxyl radical
thf	Tetrahydrofuran
TMS	Trimethylsilyl
UV	Ultraviolet
λ_{em}	Wavelength of emission (nm)
λ_{exc}	Wavelength of excitation (nm)

Table of Contents

Declaration	i
Acknowledgements.....	ii
Statement of the contribution of others.....	iv
Abstract	v
Abbreviations	viii
Table of Contents	xi
Chapter 1: Introduction to the rare earth elements	1
1.1 The rare earth elements.....	1
1.2 Properties of the rare earth elements.....	2
1.3 Applications of rare earth elements	3
1.4 Rare earth organometallic chemistry.....	3
1.4.1 Metathesis reactions	3
1.4.2 Protolysis reactions.....	4
1.4.3 Redox transmetallation reactions	5
1.4.4 Redox transmetallation/protolysis reactions	5
1.5 Rare earth biphenolate chemistry.....	7
1.6 Superbulky cyclopentadienyl rare earth chemistry	10
1.7 Carbon-fluorine bond activation by rare earth metals	14
1.8 References	16

Chapter 2: Synthesis of lanthanoid biphenolate complexes and their further reactivity 24

2.1 Introduction	24
2.1.1 Synthesis of divalent lanthanoid biphenolate complexes	24
2.1.2 Synthesis of trivalent lanthanoid biphenolate complexes	26
2.1.3 Synthesis of tetravalent lanthanoid biphenolate complexes	40
2.2 Results and discussion	41
2.2.1 Synthesis of lanthanoid biphenolate complexes by RTP	41
2.2.2 Further reactivity of lanthanoid biphenolates with trimethyl aluminium	48
2.2.3 Ring opening polymerisation reactions of <i>rac</i>-lactide	55
2.3 Conclusion	58
2.4 Experimental	60
2.4.1 Syntheses	60
2.4.2 Typical procedure for polymerisation reactions	64
2.5 Crystal and refinement data	66
2.6 References	70

Chapter 3: Synthesis of bulky octa- and deca-phenyl metallocenes by selective carbon-phosphorus bond cleavage..... 73

3.1 Introduction	73
3.1.1 Divalent polyarylcyclopentadienyl lanthanoid complexes	73
3.1.2 Carbon-phosphorus bond cleavage by lanthanoid metals	78
3.2 Results and discussion	82
3.2.1 Pro-ligand synthesis	82

3.2.2 Carbon-phosphorus cleavage reactions to yield divalent octaphenyl lanthanocenes	88
3.2.3 Carbon-phosphorus cleavage reactions to yield divalent decaphenyl lanthanocenes	92
3.2.4 Altered conditions for the carbon-phosphorus cleavage of pentaphenylcyclopentadienyldiphenylphosphine	97
3.2.5 Attempted synthesis of group 2 decaphenyl metallocenes by C-P cleavage..	100
3.2.6 Attempted synthesis of trivalent pentaphenylcyclopentadienyl complexes...	101
3.2.7 Reaction monitoring by ³¹ P NMR spectroscopy and trapping studies with C ₆ F ₅ H.....	104
3.3 Conclusion.....	108
3.4 Experimental.....	110
3.4.1 Syntheses.....	110
3.4.2 Trapping reactions	114
3.5 Crystal and refinement data.....	116
3.6 References	118
Chapter 4: Synthesis of alkaline earth and lanthanoid octaphenyl <i>ansa</i> metallocene complexes by reductive dimerisation.....	121
4.1 Introduction	121
4.1.1 Rare earth <i>ansa</i> metallocene complexes	122
4.1.2 Alkaline earth <i>ansa</i> metallocene complexes	125
4.2 Current study.....	126

4.3 Results and discussion	128
4.3.1 Synthesis and characterisation of 1,2,3,4-tetraphenylfulvene.....	128
4.3.2 Synthesis and characterisation of alkaline earth <i>ansa</i> metallocene complexes	130
4.3.3 Synthesis and characterisation of rare earth <i>ansa</i> metallocene complexes...	139
4.4 Conclusion.....	145
4.5 Experimental.....	146
4.6 Crystal and refinement data.....	151
4.7 References	153
 Chapter 5: Carbon-fluorine bond activation of pentafluorobenzene by lanthanoid metals and applications in organolanthanoid synthesis.....	
5.1 Introduction	156
5.1.1 Redox transmetallation/protolysis based C-F activation of aromatic fluorides	156
5.1.2 Other examples of C-F bond activation of aromatic fluorides	162
5.2 Results and discussion	167
5.2.1 C-F activation studies of pentafluorobenzene by lanthanoid metals.....	167
5.2.2 Synthesis of divalent cyclopentadienyl lanthanoid complexes by C-F activation/protolysis from Ln metal and pentafluorobenzene.....	175
5.2.3 Synthesis of lanthanoid fluoride half sandwich complexes by redistribution with [LnF₂(thf)_x].....	185
5.2.4 Synthesis of other divalent lanthanoid complexes.....	191

5.3 Conclusion.....	194
5.4 Experimental.....	196
5.4.1 Typical procedure for the C-F activation of pentafluorobenzene with quantification	196
5.4.2 Syntheses.....	196
5.5 Crystal and refinement data.....	202
5.6 References	203
Appendix One.....	205
Materials and general procedures.....	205
X-ray crystallography.....	206
Appendix Two	208
List of publications	208

Chapter 1: Introduction to the rare earth elements

1.1 The rare earth elements

The International Union of Pure and Applied Chemistry (IUPAC) defines the rare earth elements (REEs) as a set of 17 chemical elements in the periodic table, composed of the lanthanoids (lanthanum to lutetium – atomic numbers 57 to 71) and scandium and yttrium.^[1] Whilst widely adopted, the term “rare earth elements” inaccurately describes these elements as scarce, when in actuality they are more abundant in the Earth’s crust than gold.^[2–4] The misnomer stems from the reluctance of REEs to be found in exploitable ore deposits, like that of base metals. Alongside this, owing to their similar chemical properties, the extraction and separation of REEs is non-trivial, contributing to their perceived rarity.^[5] The primary source of REEs are the minerals bastnaesite (rare earth fluorocarbonates), monazite and xenotime (rare earth phosphates).^[6–8]

Whilst mixtures of REE oxides can be useful as catalysts, they are also required in their pure, elemental forms for a variety of applications. When separating REEs, the first element isolated is cerium, by treatment with air and base to oxidise Ce^{3+} to Ce^{4+} , forming insoluble CeO_2 , which is readily removed from the mixture. Secondly, europium is isolated, owing to the stability of the Eu^{2+} ion forming insoluble EuSO_4 . The remaining Ln^{3+} ions are then separated by solvent extraction, or ion exchange chromatography, depending on the scale of the separation, and desired purity.^[4,9] The resulting, purified REE ions are then reduced either by treatment with calcium, or lanthanum metal (at elevated temperatures), or electrochemically.^[10] With improvements in separation techniques has come a decrease in the cost of REEs, leading to an increase in accessibility, and interest in rare earth chemistry research.

1.2 Properties of the rare earth elements

The REEs possess very similar chemical properties, contributing to the difficulty of their separation from one another. When in their metallic form, rare earth metals readily react with air and moisture to form hydroxides and oxides, the former producing hydrogen gas in the process.^[10] The most common, and stable, oxidation state of the lanthanoids is +3, however, all of the lanthanoids have been isolated in the +2 oxidation state, and a selection in the +4 oxidation state. Of these unique oxidation states, the most common ions are Eu^{2+} , Sm^{2+} , Yb^{2+} and Ce^{4+} , however, less common examples include Pr^{2+} and Pr^{4+} .^[10,11] Owing to unpaired *f* electrons, the majority of rare earth ions exhibit paramagnetism, with the exceptions of Sc^{3+} , Y^{3+} , La^{3+} , Ce^{4+} , Yb^{2+} , and Lu^{3+} which are diamagnetic.

One of the most noteworthy characteristics of the lanthanoid metals is the lanthanoid contraction, which is the gradual decrease in the radii of the lanthanoid elements (and ions) across the period, resulting in a decrease of approximately 0.2 Å from La to Lu.^[5,12] This contraction arises from poor attraction between the 4*f* electrons and the lanthanoid nucleus, and consequently the 6*s* electrons are drawn inwards, causing the observed decrease in atomic and ionic radii. This results in a high charge-density, classifying the lanthanoids as hard Lewis acids,^[13] making ligands with nitrogen or oxygen donor atoms, or fluoride ions highly preferable.^[3,4,6] Due to the relatively large ionic radii of lanthanoid ions, and their inability to form covalent bonds,^[14] the coordination number of lanthanoid complexes are typically 8-10, however, with an increase in steric demand of the ligands, this can be reduced to coordination numbers as low as two.^[15,16] This high variability in coordination numbers results in lanthanoid complexes exhibiting a wide variety of coordination geometries,^[15] dictated by the steric bulk, charge, and geometry of the ligands.

1.3 Applications of rare earth elements

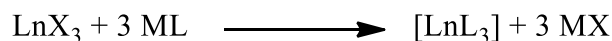
REEs have a plethora of applications in a range of industries and have become increasingly utilised since their extraction and separation methods were improved during World War II, leading to increased production and availability.^[4,17,18] Initially used in commercial lighting products,^[19] the use of rare earths has since expanded to applications in agriculture as an addition to feedstock to promote growth in animals^[20] and plants,^[21–24] in medicine as anticoagulants, anticancer, and contrast agents for MRI (magnetic resonance imaging),^[25–30] and as powerful magnets in headphones, mobile phones, electric vehicles, and even roller coasters.^[31,32] REEs have also shown to be potent catalysts for a range of chemical processes including fluid catalytic cracking of petrochemicals,^[33,34] catalytic combustion of natural gas and fossil fuels,^[35–37] the purification of automotive emissions and industrial waste air,^[38–40] and use in solid oxide fuel cells.^[41–43]

1.4 Rare earth organometallic chemistry

Several major methods exist for the synthesis of organometallic rare earth complexes, the most popular being salt metathesis, protolysis, redox transmetallation, and most recently, redox transmetallation/protolysis (RTP). These four major synthetic routes are discussed in more detail below.

1.4.1 Metathesis reactions

Metathesis (or salt elimination) reactions involve the treatment of a rare earth halide with an alkali metal salt of a ligand, eliminating the alkali halide, and resulting in the desired rare earth complex (Equation 1.1).^[16,44,45]



Ln = Lanthanoid metal

X = Halide

M = Alkali metal

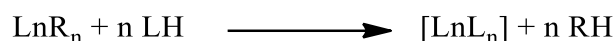
L = Anionic ligand

Equation 1.1 - General metathesis (salt elimination) reaction to form rare earth complexes.^[16,44,45]

The metathesis pathway, while very versatile, suffers from several issues, namely the low solubility of unsolvated LnX_n species^[46] leading to low yields and formation of undesired heteroleptic complexes, and alkali/halide inclusion into the complex, forming undesired lanthanoid metallate complexes.^[45,47,48] Alongside this, the alkali metal halide produced typically has some solubility in polar solvents, which can lead to isolation difficulties and also contributing to undesired inclusion.

1.4.2 Protolysis reactions

Protolysis reactions involve the treatment of a lanthanoid reagent (LnR_n – where R is a basic, anionic ligand) with a protic reagent (LH) (Equation 1.2).



Ln = Lanthanoid metal

R = Basic, anionic ligand

LH = Protic ligand

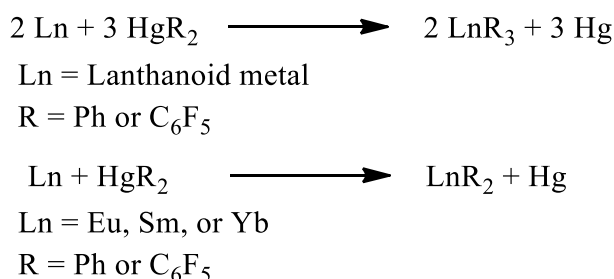
Equation 1.2 – General protolysis reaction to form rare earth complexes.^[45-48]

The lanthanoid precursors for protolysis reagents are typically much more soluble than their metathesis counterparts, allowing for a more versatile synthetic approach for both hetero and homoleptic lanthanoid species. While seemingly more reliable than metathesis for avoiding “ate” complex formation, these LnR_n precursors are typically synthesised from rare earth

halides *via* metathesis routes, and thus can suffer the same drawbacks. The synthesis and purification of these precursors for further use can also be non-trivial.^[46,47]

1.4.3 Redox transmetallation reactions

Redox transmetallation (RT) reactions utilise the free lanthanoid metal, which is treated with a metal complex with a more positive standard reduction potential (typically Hg,^[49–51] Tl,^[44,49] or Bi^[50,51]). The lanthanoid metal is readily oxidised, the RT reagent is reduced, and the ligands coordinate to the Ln ion, forming the desired complex (Equation 1.3).



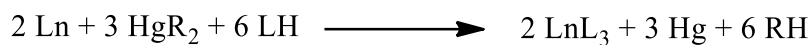
Equation 1.3 – General redox transmetallation reaction to form both trivalent and divalent lanthanoid reagents.^[49-51]

This synthetic approach allows for a facile synthesis of lanthanoid reagents, however, is heavily gated by the accessibility of appropriate metal reagents. Again, these reagents can sometimes be non-trivial to synthesise.

1.4.4 Redox transmetallation/protolysis reactions

As the name suggests, redox transmetallation/protolysis (RTP) reactions incorporate elements of both redox transmetallation and protolysis reactions, to synthesise rare earth complexes. The first step is redox transmetallation, where the lanthanoid metal is oxidised, the mercury is reduced, and the basic anions coordinate to the Ln cation. The second step is the subsequent

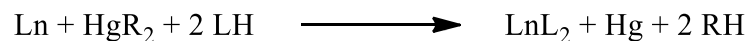
protolysis whereby the basic anions abstract a proton from the protic ligands, resulting in the desired lanthanoid complex (Equation 1.4).^[52,53]



Ln = Lanthanoid metal

R = Ph or C₆F₅

LH = Protic ligand



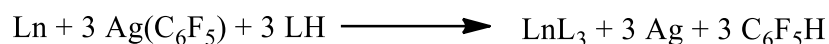
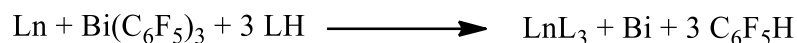
Ln = Eu, Sm, or Yb

R = Ph or C₆F₅

LH = Protic ligand

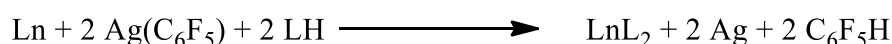
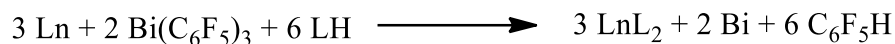
Equation 1.4 – General redox transmetallation/protolysis reaction to form both trivalent and divalent lanthanoid complexes.^[52,53]

This synthetic pathway offers many advantages over metathesis, protolysis, and redox transmetallation reactions, as the reactions can be performed in one pot, with only one air sensitive reagent (the Ln metal). The workup and isolation of the desired complexes is also facile, as the soluble LnL_x can be isolated from excess Ln and Hg metal by filtration, and the formed RH (benzene, or pentafluorobenzene) can be removed easily under reduced pressure. Owing to its versatility, and reliability, the RTP reaction has been used extensively in Chapter 2 of this thesis. The major drawback of the RTP reaction is the use of toxic mercury reagents, however, recent advances have utilised silver and bismuth reagents (Equation 1.5) in place of the organomercury compounds used here, affording an analogous, mercury-free synthetic pathway.^[52,54]



Ln = Lanthanoid metal

LH = Protic ligand



Ln = Eu, Sm, or Yb

LH = Protic ligand

Equation 1.5 – Redox transmetallation/protolysis reactions utilising $\text{Bi}(\text{C}_6\text{F}_5)_3$ and AgC_6F_5 to synthesise both trivalent and divalent lanthanoid complexes.^[52,54]

1.5 Rare earth biphenolate chemistry

Rare earth complexes bearing alkoxide and aryloxy ligands have become increasingly studied in the past two decades, primarily acting as high steric bulk ligands giving access to low coordination number complexes.^[45,48,55] While monodentate phenols have been studied extensively, their biphenol counterparts have received considerably less attention. Biphenolate ligands are able to act as mono- or di-anionic ligands, and offer the potential to chelate, providing some stability to the corresponding complexes towards redistribution. They also offer a stereochemically rigid framework for the metal, which can potentially influence stereospecific transformations. Lanthanoid biphenolate complexes have exhibited activity towards a range of polymerisation reactions, namely ring opening polymerisation of cyclic esters (e.g. L-lactide, ϵ -caprolactone, and the highly heteroselective polymerisation of rac-lactide).^[56-59] Furthermore, lanthanoid biphenolates have been shown to be efficient catalysts towards the Diels-Alder reaction of cyclopentadiene with methyl methacrylate,^[60] and also have seen applications in sol gel methods,^[45] and as feedstocks in both MOCVD (metal organic chemical vapour deposition) and ALD (atomic layer deposition) of oxide layers.^[61]

Methylene bridged biphenols are a versatile class of ligand. They are very tuneable, as changing the substituents in the *ortho* and *para* positions allows for manipulation of the coordination number, and solubility of the resulting complexes respectively, as well as the electronic properties of the substituents influencing the acidity of the phenolic proton. In this work, the ligand 2,2'-methylenebis(6-*tert*-butyl-4-methylphenol) (mbmpH₂) (Figure 1.1) has been utilised extensively. The *tert*-butyl groups in the *ortho* positions provide some crowding around the coordinating oxygen atoms, while the methyl groups in the *para* positions aid in the solubility of the formed complexes. The methylene bridge between the two phenyl moieties provides some flexibility to the molecule, which can result in a range of interesting geometries with different metals.

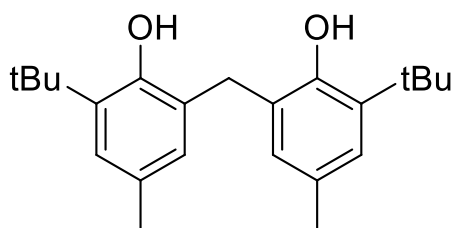


Figure 1.1 – Structure of 2,2'-methylenebis(6-*tert*-butyl-4-methylphenol) (mbmpH₂).

The primary factors that affect the coordination environment of a phenolate ligand with a lanthanoid metal are the steric effects of substituents in the *ortho* positions (adjacent to the oxygen donors), and the ionic radius of the metal centre(s).^[62–64] Even with a static ligand set, a range of coordination environments can be achieved (Figure 1.2). These environments range from very simple mononuclear lanthanoid biphenolate complexes, to larger, tetranuclear heterobimetallic species.

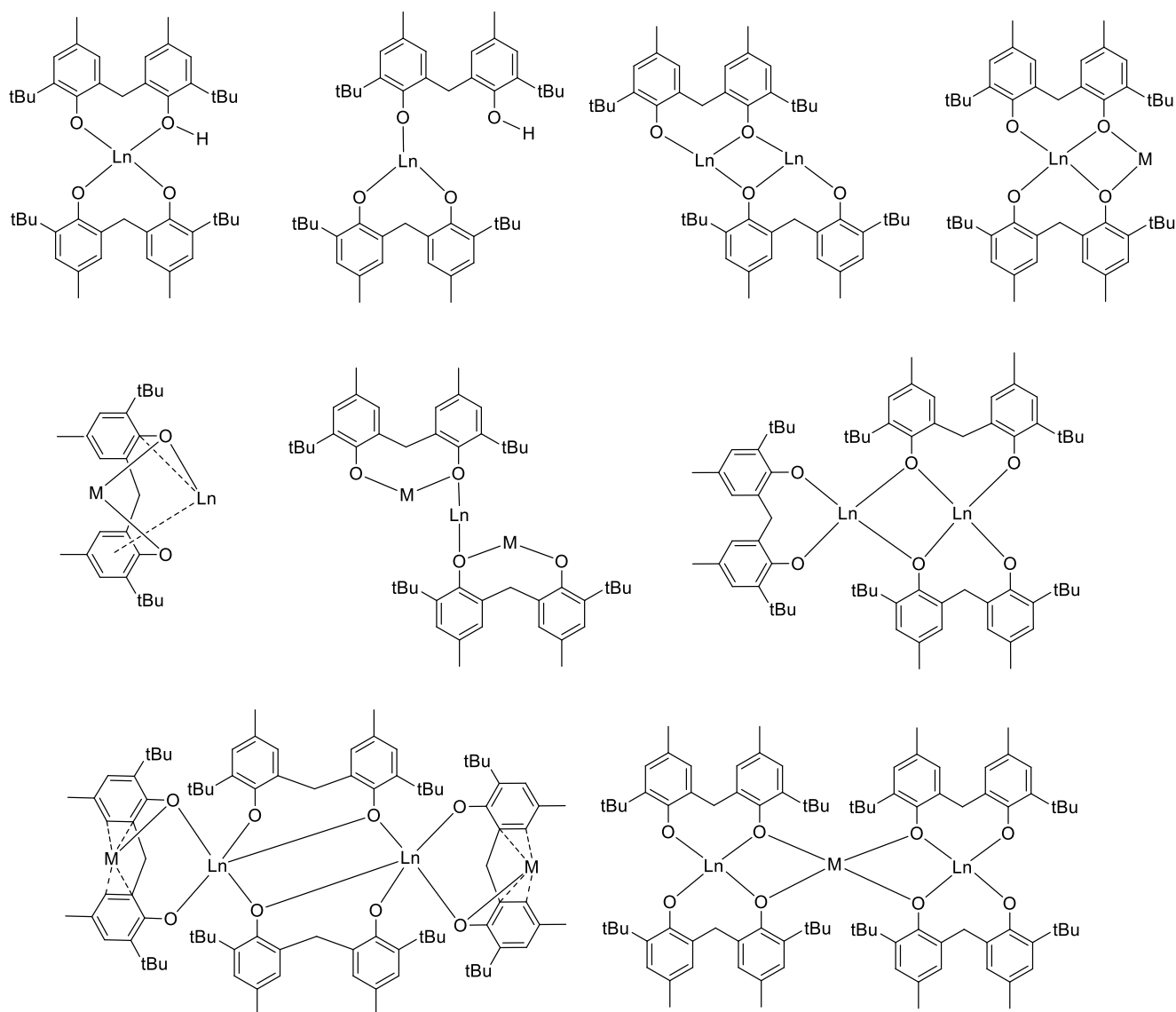


Figure 1.2 - A range of coordination modes of the mbmp^{2-} ligand in rare earth, and rare earth/main group heterobimetallic complexes.

Two major synthetic routes have been used to access lanthanoid biphenolate complexes: salt metathesis, and protolysis/ligand exchange reactions. With the previously discussed disadvantages of both salt metathesis and protolysis reactions, it is surprising that until recently, redox transmetallation/protolysis reactions had not been employed for the synthesis of lanthanoid biphenolate complexes.^[65] In light of the successful synthesis of their monodentate aryloxy counterparts,^[66,67] application of redox transmetallation/protolysis reactions to

synthesise lanthanoid biphenolate complexes, in order to avoid the complications which arise from salt metathesis and protolysis, is the next logical step.

1.6 Superbulky cyclopentadienyl rare earth chemistry

The chemistry of the cyclopentadienyl ligand and its complexes has been an emerging and well-studied area since the discovery of ferrocene in 1952.^[68] Shortly thereafter, the first rare earth cyclopentadienyl complexes were reported,^[69] however, progress in the area of rare earth cyclopentadienyl chemistry came to a halt for nearly 30 years, until introduction of the Cp* (C₅Me₅⁻) ligand caused a resurgence in interest. The Cp* ligand offers better solubility to its corresponding metallocenes in non-polar solvents, an increase in kinetic stability owing to steric bulk about the metal centre, and reduced tendency to form polymeric complexes.^[70] The Cp* ligand was used to synthesise the first soluble, divalent organosamarium species, [Sm(Cp*)₂(thf)₂] by the Evans group (Figure 1.3),^[71] alongside a variety of trivalent organolanthanoid complexes of the form [Ln(Cp*)₃].^[72-74] The divalent [Sm(Cp*)₂(thf)₂], and unsolvated [Sm(Cp*)₂] were shown to be incredibly reactive,^[75-77] even reacting with nitrogen gas to form the N₂ bridged complex [$\{\text{Sm}(\text{Cp}^*)_2\}_2(\mu\text{-}\eta^2\text{:}\eta^2\text{-N}_2)$].^[78] Placing the dinitrogen complex under vacuum for several hours allows the reaction to be reversed.^[78]

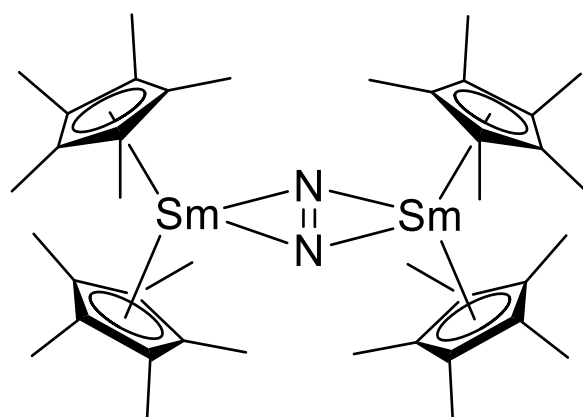
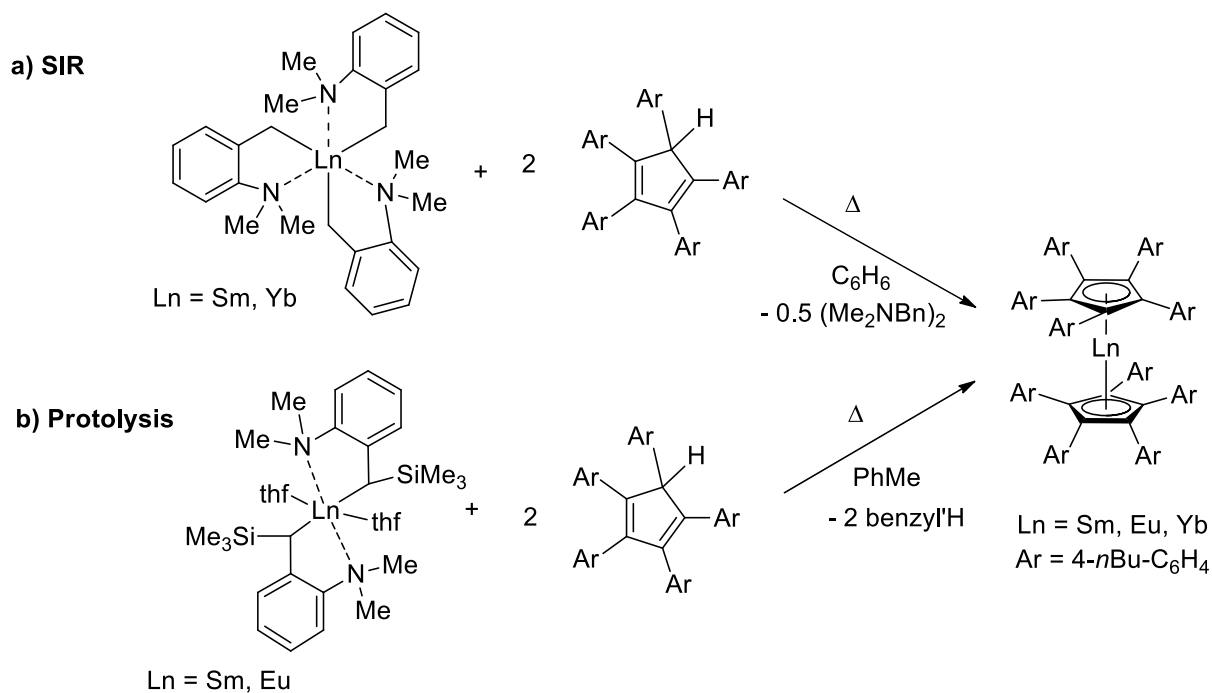


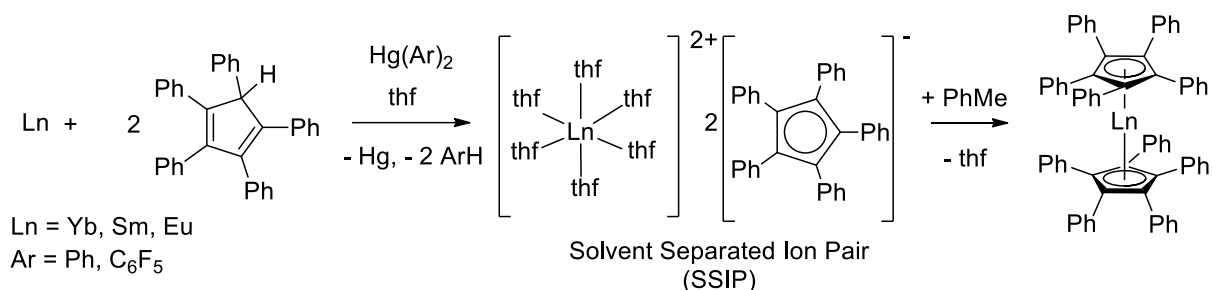
Figure 1.3 – Dinitrogen divalent samarium complex [Sm(Cp*)₂(thf)₂].^[78]

Since then, major developments have been made with the field of rare earth cyclopentadienyl chemistry continuing to expand and progress. One such avenue is the synthesis of bulky polyarylcyclopentadienyl rare and alkaline earth metal complexes. Polyarylcyclopentadienyl ligands typically employ three, four or five aryl groups on the cyclopentadienyl ring, which influences their structure, reactivity, and other physical properties tremendously, compared to alkyl- and silyl- substituted cyclopentadienyl ligands. As such, divalent lanthanocenes with multiple aryl groups are desirable targets, as they show high stability, limited reactivity, and for the europium species, interesting luminescence properties.^[79–82] One of the major hurdles of undertaking synthesis with these bulky cyclopentadienyl ligands is their low solubility, and the low solubility of their complexes. These solubility issues have been overcome by addition of alkyl or aryl substituents onto the phenyl rings (e.g., Cp^{BIG} = C₅(4-*n*BuC₆H₄)₅),^[83,84] dramatically increasing their solubility in organic, non-polar solvents.

The synthesis of polyarylcyclopentadienyl lanthanocenes has largely been achieved by two methods: protolysis reactions with the protonated cyclopentadiene starting material, using highly reactive lanthanoid benzyl precursors (Scheme 1.1) (sometimes accompanied by sterically induced reduction (SIR)),^[83,84] or alternatively through redox transmetallation/protolysis with the protonated cyclopentadiene ligand and the free lanthanoid metal (Scheme 1.2).^[79–82] The former requires the synthesis and careful handling of these reactive precursors, whilst the latter does not rely on air and moisture sensitive reagents, however, utilises organomercurial reagents and has potential for C-F bond activation owing to the formation of the pentafluorobenzene by-product when using Hg(C₆F₅)₂.^[82]

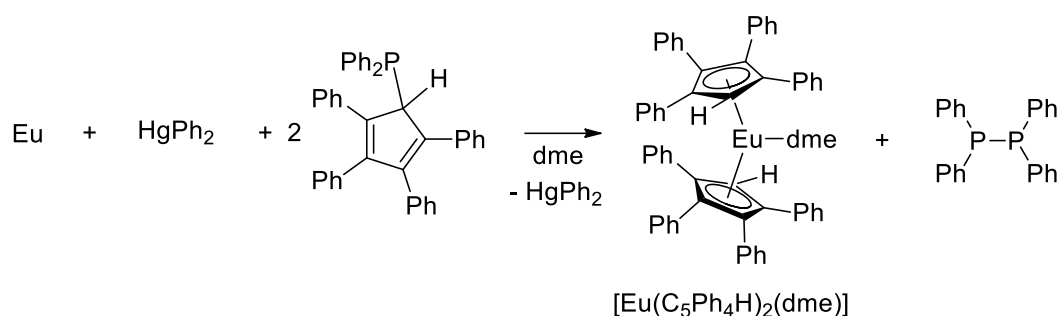


Scheme 1.1 – Synthesis of superbuly lanthanocenes by a) protolysis accompanied by sterically induced reduction (SIR) and b) protolysis.^[83,84]



Scheme 1.2 – Synthesis of decaphenyl lanthanocenes by redox transmetallation/protolysis.^[79–82]

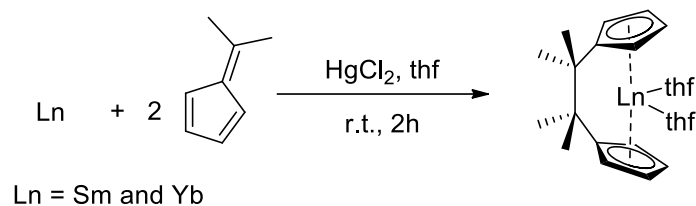
A largely unexplored alternative synthetic method, discovered by the Deacon group, involves preparation of a phosphinated cyclopentadienyl pro-ligand, which can undergo selective carbon-phosphorus bond cleavage to form the desired sandwich complex, eliminating the phosphorus coupled tetraphenyldiphosphine in the process (Scheme 1.3).^[85]



Scheme 1.3 – Synthesis of octaphenyl europocene by selective C-P cleavage of a phosphinated cyclopentadienyl pro-ligand.^[85]

While using much less sensitive lanthanoid reagents than the protolysis route and offering a mercury-free synthetic pathway compared to the RTP reactions, the C-P cleavage route has only been shown to be effective with europium metal, and tetraphenylcyclopentadienyldiphenylphosphine as a pro-ligand, with no extension made to other lanthanoid metals or polyarylcyclopentadiene based ligand systems.

Lanthanocenes can be further diversified by introduction of a bridging group between the two cyclopentadienyl rings which can greatly influence the structural and chemical properties, as well as the reactivity of the resulting sandwich complexes, known as *ansa* lanthanocenes.^[86] Much like polyaryl sandwich complexes, polyaryl *ansa* complexes are of great interest, as when compared to their untethered counterparts, they can offer a higher degree of reactivity owing to the tether's influence on the planar angle of the cyclopentadienyl rings, facilitating access to the metal centre. Typically, these complexes have been synthesised by protolysis, or salt metathesis, with very few examples of reductive dimerisation,^[87] whereby a fulvene is reduced into a radical by the activated lanthanoid metal, and undergoes coupling to produce the bridged ligand species, which readily coordinates to the oxidised metal centre (Scheme 1.4).^[88]



Scheme 1.4 – Reductive dimerisation of 6,6'-dimethylfulvene by Sm and Yb metal (activated with HgCl_2) to form $\text{Ln}(\textit{ansa})$ complexes.^[88]

1.7 Carbon-fluorine bond activation by rare earth metals

Carbon-fluorine bonds represent the strongest single bonds in organic chemistry, with a bond dissociation energy of 441 kJ/mol.^[89] This bond strength results in a decrease in the reactivity, and increase in the thermal stability of C-F bond containing compounds when compared to their C-H counterparts.^[90] These enticing properties have led to incorporation of C-F moieties into chemicals that are widespread within the agriculture and pharmaceutical sectors.^[91] One of the major detriments of this is the longevity and persistence of C-F containing compounds long after their intended application. A sinister example being polyfluoroalkylated substances (PFAS), which have become an increasing concern in recent years, owing to their detection across many different environments, alongside their persistence, bioaccumulation/magnification, and potential health implications.^[92] Treatment of these fluorinated compounds by combustion leads to release of greenhouse gases, and thus an area of great interest is the activation of C-F bonds in order to cleave these otherwise stable bonds.

Research efforts on C-F activation by metal centres have largely focussed on the use of transition metals complexes.^[90,91,93–99] These reports are primarily on intramolecular C-F activation, whereby the C-F bond of a coordinated ligand is cleaved by the metal centre. Whilst examples of rare earth metal centres being used for C-F activation are not as widely reported as their transition metal counterparts, their high fluorophilicity facilitates interactions between

fluorine and the metal, weakening the C-F bond, and promoting subsequent C-F activation.^[90] Whilst typical C-F bond dissociation energies are very high, this bond strength can be offset by the higher dissociation energy of the Ln-F bond which is formed in the process of C-F activation by a lanthanoid metal species. Reports of rare earth induced C-F activation have typically utilised organolanthanoid complexes and inorganic lanthanoid salts, with only a small series of examples involving the free lanthanoid metal.

1.8 References

- [1] N. G. Connelly, T. Damhus, R. M. Hartshorn, A. T. Hutton, *Nomenclature of Inorganic Chemistry*, Royal Society of Chemistry, Cambridge, **2005**.
- [2] T. Imamoto, *Lanthanides in Organic Chemistry*, Academic Press, London, **1994**.
- [3] B. T. Kilbourn, *A Lanthanide Lanthology, Part I, A-L*, Academic Press, New York, **1993**.
- [4] S. Cotton, *Lanthanide and Actinide Chemistry*, John Wiley And Sons, Chichester, **2006**.
- [5] N. Krishnamurthy, C. K. Gupta, *Extractive Metallurgy of Rare Earths*, CRC Press, Boca Raton, **2016**.
- [6] B. T. Kilbourn, *A Lanthanide Lanthology, Part II, M-Z*, Molycorp, New York, **1993**.
- [7] D. N. Trifonov, *The Rare Earth Elements*, Pergamon Press, Oxford, **1963**.
- [8] F. H. Spedding, *Handbook on the Physics and Chemistry of Rare Earths*, North-Holland Publishing Company, Amsterdam, **1978**.
- [9] K. L. Nash, G. R. Choppin, *Separation of the Elements*, Plenum, New York, **1995**.
- [10] F. A. Cotton, G. Wilkinson, C. A. Murillo, M. Bochmann, *Advanced Inorganic Chemistry: A Comprehensive Text*, John Wiley And Sons, New York, **1999**.
- [11] W. T. Carnal, *Handbook on the Physics and Chemistry of Rare Earths*, North-Holland Publishing Company, Amsterdam, **1979**.
- [12] R. E. Krebs, *The History and Use of Our Earth's Chemical Elements: A Reference Guide*, Greenwood Press, Connecticut, **1998**.

- [13] Ralph G. Pearson, *J. Am. Chem. Soc.* **1963**, *85*, 3533–3539.
- [14] V. I. Spitsyn, L. I. Martynenko, *Coordination Chemistry of Rare Earth Elements*, Izd. MGU, Moscow, **1973**.
- [15] N. N. Greenwood, A. Earnshaw, *Chemistry of the Elements*, Butterworth-Heinemann, Oxford, **1997**.
- [16] S. A. Cotton, *Comprehensive Coordination Chemistry II*, Elsevier, Oxford, **2004**.
- [17] I. Olmez, E. R. Sholkovtztz, D. Hermann, R. P. Eganhouse, *Environ. Sci. Technol.* **1991**, *25*, 310–316.
- [18] Y. Nozaki, D. Lerche, D. S. Alibo, M. Tsutsumi, *Dissolved Indium and Rare Earth Elements in Three Japanese Rivers and Tokyo Bay: Evidence for Anthropogenic Gd and In*, **2000**.
- [19] E. Greinacher, in *Ind. Appl. Rare Earth Elem.* (Ed.: K.A. Gschneider), ACS Symposium Series, **1981**, pp. 3–17.
- [20] M. L. He, D. Ranz, W. A. Rambeck, *J. Anim. Physiol. Anim. Nutr. (Berl)*. **2001**, *85*, 263–270.
- [21] E. Delhaize, P. R. Ryan, P. J. Randall, *Plant Physiol.* **1993**, *103*, 695–702.
- [22] C. J. Asher, F. W. Smith, *J. Plant Nutr.* **1995**, *18*, 1963–1976.
- [23] C. J. Asher, F. W. Smith, *J. Plant Nutr.* **1995**, *18*, 1977–1989.
- [24] C. J. Asher, F. W. Smith, *J. Plant Nutr.* **1995**, *18*, 1991–2003.
- [25] C. Picard, N. Geum, I. Nasso, B. Mestre, P. Tisnès, S. Laurent, R. N. Muller, L. Vander

- Elst, *Bioorganic Med. Chem. Lett.* **2006**, *16*, 5309–5312.
- [26] S. Aime, S. G. Crich, E. Gianolio, G. B. Giovenzana, L. Tei, E. Terreno, *Coord. Chem. Rev.* **2006**, *250*, 1562–1579.
- [27] J. T. Haley, *J. Pharmacol. Sci.* **1965**, *54*, 663–670.
- [28] S. P. Fricker, *Chem. Soc. Rev.* **2006**, *35*, 524–533.
- [29] M. Woods, D. E. Woessner, A. D. Sherry, *Chem. Soc. Rev.* **2006**, *35*, 500–511.
- [30] M. Bottrill, L. Kwok, N. J. Long, *Chem. Soc. Rev.* **2006**, *35*, 557–571.
- [31] S. Methfessel, *IEEE Trans. Magn.* **1965**, *MAG-1*, 144–155.
- [32] V. S. Sastri, J. C. Bünzli, V. R. Rao, G. V. S. Rayudu, J. R. Perumareddi, *Modern Aspects of Rare Earths and Their Complexes*, Elsevier, Amsterdam, **2003**.
- [33] G. De La Puente, E. Falabella Souza-Aguiar, F. M. Zanon Zotin, V. L. Doria Camorim, U. Sedran, *Influence of Different Rare Earth Ions on Hydrogen Transfer over Y Zeolite*, **2000**.
- [34] R. Carvajal, P. J. Chu, J. H. Lunsford, *J. Catal.* **1990**, *125*, 123–131.
- [35] T. V. Choudhary, S. Banerjee, V. R. Choudhary, *Catalysts for Combustion of Methane and Lower Alkanes*, **2002**.
- [36] S. Colussi, A. Gayen, J. Llorca, C. De Leitenburg, G. Dolcetti, A. Trovarelli, *Ind. Eng. Chem. Res.* **2012**, *51*, 7510–7517.
- [37] M. F. M. Zwinkels, S. G. Järås, P. G. Menon, T. A. Griffin, *Catal. Rev. Sci. Eng.* **1993**, *35*, 319–358.

- [38] W. C. Cheng, G. Kim, A. W. Peters, X. Zhao, K. Rajagopalan, M. S. Ziebarth, C. J. Pereira, *Catal. Rev. Sci. Eng.* **1998**, *40*, 39–79.
- [39] D. B. Hibbert, *Catal. Rev. Sci. Eng.* **1992**, *34*, 391–408.
- [40] Y. Nishihata, J. Mizuki, T. Akao, H. Tanaka, M. Uenishi, M. Kimura, T. Okamoto, N. Hamada, *Nature* **2002**, *418*, 164–167.
- [41] Z. Wang, M. Cheng, Z. Bi, Y. Dong, H. Zhang, J. Zhang, Z. Feng, C. Li, *Mater. Lett.* **2005**, *59*, 2579–2582.
- [42] Z. Wang, M. Cheng, Y. Dong, M. Zhang, H. Zhang, *J. Power Sources* **2006**, *156*, 306–310.
- [43] S. Park, J. M. Vohs, R. J. Gorte, *Nature* **2000**, *404*, 265–267.
- [44] M. N. Bochkarev, L. N. Zakharov, G. S. Kalinina, *Organoderivatives of the Rare Earth Elements*, Kluwer, Dordrecht, **1995**.
- [45] D. C. Bradley, R. C. Mehrotra, I. P. Rothwell, A. Singh, *Alkoxo and Aryloxo Derivatives of Metals*, Academic Press, London, **2001**.
- [46] W. A. Herrmann, R. Anwender, M. Kleine, W. Scherer, *Herrmann-Brauer, Synthetic Methods of Organometallic and Inorganic Chemistry*, Thieme, Stuttgart, **1997**.
- [47] D. C. Bradley, J. S. Ghotra, F. A. Hart, R. L. LaDuca, P. T. Wolczanski, *Herrmann-Brauer, Synthetic Methods of Organometallic and Inorganic Chemistry*, Thieme, Stuttgart, **1997**.
- [48] T. J. Boyle, L. A. M. Ottley, *Chem. Rev.* **2008**, *108*, 1896–1917.
- [49] G. B. Deacon, J. E. Cosgriff, E. T. Lawrenz, C. M. Forsyth, D. L. Wilkinson, *Herrmann-*

Brauer, Synthetic Methods of Organometallic and Inorganic Chemistry, Thieme, Stuttgart, **1997**.

- [50] L. N. Bochkarev, T. A. Stepantseva, L. N. Zakharov, G. K. Fukin, A. I. Yanovsky, Y. T. Struchkov, *Organometallics* **1995**, *14*, 2127.
- [51] M. N. Bochkarev, A. A. Trifonov, E. A. Fedorova, N. S. Emelyanova, T. A. Basalgina, G. S. Kalinina, G. A. Razuvaev, *J. Organomet. Chem.* **1989**, *372*, 217–224.
- [52] Z. Guo, R. Huo, Y. Q. Tan, V. Blair, G. B. Deacon, P. C. Junk, *Coord. Chem. Rev.* **2020**, *415*, 213232.
- [53] G. B. Deacon, C. M. Forsyth, S. Nickel, *J. Organomet. Chem.* **2002**, *647*, 50–60.
- [54] Z. Guo, V. Blair, G. B. Deacon, P. C. Junk, *Chem. Eur. J.* **2018**, *24*, 17464–17474.
- [55] C. J. Raub, *Handbook on the Physics and Chemistry of Rare Earths, Volume 21*, **1997**.
- [56] A. Amgoune, C. M. Thomas, J. F. Carpentier, *Pure Appl. Chem.* **2007**, *79*, 2013–2030.
- [57] X. Liu, X. Shang, T. Tang, N. Hu, F. Pei, D. Cui, X. Chen, X. Jing, *Organometallics* **2007**, *26*, 2747–2757.
- [58] Kun Nie, Xiangyong Gu, Yingming Yao, Yong Zhang, Qi Shen, *Dalton Trans.* **2010**, *39*, 6832–6840.
- [59] Y. Yao, X. Xu, B. Liu, Y. Zhang, Q. Shen, W. T. Wong, *Inorg. Chem.* **2005**, *44*, 5133–5140.
- [60] H. C. Aspinall, J. F. Bickley, J. M. Gaskell, A. C. Jones, G. Labat, P. R. Chalker, P. A. Williams, *Inorg. Chem.* **2007**, *46*, 5852–5860.

- [61] X. Xu, M. Ma, Y. Yao, Y. Zhang, Q. Shen, *J. Mol. Struct.* **2005**, *743*, 163–168.
- [62] K. G. Caulton, L. G. Hubert-Pfalzgraf, *Chem. Rev.* **1990**, *90*, 969–995.
- [63] R. C. Mehrotra, A. Singh, U. M. Tripathi, *Chem. Rev.* **1991**, *91*, 1287–1303.
- [64] J. Marçalo, A. P. De Matos, *Polyhedron* **1989**, *8*, 2431–2437.
- [65] S. H. Ali, Syntheses, Structures and Reactivity of Organolanthanoid Complexes, PhD Thesis, James Cook University, **2017**.
- [66] G. B. Deacon, T. Feng, P. MacKinnon, R. H. Newnham, S. Nickel, B. W. Skelton, A. H. White, *Aust. J. Chem* **1993**, *46*, 387–399.
- [67] M. L. Cole, G. B. Deacon, P. C. Junk, K. M. Proctor, J. L. Scott, C. R. Strauss, *Eur. J. Inorg. Chem.* **2005**, 4138–4144.
- [68] G. Wilkinson, M. Rosenblum, M. C. Whiting, R. B. Woodward, *J. Am. Chem. Soc.* **1952**, *74*, 2125–2126.
- [69] G. Wilkinson, J. M. Birmingham, *J. Am. Chem. Soc.* **1954**, *76*, 6210.
- [70] C. Elschenbroich, *Organometallics*, Wiley-VCH, Weinheim, **2006**.
- [71] W. J. Evans, I. Bloom, W. E. Hunter, J. L. Atwood, *J. Am. Chem. Soc.* **1981**, *103*, 6507–6508.
- [72] W. J. Evans, S. L. Gonzales, J. W. Ziller, *J. Am. Chem. Soc.* **1991**, *113*, 7423–7424.
- [73] W. J. Evans, J. M. Perotti, S. A. Kozimor, T. M. Champagne, B. L. Davis, G. W. Nyce, C. H. Fujimoto, R. D. Clark, M. A. Johnston, J. W. Ziller, *Organometallics* **2005**, *24*, 3916–3931.

- [74] W. J. Evans, C. A. Seibel, J. W. Ziller, *J. Am. Chem. Soc.* **1998**, *120*, 6745–6752.
- [75] W. J. Evans, D. K. Drummond, S. G. Bott, J. L. Atwood, *Organometallics* **1986**, *5*, 2389–2391.
- [76] S. N. Konchenko, N. A. Pushkarevsky, M. T. Gamer, R. Köppe, H. Schnöckel, P. W. Roesky, *J. Am. Chem. Soc.* **2009**, *131*, 5740–5741.
- [77] W. J. Evans, S. L. Gonzales, J. W. Ziller, *J. Am. Chem. Soc.* **1991**, *113*, 9880–9882.
- [78] W. J. Evans, T. A. Ulibarri, J. W. Ziller, *J. Am. Chem. Soc.* **1988**, *110*, 6877–6879.
- [79] R. P. Kelly, T. D. M. Bell, R. P. Cox, D. P. Daniels, G. B. Deacon, F. Jaroschik, P. C. Junk, X. F. Le Goff, G. Lemercier, A. Martinez, J. Wang, D. Werner, *Organometallics* **2015**, *34*, 5624–5636.
- [80] G. B. Deacon, F. Jaroschik, P. C. Junk, R. P. Kelly, *Organometallics* **2015**, *34*, 2369–2377.
- [81] G. B. Deacon, C. M. Forsyth, F. Jaroschik, P. C. Junk, D. L. Kay, T. Maschmeyer, A. F. Masters, J. Wang, L. D. Field, *Organometallics* **2008**, *27*, 4772–4778.
- [82] G. B. Deacon, F. Jaroschik, P. C. Junk, R. P. Kelly, *Chem. Commun.* **2014**, *50*, 10655–10657.
- [83] S. Harder, D. Naglav, C. Ruspic, C. Wickleder, M. Adlung, W. Hermes, M. Eul, R. Pöttgen, D. B. Rego, F. Poineau, K. R. Czerwinski, R. H. Herber, I. Nowik, *Chem. Eur. J.* **2013**, *19*, 12272–12280.
- [84] C. Ruspic, J. R. Moss, M. Schürmann, S. Harder, *Angew. Chem. Int. Ed.* **2008**, *47*, 2121–2126.

- [85] D. P. Daniels, Substituted Cyclopentadienyl Chemistry of the Alkaline Earth and Rare Earth Elements, PhD Thesis, Monash University, **2011**.
- [86] P. J. Shapiro, *Coord. Chem. Rev.* **2002**, *231*, 67–81.
- [87] A. Recknagel, F. T. Edelmann, *Angew. Chem., Int. Ed. Engl.* **1991**, *30*, 693–694.
- [88] F. T. Edelmann, M. Rieckhoff, I. Haiduc, I. Silaghi-Dumitrescu, *J. Organomet. Chem.* **1993**, *447*, 203–208.
- [89] D. O'hagan, *Chem. Soc. Rev.* **2008**, *37*, 308–319.
- [90] A. E. Shilov, G. B. Shul'pin, *Chem. Rev.* **1997**, *97*, 2879–2932.
- [91] H. Amii, K. Uneyama, *Chem. Rev.* **2009**, *109*, 2119–2183.
- [92] A. Chohan, H. Petaway, V. Rivera-Diaz, A. Day, O. Colaianni, M. Keramati, *Rev. Environ. Health* **2021**, *36*, 235–259.
- [93] K. Uneyama, H. Amii, *J. Fluor. Chem.* **2002**, *114*, 127–131.
- [94] W. D. Jones, *J. Chem. Soc. Dalton Trans.* **2003**, *3*, 3991–3995.
- [95] T. Braun, R. N. Perutz, *Chem. Commun.* **2002**, *2*, 2749–2757.
- [96] A. D. Sun, J. A. Love, *Dalton Trans.* **2010**, *39*, 10362–10374.
- [97] T. Braun, F. Wehmeier, *Eur. J. Inorg. Chem.* **2011**, 613–625.
- [98] E. Clot, O. Eisenstein, N. Jasim, S. A. MacGregor, J. E. McGrady, R. N. Perutz, *Acc. Chem. Res.* **2011**, *44*, 333–348.
- [99] M. Klahn, U. Rosenthal, *Organometallics* **2012**, *31*, 1235–1244.

Chapter 2: Synthesis of lanthanoid biphenolate complexes and their further reactivity

2.1 Introduction

The biphenol 2,2'-methylenebis(6-*tert*-butyl-4-methylphenol) (mbmpH₂) (Figure 2.1) has been the primary pro-ligand used in lanthanoid biphenolate chemistry, yielding a variety of lanthanoid biphenolate complexes through two major synthetic pathways used for lanthanoid aryloxide synthesis: salt metathesis of the corresponding alkali metal salt of mbmp²⁻, or through protolysis reactions utilising a variety of lanthanoid precursors.^[1] These two methods have given access to molecular divalent, and both molecular and charge separated trivalent metal complexes. Whilst seemingly versatile, both methods have distinct restrictions, typically involving the incorporation of halides, or alkali metal ion inclusion into the desired complex.

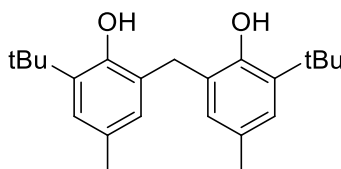
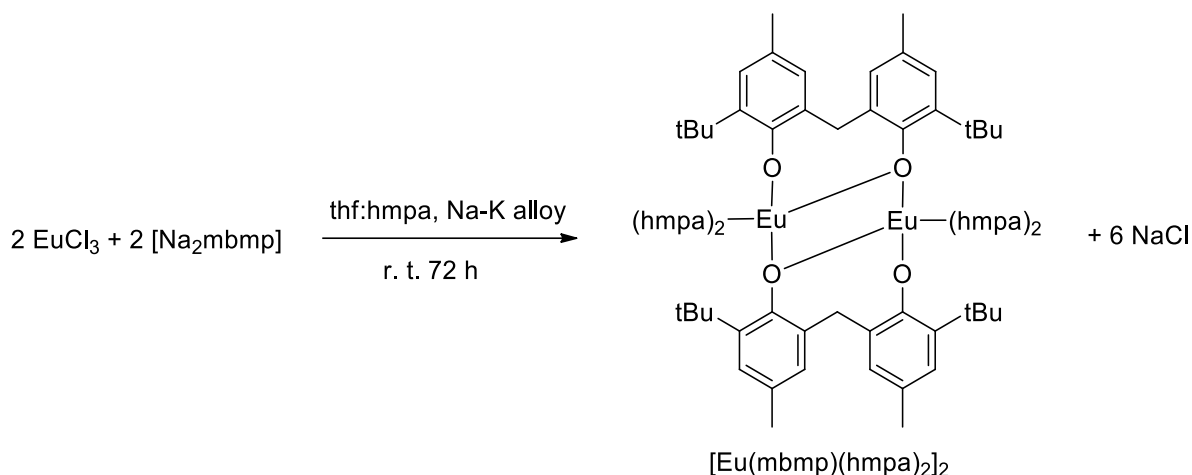


Figure 2.1 – Structure of 2,2'-methylenebis(6-*tert*-butyl-4-methylphenol) (mbmpH₂).

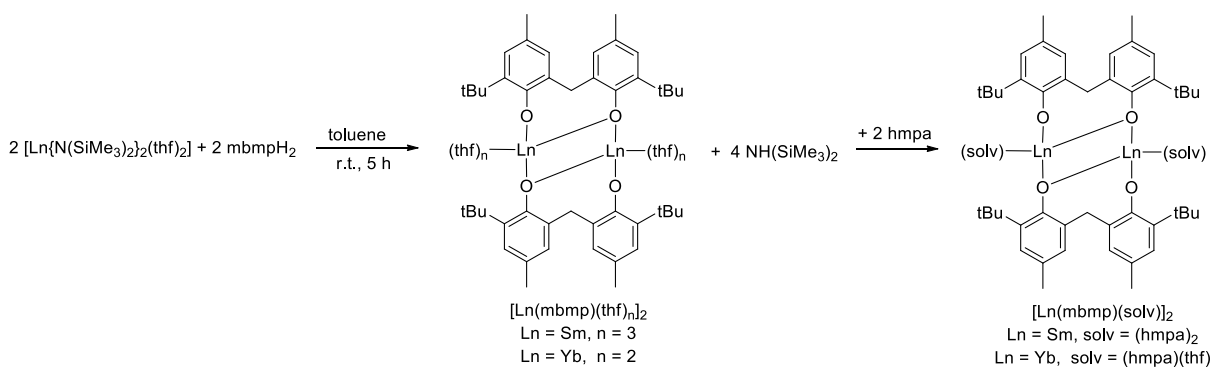
2.1.1 Synthesis of divalent lanthanoid biphenolate complexes

Divalent lanthanoid biphenolates with the mbmp²⁻ ligand are not widely reported compared to their trivalent counterparts, with only a few examples in the literature. The Shen group have prepared the first such divalent carbon-bridged biphenolate europium complex by salt metathesis of EuCl₃ with Na₂mbmp, and subsequent reduction of Eu³⁺ to Eu²⁺ by a Na-K alloy in thf:hmpa (Scheme 2.1).^[2]



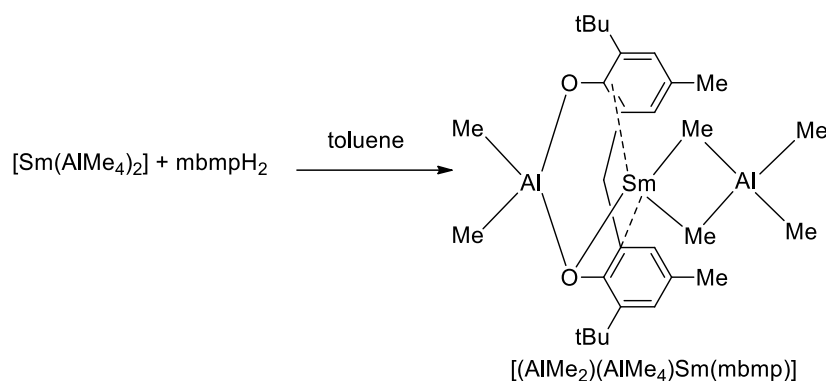
Scheme 2.1 – Synthesis of $[\text{Eu}(\text{mbmp})(\text{hmpa})_2]_2$ from salt metathesis of EuCl_3 and Na_2mbmp , and reduction by Na-K alloy.^[2]

The Shen group synthesised analogous samarium and ytterbium complexes by protolysis, using $[\text{Ln}\{\text{N}(\text{SiMe}_3)_2\}_2(\text{thf})_2]$ reagents, and treating them with the mbmpH_2 pro-ligand in thf , and further treated with hmpa to solubilise them and obtain crystals (Scheme 2.2).^[3]



Scheme 2.2 – Synthesis of $[\text{Ln}(\text{mbmp})(\text{thf})_n]_2$ and $[\text{Ln}(\text{mbmp})(\text{solv})]_2$ by protolysis of $[\text{Ln}\{\text{N}(\text{SiMe}_3)_2\}_2(\text{thf})_2]$ and mbmpH_2 .^[3]

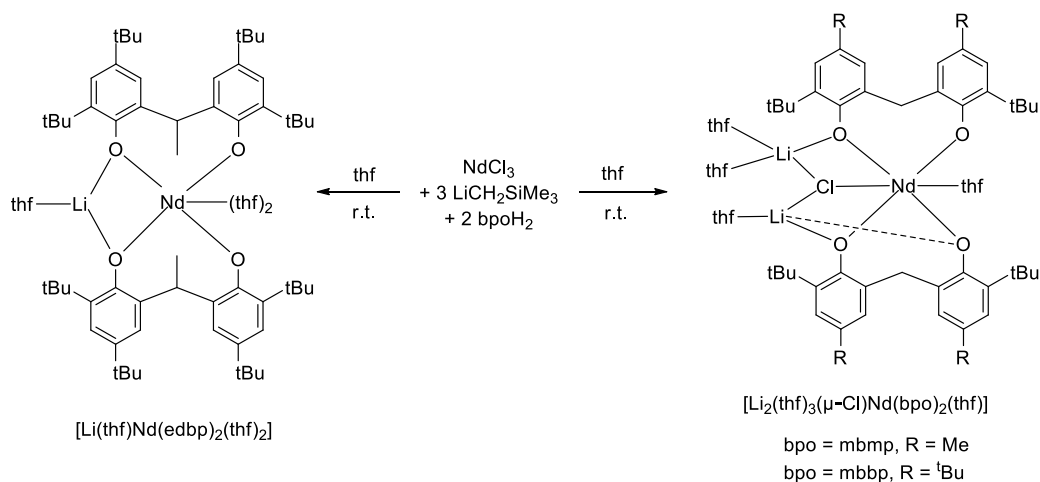
The divalent, peralkylated aluminate samarium species $[\text{Sm}(\text{AlMe}_4)_2]$ has also been used as a protolysis reagent to access the divalent $[(\text{AlMe}_2)(\text{AlMe}_4)\text{Sm}(\text{mbmp})]$ species (Scheme 2.3).^[4]



Scheme 2.3 – Synthesis of divalent heterobimetallic $[(\text{AlMe}_2)(\text{AlMe}_4)\text{Sm}(\text{mbmp})]$ species by protolysis reaction of $[\text{Sm}(\text{AlMe}_4)_2]$ and mbmpH_2 .^[4]

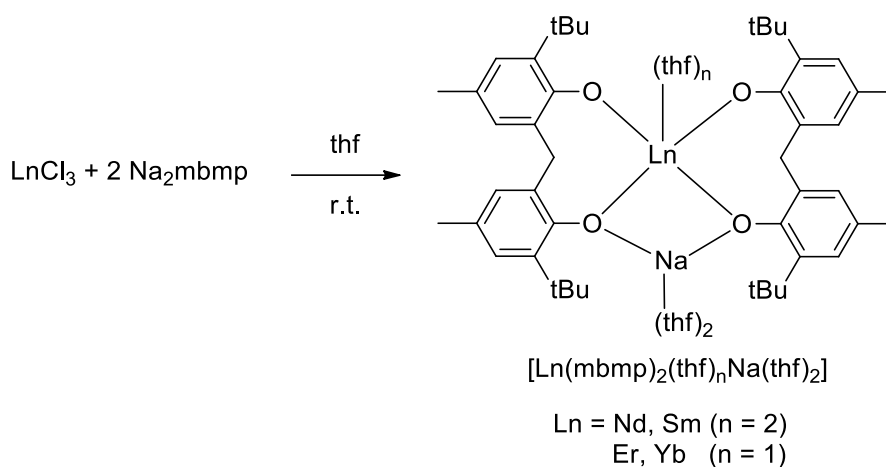
2.1.2 Synthesis of trivalent lanthanoid biphenolate complexes

Comparatively, there are a wide array of trivalent lanthanoid species synthesised by both salt metathesis and protolysis reactions. These complexes can potentially suffer the same fate as their divalent counterparts, where inclusion of alkali metal or halide ions are observed. For example, the salt metathesis reaction of NdCl_3 and $\text{LiCH}_2\text{SiMe}_3$ with biphenol pro-ligands 6,6'-methylenebis(2-*tert*-butyl-4-methylphenol) (mbmpH_2), 6,6'-methylenebis(2,4-di-*tert*-butylphenol) (mbbpH_2) or 6,6'-(ethane-1,1-diyl)bis(2,4-di-*tert*-butylphenol) (edbpH_2), yields both the lithium ion incorporated product $[\text{Li}(\text{thf})\text{Nd}(\text{edbp})_2(\text{thf})_2]$, or the lithium and chloride ion incorporated products $[\text{Li}_2(\text{thf})_3(\mu\text{-Cl})\text{Nd}(\text{mbmp})_2(\text{thf})]$ and $[\text{Li}_2(\text{thf})_3(\mu\text{-Cl})\text{Nd}(\text{mbbp})_2(\text{thf})]$ (Scheme 2.4).^[5] Attempts were made to avoid the redistribution by performing the reaction at reduced temperatures, and with shorter durations, but were ultimately unsuccessful.



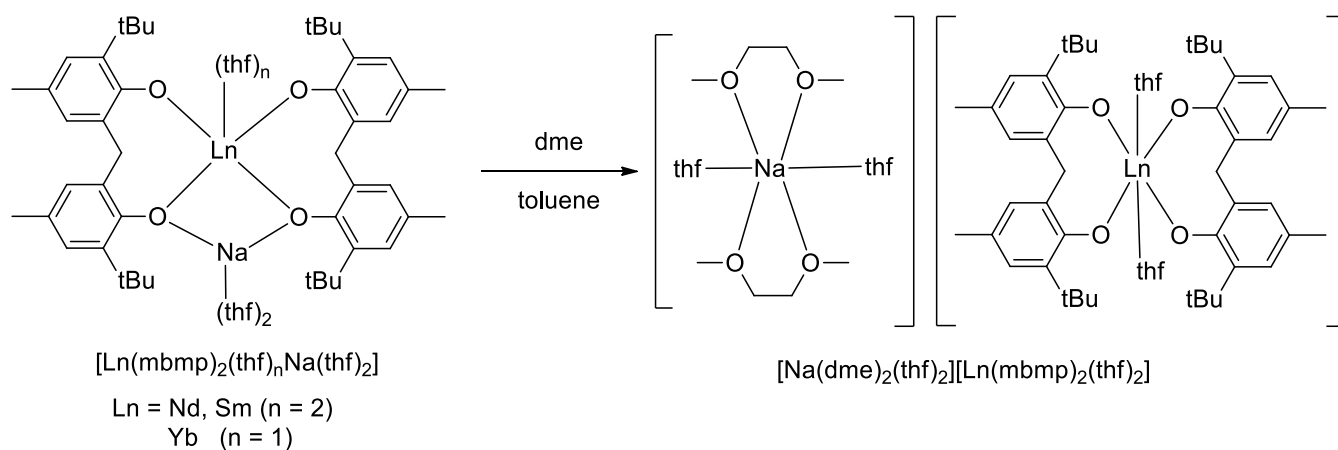
Scheme 2.4 - Salt metathesis reactions of NdCl_3 yielding the lithium incorporated $[\text{Li}(\text{thf})\text{Nd}(\text{edbp})_2(\text{thf})_2]$, and lithium chloride incorporated $[\text{Li}_2(\text{thf})_3(\mu\text{-Cl})\text{Nd}(\text{mbmp})_2(\text{thf})]$ and $[\text{Li}_2(\text{thf})_3(\mu\text{-Cl})\text{Nd}(\text{mbbp})_2(\text{thf})]$ complexes.^[5]

Inclusion of the alkali metal or halide ions can result in the formation of both neutral, and charged complexes, based on the solvent system used. The Shen group has demonstrated this by treatment of LnCl_3 ($\text{Ln} = \text{Nd}, \text{Sm}, \text{Er}$ and Yb) with two equivalents of Na_2mbmp in thf, yielding the corresponding molecular $[\text{Ln}(\text{mbmp})_2(\text{thf})_n\text{Na}(\text{thf})_2]$ ($\text{Ln} = \text{Nd}, \text{Sm}, n = 1$, and $\text{Ln} = \text{Er}, \text{Yb}, n = 2$) complexes (Scheme 2.5).^[6,7]



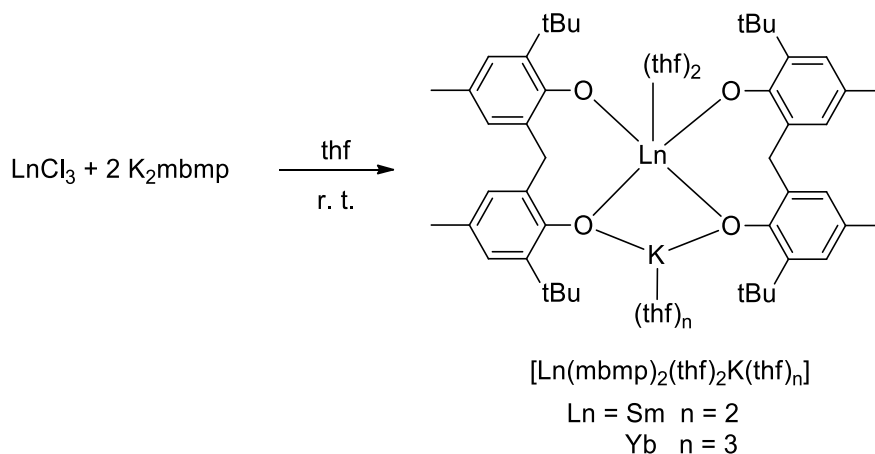
Scheme 2.5 – Salt metathesis reactions of LnCl_3 with Na_2mbmp yielding sodium-lanthanoid bimetallic biphenolate complexes $[\text{Ln}(\text{mbmp})_2(\text{thf})_n\text{Na}(\text{thf})_2]$.^[6,7]

Of these complexes, the Nd, Sm and Yb heterobimetallics were susceptible to forming the ionic complexes $[\text{Na}(\text{dme})_2(\text{thf})_2][\text{Ln}(\text{mbmp})_2(\text{thf})_2]$ when extracted into a mixture of toluene and dme (Scheme 2.6).^[7]



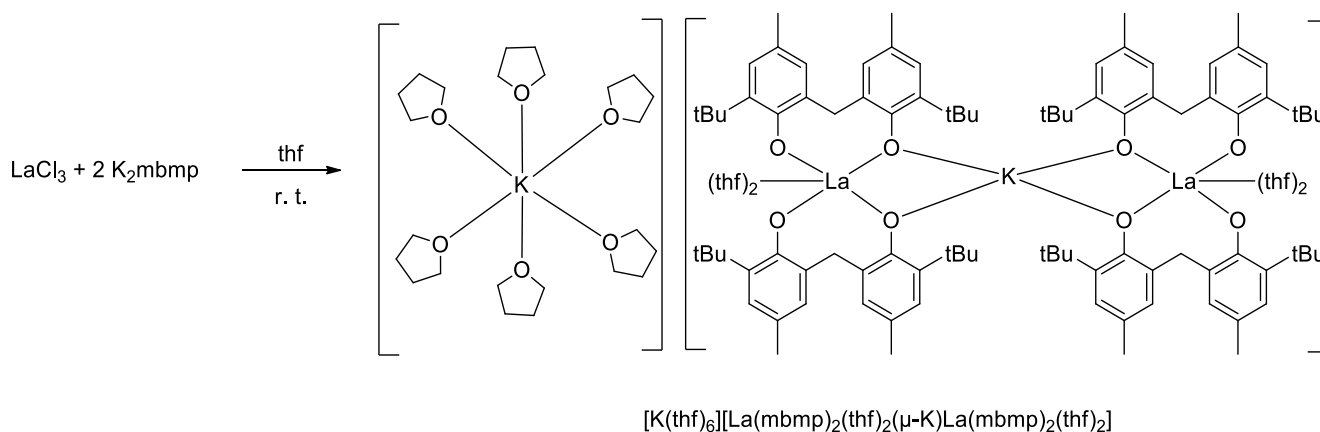
Scheme 2.6 – Formation of ionic species $[\text{Na}(\text{dme})_2(\text{thf})_2][\text{Ln}(\text{mbmp})_2(\text{thf})_2]$ where Ln = Nd, Sm and Yb, upon changing solvent from thf to a dme:toluene mixture.^[7]

The variability observed in these complexes was further exaggerated when using the larger potassium cation based salt of the biphenolate ligand, K_2mbmp , whereby metathesis reactions with LnCl_3 (Ln = La, Sm, Nd and Yb), produced both molecular, and ionic complexes when synthesised in thf. The Sm and Yb complexes $[\text{Ln}(\text{mbmp})_2(\text{thf})_2\text{K}(\text{thf})_n]$ were analogous to their sodium counterparts (Scheme 2.7),^[8] whereas the La complex formed a charge separated species, with a solvated potassium cation, and a two lanthanum centred, potassium bridged, anion $[\text{K}(\text{thf})_6][\text{La}(\text{mbmp})_2(\text{thf})_2(\mu\text{-K})\text{La}(\text{mbmp})_2(\text{thf})_2]$ (Scheme 2.8),^[8] and Nd formed a large tetranuclear molecular complex $[\text{K}(\text{thf})_2\text{Nd}(\text{mbmp})_2]_2$ (Scheme 2.9).^[8]

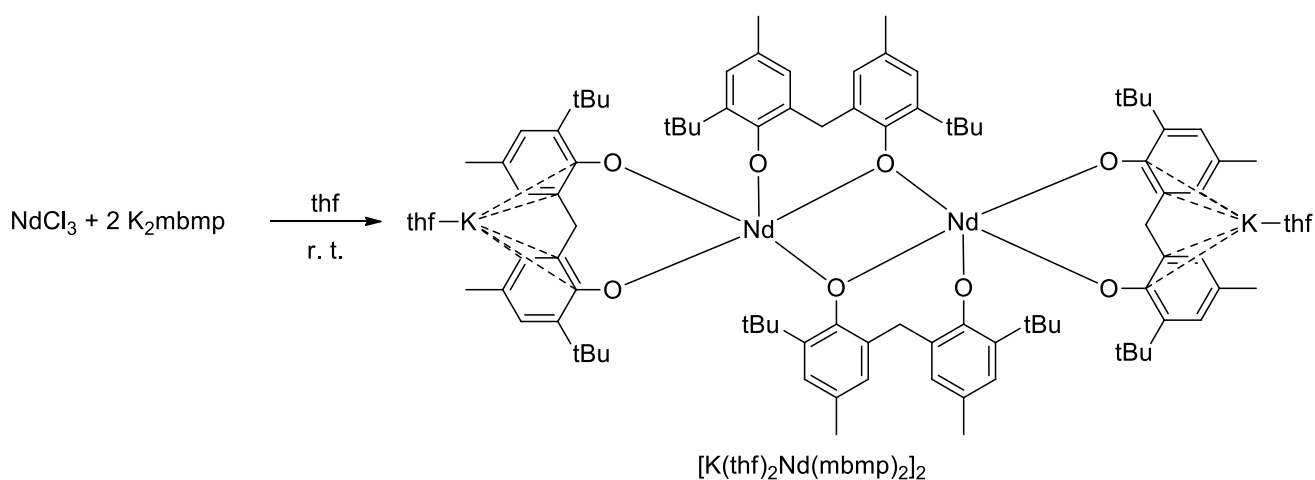


Scheme 2.7 – Metathesis reaction of LnCl_3 with K_2mbmp to form $[\text{Ln}(\text{mbmp})_2(\text{thf})_2\text{K}(\text{thf})_n]$

($\text{Ln} = \text{Sm}$, $n = 2$, and $\text{Ln} = \text{Yb}$, $n = 3$).^[8]

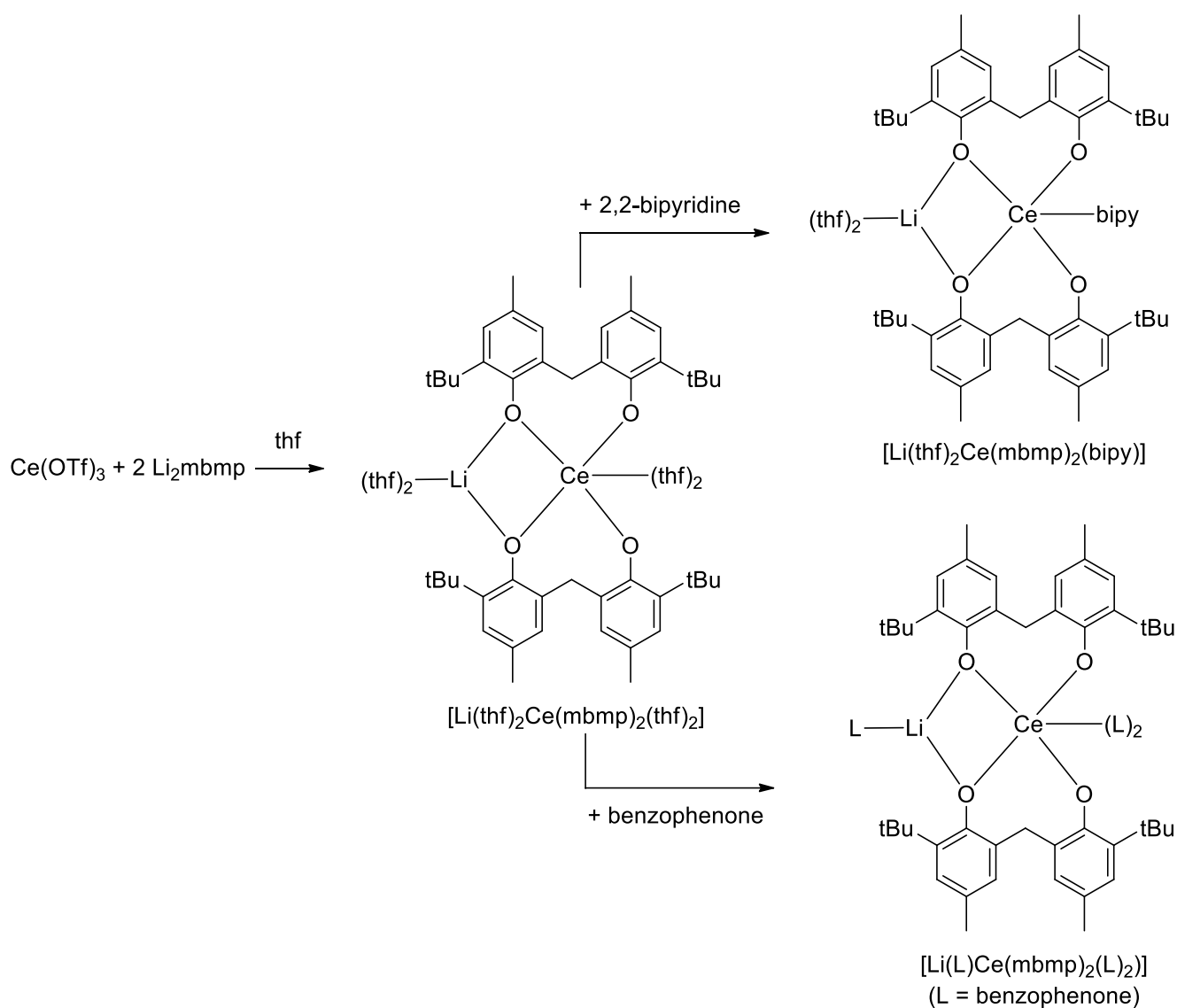


Scheme 2.8 – Formation of the charge separated ionic species $[\text{K}(\text{thf})_6][\text{La}(\text{mbmp})_2(\text{thf})_2(\mu\text{-K})\text{La}(\text{mbmp})_2(\text{thf})_2]$.^[8]



Scheme 2.9 – Synthesis of tetranuclear Nd-K complex $[\text{K}(\text{thf})_2\text{Nd}(\text{mbmp})_2]_2$.^[8]

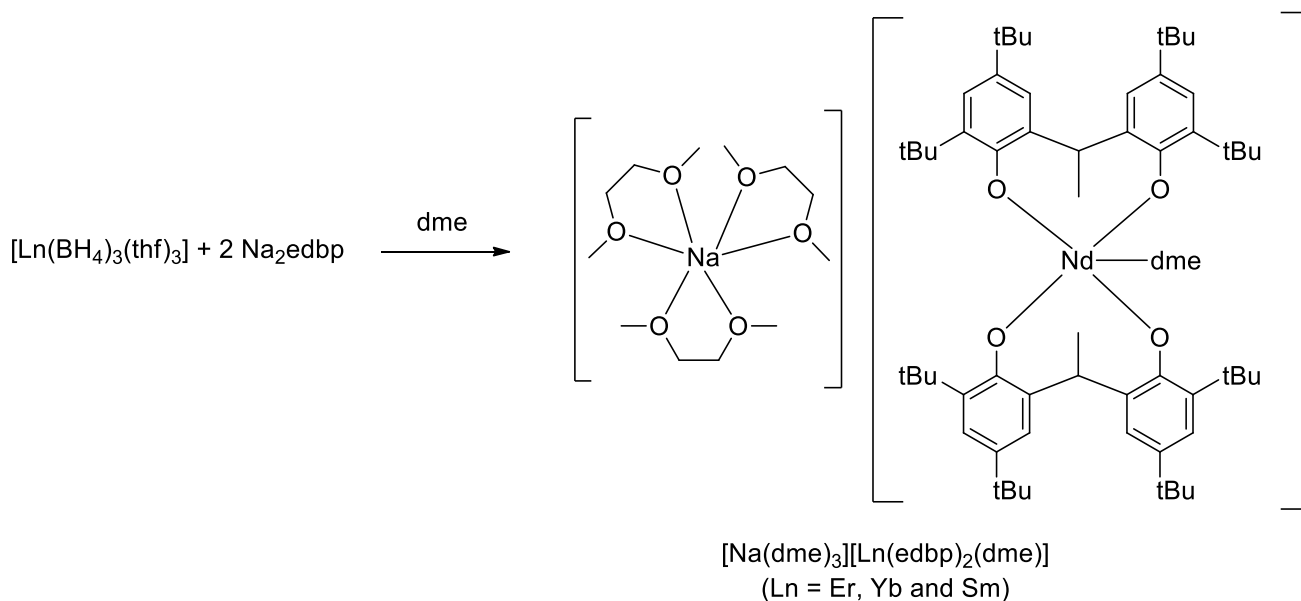
A cerium(III) biphenolate complex has also been synthesised by the Schelter group *via* salt metathesis, utilising $\text{Ce}(\text{OTf})_3$ and Li_2mbmp to form the lithium/cerium heterobimetallic complex $[\text{Li}(\text{thf})_2\text{Ce}(\text{mbmp})_2(\text{thf})_2]$ (Scheme 2.10).^[9] The thf coordinated to the Ce^{3+} cation could be displaced by addition of 2,2'-bipyridine to yield $[\text{Li}(\text{thf})_2\text{Ce}(\text{mbmp})_2(\text{bipy})]$, whereas addition of benzophenone displaced the coordinated thf on both the Ce^{3+} and Li^+ cations, yielding $[\text{Li}(\text{L})\text{Ce}(\text{mbmp})_2(\text{L})_2]$ (L = benzophenone) (Scheme 2.10).^[9]



Scheme 2.10 – Metathesis reactions utilising $\text{Ce}(\text{OTf})_3$ with the Li_2mbmp to synthesise the cerium-lithium heterobimetallic $[\text{Li}(\text{thf})_2\text{Ce}(\text{mbmp})_2(\text{thf})_2]$, and subsequent treatment with 2,2-bipyridine to yield $[\text{Li}(\text{thf})_2\text{Ce}(\text{mbmp})_2(\text{bipy})]$, and treatment with benzophenone to yield $[\text{Li}(\text{L})\text{Ce}(\text{mbmp})_2(\text{L})_2]$ (where L = benzophenone).^[9]

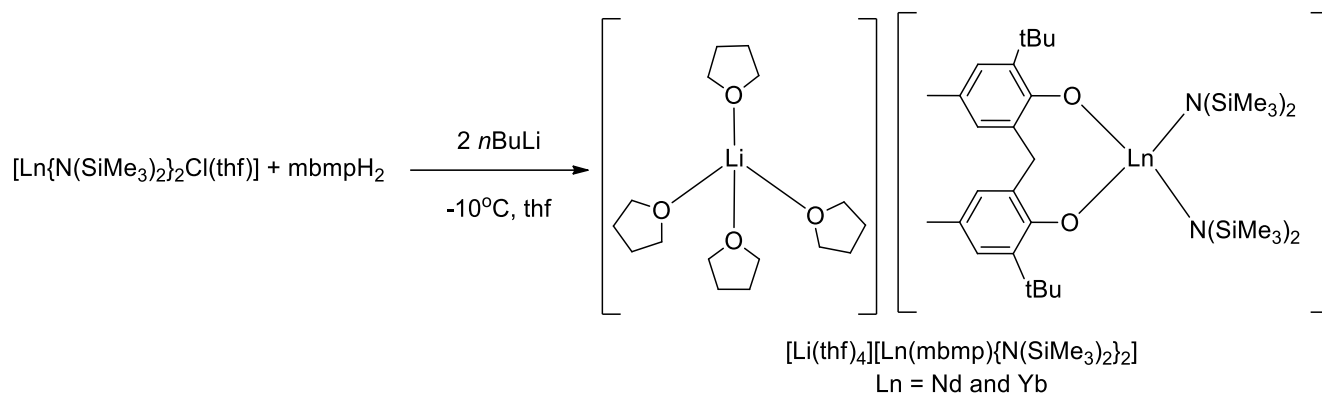
Similarly, the Shen group have also utilised lanthanoid borohydrides for the synthesis of biphenolate complexes by salt metathesis. Sodium lanthanoid ionic complexes have been synthesised by treatment of $[\text{Ln}(\text{BH}_4)_3(\text{thf})_3]$ (Ln = Er, Yb and Sm) with Na_2edbp in dme to

yield the ionic complexes $[\text{Na}(\text{dme})_3][\text{Ln}(\text{edbp})_2(\text{dme})]$ (Scheme 2.11).^[10] This synthetic approach avoids the solubility issues associated with lanthanoid halide starting materials.



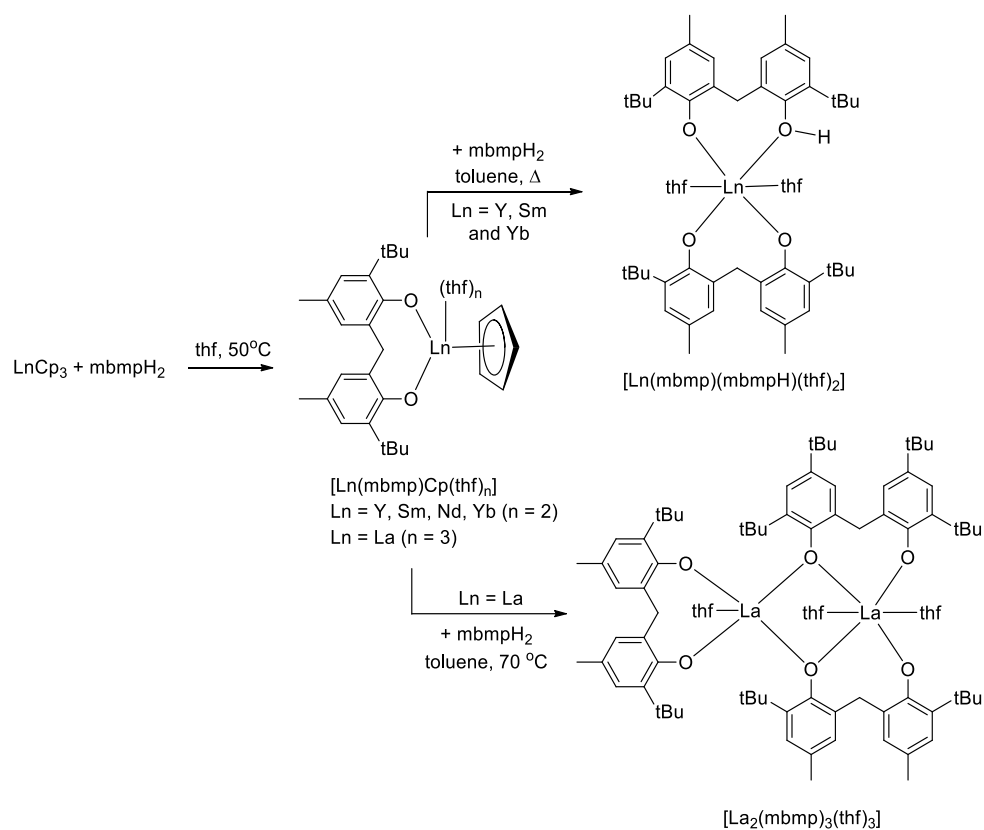
Scheme 2.11 - Synthesis of $[\text{Na}(\text{dme})_3][\text{Ln}(\text{edbp})_2(\text{dme})]$ (Ln = Er, Yb and Sm) from lanthanoid borohydride starting materials.^[10]

The Shen group also employed the use of lanthanoid amide halide starting materials to form heteroleptic ionic biphenolate amide complexes by salt metathesis. Treatment of $[\text{Ln}\{\text{N}(\text{SiMe}_3)_2\}_2\text{Cl}(\text{thf})]$ (Ln = Nd and Yb) with mbmpH_2 in the presence of two equivalents of *n*-butyllithium at $-10\text{ }^\circ\text{C}$ in thf yielded the ionic complexes $[\text{Li}(\text{thf})_4][\text{Ln}(\text{mbmp})\{\text{N}(\text{SiMe}_3)_2\}_2]$ (Scheme 2.12).^[11]



Scheme 2.12 – Synthesis of $[\text{Li}(\text{thf})_4][\text{Ln}(\text{mbmp})\{\text{N}(\text{SiMe}_3)_2\}_2]$ by metathesis from heteroleptic lanthanoid amide halide starting material.^[11]

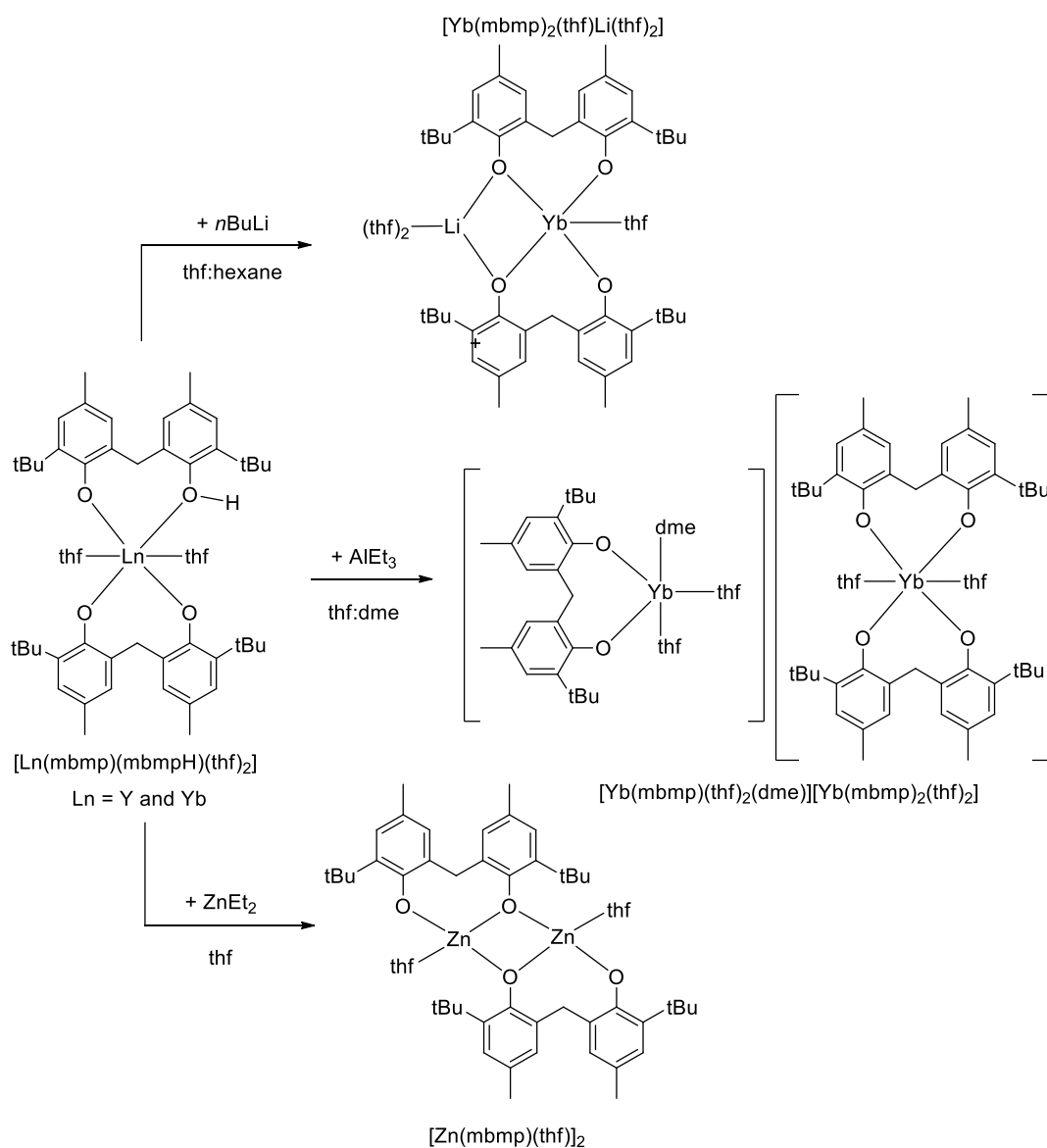
The use of protolysis/ligand exchange reactions reduces (and can even eliminate) the probability of halide or alkali metal ion inclusion, and until recently, has been the only means of synthesising halide/alkali-free trivalent lanthanoid biphenolate complexes. The simplest lanthanoid biphenolate complexes have been synthesised by protolysis reactions of lanthanoid Cp reagents with mbmpH_2 in a stepwise manner (Scheme 2.13).^[12,13]



Scheme 2.13 – Synthesis of heteroleptic $[\text{Ln}(\text{mbmp})\text{Cp}(\text{thf})_n]$ where $\text{Ln} = \text{Y, Sm, Nd}$ ($n = 2$) and La ($n = 3$), and subsequent treatment with mbmpH_2 to yield either $[\text{Ln}(\text{mbmp})(\text{mbmpH})(\text{thf})_2]$ ($\text{Ln} = \text{Y, Sm}$ and Yb) or $[\text{La}_2(\text{mbmp})_3(\text{thf})_3]$.^[12,13]

Treatment of the lanthanoid tris(cyclopentadienyl) complex with one equivalent of mbmpH_2 in thf at 50°C yielded the heteroleptic $[\text{Ln}(\text{mbmp})\text{Cp}(\text{thf})_n]$ complexes of yttrium, lanthanum, neodymium, samarium, and ytterbium. Further treatment with another equivalent of mbmpH_2 led to either the partially protonated biphenoate complexes $[\text{Ln}(\text{mbmp})(\text{mbmpH})(\text{thf})_2]$ of yttrium, samarium, and ytterbium, or alternatively, the dinuclear lanthanum complex $[\text{La}_2(\text{mbmp})_3(\text{thf})_3]$.^[12] The partially protonated yttrium and ytterbium complexes are of particular interest owing to the protonated phenolic portion of the ligand, which can potentially undergo further protolysis reactions with basic organometallic reagents.

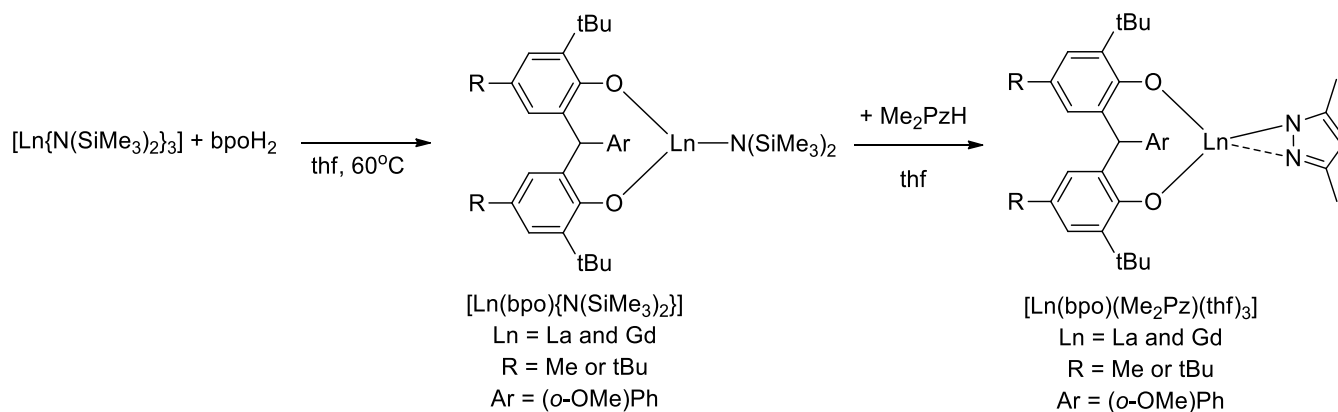
The Shen group explored this reactivity by treatment of the $[\text{Ln}(\text{mbmp})(\text{mbmpH})(\text{thf})_2]$ ($\text{Ln} = \text{Y}$ and Yb) species with basic organometallic reagents, to form heterobimetallic complexes, however with limited success. Treatment of $[\text{Yb}(\text{mbmp})(\text{mbmpH})(\text{thf})_2]$ with one equivalent of AlEt_3 yielded the redistribution product as a discrete ion pair $[\text{Yb}(\text{mbmp})(\text{thf})_2(\text{dme})][\text{Yb}(\text{mbmp})_2(\text{thf})_2]$ (Scheme 2.14).^[12] Comparatively, treatment of the same Yb complex with $n\text{BuLi}$ yielded the lithium ytterbium heterobimetallic complex $[\text{Yb}(\text{mbmp})_2(\text{thf})\text{Li}(\text{thf})_2]$ (Scheme 2.14).^[12] Treatment of the partially protonated Y and Yb complexes with ZnEt_2 both yielded the redistribution product $[\text{Zn}(\text{mbmp})(\text{thf})]_2$ (Scheme 2.14).^[12]



Scheme 2.14 – Further reactivity of $[Ln(mbmp)(mbmpH)(thf)_2]$ ($Ln = Y$ and Yb) complexes towards $nBuLi$, $AlEt_3$ and $ZnEt_2$.^[12]

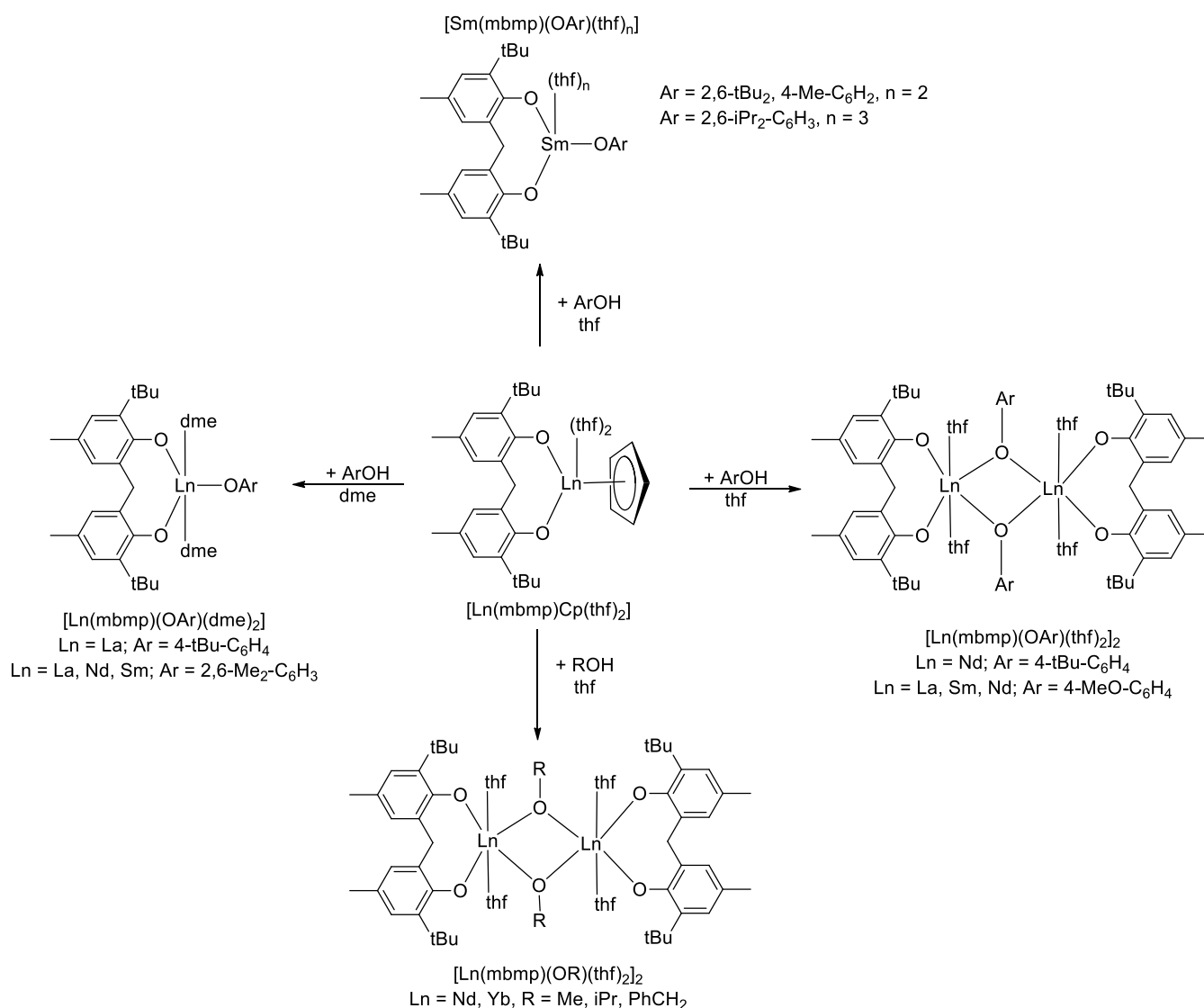
This stepwise protolysis (as per Scheme 2.13) of lanthanoid reagents allows for the facile synthesis of diverse heteroleptic complexes. The Shen group has utilised a similar approach to that described in Scheme 2.13, using the lanthanoid silylamide starting materials $[Ln\{N(SiMe_3)_2\}_3]$ ($Ln = La$ and Gd) alongside the bulkier biphenol pro-ligands 6,6'-((2-methoxyphenyl)methylene)bis(2-(*tert*-butyl)-4-methylphenol) ($mbmpaH_2$) and 6,6'-((2-methoxyphenyl)methylene)bis(2,4-di-*tert*-butylphenol) ($mbbpaH_2$). Treatment of

$[\text{Ln}\{\text{N}(\text{SiMe}_3)_2\}_3]$ with one equivalent of a biphenol (bpoH_2) at $60\text{ }^\circ\text{C}$ led to formation of $[\text{Ln}(\text{bpo})\{\text{N}(\text{SiMe}_3)_2\}]$, which could undergo further protolysis with 3,5-dimethylpyrazole, yielding $[\text{Ln}(\text{bpo})(\text{Me}_2\text{Pz})(\text{thf})_3]$ (Scheme 2.15).^[14]



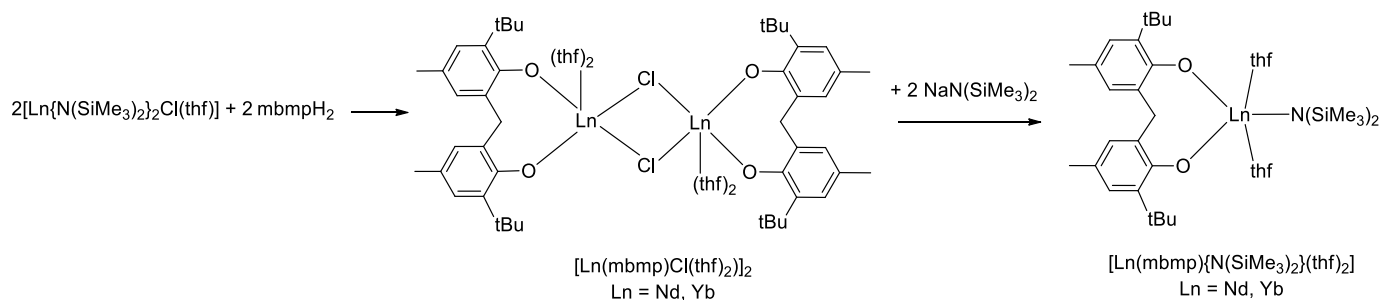
Scheme 2.15 – Stepwise protolysis of lanthanoid silylamide starting materials with bulky biphenols (mbmpaH_2 and mbbpaH_2) yielding heteroleptic $[\text{Ln}(\text{bpo})\{\text{N}(\text{SiMe}_3)_2\}]$ complexes, and subsequent protolysis with 3,5-dimethylpyrazole yielding $[\text{Ln}(\text{bpo})(\text{Me}_2\text{Pz})(\text{thf})_3]$.^[14]

In a similar fashion, a variety of phenols and alcohols of varying steric bulk were used to synthesise heteroleptic alkoxide and aryloxide biphenolate complexes from $[\text{Ln}(\text{mbmp})\text{Cp}(\text{thf})_2]$ ($\text{Ln} = \text{La, Sm, Nd and Yb}$) starting materials, yielding a range of mono- and di-nuclear complexes (Scheme 2.16).^[15,16]



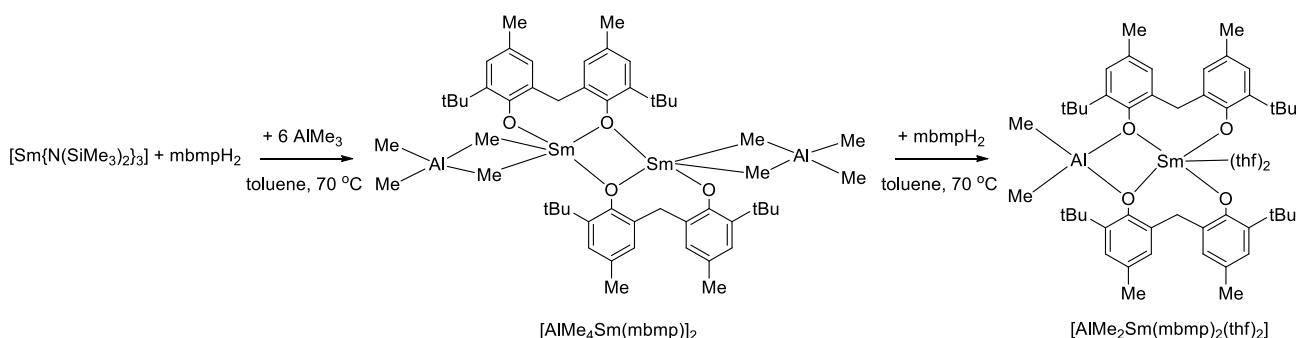
Scheme 2.16 – Reactions of alcohols and phenols with $[\text{Ln}(\text{mbmp})\text{Cp}(\text{thf})_2]$ yielding both mono- and di-nuclear complexes.^[15,16]

Just as heteroleptic lanthanoid silylamide halide starting materials have been used in metathesis reactions (Scheme 2.12) these reagents can also be utilised directly for protolysis reactions owing to the basic silylamide ligand. The heteroleptic $[\text{Ln}\{\text{N}(\text{SiMe}_3)_2\}_2\text{Cl}(\text{thf})]$ (where $\text{Ln} = \text{Nd}$, and Yb) can be treated with one equivalent of mbmpH_2 to yield $[\text{Ln}(\text{mbmp})\text{Cl}(\text{thf})_2]_2$ (Scheme 2.17).^[17] The bridging chloride between the two Ln atoms allowed for subsequent metathesis reactions to be performed with $\text{NaN}(\text{SiMe}_3)_2$, to yield $[\text{Ln}(\text{mbmp})\{\text{N}(\text{SiMe}_3)_2\}(\text{thf})_2]$ (Scheme 2.17).^[17]



Scheme 2.17 – Protolysis reaction of lanthanoid amide halides followed by subsequent metathesis to yield heteroleptic $[\text{Ln}(\text{mbmp})\{\text{N}(\text{SiMe}_3)_2\}(\text{thf})_2]$ ($\text{Ln} = \text{Nd}$ and Yb) complexes.^[17]

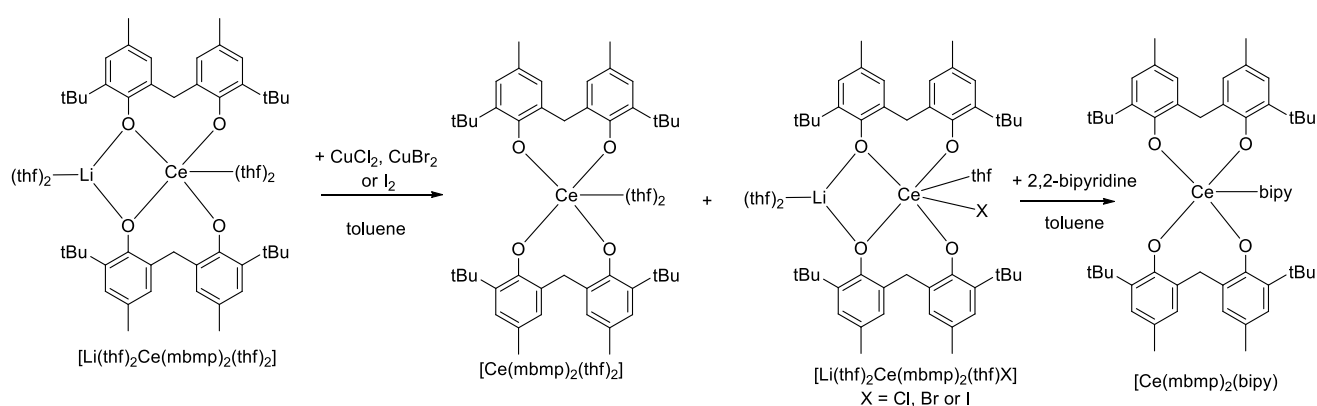
In contrast, the homoleptic $[\text{Sm}\{\text{N}(\text{SiMe}_3)_2\}_3]$ starting material has been used to synthesise the unsolvated samarium aluminium biphenolate complex $[\text{AlMe}_4\text{Sm}(\text{mbmp})]_2$, by treatment with AlMe_3 and mbmpH_2 in toluene at 70°C (Scheme 2.18).^[4]



Scheme 2.18 – Synthesis of dinuclear samarium aluminium biphenolate $[\text{AlMe}_4\text{Sm}(\text{mbmp})]_2$ and subsequent protolysis yielding $[\text{AlMe}_2\text{Sm}(\text{mbmp})_2(\text{thf})_2]$.^[4]

2.1.3 Synthesis of tetravalent lanthanoid biphenolate complexes

Reports of tetravalent lanthanoid biphenolates are quite limited in the literature, with only a few examples reported. The Schelter group has synthesised cerium(IV) complexes, firstly by salt metathesis with $[\text{Ce}(\text{OTf})_3]$ and Li_2mbmp , yielding the previously discussed $[\text{Li}(\text{thf})_2\text{Ce}(\text{mbmp})_2(\text{thf})_2]$, and then further oxidising this complex with copper halide reagents (CuCl_2 , or CuBr_2), or elemental iodine, resulting in a mixture of the mononuclear $[\text{Ce}(\text{mbmp})_2(\text{thf})_2]$ and the heterobimetallic $[\text{Li}(\text{thf})_n\text{Ce}(\text{mbmp})_2(\text{thf})\text{X}]$ ($\text{X} = \text{Cl}, \text{Br}$ or I , depending on the oxidant used) (Scheme 2.19).^[9] Treatment of this mixture with 2,2'-bipyridine (bipy) led to isolation of the standalone complex $[\text{Ce}(\text{mbmp})_2(\text{bipy})]$ in good yields (Scheme 2.19).^[9]

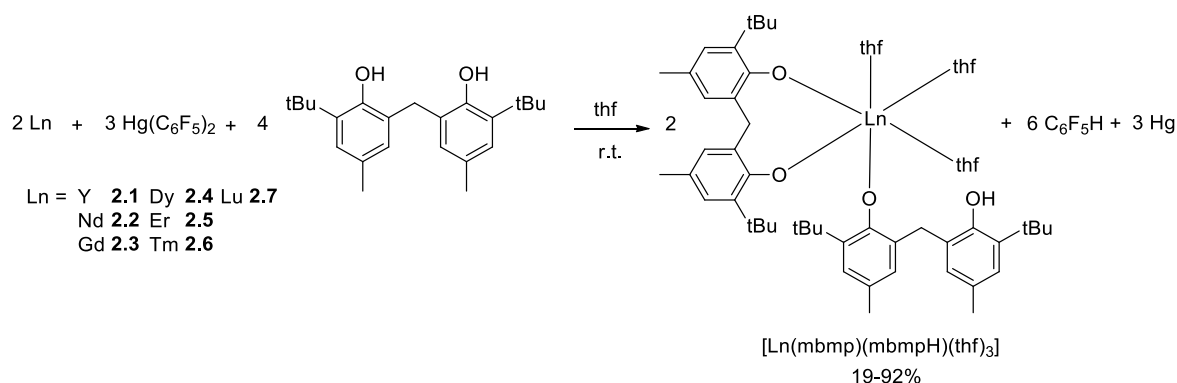


Scheme 2.19 – Synthesis of tetravalent cerium complexes by oxidation of trivalent cerium species.^[9]

2.2 Results and discussion

2.2.1 Synthesis of lanthanoid biphenolate complexes by RTP

The RTP reaction has been used extensively in the synthesis of lanthanoid aryloxide complexes,^[1] however, it has not seen widespread adoption in the synthesis of lanthanoid biphenolate complexes, with only a few examples synthesised.^[18] As discussed in Chapter 1, the RTP reaction involves treatment of a free metal with bis(pentafluorophenyl)mercury ($\text{Hg}(\text{C}_6\text{F}_5)_2$) and a protic pro-ligand (2,2'-methylenebis(6-*tert*-butyl-4-methylphenol) (mbmpH_2)) in an appropriate solvent. In all cases, the mbmpH_2 : metal : $\text{Hg}(\text{C}_6\text{F}_5)_2$ mole ratio utilised was 4 : 3 (excess) : 3 (Scheme 2.20). The resulting $[\text{Ln}(\text{mbmp})(\text{mbmpH})(\text{thf})_3]$ complex possesses one completely deprotonated, bidentate mbmp^{2-} ligand, one partially protonated, monodentate mbmpH^- ligand, and three coordinated thf molecules.



Scheme 2.20 - RTP reaction of lanthanoid metals with $\text{Hg}(\text{C}_6\text{F}_5)_2$ and mbmpH_2 .

All reactions were carried out in thf at room temperature and included a drop of Hg metal to form a reactive lanthanoid-mercury amalgam, thereby activating the lanthanoid metal. Reaction progress was monitored by ^{19}F NMR spectroscopy until $\text{Hg}(\text{C}_6\text{F}_5)_2$ was totally consumed, and only $\text{C}_6\text{F}_5\text{H}$ was detected. The reaction mixtures were then allowed to stand so that excess Ln metal and produced mercury could settle, and the supernatant solution isolated

by filtration. The filtrate was then concentrated under reduced pressure, leading to isolation of complexes **2.1-2.7** (Scheme 2.20) as crystalline material. The yields range significantly from 19 – 92%, which are largely comparable to previous syntheses of similar complexes of the general form $[\text{Ln}(\text{mbmp})(\text{mbmpH})(\text{thf})_2]$ ($\text{Ln} = \text{Y}, \text{Yb}$ and Sm) from LnCp_3 precursors.^[12,13] Syntheses with all lanthanoid metals were attempted, however, La, Ce, Pr, and Ho produced low solubility products and were therefore not studied further. Synthesis by RTP offers a distinct advantage over the protolysis reactions, in that the prior synthesis (or purchase) of LnCp_3 reagents is not required, and that the synthesis is not restricted to only Y, Yb and Sm.

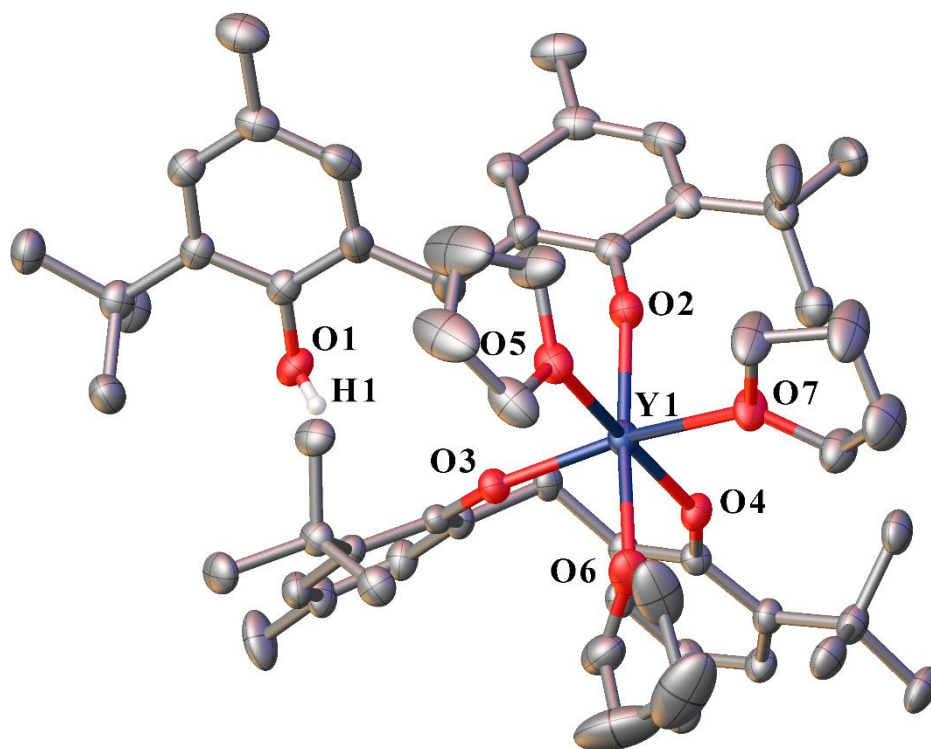


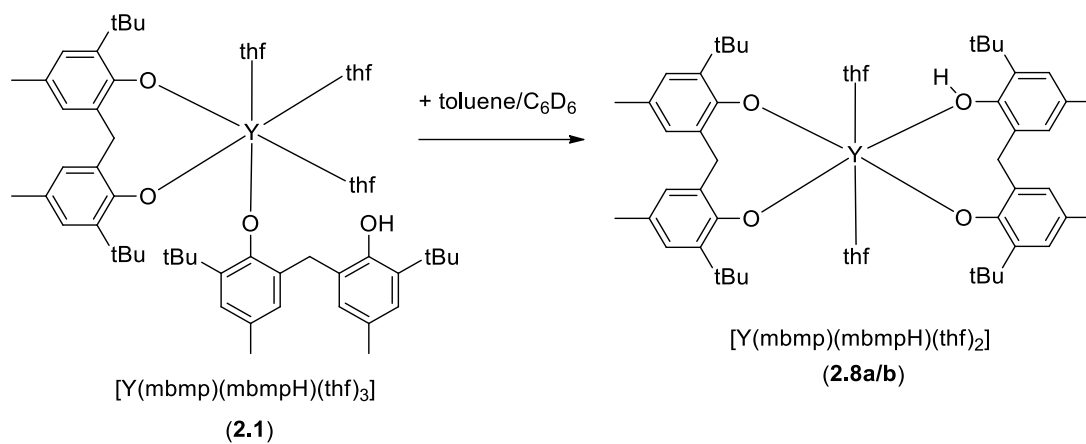
Figure 2.2 – ORTEP diagram of complex **2.1** (also representative of **2.2-2.7**) showing atom-numbering scheme for relevant atoms. Thermal ellipsoids are drawn at the 50% probability level. Hydrogen atoms (except the phenolic H) and lattice thf are omitted for clarity. Selected bond lengths are summarised in Table 2.1.

Complexes **2.1-2.7** crystallise in the monoclinic space group $P2_1/c$. When crystallised from thf, complexes **2.1-2.7** are isostructural, with the general form $[\text{Ln}(\text{mbmp})(\text{mbmpH})(\text{thf})_3] \cdot 3\text{thf}$ (Figure 2.2). Complexes **2.1-2.7** are composed of a six-coordinate, octahedral Ln centre, ligated by one bidentate mbmp^{2-} ligand (O3 and O4, in equatorial sites), one partially protonated, monodentate mbmpH^- ligand in an axial position (O2), and three facially coordinate thf molecules (O5, O6 and O7). The dianionic mbmp^{2-} ligand is bidentate, whilst the partially protonated mbmpH^- is monodentate, only coordinating through the phenolate's O⁻. The bond angles between the bound thf ligands of **2.1** are $\text{O}(5)\text{-Y}(1)\text{-O}(6) = 89.11(13)^\circ$, $\text{O}(5)\text{-Y}(1)\text{-O}(7) = 77.66(11)^\circ$, and $\text{O}(6)\text{-Y}(1)\text{-O}(7) = 77.81(12)^\circ$ and are representative of complexes **2.2-2.7** also. Whilst the crystal structure of **2.2** was obtained, it could only be used for connectivity.

The average bond lengths of complexes **2.1-2.7** have been summarised in Table 2.1. The average Ln-O_(phenolate) bond distances for each complex are in agreement with those reported for the previously synthesised $[\text{Ln}(\text{mbmp})(\text{mbmpH})(\text{thf})_2]$ (Ln = Y and Yb, where average Ln-O_(phenolate) = 2.101, and 2.140 Å respectively).^[12] The decrease in average Ln-O_(phenolate) bond length is in accordance with the decrease in ionic radii of the Ln³⁺ centre, owing to lanthanoid contraction, from six-coordinate Nd³⁺ (0.983 Å) to six-coordinate Lu³⁺ (0.861 Å).^[19]

The lanthanoid biphenolate complexes synthesised through RTP in thf differ distinctly from the Y, Sm and Yb complexes synthesised through protolysis in toluene, as the latter exhibit coordination of all three phenolate oxygens, alongside the protonated phenolic oxygen, and two molecules of thf.^[12,13] However, this coordination arrangement could be achieved by recrystallisation of **2.1** in non-coordinating solvents (e.g. toluene or C₆D₆) (Scheme 2.21), resulting in one coordinated molecule of thf being displaced by the protonated phenol upon heating, yielding $[\text{Y}(\text{mbmp})(\text{mbmpH})(\text{thf})_2] \cdot \text{solv}$ (solv = PhMe (**2.8a**) or 2C₆D₆ (**2.8b**)) (Figure

2.3), which are both isostructural with the reported yttrium complex synthesised through protolysis in toluene.^[12]



Scheme 2.21 – Coordination of phenolic OH by crystallising from a hot, non-coordinating solvent.

Table 2.1 - Selected bond lengths (Å) of [Ln(mbmp)(mbmpH)(thf)₃] (Ln = Y, Nd, Gd, Dy, Er, Tm, Lu) with average bond lengths italicised.

Bond Lengths (Å)	2.1 (Y)	2.2 (Nd)	2.3 (Gd)	2.4 (Dy)	2.5 (Er)	2.6 (Tm)	2.7 (Lu)
Ln(1)-O(2)	2.113(3)	2.205(10)	2.148(3)	2.130(3)	2.105(3)	2.094(4)	2.080(6)
Ln(1)-O(3)	2.127(3)	2.226(8)	2.164(3)	2.144(3)	2.116(3)	2.094(4)	2.101(5)
Ln(1)-O(4)	2.132(3)	2.214(9)	2.162(2)	2.144(3)	2.126(3)	2.103(4)	2.099(5)
<i><Ln(1)-O_(phenolate)>*</i>	<i>2.124(5)</i>	<i>2.215(16)</i>	<i>2.164(5)</i>	<i>2.139(5)</i>	<i>2.116(5)</i>	<i>2.097(7)</i>	<i>2.093(9)</i>
Ln(1)-O(5)	2.430(3)	2.545(8)	2.466(3)	2.457(3)	2.415(3)	2.396(5)	2.404(6)
Ln(1)-O(6)	2.402(4)	2.515(6)	2.448(3)	2.427(3)	2.399(4)	2.373(4)	2.371(6)
Ln(1)-O(7)	2.445(3)	2.543(8)	2.484(3)	2.462(3)	2.433(3)	2.406(4)	2.407(5)
<i><Ln(1)-O_(thf)>*</i>	<i>2.426(6)</i>	<i>2.534(13)</i>	<i>2.466(5)</i>	<i>2.449(5)</i>	<i>2.416(6)</i>	<i>2.392(8)</i>	<i>2.394(10)</i>

*Average e.s.d.'s are calculated using the expression $\sigma_{\text{avg}} = [\sum(l - \bar{l})^2 / (m - 1)]^{\frac{1}{2}}$ where m is the number of values averaged and $(l - \bar{l})^2$ is the difference between each value and the average.^[20]

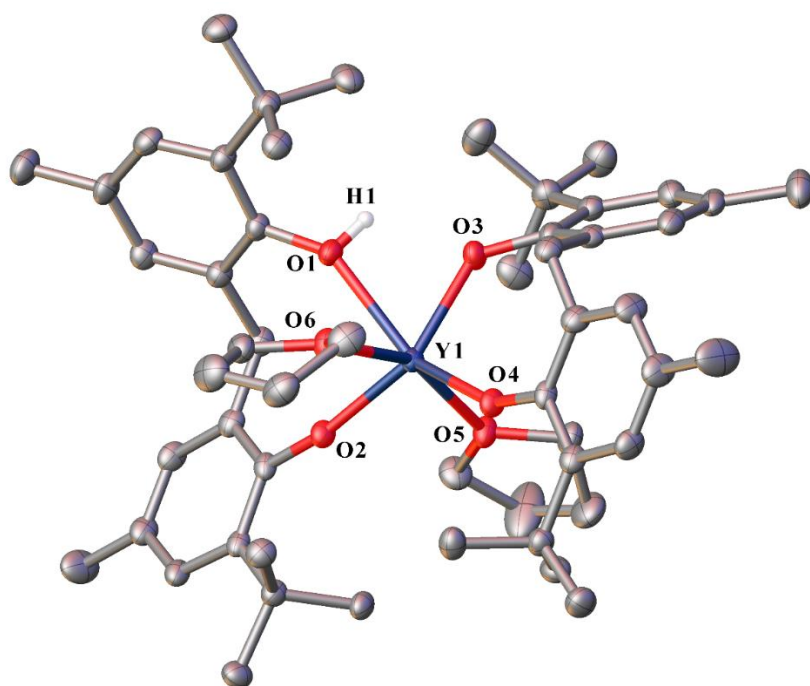


Figure 2.3 - ORTEP diagram of complex **2.8a** (also representative of **2.8b**) showing atom-numbering scheme for relevant atoms. Thermal ellipsoids are drawn at the 50% probability level. Hydrogen atoms (except the phenolic H) and lattice toluene are omitted for clarity.

Both complexes **2.8a** and **2.8b** are isostructural, varying only in their solvent of crystallisation (**2.8a** = toluene, **2.8b** = 2 C₆D₆). Complex **2.8a** crystallises in the triclinic space group *P*- with one molecule in the asymmetric unit, whilst complex **2.8b** crystallises in the monoclinic space group *C2/c* with half a molecule in the asymmetric unit. The latter displays disorder between the phenolic OH and the phenolate O⁻, as well as the lattice solvent. Both complexes possess a distorted octahedral yttrium atom, which is coordinated to one fully deprotonated mbmp²⁻ ligand, and one partially protonated mbmpH⁻ in the equatorial positions, alongside two coordinated thf molecules in the axial positions. (O(5)-Y(1)-O(6) = 155.35(7)° (**2.8a**), and 160.09(9)° (**2.8b**)). Both complexes exhibit coordination of the OH to the metal centre, which is consistent with the reported Y, Sm and Yb complexes previously reported.^[12,13] The metal to oxygen bond lengths of the protonated phenol (Y(1)-O(1) = 2.4106(18) Å (**2.8a**) and

2.389(10) Å (**2.9b**)) are similar to that of the metal to oxygen bond lengths for the coordinated thf molecules ($Y(1)-O_{(thf)}$ average = 2.3714(35) Å) and are considerably longer than the average metal to oxygen bond of the coordinated phenolates ($Y(1)-O_{(phenolate)}$ average = 2.152(45) Å) in the same complexes.

The IR spectra of complexes **2.1-2.7**, **2.8a** and **2.8b** are consistent with the X-ray crystal structures, exhibiting only a single, sharp OH stretching frequency at approximately 3510 cm^{-1} , attributed to the protonated phenol. Partial hydrolysis could sometimes be observed in the IR spectra, appearing as two discrete stretching bands at approximately 3600 cm^{-1} and 3390 cm^{-1} , corresponding to $\nu(OH)$ of the free mbmpH₂ ligand. In these cases, Nujol was not sufficient for the protection of the highly air and moisture sensitive complexes, allowing some hydrolysis to occur in the time it took to record the IR spectra.

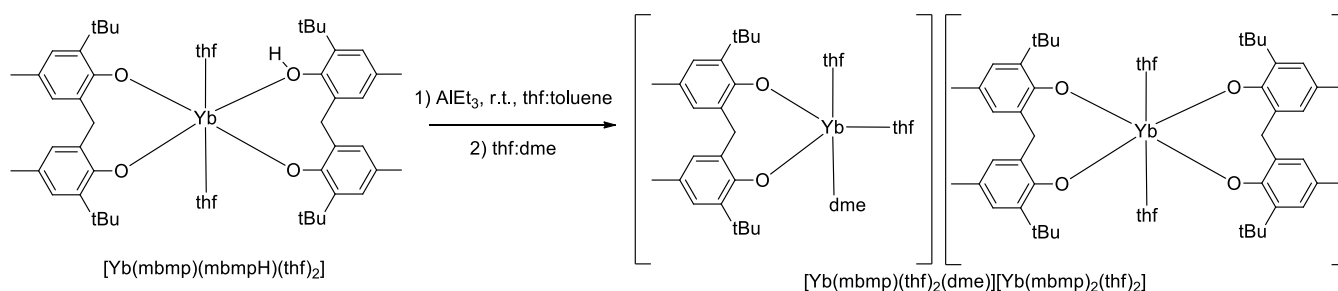
As many of the synthesised complexes are paramagnetic in nature, interpretable ¹H NMR spectra were only collected for complexes **2.1** and **2.7**. The paramagnetic complexes **2.2 – 2.6** either produced uninterpretable spectra with significant broadening or were unable to be recorded at all. The phenolic OH resonance was not observed in complex **2.1**, however in complex **2.7** a broad singlet was observed at 5.75 ppm. The ligand to thf ratios observed in the ¹H NMR spectra for both **2.1** and **2.7** agreed with the X-ray crystal structures obtained. As observed in the IR spectra, partial hydrolysis was also observed in the ¹H NMR spectra, exhibited by signals corresponding to small amounts of free ligand.

Satisfactory elemental analysis of each complex was obtained after drying under reduced pressure. Variable loss of lattice solvent, and in the case of **2.5**, coordinated solvent, was observed. Complexes **2.1**, **2.3**, and **2.8b** lost all lattice solvent, **2.2** lost one lattice thf, **2.5** lost all lattice, and two coordinated thf, and **2.4**, **2.6**, and **2.7** retained their lattice solvent. The

elemental analysis for most complexes was supported by complexometric titration to determine the metal percentage.

2.2.2 Further reactivity of lanthanoid biphenolates with trimethyl aluminium

As already outlined, the presence of a phenolic proton on complexes **2.1** – **2.7**, and **2.8a/b** allows for these complexes to undergo further protolysis with organometallic bases to form heterobimetallic species. Previous attempts to synthesise the ytterbium-aluminium heterobimetallic has been attempted with an ytterbium complex analogous to **2.8a/b**. Treatment of the Yb complex with triethylaluminium yielded the discrete ion pair complex $[\text{Yb}(\text{mbmp})(\text{thf})_2(\text{dme})][\text{Yb}(\text{mbmp})_2(\text{thf})_2]$ rather than the expected molecular heterobimetallic complex (Scheme 2.22).^[12] No aluminium containing species were isolated.

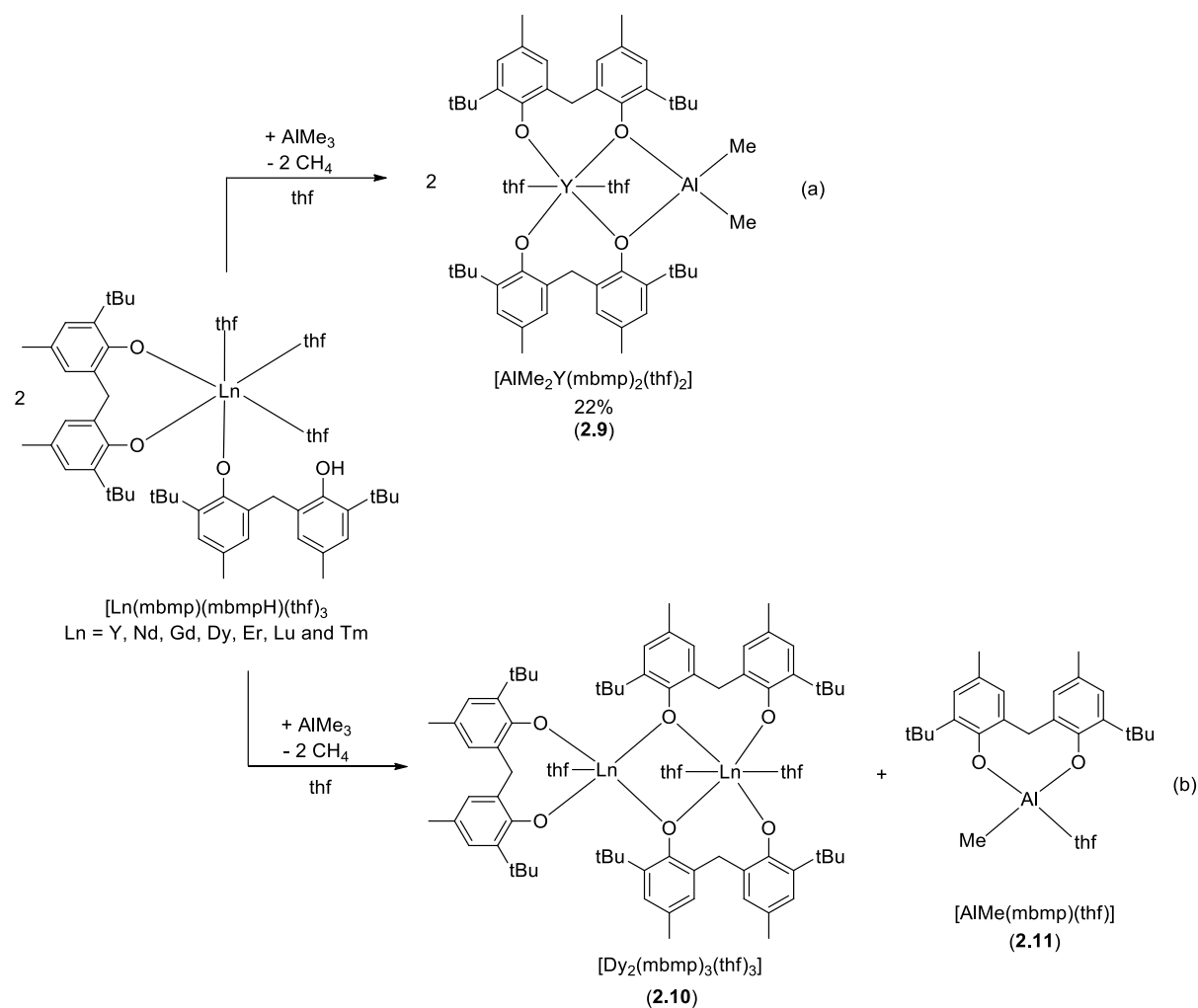


Scheme 2.22 – Attempted synthesis of an ytterbium-aluminium heterobimetallic by treatment of the partially protonated ytterbium biphenolate with triethylaluminium.

Whilst the one reported attempt of using protolysis to yield the aluminium-ytterbium complex was unsuccessful, it is possible that using a toluene-based solution, driving the formation of the coordinated phenol complex, alongside using AlEt_3 instead of the slightly less bulky AlMe_3 could have hindered the formation. To avoid this result when attempting the protolysis reactions with complexes **2.1-2.7**, the complexes were first dissolved in thf, and then one equivalent of trimethylaluminium in toluene was added at room temperature. Crystals were isolated from all reactions upon standing at $-18\text{ }^\circ\text{C}$ for several days. Initially, only two different

products were isolated from these reactions. When treating **2.1** with trimethylaluminium, the desired yttrium-aluminium heterobimetallic complex $[\text{AlMe}_2\text{Y}(\text{mbmp})_2(\text{thf})_2]$ (**2.9**) was isolated as a yellow solid (Scheme 2.23(a) and Figure 2.4), crystals suitable for X-ray diffraction studies were grown from a solution of C_6D_6 . Absence of a $\nu(\text{OH})$ band in the IR spectrum at approximately 3510 cm^{-1} confirmed that the protolysis was successful, alongside obtaining satisfactory microanalysis, supported by complexometric titration (with masking for aluminium).

When picking crystals for X-ray diffraction from the reaction of the dysprosium complex **2.4** with trimethylaluminium, two discrete sets of crystals were isolated from the concentrated solution: a dinuclear dysprosium complex $[\text{Dy}_2(\text{mbmp})_3(\text{thf})_3]$ (**2.10**) (Scheme 2.23(b) and Figure 2.5) and an aluminium biphenolate complex $[\text{AlMe}(\text{mbmp})(\text{thf})]$ (**2.11**) (Scheme 2.23(b) and Figure 2.6). This suggested that the AlMe_3 reagent instigated redistribution, yielding the two complexes. In all other cases, only the aluminium complex **2.11** was isolated, inferring that the same redistribution was occurring, however no analogues of **2.10** could be crystallised.



Scheme 2.23 - Reaction of lanthanoid biphenolate complexes with trimethyl aluminium to yield (a) an yttrium aluminium heterobimetallic species, or (b) the aluminium biphenolate complex **2.11** via redistribution (and **2.10** in the case of Dy).

A similar redistribution of $[\text{Ln}(\text{mbmp})(\text{mbmpH})(\text{thf})_2]$ ($\text{Ln} = \text{Y}$ and Yb) species has been reported when treated with diethylzinc, yielding the zinc biphenolate complex $[\text{Zn}(\text{mbmp})(\text{thf})_2]$.^[12]

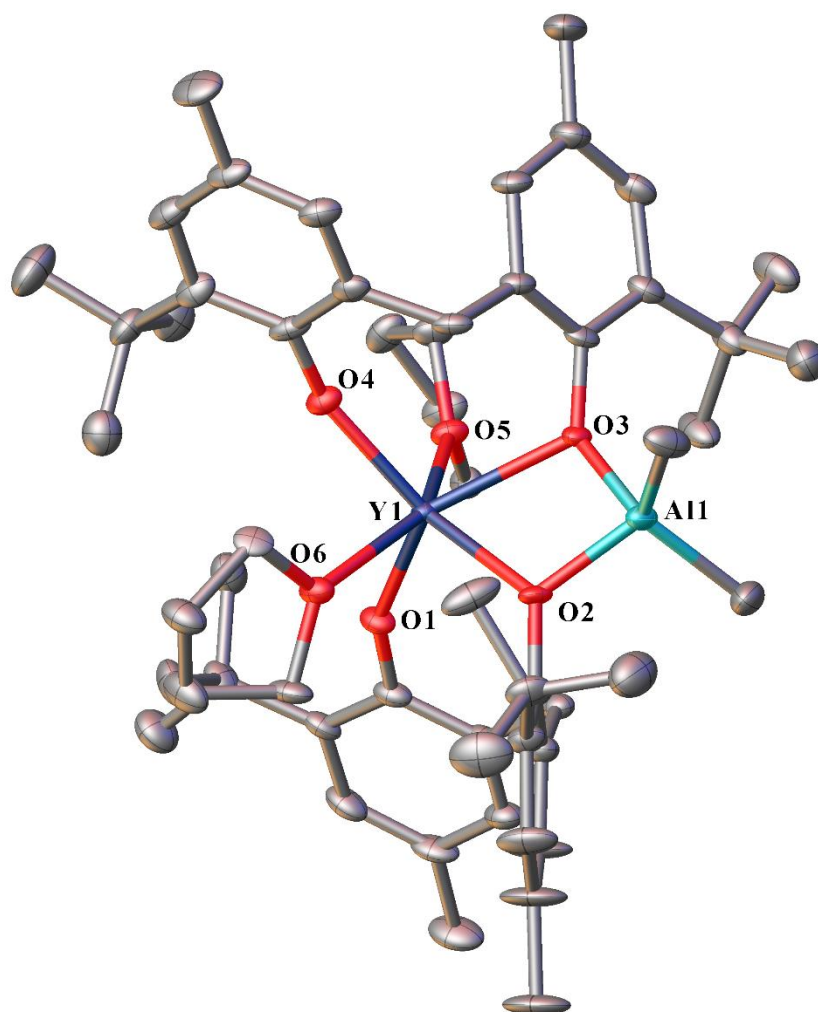


Figure 2.4 – ORTEP diagram of complex **2.9** showing atom-numbering scheme for relevant atoms. Thermal ellipsoids are drawn at the 50% probability level. Hydrogen atoms and lattice C_6D_6 are omitted for clarity. Selected bond lengths (Å): Y(1)-O(1) 2.093(3), Y(1)-O(2) 2.375(3), Y(1)-O(3) 2.388(3), Y(1)-O(4) 2.110(3), Y(1)-O(5) 2.399(4), Y(1)-O(6) 2.408(4), Al(1)-O(2) 1.834(4), Al(1)-O(3) 1.827(4).

Complex **2.9** crystallises in the monoclinic space group $P2_1/n$. It is composed of a six-coordinate, distorted octahedral yttrium atom, and a four-coordinate, distorted tetrahedral aluminium atom. The yttrium is coordinated to two deprotonated $mbmp^{2-}$ ligands in equatorial positions, and two thf molecules (O(5) and O(6)) in the axial sites ($O(5)-Y(1)-O(6) = 148.70(14)^\circ$). One oxygen on both $mbmp^{2-}$ ligands is bound solely to the yttrium (O(1) and

O(4)), whilst the other is bridging between the yttrium and aluminium (O(2) and O(3)). The aluminium atom is coordinated to two bridging mbmp²⁻ moieties, and two methyl groups. The bridging oxygens of the mbmp²⁻ ligands exhibit longer Y-O bond lengths than their non-bridging counterparts, as expected. Complex **2.9** is isostructural with a reported samarium-aluminium heterobimetallic biphenolate complex, with the same general formula.^[4] The bridging Sm-O bond lengths are 2.450 and 2.457 Å, whilst the bridging Al-O bond lengths are 1.836 and 1.839 Å, consistent with the bond lengths observed in **2.9**, after considering the decrease in ionic radius from Sm³⁺ to Y³⁺.^[19]

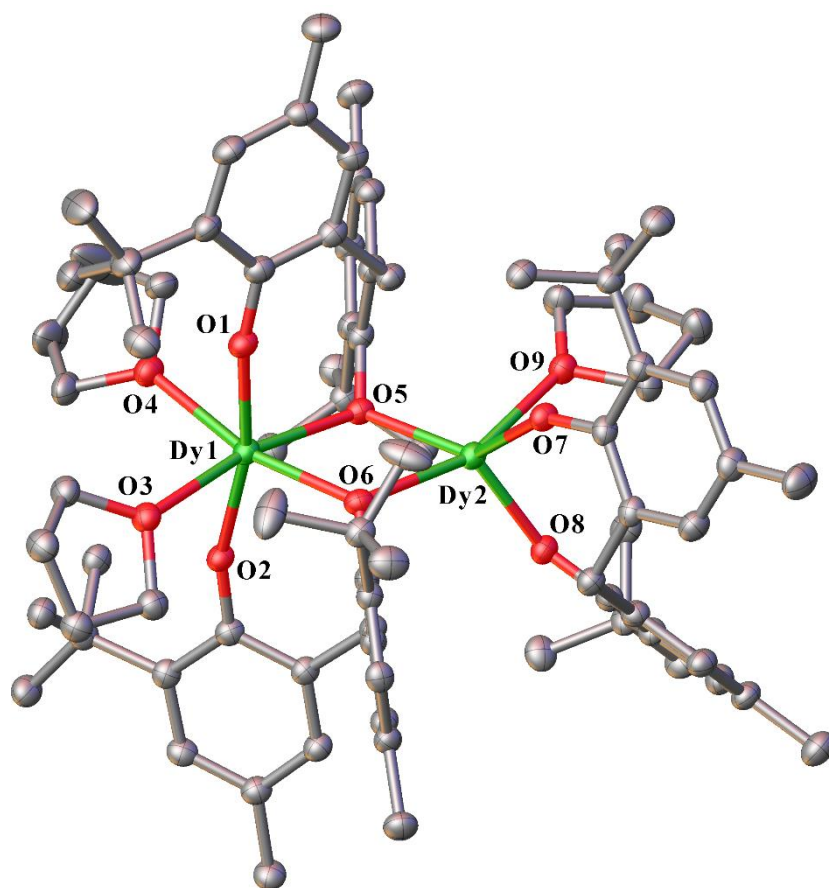


Figure 2.5 – ORTEP diagram of complex **2.10** showing atom-numbering scheme for relevant atoms. Thermal ellipsoids are drawn at the 30% probability level. Hydrogen atoms and lattice toluene are omitted for clarity. Selected bond lengths (Å): Dy(1)-O(1) 2.173(4), Dy(1)-O(2) 2.170(4), Dy(1)-O(3) 2.415(4), Dy(1)-O(4) 2.424(4), Dy(1)-O(5) 2.361(4), Dy(1)-O(6)

2.296(3), Dy(2)-O(5) 2.311(3), Dy(2)-O(6) 2.340(4), Dy(2)-O(7) 2.094(3), Dy(2)-O(8) 2.105(4), Dy(2)-O(9) 2.426 (4).

Complex **2.10** crystallises in the triclinic space group $P\bar{1}$ as an asymmetrical dinuclear dysprosium complex. It is analogous to the reported lanthanum complex $[\text{La}(\text{mbmp})_3(\text{thf})_3]$.^[12] One dysprosium atom (Dy(1)) is six-coordinate with a distorted octahedral geometry. There are two bidentate mbmp^{2-} ligands coordinated with one oxygen bound solely to Dy(1), whilst the other is bridging between the two dysprosium atoms, alongside two coordinated thf molecules. The other dysprosium atom (Dy(2)) is five-coordinate, with a distorted square pyramidal geometry, and is coordinated by the two bridging mbmp^{2-} oxygens, a third, terminal mbmp^{2-} , and one molecule of thf. The bridging oxygens of the mbmp^{2-} ligands display significantly longer Dy-O bond lengths than their non-bridging counterparts, and the bond lengths of Dy(1)-O(1) and Dy(1)-O(2) are significantly longer than Dy(2)-O(7) and Dy(2)-O(8) consistent with the difference in coordination number of the two Dy atoms. However, the Dy-O_(thf) bond lengths are largely unaffected. Complex **2.10** may be viewed as a precursor of a charge separated species, namely $[\text{Dy}(\text{mbmp})(\text{thf})_4][\text{Dy}(\text{mbmp})_2(\text{thf})_2]$, analogous to that of the reported ytterbium complex $[\text{Yb}(\text{mbmp})(\text{thf})_2(\text{dme})][\text{Yb}(\text{mbmp})_2(\text{thf})_2]$.^[12]

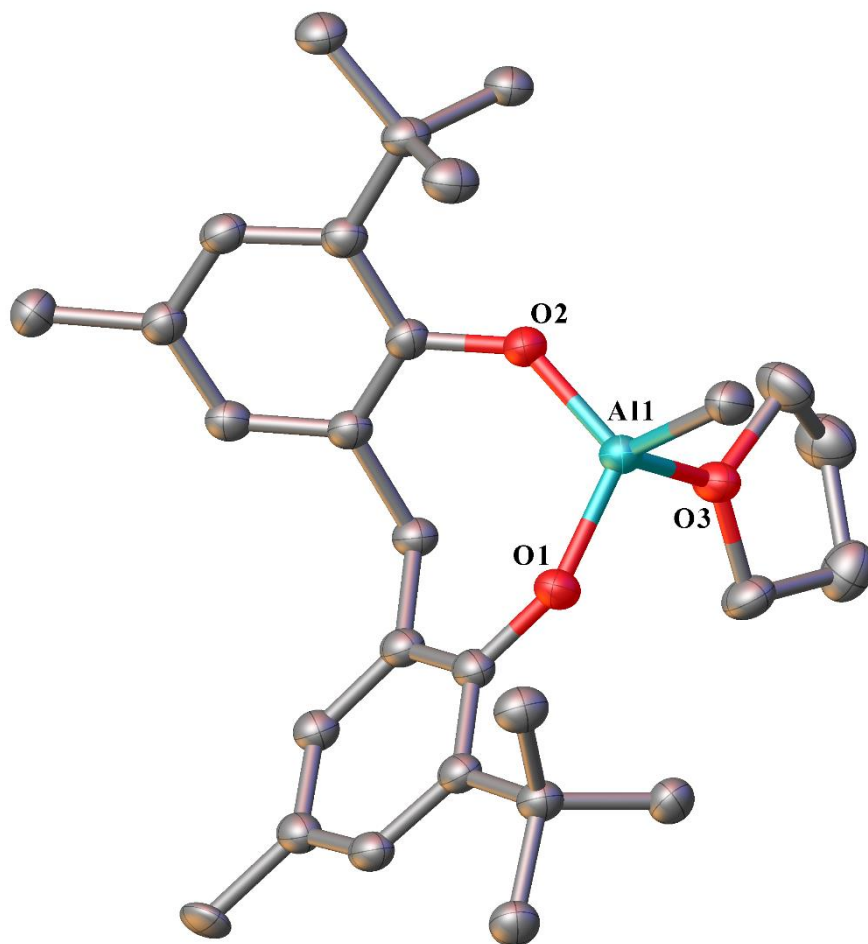
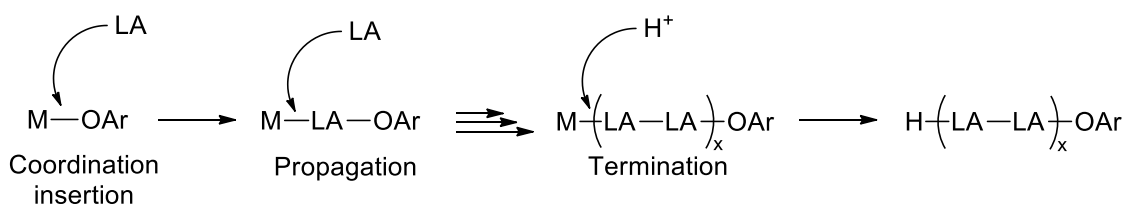


Figure 2.6 - ORTEP diagram of complex **2.11** showing atom-numbering scheme for relevant atoms. Thermal ellipsoids are drawn at the 40% probability level. Hydrogen atoms and lattice toluene are omitted for clarity. Selected bond lengths (Å): Al(1)-O(1) 1.7118(14), Al(1)-O(2) 1.7253(16), Al(1)-O(3) 1.8851(15).

Crystals of complex **2.11** were isolated from reactions of **2.2-2.7** with trimethylaluminium, as well as synthesised directly from trimethylaluminium and mbmpH₂ in thf. Complex **2.11** crystallises in the monoclinic space group *C2/c*. It is composed of an aluminium atom in a tetrahedral geometry, coordinated to one fully deprotonated mbmp²⁻ ligand, one methyl group, and one molecule of thf. The X-ray and ¹H NMR data agreed with reports of the analogous diethyl ether complex.^[21]

2.2.3 Ring opening polymerisation reactions of *rac*-lactide

Many rare earth alkoxide and aryloxy complexes have exhibited initiation capabilities for the ring opening polymerisation (ROP) of cyclic esters, usually initiating polymerisation at room temperature and going to completion within minutes.^[22–25] The Lewis acidic lanthanoid metal centre readily instigates polymerisation by a coordination-insertion chain growth mechanism (Scheme 2.24).^[23,26–30]



Scheme 2.24 – Polymerisation of LA (*rac*-lactide) by a coordination insertion mechanism in the presence of a simplified lanthanoid aryloxy complex.

The bulky, mononuclear biphenolate complexes of Dy, Nd, and Lu (**2.2**, **2.4** and **2.7**), as well as a mixture of the dinuclear dysprosium and aluminium biphenolate complexes (**2.10** and **2.11**), and the standalone aluminium biphenolate (**2.11**) were assessed for the ROP initiation of *rac*-lactide. All lanthanoid complexes were found to be active for the ROP at 70 °C in toluene, but displayed slow reaction rates, poor yields, and high PDIs, while the standalone aluminium complex (**2.11**) was inactive (Table 2.2).

Table 2.2 - Polymerisation of *rac*-lactide initiated by biphenolate complexes^a.

Entry	Initiator	[M] ₀ :[I]	Time (h)	Yield (%)	M _n (g.mol ⁻¹) ^b	PDI ^b
1	2.2 (Y)	100	10	75	3653	6.99
2	2.4 (Dy)	100	10	63	2829	3.49
3	2.4 (Dy)	100	20	84	4283	6.62
4	2.7 (Lu)	100	10	30	2644	2.62
5	2.10 (Dy₂) + 2.11 (Al)	100	10	29	5682	2.52
6	2.11 (Al)	100	10	0	-	-

^a Conditions [M]₀ = 0.7 M, solvent: toluene; 70 °C.

^b Measured by GPC against polystyrene standards.

Complex **2.2** was initially trialled with a 10-hour duration, showing conversion of 75% of monomer to polymer. A similar result was achieved with complex **2.4** (63% conversion). Upon extending the reaction duration with complex **2.4** to 20 hours, an increase in conversion was observed (84% conversion), alongside a significant increase in PDI, which can be ascribed to transesterification, resulting in lengthened, shortened, or cyclised polymer chains.^[31] Most notably, the efficacy of the complexes varied significantly with a change in metal centre, considerably decreasing with a decrease in ionic radius from the larger Nd and Dy complexes (**2.2** and **2.4**) to the smaller Lu complex (**2.7**). This was demonstrated by the decreased yields, and number average molecular weight (M_n) decreasing with a decrease in radius. In contrast to these negative implications, the PDI also decreased with a decrease in ionic radius, suggesting a more controlled polymerisation was occurring.

As **2.10** and **2.11** could not be easily separated, the mixture was assessed for its ROP initiation capabilities. When compared to the mononuclear dysprosium **2.4**, the mixture showed very low activity, likely owing to the reduced accessibility to the dysprosium active sites. In contrast, there was a significant increase in M_n . Complex **2.11** alone showed no activity whatsoever, suggesting that the activity of the mixture was solely dependent on **2.10**. **2.11**'s lack of activity could be attributed to the crowding about the Al^{3+} centre, which has a significantly smaller ionic radius than that of the Ln^{3+} ions. This agrees with reports of altering steric bulk in the *ortho* positions of monodentate phenolate ligands, with an increase in bulk reducing the performance, owing to hindered access to the metal centre.^[29,32] This results in reduced PDIs and M_n values.

Despite complexes **2.2**, **2.4**, **2.7**, and **2.10** displaying ROP activity, these high steric bulk biphenolate complexes show considerably reduced efficacy than their lower steric bulk, monodentate rare earth aryloxide counterparts, requiring significantly longer reaction durations, and exhibiting lower yields and number average molecular weights, alongside higher polydispersity indices.

2.3 Conclusion

The redox transmetallation/protolysis reaction with bis(pentafluorophenyl)mercury has been used to synthesise a range of new heteroleptic, rare earth biphenolate complexes from the free rare earth metal, and the ligand 2,2'-methylenebis(6-*tert*-butyl-4-methylphenol) (mbmpH₂), yielding biphenolate complexes of the general form [Ln(mbmp)(mbmpH)(thf)₃]. These complexes had their further reactivity towards trimethylaluminium trialled in attempts to form lanthanoid-aluminium heterobimetallic species, as well as their initiation efficacy assessed for the ring opening polymerisation of *rac*-lactide. Complexes **2.1-2.7** are isostructural, and consist of a distorted octahedral core, with one chelating mbmp²⁻ ligand, and one partially protonated mbmpH⁻ ligand, bound only through the phenolate oxygen, and three *fac* thf molecules. In the case of **2.1**, this complex could be recrystallised from non-coordinating solvents (such as toluene or C₆D₆) to force the coordination of the protonated phenol, yielding [Y(mbmp)(mbmpH)(thf)₂] \cdot solv (solv = PhMe, (**2.8a**) or 2 C₆D₆, (**2.8b**)). Treatment of complex **2.1** with trimethylaluminium, led to the formation of the yttrium-aluminium heterobimetallic [AlMe₂Y(mbmp)₂(thf)₂] (**2.9**). Complexes **2.2-2.7** with trimethylaluminium yielded the redistribution product [AlMe(mbmp)(thf)] (**2.11**). In the case of the dysprosium complex (**2.4**), a dinuclear dysprosium complex [Dy₂(mbmp)₃(thf)₃] (**2.10**) was also isolated, alongside the aluminium complex **2.11**, suggesting that trimethylaluminium instigates the redistribution reaction. A sample of the monometallic biphenolate complexes (**2.2**, **2.4**, and **2.7**) as well as a mixture of the dinuclear dysprosium and aluminium complexes (**2.10** and **2.11**), and the standalone aluminium complex (**2.11**) were assessed for their initiation capabilities for the ring opening polymerisation of *rac*-lactide in toluene at 70 °C. All lanthanoid complexes were found to be active, however, they were found to be poor initiators compared to rare earth complexes of monodentate aryloxides. Their efficacy, however, was observed to increase with an increase in the ionic radius of the metal centre used. The use of the RTP reaction with Hg(C₆F₅)₂ has

facilitated an expansion of the library of lanthanoid biphenolate complexes with mbmp²⁻ and mbmpH⁻ ligands, which has opened the door for the synthesis of many more heterobimetallic complexes by treatment with organometallic bases. Further diversification of the heterobimetallic species known, alongside assessment of the catalytic activity of these mixed metallic systems is a potential route for future work within the growing area of lanthanoid biphenolate chemistry.

2.4 Experimental

For materials and general procedures, see Appendix One.

2.4.1 Syntheses

[Y(mbmp)(mbmpH)(thf)₃]**·3thf (2.1)**

A Schlenk flask equipped with a magnetic stirrer bar was charged with mbmpH₂ (1.36g; 4.00 mmol), Hg(C₆F₅)₂ (1.60 g; 3.00 mmol), one drop of Hg metal (to form a reactive lanthanoid-mercury amalgam) and excess yttrium filings (0.27 g; 3.0 mmol). Anhydrous thf (~20 mL) was added by cannula, and the reaction mixture stirred at room temperature for 3 days. Excess yttrium metal and mercury were allowed to settle before isolating the supernatant liquid by a filtration cannula. The resulting filtrate was concentrated under reduced pressure to ~10 mL and allowed to stand at room temperature to crystallise, yielding small, pale brown crystals (1.80 g, 92%). *Anal.* Calc. for C₅₈H₈₅O₇Y (983.19g.mol⁻¹ after loss of three lattice thf): C, 70.85; H, 8.71; Y, 9.04. Found: C, 70.43; H, 8.20; Y, 8.76%. ¹H-NMR (400 MHz, C₆D₆, 25 °C): δ 7.40 (d, 4H, ArH), 7.16 (d, 4H, ArH), 3.73 (s, 4H, CH₂), 3.57 (m, 24H, thf), 2.28 (s, 12H, ArCH₃), 1.57 (s, 36H, C(CH₃)₃), 1.31 (s, 24H, thf). IR (Nujol, cm⁻¹): 3501 s, 1960 w, 1887 w, 1740 s, 1568 s, 1254 w, 1070 m, 1012 m, 914 s, 861 m, 792 w, 726 m, 669 s.

[Nd(mbmp)(mbmpH)(thf)₃]**·3thf (2.2)**

The synthesis of complex **2.2** was carried out in the same way as that described for complex **2.1**, but neodymium filings (0.43 g; 3.0 mmol) were used in place of yttrium. Blue-green crystals were obtained from ~10 mL of thf at 4 °C (1.20 g, 51%). *Anal.* Calc. for C₆₆H₁₀₁O₉Nd (1182.74g.mol⁻¹ after loss of one lattice thf): C, 67.02; H, 8.61; Nd, 12.20. Found: C, 66.05; H, 8.43; Nd, 12.08%. IR (Nujol, cm⁻¹): 3509 s, 1966 w, 1742 m, 1603 s, 1562 w, 1532 w, 1459 m, 1378 m, 1161 m, 1069 m, 1023 m, 862 m, 818 m, 794 m, 752 w, 723 w, 668 m.

[Gd(mbmp)(mbmpH)(thf)₃] \cdot 3thf (2.3)

The synthesis of complex **2.3** was carried out in the same way as that described for complex **2.1**, but gadolinium powder (0.48 g; 3.0 mmol) was used in place of yttrium. Brown crystals were obtained from ~10 mL of thf at -18 °C (0.40g, 19%). *Anal.* Calc. for C₅₈H₈₅O₇Gd (1051.54 g.mol⁻¹ after loss of three lattice thf): C, 66.25; H, 8.15; Gd, 14.95. Found: C, 65.87; H, 7.95; Gd, 14.80%. IR (Nujol, cm⁻¹): 3505 s, 1744 m, 1712 w, 1645 s, 1604 m, 1533 w, 1509 m, 1456 m, 1378 m, 1262 m, 1179 m, 1072 m, 955 m, 941 m, 913 m, 862 m, 820 m, 718 m, 672 m.

[Dy(mbmp)(mbmpH)(thf)₃] \cdot 3thf (2.4)

The synthesis of complex **2.4** was carried out in the same way as that described for complex **2.1**, but dysprosium powder (0.49 g, 3 mmol) was used in place of yttrium. Dark yellow crystals were obtained from ~10 mL of thf at 4 °C (1.87 g, 70%). *Anal.* Calc. for C₇₀H₁₀₉O₁₀Dy (1273.10g.mol⁻¹): C, 66.04; H, 8.63; Dy, 12.76. Found: C, 66.07; H, 8.92%. IR (Nujol, cm⁻¹): 3508 s, 1741 m, 1604 s, 1560 w, 1533 w, 1463 m, 1378 m, 1263 m, 1212 m, 1161 m, 1070 m, 1019 m, 956 w, 913 m, 863 m, 820 m, 794 m, 770 m, 723 w, 669 m.

[Er(mbmp)(mbmpH)(thf)₃] \cdot 3thf (2.5)

The synthesis of complex **2.5** was carried out in the same way as that described for complex **2.1**, but erbium powder (0.50 g, 3 mmol) was used in place of yttrium. Orange crystals were obtained from ~10 mL of thf at 4 °C (0.53g, 29%). *Anal.* Calc. for C₅₀H₆₉O₅Er (917.34 g.mol⁻¹ after loss of two thf of solvation and three lattice thf): C, 65.46; H, 7.58; Er, 18.23. Found: C, 65.11; H, 7.19; Er, 18.02%. IR (Nujol, cm⁻¹): 3509 s, 1740 m, 1713 w, 1607 s, 1560 m, 1370 m, 1262 m, 1069 m, 965 m, 861 m, 810 m.

[Tm(mbmp)(mbmpH)(thf)₃·3thf (2.6)

The synthesis of complex **2.6** was carried out in the same way as that described for complex **2.1**, but thulium filings (0.51 g, 3 mmol) were used in place of yttrium. Green crystals were obtained from ~10 mL of thf at -18 °C (0.69 g, 25%) *Anal. Calc.* for C₇₀H₁₀₉O₁₀Tm (1279.54g.mol⁻¹): C, 65.71; H, 8.59; Tm, 13.20. Found: C, 65.86; H, 8.67; Tm, 12.53%. IR (Nujol, cm⁻¹): 3508 s, 1741 m, 1639 s, 1604 s, 1548 w, 1532 m, 1166, m, 1045 m, 967 m, 857 m, 770 m, 752 m, 718 w 670 m.

[Lu(mbmp)(mbmpH)(thf)₃·3thf (2.7)

The synthesis of complex **2.7** was carried out in the same way as that described for complex **2.1**, but lutetium filings (0.53 g, 3 mmol) were used in place of yttrium. Pale brown crystals were obtained from ~10 mL of thf at 4 °C (1.75 g, 68%) *Anal. Calc.* for C₇₀H₁₀₉O₁₀Lu (1285.57g.mol⁻¹): C, 65.40; H, 8.55. Found: C, 65.27; H, 8.38; .¹H-NMR (400 MHz, C₆D₆, 25 °C): δ 7.34 (s, 4H, ArH), 7.18 (s, 4H, ArH), 5.75 (br s, 1H, ArOH), 3.98 (s, 4H, CH₂) 3.60 (s, 24H, thf), 2.28 (s, 12H, ArCH₃), 1.59 (s, 36H, C(CH₃)₃), 1.34 (s, 24H, thf). IR (Nujol, cm⁻¹): 3506 s, 1743 m, 1638 s, 1604 s, 1532 m, 1509 m, 1444 m, 1370 m, 1266 m, 1073 m, 1019 m, 967 m, 914 m, 862 m, 822 m, 795 m, 769 m, 722 m, 674 w, 613 w.

[Y(mbmp)(mbmpH)(thf)₂·PhMe (2.8a)

The synthesis of complex **2.8a** was carried out in the same way as that described for complex **2.1**, but, after filtration, all solvent was removed under vacuum, and the residue recrystallised by slow cooling of a hot toluene solution (~10 mL) giving single crystals of **2.8a**.

[Y(mbmp)(mbmpH)(thf)₂·2C₆D₆ (2.8b)

The synthesis of complex **2.8b** was carried out in the same was as that described for complex **2.8a**, but **2.8b** was a result of recrystallising from hot deuterated benzene. *Anal. Calc.* for

$C_{54}H_{77}O_6Y$ (911.09 g.mol⁻¹ after loss of two lattice C_6D_6): C, 71.19; H, 8.52; Y, 9.76. Found: C, 70.83; H, 8.13; Y, 9.37%.

[AlMe₂Y(mbmp)₂(thf)₂]·2C₆D₆ (2.9)

A Schlenk flask was charged with **2.1** (1.80 g, 1.8 mmol) and dissolved in anhydrous toluene (~10 mL), and a 2.0 M solution of trimethylaluminium in toluene (0.90 mL, 1.8 mmol) was added at room temperature. The solution was cooled to -18 °C, and small crystals unsuitable for X-ray analysis were obtained. The supernatant solution was removed by filtration, and the crystalline material was dried under reduced pressure, and recrystallised from hot deuterated benzene yielding colourless crystals (0.45 g, 22%). *Anal.* Calc. for $C_{56}H_{82}AlO_6Y$ (967.13 g.mol⁻¹ after loss of two lattice C_6D_6): C, 69.55; H, 8.55; Y, 9.19. Found: C, 69.22; H, 8.33; Y, 9.03%. ¹H NMR (400 MHz, C_6D_6 , 25 °C): δ = 7.26 (d, 4H, ArH, J = 2.1 Hz), 7.15 (d, 4H, ArH, J = 2.1 Hz), 4.18 (d, 2H, CH₂, J = 13.7 Hz), 3.68 (d, 2H, CH₂, J = 13.7 Hz), 3.58 (m, 24H, thf), 2.27 (s, 12H, ArCH₃), 1.60 (s, 36H, C(CH₃)₃), 1.21 (m, 24H, thf), -0.28 (s, 6H, AlCH₃). Although the NMR sample contained an excess of thf, it establishes the mbmp:Me ratio. IR (Nujol, cm⁻¹): 2725 w, 2369 w, 2214 w, 1891 m, 1740 s, 1605 s, 1258 w, 1012 w, 800 w, 722 m, 669 m, 587 m, 518 m.

[Dy₂(mbmp)₃(thf)₃]·2PhMe (2.10)

The synthesis of complex **2.10** was carried out in the same way as that described for complex **2.9**, but complex **2.4** (1.87 g, 1.4 mmol) was used in place of complex **2.1**, and a 2.0 M solution of trimethylaluminium in toluene (0.70 mL, 1.4 mmol) was added. Amber crystals suitable for X-ray analysis were obtained from the toluene solution at -18 °C, alongside crystals of **2.10**. As **2.10** and **2.11** were obtained as a mixture, discrete spectroscopic and elemental analysis was not able to be obtained.

[AlMe(mbmp)(thf)]·PhMe (2.11)

Method A: A Schlenk flask was charged with **2.2-2.6** (1 equivalent) and dissolved in anhydrous toluene (~10 mL), and a 2.0 M solution of trimethylaluminium in toluene (1 equivalent) was added at room temperature. The solution was cooled to -18 °C, and colourless crystals of **2.11** were obtained and were identified by X-ray crystallography.

Method B: A Schlenk flask equipped with a magnetic stirrer bar was charged with mbmpH₂ (0.89 g, 2.6 mmol) and dissolved in anhydrous thf (~30 mL). The solution was cooled to 0 °C, and a 2.0 M solution of trimethylaluminium in toluene (1.2 mL, 2.4 mmol) was added dropwise. The resulting solution was allowed to warm to room temperature and was stirred for 3 hours before removing the solvent under reduced pressure. The solids were resuspended in anhydrous toluene, and the solution removed by filter cannula. Yellow/orange crystals were obtained from the solution at -18 °C (0.44 g, 45%). *Anal.* Calc. for C₂₈H₄₁O₃Al (452.60 g·mol⁻¹ after loss of one lattice toluene): C, 74.30; H, 9.13. Found: C, 74.12; H, 8.95%. ¹H NMR (400 MHz, C₆D₆, 25 °C): δ = 7.27 (d, 2H, ArH, *J* = 1.9 Hz), 7.14 (d, 2H, ArH, *J* = 1.9 Hz), 4.22 (d, 1H, CH₂, *J* = 13.7 Hz), 3.58 (d, 1H, *J* = 13.7 Hz), 3.53 (m, 4H, thf), 2.27 (s, 6H, ArCH₃), 1.60 (s, 18H, C(CH₃)₃), 0.95 (m, 4H, thf), -0.28 (s, 3H, AlCH₃). IR (Nujol, cm⁻¹): 2377 m, 2214 w, 2054 w, 1940 w, 1854 m, 1744 m, 1638 s, 1462 m, 1255 m, 1074 s, 955 m, 804 w, 722 s.

2.4.2 Typical procedure for polymerisation reactions

A Schlenk flask equipped with a magnetic stirrer bar was charged with *rac*-lactide (0.20 g, 1.39 mmol) and anhydrous toluene (1.5 mL). The contents of the flask were heated to 70 °C with stirring, and the initiator (**2.2**, **2.4**, **2.7**, **2.10** + **2.11**, or **2.11**) (1.39 x 10⁻² mmol) in anhydrous toluene (0.5 mL) was added slowly by syringe. The solution was stirred for 10 hours and then quenched with ethanol (2 mL) and concentrated hydrochloric acid (2-3 drops), before being

poured into hexanes (40 mL) to precipitate the polymer. The suspension was filtered, and the polymer dried in a vacuum oven at 40 °C overnight to remove residual solvent.

As complexes **2.1-2.7** are isostructural, catalytic studies were undertaken on metal centres that represented a range of relative ionic radii: large (Nd = **2.2**), medium (Dy = **2.4**), and small (Lu = **2.7**).

2.5 Crystal and refinement data**[Y(mbmp)(mbmpH)(thf)₃] \cdot 3thf (2.1)**

C₇₀H₁₀₉O₁₀Y (*M* = 1199.48 g/mol): monoclinic, space group *P*2₁/*c* (no. 14), *a* = 13.254(3) Å, *b* = 17.600(4) Å, *c* = 28.387(6) Å, β = 93.72(3)°, *V* = 6608(2) Å³, *Z* = 4, *T* = 100(2) K, μ (Synchrotron) = 0.938 mm⁻¹, *D*_{calc} = 1.206 g/cm³, 83342 reflections measured (2.724° ≤ 2 Θ ≤ 55.822°), 15405 unique (*R*_{int} = 0.0632, *R*_{sigma} = 0.0363) which were used in all calculations. The final *R*₁ was 0.0539 (*I* > 2 σ (*I*)) and *wR*₂ was 0.1365 (all data).

[Nd(mbmp)(mbmpH)(thf)₃] \cdot 3thf (2.2)

C₇₀H₁₀₉NdO₁₀ (*M* = 1254.81 g/mol): monoclinic, space group *P*2₁/*c* (no. 14), *a* = 13.176(3) Å, *b* = 17.631(4) Å, *c* = 28.491(6) Å, β = 93.50(3)°, *V* = 6606(2) Å³, *Z* = 4, *T* = 100(2) K, μ (Synchrotron) = 0.841 mm⁻¹, *D*_{calc} = 1.262 g/cm³, 76138 reflections measured (2.718° ≤ 2 Θ ≤ 49.998°), 11605 unique (*R*_{int} = 0.0748, *R*_{sigma} = 0.0455) which were used in all calculations. The final *R*₁ was 0.1274 (*I* > 2 σ (*I*)) and *wR*₂ was 0.3659 (all data).

[Gd(mbmp)(mbmpH)(thf)₃] \cdot 3thf (2.3)

C₇₀H₁₀₉GdO₁₀ (*M* = 1267.82 g/mol): monoclinic, space group *P*2₁/*c* (no. 14), *a* = 13.228(3) Å, *b* = 17.675(4) Å, *c* = 28.481(6) Å, β = 94.11(3)°, *V* = 6642(2) Å³, *Z* = 4, *T* = 100(2) K, μ (Synchrotron) = 1.054 mm⁻¹, *D*_{calc} = 1.268 g/cm³, 88343 reflections measured (2.714° ≤ 2 Θ ≤ 55.848°), 15703 unique (*R*_{int} = 0.0341, *R*_{sigma} = 0.0215) which were used in all calculations. The final *R*₁ was 0.0352 (*I* > 2 σ (*I*)) and *wR*₂ was 0.0888 (all data).

[Dy(mbmp)(mbmpH)(thf)₃]·3thf (2.4)

$C_{70}H_{109}DyO_{10}$ ($M=1273.07$ g/mol): monoclinic, space group $P2_1/c$ (no. 14), $a = 13.212(3)$ Å, $b = 17.539(4)$ Å, $c = 28.459(6)$ Å, $\beta = 93.44(3)^\circ$, $V = 6583(2)$ Å³, $Z = 4$, $T = 100(2)$ K, $\mu(\text{Synchrotron}) = 1.191$ mm⁻¹, $D_{\text{calc}} = 1.285$ g/cm³, 113072 reflections measured ($2.728^\circ \leq 2\Theta \leq 60^\circ$), 18449 unique ($R_{\text{int}} = 0.0435$, $R_{\text{sigma}} = 0.0256$) which were used in all calculations. The final R_1 was 0.0511 ($I > 2\sigma(I)$) and wR_2 was 0.1473 (all data).

[Er(mbmp)(mbmpH)(thf)₃]·3thf (2.5)

$C_{70}H_{109}ErO_{10}$ ($M=1277.83$ g/mol): monoclinic, space group $P2_1/c$ (no. 14), $a = 13.282(3)$ Å, $b = 17.590(4)$ Å, $c = 28.362(6)$ Å, $\beta = 93.80(3)^\circ$, $V = 6612(2)$ Å³, $Z = 4$, $T = 100(2)$ K, $\mu(\text{Synchrotron}) = 1.325$ mm⁻¹, $D_{\text{calc}} = 1.284$ g/cm³, 54558 reflections measured ($2.726^\circ \leq 2\Theta \leq 55.866^\circ$), 15644 unique ($R_{\text{int}} = 0.0546$, $R_{\text{sigma}} = 0.0438$) which were used in all calculations. The final R_1 was 0.0391 ($I > 2\sigma(I)$) and wR_2 was 0.0967 (all data).

[Tm(mbmp)(mbmpH)(thf)₃]·3thf (2.6)

$C_{70}H_{109}O_{10}Tm$ ($M=1279.50$ g/mol): monoclinic, space group $P2_1/c$ (no. 14), $a = 13.200(3)$ Å, $b = 17.530(4)$ Å, $c = 28.420(6)$ Å, $\beta = 93.32(3)^\circ$, $V = 6565(2)$ Å³, $Z = 4$, $T = 100(2)$ K, $\mu(\text{Synchrotron}) = 1.407$ mm⁻¹, $D_{\text{calc}} = 1.294$ g/cm³, 157911 reflections measured ($2.73^\circ \leq 2\Theta \leq 51.364^\circ$), 11559 unique ($R_{\text{int}} = 0.0450$, $R_{\text{sigma}} = 0.0165$) which were used in all calculations. The final R_1 was 0.0463 ($I > 2\sigma(I)$) and wR_2 was 0.1271 (all data).

[Lu(mbmp)(mbmpH)(thf)₃]·3thf (2.7)

$C_{70}H_{109}LuO_{10}$ ($M=1285.54$ g/mol): monoclinic, space group $P2_1/c$ (no. 14), $a = 13.210(3)$ Å, $b = 17.490(4)$ Å, $c = 28.400(6)$ Å, $\beta = 93.23(3)^\circ$, $V = 6551(2)$ Å³, $Z = 4$, $T = 100(2)$ K, $\mu(\text{Synchrotron}) = 1.563$ mm⁻¹, $D_{\text{calc}} = 1.303$ g/cm³, 70227 reflections measured

($2.736^\circ \leq 2\Theta \leq 50.078^\circ$), 11194 unique ($R_{\text{int}} = 0.0685$, $R_{\text{sigma}} = 0.0408$) which were used in all calculations. The final R_1 was 0.0612 ($I > 2\sigma(I)$) and wR_2 was 0.1796 (all data).

[Y(mbmp)(mbmpH)(thf)₂]·PhMe (2.8a)

$\text{C}_{61}\text{H}_{85}\text{O}_6\text{Y}$ ($M = 1003.19$ g/mol): triclinic, space group $P\bar{1}$ (no. 2), $a = 12.386(3)$ Å, $b = 14.465(3)$ Å, $c = 17.062(3)$ Å, $\alpha = 106.74(3)^\circ$, $\beta = 106.42(3)^\circ$, $\gamma = 93.08(3)^\circ$, $V = 2777.3(11)$ Å³, $Z = 2$, $T = 100(2)$ K, $\mu(\text{Synchrotron}) = 1.098$ mm⁻¹, $D_{\text{calc}} = 1.200$ g/cm³, 34526 reflections measured ($2.624^\circ \leq 2\Theta \leq 50.052^\circ$), 9003 unique ($R_{\text{int}} = 0.0404$, $R_{\text{sigma}} = 0.0325$) which were used in all calculations. The final R_1 was 0.0413 ($I > 2\sigma(I)$) and wR_2 was 0.1104 (all data).

[Y(mbmp)(mbmpH)(thf)₂]·2C₆D₆ (2.8b)

$\text{C}_{66}\text{H}_{77}\text{D}_{12}\text{O}_6\text{Y}$ ($M = 1079.28$ g/mol): monoclinic, space group $C2/c$ (no. 15), $a = 23.753(5)$ Å, $b = 12.686(3)$ Å, $c = 19.936(4)$ Å, $\beta = 103.50(3)^\circ$, $V = 5841(2)$ Å³, $Z = 4$, $T = 100.15$ K, $\mu(\text{Synchrotron}) = 1.048$ mm⁻¹, $D_{\text{calc}} = 1.214$ g/cm³, 17573 reflections measured ($4.012^\circ \leq 2\Theta \leq 49.99^\circ$), 4738 unique ($R_{\text{int}} = 0.0964$, $R_{\text{sigma}} = 0.0967$) which were used in all calculations. The final R_1 was 0.0451 ($I > 2\sigma(I)$) and wR_2 was 0.1251 (all data).

[AlMe₂Y(mbmp)₂(thf)₂]·2C₆D₆ (2.9)

$\text{C}_{68}\text{H}_{94}\text{AlO}_6\text{Y}$ ($M = 1123.32$ g/mol): monoclinic, space group $P2_1/n$ (no. 14), $a = 9.845(2)$ Å, $b = 19.536(4)$ Å, $c = 32.429(7)$ Å, $\beta = 94.32(3)^\circ$, $V = 6219(2)$ Å³, $Z = 4$, $T = 100(2)$ K, $\mu(\text{Synchrotron}) = 1.001$ mm⁻¹, $D_{\text{calc}} = 1.200$ g/cm³, 76823 reflections measured ($2.436^\circ \leq 2\Theta \leq 49.996^\circ$), 10557 unique ($R_{\text{int}} = 0.0746$, $R_{\text{sigma}} = 0.0388$) which were used in all calculations. The final R_1 was 0.0998 ($I > 2\sigma(I)$) and wR_2 was 0.2733 (all data).

[Dy₂(mbmp)₃(thf)₃]·2PhMe (2.10)

C₉₅H₁₃₀Dy₂O₉ ($M=1740.98$ g/mol): triclinic, space group $P\bar{1}$ (no. 2), $a = 13.158(3)$ Å, $b = 16.671(3)$ Å, $c = 22.238(4)$ Å, $\alpha = 70.76(3)^\circ$, $\beta = 76.21(3)^\circ$, $\gamma = 68.48(3)^\circ$, $V = 4246.1(19)$ Å³, $Z = 2$, $T = 100(2)$ K, $\mu(\text{Synchrotron}) = 1.802$ mm⁻¹, $D_{\text{calc}} = 1.362$ g/cm³, 51459 reflections measured ($2.726^\circ \leq 2\Theta \leq 51.36^\circ$), 14588 unique ($R_{\text{int}} = 0.0301$, $R_{\text{sigma}} = 0.0263$) which were used in all calculations. The final R_1 was 0.0379 ($I > 2\sigma(I)$) and wR_2 was 0.1026 (all data).

[AlMe(mbmp)(thf)]·PhMe (2.11)

C₃₅H₄₉AlO₃ ($M=544.72$ g/mol): monoclinic, space group $C2/c$ (no. 15), $a = 16.725(3)$ Å, $b = 16.410(3)$ Å, $c = 24.286(5)$ Å, $\beta = 108.39(3)^\circ$, $V = 6325(2)$ Å³, $Z = 8$, $T = 100(2)$ K, $\mu(\text{Synchrotron}) = 0.096$ mm⁻¹, $D_{\text{calc}} = 1.144$ g/cm³, 38583 reflections measured ($3.534^\circ \leq 2\Theta \leq 51.37^\circ$), 5741 unique ($R_{\text{int}} = 0.0412$, $R_{\text{sigma}} = 0.0209$) which were used in all calculations. The final R_1 was 0.0505 ($I > 2\sigma(I)$) and wR_2 was 0.1479 (all data).

2.6 References

- [1] F. Ortu, *Chem. Rev.* **2022**, *122*, 6040–6116.
- [2] B. Liu, Y. Yao, M. Deng, Y. Zhang, Q. Shen, *J. Rare Earths* **2006**, *24*, 264–267.
- [3] M. Deng, Y. Yao, Q. Shen, Y. Zhang, S. Jin, *Dalton Trans.* **2004**, *4*, 944–950.
- [4] I. Korobkov, S. Gambarotta, *Organometallics* **2009**, *28*, 4009–4019.
- [5] Z. Liang, X. Ni, X. Li, Z. Shen, *Inorg. Chem. Commun.* **2011**, *14*, 1948–1951.
- [6] X. Xu, M. Ma, Y. Yao, Y. Zhang, Q. Shen, *J. Mol. Struct.* **2005**, *743*, 163–168.
- [7] X. Xu, M. Ma, Y. Yao, Y. Zhang, Q. Shen, *Eur. J. Inorg. Chem.* **2005**, 676–684.
- [8] B. Xu, L. Huang, Z. Yang, Y. Yao, Y. Zhang, Q. Shen, *Organometallics* **2011**, *30*, 3588–3595.
- [9] B. D. Mahoney, N. A. Piro, P. J. Carroll, E. J. Schelter, *Inorg. Chem.* **2013**, *52*, 5970–5977.
- [10] J. Yu, G. Wu, J. Huang, W. Sun, Z. Shen, *Sci. China, Ser. B Chem.* **2009**, *52*, 1711–1714.
- [11] X. Xu, M. Hu, Y. Yao, R. Qi, Y. Zhang, Q. Shen, *J. Mol. Struct.* **2007**, *829*, 189–194.
- [12] R. Qi, B. Liu, X. Xu, Z. Yang, Y. Yao, Y. Zhang, Q. Shen, *Dalton Trans.* **2008**, 5016–5024.
- [13] Y. F. Tan, X. P. Xu, K. Guo, Y. M. Yao, Y. Zhang, Q. Shen, *Polyhedron* **2013**, *61*, 218–224.

- [14] Y. X. Zhou, J. Zhao, L. Peng, Y. L. Wang, X. Tao, Y. Z. Shen, *RSC Adv.* **2016**, *6*, 22269–22276.
- [15] L. Fang, Y. Yao, Y. Zhang, Q. Shen, Y. Wang, *Z. Anorg. Allg. Chem.* **2013**, *639*, 2324–2330.
- [16] Y. Yao, X. Xu, B. Liu, Y. Zhang, Q. Shen, W. T. Wong, *Inorg. Chem.* **2005**, *44*, 5133–5140.
- [17] X. Xu, Z. Zhang, Y. Yao, Y. Zhang, Q. Shen, *Inorg. Chem.* **2007**, *46*, 9379–9388.
- [18] S. H. Ali, Syntheses, Structures and Reactivity of Organolanthanoid Complexes, PhD Thesis, James Cook University, **2017**.
- [19] R. D. Shannon, *Acta Crystallogr. Sect. A* **1976**, *32*, 751–767.
- [20] F. C. March, G. Ferguson, *Can. J. Chem.* **1971**, *49*, 3590.
- [21] B. T. Ko, Y. C. Chao, C. C. Lin, *Inorg. Chem.* **2000**, *39*, 1463–1469.
- [22] D. M. Lyubov, A. O. Tolpygin, A. A. Trifonov, *Coord. Chem. Rev.* **2019**, *392*, 83–145.
- [23] R. H. Platel, L. M. Hodgson, C. K. Williams, *Polym. Rev.* **2008**, *48*, 11–63.
- [24] L. Clark, G. B. Deacon, C. M. Forsyth, P. C. Junk, P. Mountford, J. P. Townley, *Dalton Trans.* **2010**, *39*, 6693–6704.
- [25] L. Clark, G. B. Deacon, C. M. Forsyth, P. C. Junk, P. Mountford, J. P. Townley, J. Wang, *Dalton Trans.* **2013**, *42*, 9294–9312.
- [26] B. J. O’Keefe, M. A. Hillmyer, W. B. Tolman, *J. Chem. Soc. Dalton Trans.* **2001**, 2215–2224.

Chapter Two

- [27] O. Dechy-Cabaret, B. Martin-Vaca, D. Bourissou, *Chem. Rev.* **2004**, *104*, 6147–6176.
- [28] S. Agarwal, C. Mast, K. Dehnicke, A. Greiner, *Macromol. Rapid Commun.* **2000**, *21*, 195–212.
- [29] I. Palard, M. Schappacher, A. Soum, S. M. Guillaume, *Polym. Int.* **2006**, *55*, 1132–1137.
- [30] A. Amgoune, C. M. Thomas, J. F. Carpentier, *Pure Appl. Chem.* **2007**, *79*, 2013–2030.
- [31] W. J. Evans, H. Katsumata, *Macromolecules* **1994**, *27*, 2330–2332.
- [32] W. M. Stevels, M. J. K. Ankoné, P. J. Dijkstra, J. Feijen, *Macromolecules* **1996**, *29*, 6132–6138.

Chapter 3: Synthesis of bulky octa- and deca-phenyl metallocenes by selective carbon-phosphorus bond cleavage

3.1 Introduction

3.1.1 Divalent polyarylcyclopentadienyl lanthanoid complexes

As discussed in Chapter 1, polyarylcyclopentadienyl based ligands have become interesting targets owing to their desirable stability and reactivity properties, however, examples of rare earth complexes of these ligands are scarce. These bulky ligand systems often afford lower solubility compared to their alkyl- and silyl-cyclopentadienyl substituted counterparts, making them significantly more challenging to work with. Typical synthetic approaches such as protolysis, or metathesis are often unsuitable to access polyarylcyclopentadienyl complexes, owing to reactivity and purification issues.^[1] Despite these unfavourable traits, these ligand systems are very desirable, as the stabilisation of the negative charge by the aryl groups significantly decreases the Lewis basicity of the ligands which results in a poorer donor ability than the alkyl and silyl substituted ligands, which may also lead to increased stability of strongly reducing divalent lanthanoid ions. Only a few ligand systems have been reported as capable of stabilising this low-valent lanthanoid complexes, such as Tm(II), Nd(II) and Dy(II).^[2] A small selection of polyarylcyclopentadiene ligands have been used in rare earth chemistry, primarily tetraphenylcyclopentadiene ($C_5Ph_4H_2$) and pentaphenylcyclopentadiene (C_5Ph_5H) (Figure 3.1), which may also be contenders for the synthesis of low-valent lanthanoid complexes.

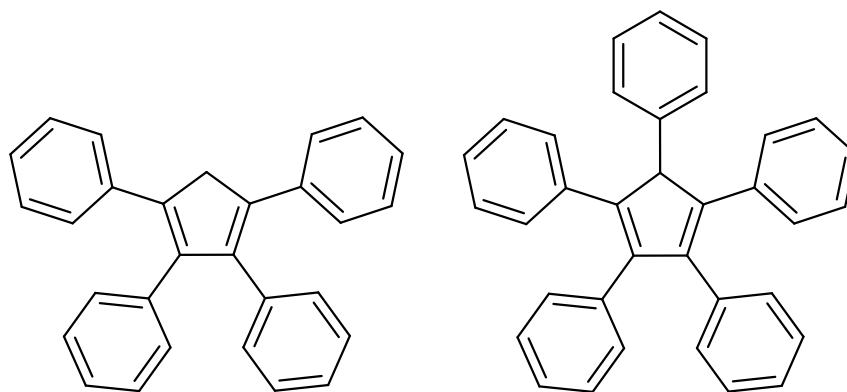
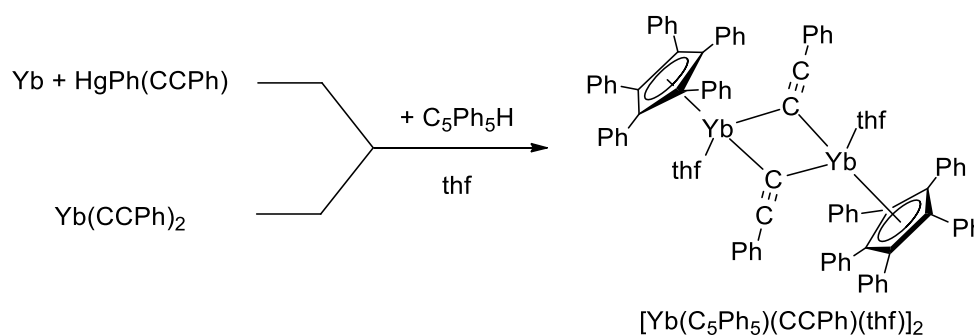


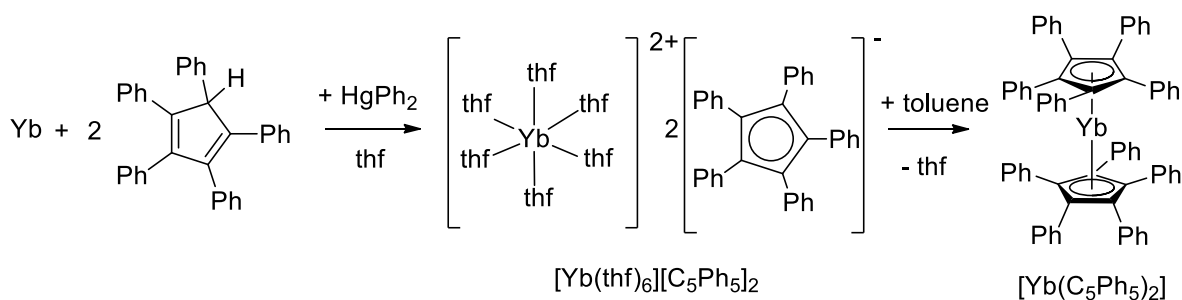
Figure 3.1 – Molecular structure of tetraphenylcyclopentadiene ($C_5Ph_4H_2$) and pentaphenylcyclopentadiene (C_5Ph_5H).

Great advancements on the synthesis of pentaphenylcyclopentadienyl sandwich complexes of the rare earth elements have been achieved in recent years, owing to the use of the redox transmetallation/protolysis (RTP) reaction, which avoids the aforementioned purification and reactivity issues of protolysis and metathesis reactions. The Deacon group reported the first structural characterisation of a lanthanoid C_5Ph_5 complex, $[Yb(C_5Ph_5)(CCPh)(thf)]_2$ by RTP synthesis in 2006 (Scheme 3.1).^[3]



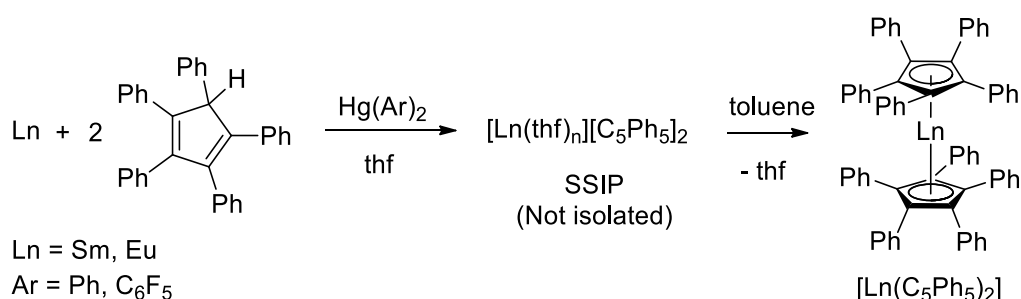
Scheme 3.1 – Synthesis of $[Yb(C_5Ph_5)(CCPh)(thf)]_2$ by redox transmetallation/protolysis.^[3]

The Deacon group continued to make developments in 2008 with the isolation and characterisation of the first sandwich complex of C_5Ph_5 , $[Yb(C_5Ph_5)_2]$, from desolvating the solvent separated ion pair (SSIP) $[Yb(thf)_6][C_5Ph_5]_2$, also synthesised by RTP (Scheme 3.2).^[4]



Scheme 3.2 – Synthesis of the SSIP $[\text{Yb}(\text{thf})_6][\text{C}_5\text{Ph}_5]_2$ and desolvation to yield the sandwich complex $[\text{Yb}(\text{C}_5\text{Ph}_5)_2]$.^[4]

The Deacon group further prepared the samarium and europium analogues, again by RTP, in 2015, however the SSIPs were not isolated (Scheme 3.3).^[5] Both HgPh_2 and $\text{Hg}(\text{C}_6\text{F}_5)_2$ could be used for the synthesis of the Eu sandwich complex (if performed at room temperature) however only HgPh_2 could be used for the synthesis of the Sm analogue.



Scheme 3.3 – Syntheses of Sm and Eu sandwich complexes $[\text{Ln}(\text{C}_5\text{Ph}_5)_2]$ by RTP.^[5]

In 2008 the Harder group overcame the challenges associated with the low solubility of the C_5Ph_5 ligand and its complexes by addition of an *n*-butyl group in the *para* position of each phenyl ring, coined Cp^{BIG} (Figure 3.2).^[6]

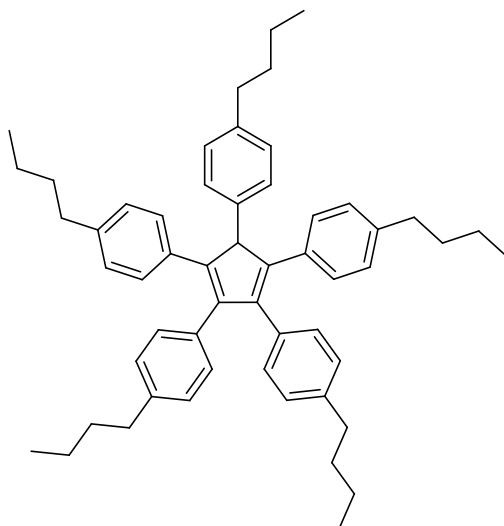
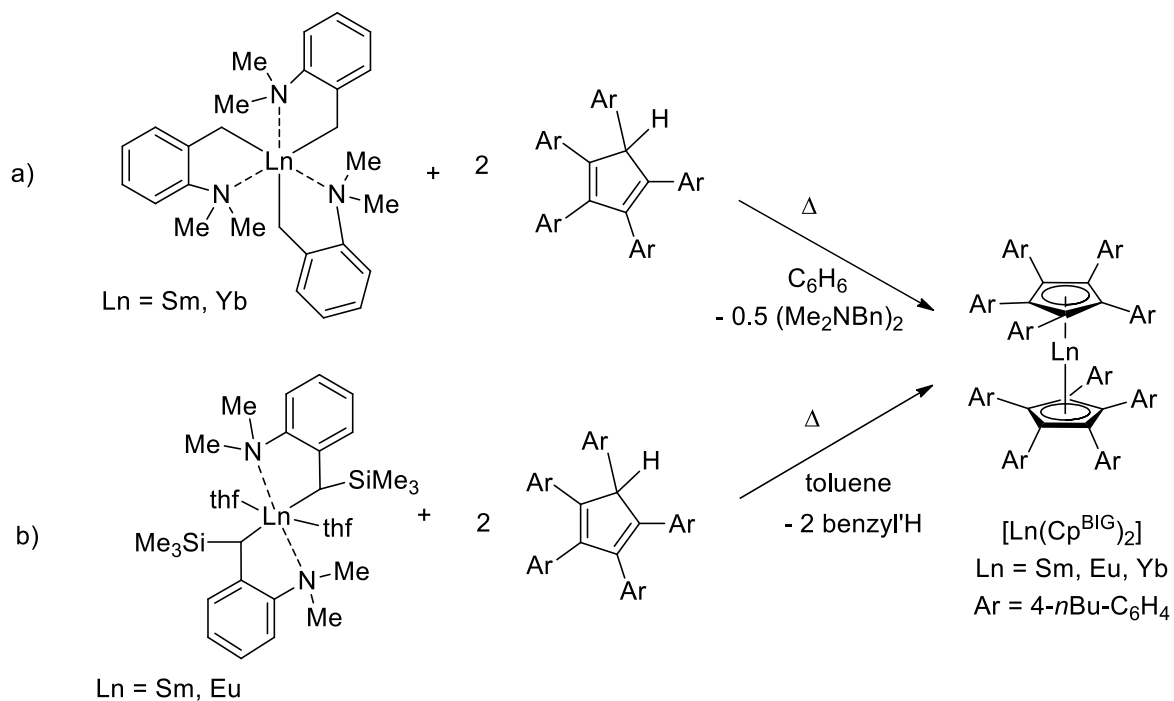


Figure 3.2 – Molecular structure of Harder's $\text{Cp}^{\text{BIG}}\text{H}$ ($\text{C}_5(4\text{-}n\text{BuC}_6\text{H}_4)_5\text{H}$).^[6]

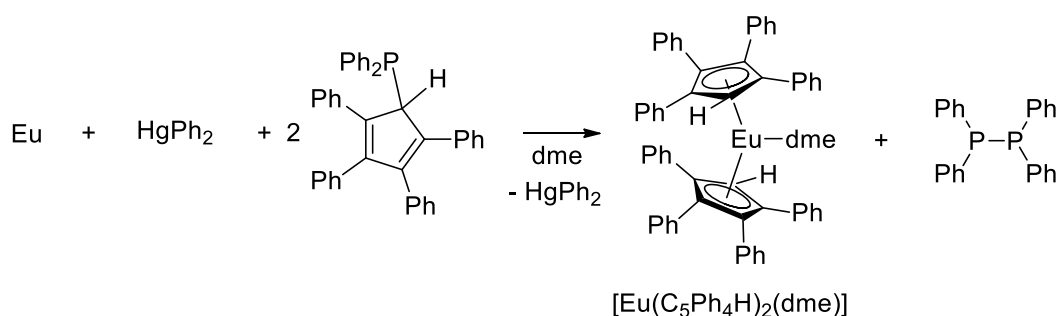
The Harder group successfully synthesised divalent sandwich complexes of samarium, europium, and ytterbium by treating the Cp^{BIG} ligand with highly reactive lanthanoid benzyl reagents (Scheme 3.4).^[6-8]



Scheme 3.4 – Two complementary pathways to $[\text{Ln}(\text{Cp}^{\text{BIG}})_2]$ complexes by a) protolysis with sterically induced reduction (SIR) and b) protolysis.^[6-8]

Remarkably, when $\text{Cp}^{\text{BIG}}\text{H}$ was treated with trivalent lanthanoid reagents $[\text{Ln}(\text{Bn}^*)_3]$ ($\text{Ln} = \text{Sm}, \text{Yb}$; $\text{Bn}^* = \text{CH}_2\text{C}_6\text{H}_4\text{-2-NMe}_2$) the divalent sandwich complexes $[\text{Ln}(\text{Cp}^{\text{BIG}})_2]$ were isolated, and half an equivalent of the coupled $(\text{Me}_2\text{NC}_6\text{H}_4\text{CH}_2)_2$ species was eliminated (Scheme 3.4(a)). This method, dubbed sterically induced reduction (SIR), provided access to the sandwich complexes of Cp^{BIG} for both samarium and ytterbium, whilst conversely, simple protolysis from the divalent trimethylsilane substituted benzyl reagents ($[\text{Ln}(\text{CH}(\text{SiMe}_3)\text{C}_6\text{H}_4\text{-2-NMe}_2)_2]$) of samarium and europium could also be used to access these complexes (Scheme 3.4 (b)).

An alternative approach to overcoming the low solubility of the C_5Ph_5 ligand involves simply removing one of the phenyl rings. Tetraphenylcyclopentadiene and its complexes are significantly more soluble in organic solvents than their pentaphenyl counterparts,^[1,9–11] yet even still, only a few examples of divalent octaphenyl lanthanocenes have been reported. The first divalent lanthanoid sandwich complex of the $\text{C}_5\text{Ph}_4\text{H}$ ligand was reported by the Deacon group when initially attempting to synthesise $[\text{Eu}(\text{C}_5\text{Ph}_4\text{HPPH}_2)_2]$ by RTP.^[12] Instead of forming the desired phosphinated sandwich complex, the ligand underwent carbon-phosphorus bond cleavage, yielding instead $[\text{Eu}(\text{C}_5\text{Ph}_4\text{H})_2(\text{dme})]$ and eliminating $\text{Ph}_2\text{P-PPh}_2$ (Scheme 3.5).



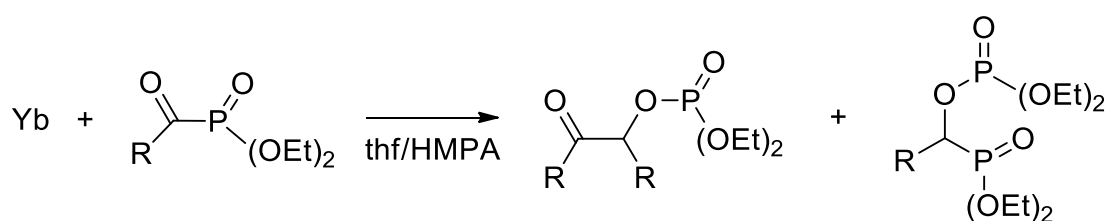
Scheme 3.5 – C-P cleavage of $\text{C}_5\text{Ph}_4\text{HPPH}_2$ by Eu metal, yielding $[\text{Eu}(\text{C}_5\text{Ph}_4\text{H})_2(\text{dme})]$.^[12]

A deliberate synthesis was then attempted using $\text{C}_5\text{Ph}_4\text{H}_2$ in an RTP reaction, also successfully synthesising the octaphenyl europocene sandwich complex, however extension to ytterbium

resulted in the solvent separated ion pair (SSIP) $[\text{Yb}(\text{dme})_4][\text{C}_5\text{Ph}_4\text{H}]_2$. The Deacon group later synthesised both the ytterbium and samarium sandwich complexes successfully through RTP reactions in thf.^[5,13,14] Despite the RTP reaction showing to be an effective method of synthesising these complexes, the C-P cleavage proved to be an interesting alternative route to access them, however no further investigation into this method was undertaken.

3.1.2 Carbon-phosphorus bond cleavage by lanthanoid metals

Lanthanoid metals are well known for the cleavage of C-X bonds (X = halides),^[15] however, only a few examples of C-P cleavage are reported in the literature, including the already outlined C-P cleavage of $\text{C}_5\text{Ph}_4\text{HPPH}_2$ by Eu metal.^[12] The first report of C-P cleavage by lanthanoids was by Fujiwara and Takaki, who reported the insertion of both Yb and Sm metals into acylphosphonates. A range of diethylacylphosphonates were treated with ytterbium metal (and in one example samarium metal), with methyl iodide for activation in a thf : HMPA solution (4:1) and stirred for several hours. Upon quenching with water and extracting with diethyl ether, a mixture of the α -ketophosphate and the phosphoryloxy phosphonate were isolated (Scheme 3.6).^[16]

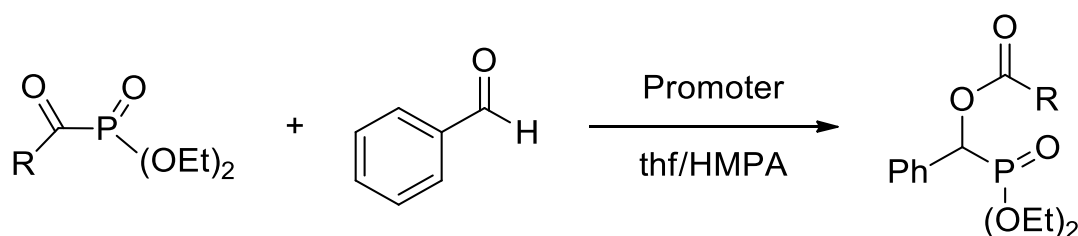


Scheme 3.6 – General C-P cleavage reaction of acylphosphonates with Yb metal.^[16]

The C-P cleavage mechanism has been proposed by a two-electron transfer from the Yb metal to the weak C-P bond, affording a phosphoryl acylytterbium intermediate, which can then attack the starting acylphosphonate at either the C or P sites, yielding the two products. Samarium metal could also be used for C-P cleavage in this system, however, was only

effective at higher temperatures, and only produced the phosphoryloxy phosphonate with low yields.

Fujiwara and Takaki further explored the use of samarium and ytterbium metal and samarium diiodide as C-P cleavage reagents for the coupling of acylphosphonates and aldehydes (Scheme 3.7).^[17] The reaction is thought to proceed, by reductive cleavage of the acylphosphonate by Sm or SmI₂ yielding a samarium phosphonate, which can undergo addition with the aldehyde, affording a samarium alkoxide, which can then abstract an acyl group from another equivalent of the acylphosphonate, resulting in the acyloxyphosphonate.

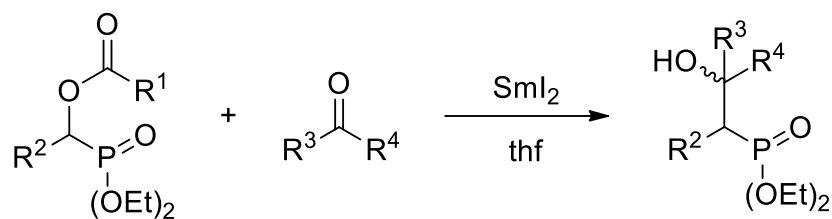


R = *p*-MeC₆H₄, promoter = Sm, Yb

R = Ph, promoter = Sm, SmI₂

Scheme 3.7 – C-P cleavage mediated coupling of acylphosphonates with benzaldehyde induced by Sm, SmI₂ and Yb metal to form acyloxyphosphonates.^[17]

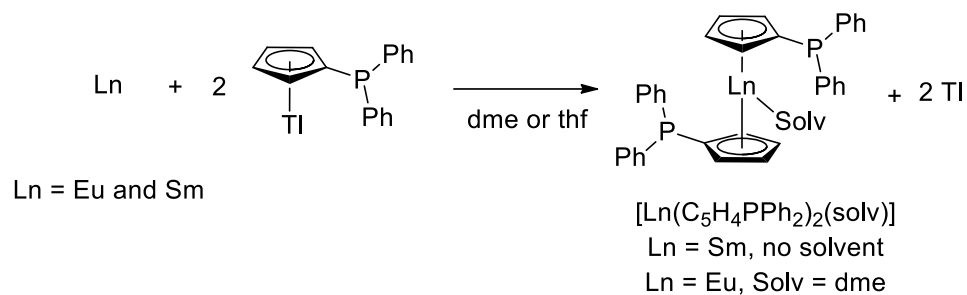
Samarium metal alone gave the best yields of the acyloxyphosphonates, and the scope was expanded to a wide range of acylphosphonate starting materials and aldehyde reagents, yielding an array of acyloxyphosphonates, which could undergo further C-P cleavage mediated coupling with aldehydes and ketones, induced by SmI₂ (Scheme 3.8).



Scheme 3.8 – General coupling reaction of acyloxyphosphonates and ketones/aldehydes mediated by SmI₂ to yield β-hydroxyphosphonates.^[17]

Lastly, the Chen group have reported C-P cleavage of triphenylphosphine oxide by an yttrium anilido hydride complex $[(L)Y(NH(DIPP))(\mu-H)]_2$ ($L = MeC(N(DIPP))-CHC(Me)(MCH_2CH_2NMe_2)^-$, $DIPP = 2,6-iPr_2C_6H_3$) forming an yttrium anilido phosphinoyl complex $[(L)Y(NH(2,6-iPr_2-C_6H_3)(OPPH_2))]$, whereby one of the C-P bonds is cleaved, and an $[O-PPh_2]^-$ anion is formed.^[18]

The Deacon group have also reported C-P cleavage when performing redox transmetallation reactions with $[Ti(C_5H_4PPh_2)]$ and an excess of samarium or europium metal (Scheme 3.9). Whilst the desired phosphinated sandwich complexes were isolated, the ³¹P NMR spectra of the reaction mixtures showed the presence of a variety of other phosphorus containing compounds, indicative of C-P cleavage processes, although none were isolated or characterised.^[19]

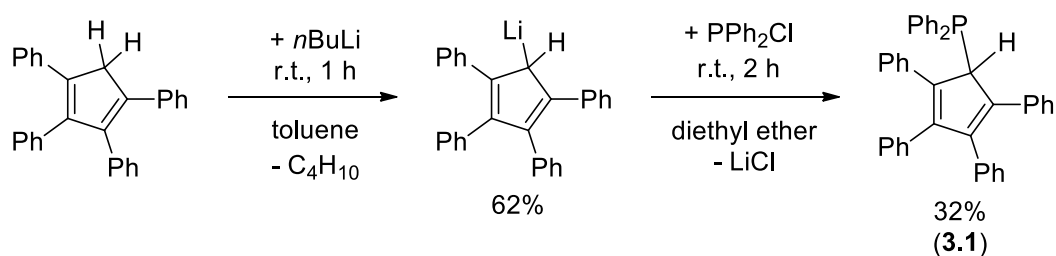


Scheme 3.9 – Redox transmetallation of europium and samarium with cyclopentadienyldiphenylphosphine thallium, yielding $[\text{Ln}(\text{C}_5\text{H}_4\text{PPh}_2)_2(\text{solv})]$ and other C-P cleavage products.^[19]

3.2 Results and discussion

3.2.1 Pro-ligand synthesis

The synthesis of polyarylcyclopentadienyl lanthanoid complexes by carbon-phosphorus bond cleavage requires, firstly, that a suitable pro-ligand with an appropriately exploitable C-P bond is synthesised. One such pro-ligand, which was serendipitously discovered to undergo this C-P cleavage in the presence of activated europium metal, is tetraphenylcyclopentadienyldiphenylphosphine ($C_5Ph_4HPPH_2$ (**3.1**)).^[12] This pro-ligand was initially synthesised by a two-step pathway from tetraphenylcyclopentadiene. Firstly, synthesising, and isolating tetraphenylcyclopentadienyl lithium after treatment with *n*-butyllithium in toluene, and then treatment of this solid, as a suspension in diethyl ether, with chlorodiphenylphosphine, and crystallising from the filtered ethereal solution (Scheme 3.10).

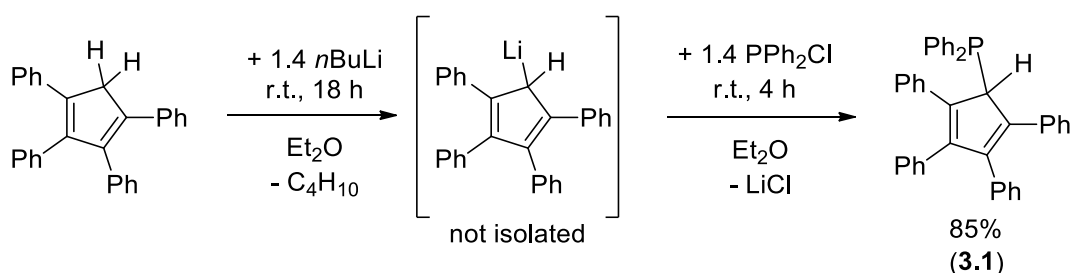


Scheme 3.10 – Reported synthesis of $C_5Ph_4HPPH_2$ (**3.1**).^[12]

Despite the synthesis resulting in a pure, crystalline starting material, the low yield of **3.1** presented a significant barrier to creating an efficient alternative to the other well-known synthetic routes. When synthesising **3.1** by the reported method above, it was observed in the ^{31}P NMR of the crude product that considerable amounts of PPh_2Cl remained after addition to the lithiated cyclopentadienyl species. This suggested that a) complete lithiation of the tetraphenylcyclopentadiene starting material was not occurring, b) some of the lithiated

cyclopentadiene was decomposing during the isolation or solvent changing step, or c) the reaction of the lithiated cyclopentadiene with PPh_2Cl was not going to completion.

To overcome these potential issues, the reaction was attempted without changing solvent systems, i.e., using diethyl ether for both steps, the lithiated cyclopentadiene intermediate was not isolated (as this step was no longer required), and 1.4 molar equivalents of *n*-butyllithium were used alongside an increased reaction duration to ensure complete lithiation. Without changing the solvent to toluene, 1.4 equivalents of PPh_2Cl were added to the lithiated cyclopentadiene suspension in diethyl ether and stirred for four hours. The diethyl ether was then removed under reduced pressure, and the solids were extracted with toluene to remove **3.1** from the formed lithium chloride. Once isolated, the toluene solution was dried under reduced pressure, and washed with anhydrous hexanes to remove any unreacted PPh_2Cl or *n*-butyl diphenylphosphine (from reaction of excess *n*-butyllithium with excess chlorodiphenylphosphine) by-product, yielding **3.1** as an off-white powder (Scheme 3.11). Crystals were grown from an anhydrous diethyl ether solution.

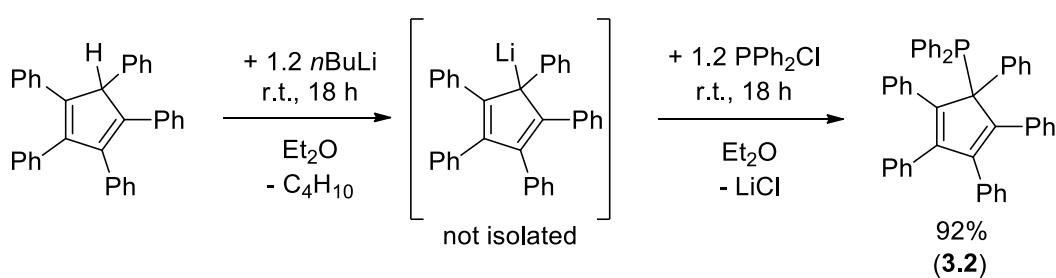


Scheme 3.11 – Improved synthesis of tetraphenylcyclopentadienyldiphenylphosphine (**3.1**) from tetraphenylcyclopentadiene.

This improved synthesis offers a more facile procedure, as only one workup was required at the end of the synthesis, as well as offering greatly improved yield (85% for the new approach vs 32% for the old approach).

^1H , ^{13}C and ^{31}P NMR spectroscopy with C_6D_6 as a solvent were used to confirm the identity and purity of **3.1**. The CpH proton signal shifts from 4.0 ppm in the ^1H NMR spectrum of tetraphenylcyclopentadiene, to 5.36 ppm in the ^1H NMR spectrum of **3.1** after substitution with the diphenylphosphine moiety. The ^{31}P NMR spectrum showed only one singlet at 13.36 ppm, confirming removal of excess PPh_2Cl , and any formed $\text{PPh}_2(\text{C}_4\text{H}_9)$. These spectral data were in accordance with those previously reported for the pure compound.^[12] Single crystal X-ray crystallography was also used to confirm the structure of **3.1**.

In a similar fashion, the previously unreported pentaphenylcyclopentadienyldiphenylphosphine pro-ligand was also synthesised by the same route, utilising pentaphenylcyclopentadiene as a starting material (Scheme 3.12).



Scheme 3.12 – Synthesis of pentaphenylcyclopentadienyldiphenylphosphine (**3.2**) from pentaphenylcyclopentadiene.

As the solubility of the pentaphenylcyclopentadiene starting material was much lower than that observed for the tetraphenylcyclopentadiene, a longer reaction duration was employed after the addition of PPh_2Cl . $n\text{BuLi}$ and PPh_2Cl were added with 1.2 stoichiometric equivalents and shown to still be effective in this reduced excess. Otherwise, only the workup differed, in that the synthesised **3.2** is also largely insoluble in toluene. Thus, the crude solids were first washed with anhydrous hexanes to remove any excess PPh_2Cl or formed $\text{PPh}_2(\text{C}_4\text{H}_9)$, and then, when extracting the organic solids from the formed LiCl , the toluene solution was heated to $60\text{ }^\circ\text{C}$

and filtered while hot. The hot solution gradually became purple in colour, indicative of some $C_5Ph_5\bullet$ radical formation.^[20] This heating step ensured that **3.2** was in solution and able to be removed from the LiCl precipitate. The hot toluene solution was allowed to cool, and then removed under reduced pressure, yielding a pale purple solid. The solid was washed again with anhydrous hexanes, yielding **3.2** as a pale-yellow solid in excellent yield (92%). Crystals of **3.2** could be grown from the slow cooling of a hot toluene solution.

The identity of **3.2** was confirmed with both 1H , ^{13}C and ^{31}P NMR spectroscopy in C_6D_6 , as well as by single crystal X-ray crystallography studies. As the only CpH proton is removed during the substitution process, the signal of the CpH proton in pentaphenylcyclopentadiene at 5.09 ppm is lost upon complete substitution with the diphenylphosphine moiety. Similar to that of **3.1**, only one signal was present in the ^{31}P NMR spectrum, a singlet at 9.75 ppm, confirming no other phosphorus containing compounds were present after workup. The signal in the ^{31}P NMR spectrum is considerably shifted downfield compared to the similar tetramethylcyclopentadienyldiphenylphosphine (0.6 ppm).^[21] A satisfactory elemental analysis of **3.2** was also obtained from the crystalline material.

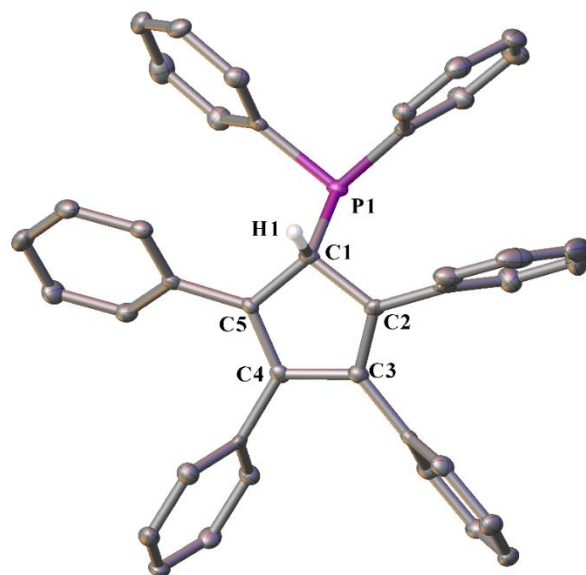


Figure 3.3 – ORTEP diagram of $C_5Ph_4HPPH_2$ (**3.1**) showing atom-numbering scheme for relevant atoms. Thermal ellipsoids are drawn at the 50% probability level. Phenyl hydrogen atoms are omitted for clarity. Selected bond lengths (\AA): C(1)-P(1) 1.890(3), C(1)-H(1) 1.000(3), C(1)-C(2) 1.502(4), C(2)-C(3) 1.361(4), C(3)-C(4) 1.486(4), C(4)-C(5) 1.366(4).

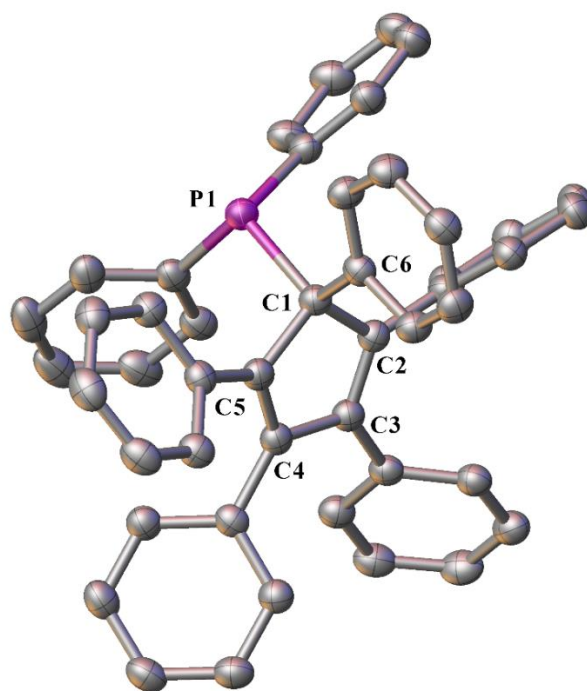
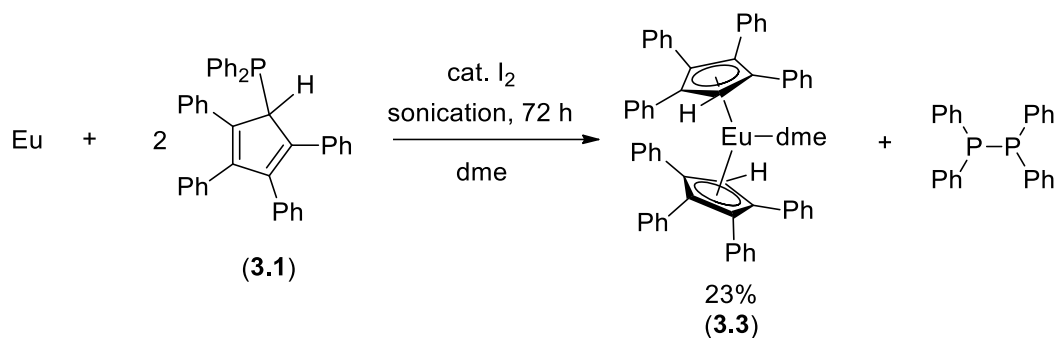


Figure 3.4 – ORTEP diagram of $C_5Ph_5PPh_2$ (**3.2**) showing atom-numbering scheme for relevant atoms. Thermal ellipsoids are drawn at 50% probability level. Hydrogen atoms are omitted for clarity. Selected bond lengths (Å): C(1)-P(1) 1.9494(16), C(1)-C(6) 1.5350(2), C(1)-C(2) 1.522(2), C(2)-C(3) 1.3606(17), C(3)-C(4) 1.4690(18), C(4)-C(5) 1.358(2).

Both pro-ligands **3.1** (Figure 3.3) and **3.2** (Figure 3.4) crystallise in the triclinic space group $P\bar{1}$ with no lattice solvent present. The most important feature of both pro-ligands **3.1** and **3.2** is the long C_{Cp} -P bond length (C(1)-P(1)). The C_{Cp} -P bond length of both **3.1** and **3.2** is significantly longer than the two C_{Phenyl} -P bond lengths of the PPh_2 moiety (**3.1** C_{Cp} -P = 1.890(3) vs C_{Phenyl} -P = 1.840(3) and 1.847(3) Å, and **3.2** C_{Cp} -P = 1.9494(16) vs C_{Phenyl} -P = 1.8361(15) and 1.8337(15) Å). These C_{Cp} -P bonds are also considerably longer than the C-P bonds reported for PPh_3 ($C-P_{(average)} = 1.831$ Å).^[22]

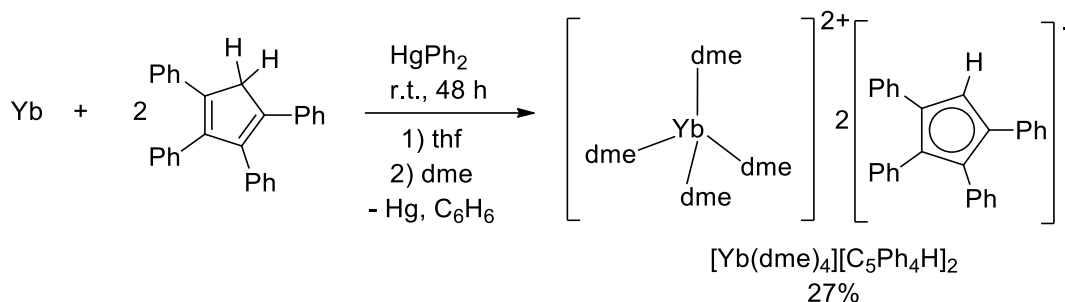
3.2.2 Carbon-phosphorus cleavage reactions to yield divalent octaphenyl lanthanocenes

With the successful report of C-P cleavage of **3.1** with activated europium metal, leading to the formation of the known complex $[\text{Eu}(\text{C}_5\text{Ph}_4\text{H})_2(\text{dme})] \cdot 1.5\text{dme}$ (**3.3**) (Scheme 3.13),^[5] this methodology was aimed to be expanded to form the corresponding samar- and ytterb-ocenes.



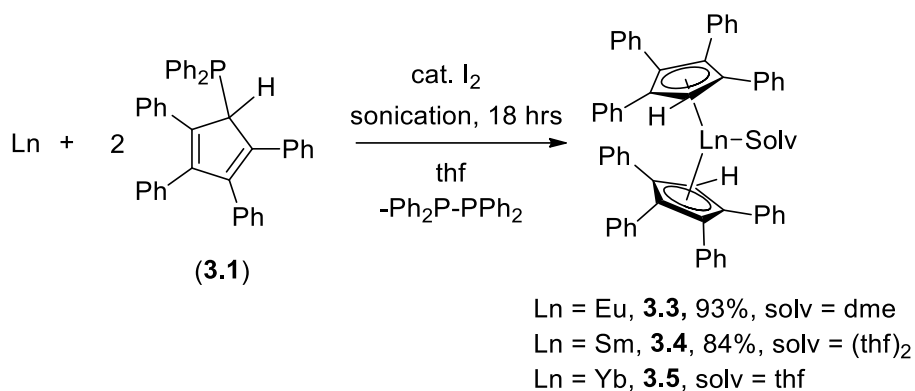
Scheme 3.13 – Synthesis of $[\text{Eu}(\text{C}_5\text{Ph}_4\text{H})_2(\text{dme})]$ by C-P cleavage of **3.1** to yield $[\text{Eu}(\text{C}_5\text{Ph}_4\text{H})_2(\text{dme})]$ (**3.3**) and $\text{PPh}_2\text{P-PPh}_2$.

Despite the successful synthesis of **3.3** in dme by C-P cleavage, analogous to the RTP synthesis of **3.3**, attempts to synthesise octaphenyl ytterbocene by RTP with diphenyl mercury (HgPh_2), tetraphenylcyclopentadiene ($\text{C}_5\text{Ph}_4\text{H}_2$), and ytterbium metal in dme resulted in the solvent separated ion pair (SSIP) $[\text{Yb}(\text{dme})_4][\text{C}_5\text{Ph}_4\text{H}]_2$ (Scheme 3.14).^[12] To avoid potential SSIP formation, the attempts of C-P cleavage of **3.1** were performed with samarium and ytterbium metal (and repeated with europium metal) in thf.



Scheme 3.14 – SSIP formation observed for the attempted synthesis of octaphenyl ytterbocene in dme by RTP.

Initial attempts of C-P cleavage involved dissolving one equivalent of **3.1** in thf, in the presence of two equivalents of Ln metal (Ln = Eu, Sm, and Yb), and a crystal of iodine, and sonicating the reaction mixture overnight (18 hours) (Scheme 3.15). During the first 4 hours of the reaction, a distinct colour change was observed as the solution progressed from a pale yellow colour into a dark orange colour. A small aliquot of the reaction mixture was removed after 18 hours, and the reaction progress followed by ^{31}P NMR spectroscopy.



Scheme 3.15 – Synthesis of octaphenyl europium, samarium, and ytterbium lanthanocenes by C-P cleavage of **3.1** in thf.

The ^{31}P NMR spectrum of the reaction mixture showed complete loss of the signal at 13.36 ppm corresponding to **3.1**, and only one signal observed at -14.6 ppm corresponding to the

coupled tetraphenyldiphosphine co-product $\text{Ph}_2\text{P-PPh}_2$.^[12] Once complete consumption of **3.1** was observed, the sonication was stopped, and the excess metal was allowed to settle, and the supernatant solution transferred to a new Schlenk flask by cannula filtration. The thf was removed under reduced pressure, and the resulting solids were washed with anhydrous hexanes to remove the formed $\text{Ph}_2\text{P-PPh}_2$ co-product and isolate the octaphenyl lanthanocenes. In the case of europium, the solids were then taken up into dme to crystallise **3.3**, whereas the samarium **3.4** and ytterbium **3.5** complexes were analysed as the thf adducts.

Identity of the paramagnetic **3.3** was confirmed by single crystal X-ray crystallography (by confirmation of a unit cell with the reported complex),^[5] alongside infrared spectroscopy, and an elemental analysis to confirm purity. Complex **3.4**, while paramagnetic, was confirmed by ^1H NMR spectroscopy (exhibiting considerable peak broadening and paramagnetic shifting), and infrared spectroscopy, producing spectra consistent with literature reports.^[5] Complex **3.5** was also confirmed by both infrared spectroscopy, and ^1H NMR spectroscopy, again, matching literature reports.^[4] The yields of **3.3** and **3.4** (93% and 84% respectively) are demonstrably higher than those reported by that of RTP reactions,^[5] with the added benefit of avoiding the use of mercurial reagents. Despite being isolated, **3.5** exhibited susceptibility to decomposition when dried under reduced pressure for long durations, and thus an accurate yield could not be obtained. Despite previous reports of $[\text{Sm}(\text{Cp}^x)_2]$ ($\text{Cp}^x = \text{C}_5\text{H}_3t\text{Bu}_2$ and C_5Me_5) complexes reacting with $\text{Ph}_2\text{P-PPh}_2$, complexes **3.3-3.5** exhibit stability in the presence of the co-product.^[23] From one reaction of **3.1** with Yb metal, a small crop of orange, needle-like crystals were obtained from the concentrated solution. Single crystal X-ray crystallography studies were undertaken, and the crystals were found to be of the iodo-ytterbium half sandwich species $[\text{Yb}(\text{C}_5\text{Ph}_4\text{H})\text{I}(\text{thf})_2]_2 \cdot 2\text{C}_6\text{D}_6$ (**3.5'**) (Figure 3.5). Owing to the limited yields, no further analysis was undertaken.

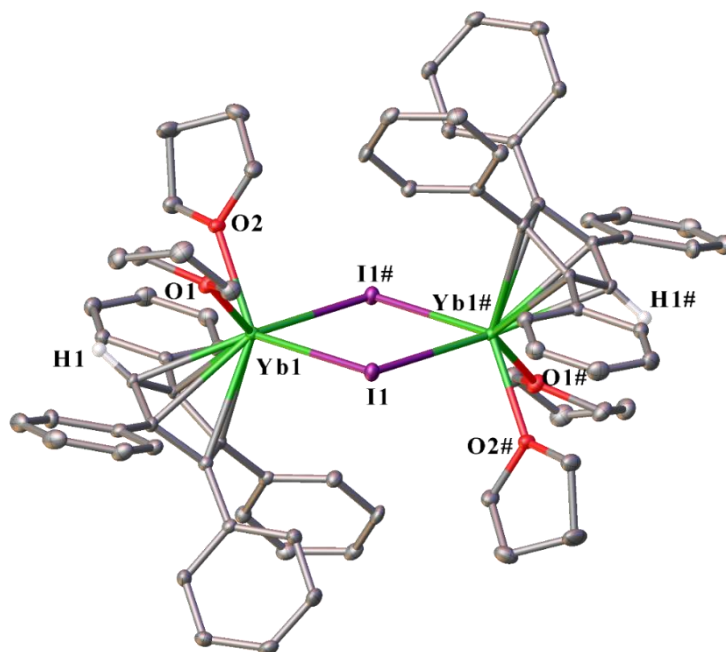
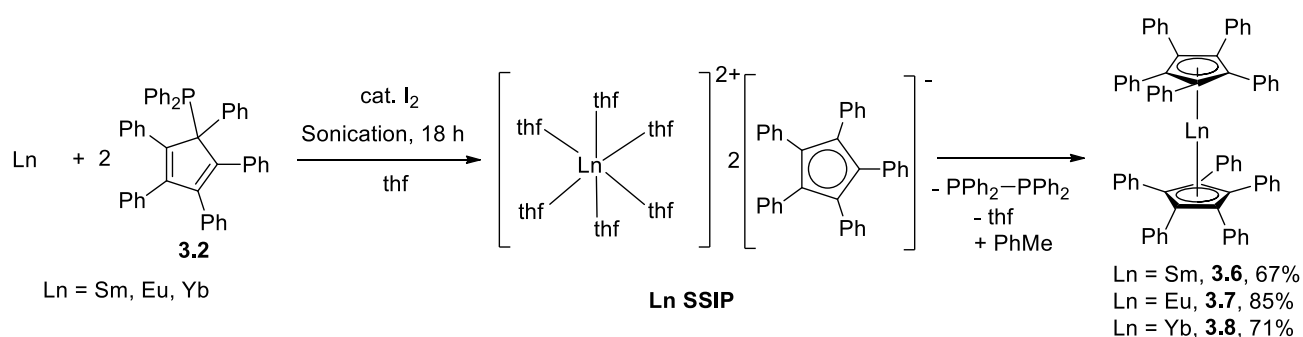


Figure 3.5 - ORTEP diagram of **3.5'** showing atom-numbering scheme for relevant atoms. Thermal ellipsoids are drawn at the 50% probability level. Phenyl hydrogen atoms and lattice C_6D_6 are omitted for clarity. # Generated by symmetry (symmetry operation used 1-X, 1-Y, 2-Z). Selected bond lengths (Å): Yb(1)-I(1) 3.1257(3), Yb(1)-I(1)# 3.1925(3), Yb(1)-C(centroid) 2.4748(14), Yb(1)-O(1) 2.450(2), Yb(1)-O(2) 2.403(2).

Complex **3.5'** crystallises in the triclinic space group $P\bar{1}$ containing half of the molecule in the asymmetric unit. It consists of two ytterbium centres in the same coordination environment, each with square based pyramidal geometries. Each ytterbium is coordinated η^5 to one $C_5Ph_4H^-$ moiety in the axial position, with two *cisoid* thf molecules, and two *cisoid* iodides, which bridge between the two ytterbium centres. The Yb-I bond lengths (3.1257(3) and 3.1925(3) Å) are consistent with the Yb-F (2.2516(19) and 2.2546(17) Å) and Yb-Br (2.8932(2) and 2.9216(3) Å) bond lengths of the analogous complexes after accounting for reduced ion size of the halides.^[13,14]

3.2.3 Carbon-phosphorus cleavage reactions to yield divalent decaphenyl lanthanocenes

When compared to the synthesis of octaphenyl metallocenes, the synthesis of decaphenyl metallocenes is significantly more challenging, owing to the limited solubility of these complexes in non-polar solvents.^[3–5,8] As the synthesis of divalent octaphenyl lanthanocenes by C-P cleavage proved to be a facile means of accessing them, the analogous divalent decaphenyl lanthanocenes were also sought to be synthesised by the C-P cleavage of **3.2** (Scheme 3.16).



Scheme 3.16 - Synthesis of decaphenyl samarium, europium, and ytterbium lanthanocenes by C-P cleavage of **3.2** in thf.

Whilst the formation of the SSIPs was aimed to be avoided with the octaphenyl lanthanocenes, in the case of the decaphenyl lanthanocenes, the formed SSIPs present a soluble alternative to the largely insoluble molecular metallocenes and can be handled during workup with less difficulty. The initial reactions with **3.2** were undertaken with the same reaction stoichiometry as those with **3.1**, in thf as a solvent and sonicated for 18 hours. Analysis of the reaction mixture by ^{31}P NMR spectroscopy after 18 hours showed complete consumption of **3.2**, and the formation of the $\text{Ph}_2\text{P-PPh}_2$ co-product. Interestingly, in some cases small amounts of PPh_2H were observed as a characteristic doublet (from ^{31}P - ^1H coupling) in the ^{31}P NMR spectra at -40 ppm. After confirmation by ^{31}P NMR spectroscopy, the reactions were stopped, and the excess metal allowed to settle before isolating the supernatant solution by cannula filtration

and removing the thf under reduced pressure. The solids were then washed with toluene, precipitating the metallocenes **3.6-3.8**. Initially, the supernatant toluene solution was removed in a concerted effort to also remove the Ph₂P-PPh₂ co-product, however, this significantly impacted the yields, as the metallocenes did exhibit some solubility in toluene. In later entries, the volume of toluene was reduced under reduced pressure after precipitating the metallocene, and then removed by filtration to facilitate removal of the Ph₂P-PPh₂ co-product, without drastically affecting the yield. Again, the yields of **3.6-3.8** from the C-P cleavage are comparable with those of the RTP reactions.^[4,5] Complexes **3.6-3.8** also exhibited stability in the presence of the Ph₂P-PPh₂ co-product.^[23]

Crystals of complexes **3.6** and **3.7** were grown from the slow cooling of hot toluene solutions (Figure 3.6 and Figure 3.7), whilst crystals of **3.8** were grown from the slow cooling of a hot C₆D₆ solution (Figure 3.8).

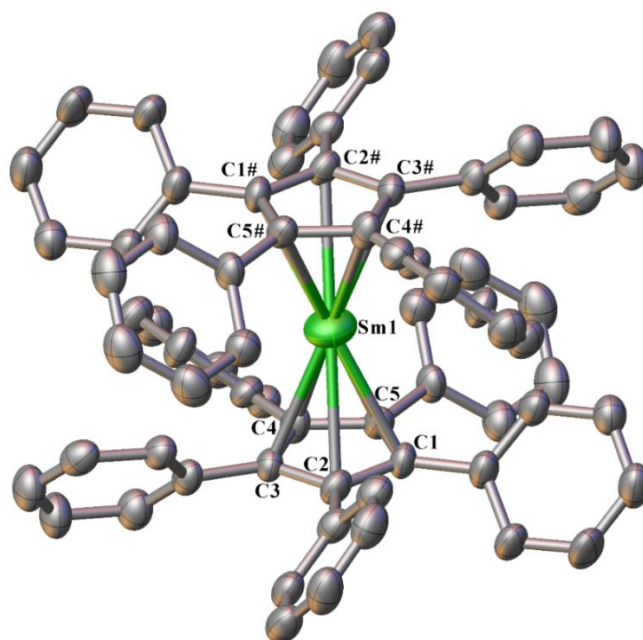


Figure 3.6 - ORTEP diagram of **3.6** showing connectivity and atom-numbering scheme for relevant atoms. Thermal ellipsoids are drawn at the 50% probability level. Phenyl hydrogen atoms and lattice toluene are omitted for clarity. # Generated by symmetry (symmetry operation used $-X, 1-Y, 1-Z$).

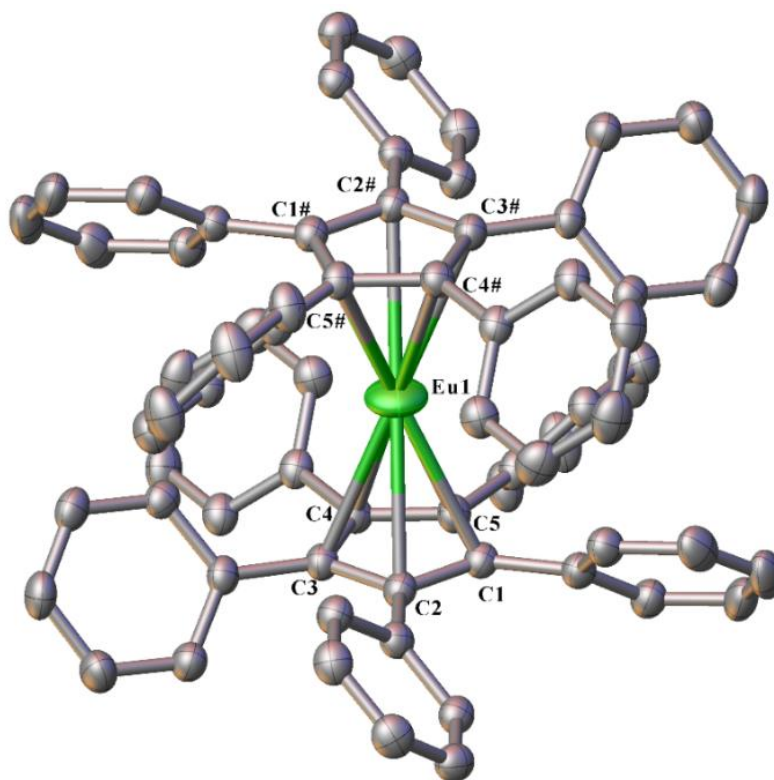


Figure 3.7 – ORTEP diagram of **3.7** showing atom-numbering scheme for relevant atoms. Thermal ellipsoids are drawn at the 50% probability level. Phenyl hydrogen atoms and lattice toluene are omitted for clarity. # Generated by symmetry (symmetry operation used 2-X, 1-Y, 1-Z).

Whilst only connectivity of complex **3.6** could be established from the X-ray crystal data, it is isomorphous with complex **3.7**, sharing the same space group ($P2_1/c$), unit cell dimensions, and both bearing one molecule of toluene in the lattice.

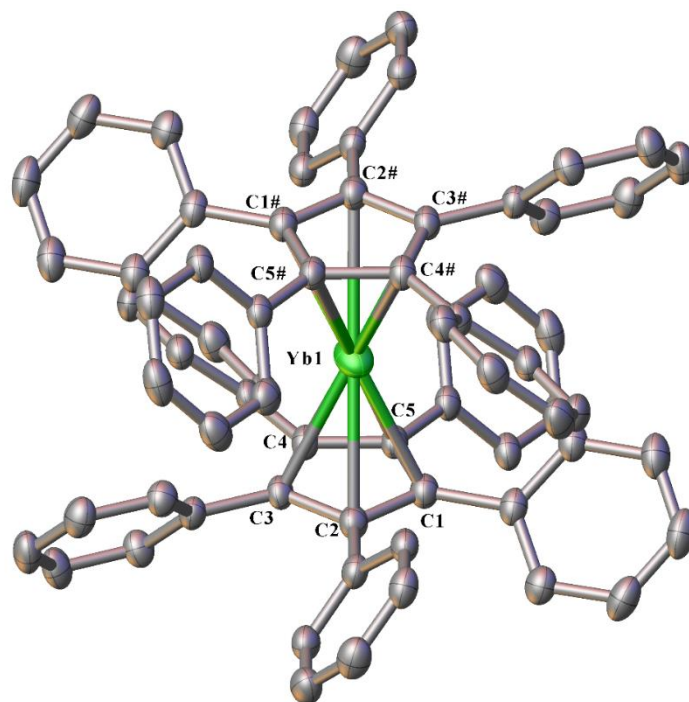


Figure 3.8 – ORTEP diagram of **3.8** showing atom-numbering scheme for relevant atoms. Thermal ellipsoids are drawn at the 50% probability level. Phenyl hydrogen atoms and lattice C_6D_6 are omitted for clarity. # Generated by symmetry (symmetry operation used $-X, 1-Y, 1-Z$).

Complex **3.8** crystallises in the triclinic space group $P\bar{1}$ bearing two half molecules in the asymmetric unit. There are 2.5 molecules of C_6D_6 in the lattice.

Complexes **3.6-3.8** all exhibit a high degree of symmetry, each displaying a parallel planar cyclopentadienyl arrangement, with a $Cn(1)-M(1)-Cn(1^\#)$ angle of 180° . The phenyl rings about the cyclopentadienyl moiety are angled in a propeller formation. Despite reported structures of decaphenyl-europocene and -ytterbocene being free of solvent of crystallisation, the bond parameters of **3.7** and **3.8** are in accordance with these previous reports.^[4,5] Similar to the Cp^{BIG} complexes of divalent lanthanoids reported by Harder, the metal centres in complexes **3.6-3.8** exhibit high displacement factors parallel to the ring planes, as a result of the metal being slightly disordered within a plane parallel to the Cp rings.^[6]

3.2.4 Altered conditions for the carbon-phosphorus cleavage of pentaphenylcyclopentadienyldiphenylphosphine

Despite the success of the C-P cleavage reactions with lanthanoid metals under the outlined conditions, there still existed potential for further improvements. The two major optimisations to be explored for the synthesis of decaphenyl lanthanocenes involved use of toluene as a solvent, so as to avoid the formation of the lanthanoid SSIP and directly form the lanthanoid sandwich complex, and secondly to attempt the reactions without iodine activation.

Initial reactions in toluene as a solvent were undertaken with **3.2** and europium metal, with iodine activation, and stirring for 18 hours. Owing to the luminescent properties of **3.7**, the initiation of the reaction could be qualitatively observed by exposing the reaction mixture to a blue light (~405 nm), with an orange emission confirming the formation of the europium sandwich complex. The ^{31}P NMR spectrum of the crude reaction mixture after 18 hours showed two signals: the expected singlet of $\text{Ph}_2\text{P-PPh}_2$ at -14.6 ppm, and a second signal at 39.4 ppm, and complete consumption of **3.2**. The resonance at 39.4 ppm was concluded to be PPh_2I ,^[24] and had not been observed for any of the prior reactions performed in thf.

Owing to the insolubility of both **3.7** and the excess europium metal in toluene, the workup to isolate **3.7** proved complicated, involving removing the toluene under reduced pressure before dissolving the solids in thf to isolate the SSIP, and then precipitating the sandwich complex from toluene, defeating the purpose of using toluene to begin with. Exploration of toluene as a solvent was discontinued, however, the formation of the PPh_2I side-product was further investigated. Thought to be a result of preferential reaction of the I_2 with **3.2** instead of the metal, the reaction of **3.2** with stoichiometric I_2 in the absence of metal was undertaken in both thf and toluene in an attempt to identify the resulting Cp containing compound and assess if its formation was critical to the mechanism. Both reactions observed complete consumption of

the **3.2** starting material after sonicating overnight, as observed by loss of the signal at 9.75 ppm in the ^{31}P NMR spectra, however depending on the solvent used, two different signals were observed. In toluene, a signal similar to that of the PPh_2I signal was observed at 37.96 ppm with the same coupling, whilst in thf a broad singlet at 30.45 ppm was observed.

Crystals were isolated from the toluene reaction mixture after exposure to air and analysed by X-ray diffraction studies. The compound was identified as the cationic 1,2,3,4,5-pentaphenylpyrylium cation, with a triiodide counter ion (Figure 3.9). The formation of pyrylium cations is possible when acidic solutions of substituted cyclopentadienes are exposed to atmospheric oxygen.^[25]

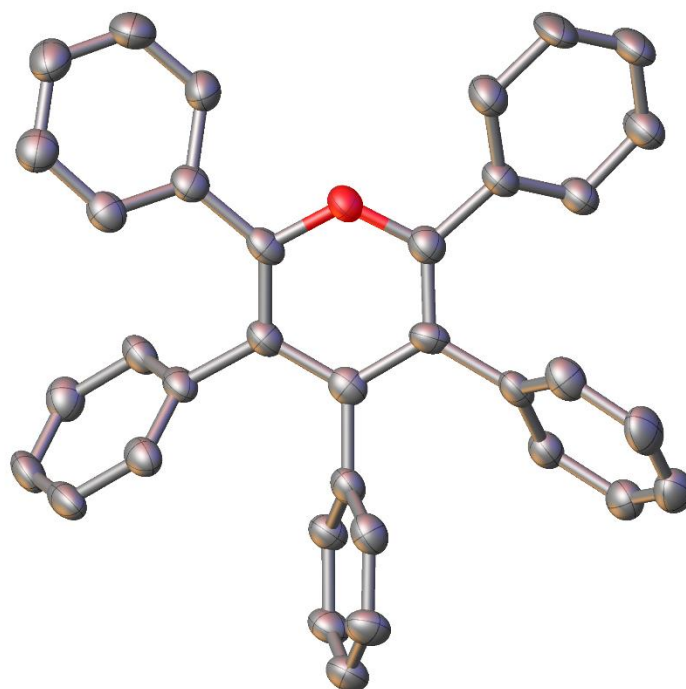


Figure 3.9 – ORTEP diagram of the isolated pyrylium cation from reaction of **3.2** with I₂ in toluene, then exposure to air. Hydrogen atoms, the triiodide anion and lattice toluene removed for clarity.

While no crystalline material could be isolated from the reaction in thf, in an effort to assess whether the I₂ reacting with **3.2** was a fundamental step in the C-P cleavage, ytterbium metal was added to the reaction mixture, and sonicated overnight. Analysis of the crude reaction mixture by ³¹P NMR spectroscopy showed no signals whatsoever, with complete loss of the signal at 30.45 ppm, but also no signs of Ph₂P-PPh₂. This instead suggested the formation of some paramagnetic Yb³⁺ species and inferred that the I₂ added at the beginning of the reaction did not influence the pathway of the C-P cleavage.

Lastly, a reaction was undertaken with ytterbium metal, and **3.2** in thf with no iodine. The reaction mixture was sonicated for 18 hours, and the crude reaction mixture analysed by ³¹P NMR spectroscopy, showing a very small amount of conversion of **3.2** to the Ph₂P-PPh₂ co-

product. The reaction was continued for 96 hours total, at which point full conversion was achieved. The sandwich complex could then be isolated by drying the SSIP and precipitating from toluene. Analogous reactions were undertaken with europium and samarium metal, with europium working effectively, but no C-P cleavage was observed in the case of samarium.

3.2.5 Attempted synthesis of group 2 decaphenyl metallocenes by C-P cleavage

Group 2 metals possess remarkable similarities with divalent lanthanoid metal ions, and so it was of great interest to determine if they would undergo C-P cleavage in a similar fashion to the divalent lanthanoid metals used. Utilising the same reaction conditions, **3.2** and the group 2 metal (M = Mg, Ca, Sr, Ba) were suspended in thf with a crystal of iodine for activation and sonicated overnight. All four crude reaction mixtures were analysed by ^{31}P NMR spectroscopy to follow the reaction progress, and whilst all four showed complete consumption of **3.2**, interestingly, only the magnesium reaction mixture exhibited formation of solely the $\text{Ph}_2\text{P-PPh}_2$ co-product. The other three metals (Ca, Ba, Sr) displayed broad singlets at approximately -18, -13, and -16 ppm respectively, possibly corresponding to diamagnetic $[\text{M}(\text{PPh}_2)_2]$ species after metal insertion into the C-P bond.

The reaction mixtures were isolated from unreacted metal by cannula filtration, and the thf removed under reduced pressure. Solids were taken up into toluene to induce precipitation of the sandwich complex (if SSIP formation was occurring, as observed with the lanthanoid metals), however, only a white precipitate formed, which was determined to be hydrolysed pentaphenylcyclopentadiene. Despite the successful C-P cleavage of the starting material **3.2**, no complexes were isolated. Further investigation into the synthesis of the group 2 metallocenes was not pursued due to time constraints.

3.2.6 Attempted synthesis of trivalent pentaphenylcyclopentadienyl complexes

Whilst samarium, europium and ytterbium metals can readily access both the divalent, and trivalent states, only the divalent metallocene complexes were isolated when synthesised by C-P cleavage of both **3.1** and **3.2**. Therefore, it was of interest to determine if metals that cannot easily access the +2 oxidation state a) would be able to undergo C-P cleavage in the same manner as samarium, europium and ytterbium, and b) whether the bulky pentaphenylcyclopentadienyl ligand could stabilise these metals in the divalent state, or form charge separated trivalent complexes. Three metals were selected as a basis for this study, lanthanum, neodymium, and thulium, representing a range of ionic radii.

The same reaction conditions were employed with these metals as previously described, using one equivalent of **3.2**, with two equivalents of metal, and a catalytic amount of I₂ in thf, and sonicating overnight (except in the case of thulium, which was stirred). The ³¹P NMR spectra of the crude reaction mixtures were analysed to monitor the reaction progress. After 18 hours, the reaction with La metal showed the expected signal at -14.6 ppm corresponding to the coupled Ph₂P-PPh₂ co-product, alongside a second signal at 98.53 ppm. Whilst this second signal was not assignable, most importantly the ³¹P NMR spectrum showed complete consumption of the starting material **3.2**, signifying the C-P cleavage was successful.

The reaction with Nd metal was similar, in that complete consumption was observed after sonicating for 18 hours, and the Ph₂P-PPh₂ product was observed in the ³¹P NMR spectrum, again at -14.6 ppm, alongside a very small, broad signal at -15.82 ppm. Again, this second signal was not assigned, but the consumption of **3.2** showed the reaction had proceeded to completion.

Lastly, the attempt with Tm metal was undertaken. Whilst sonication proved effective for the C-P cleavage with other metals, owing to the potential formation of a divalent Tm(II) complex,

and the likely instability of this complex, the reaction mixture was stirred overnight rather than sonicated to avoid complications with decomposition or undesired side reactions. The ^{31}P NMR spectrum of the crude reaction mixture after 18 hours only showed partial conversion of the starting material **3.2** to the $\text{Ph}_2\text{P-PPh}_2$ co-product ($\sim 40\%$ by NMR). The deep magenta coloured solution was allowed to continue stirring for a further 24 hours, however, after this time the colour of the solution had faded to a pale brown, suggesting oxidation to Tm^{3+} . The solution was isolated by filter cannula and concentrated before leaving to stand. Crystals grew at room temperature and were analysed by XRD and identified to be the dinuclear thulium phosphinato iodide complex $[\text{Tm}(\text{O}_2\text{PPh}_2)\text{I}_2(\text{thf})_2]_2$ (Figure 3.10), seemingly after exposure to some oxygen. Further attempts to synthesise the thulium analogue were not made due to time constraints.

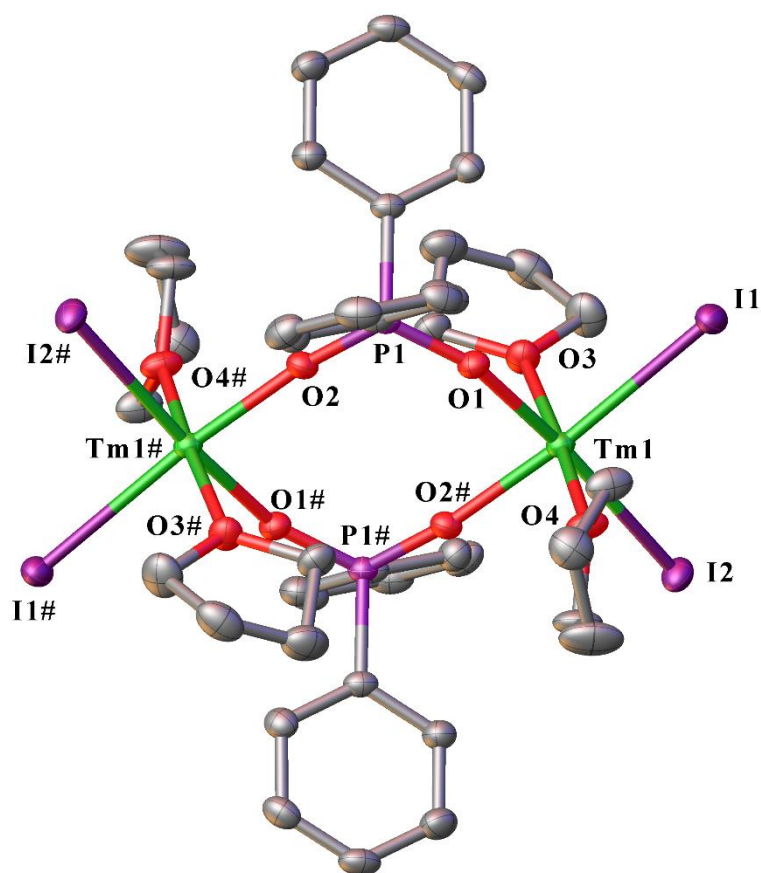


Figure 3.10 – ORTEP diagram of $[\text{Tm}(\text{O}_2\text{PPh}_2)\text{I}_2(\text{thf})_2]_2$ isolated from attempted synthesis of a pentaphenyl thulium sandwich complex. Atom-numbering scheme is shown for relevant atoms. # Generated by symmetry (Symmetry operation used (1-X, 1-Y, 1-Z).

$[\text{Tm}(\text{O}_2\text{PPh}_2)\text{I}_2(\text{thf})_2]_2$ crystallises in the orthorhombic space group $Pbca$, with half of the complex in the asymmetric unit. It is composed of two octahedral Tm^{3+} metal centres, each with two equatorial, terminal iodide ligands bound in a *cisoid* fashion, two thf molecules coordinated in the axial positions, and two diphenylphosphinato ligands which bridge the two thulium centres through the oxygen atoms.

The reaction mixtures of the La and Nd reactions were left to stand, allowing the solids to settle, and the supernatant solution isolated by filter cannula. The thf was then removed under reduced pressure, and the solids taken up into toluene to attempt to precipitate the product. In

both cases, this led to the deposition of a grey solid, whilst the supernatant solutions were pale yellow/green in colour. The supernatant solutions were isolated by filter cannula in an attempt to grow crystals, whilst the grey solids proved insoluble in both toluene, and thf. No crystals were obtained from either solution and further attempts were not undertaken.

3.2.7 Reaction monitoring by ^{31}P NMR spectroscopy and trapping studies with $\text{C}_6\text{F}_5\text{H}$

The carbon-phosphorus bond cleavage proved an effective means of synthesising bulky polyarylcyclopentadienyl complexes of samarium, europium and ytterbium, however, the precise mechanism of the cleavage was unknown. To further understand the mode of action, and hence understand the formation of the $\text{Ph}_2\text{P-PPh}_2$ product, several subsequent reactions were undertaken.

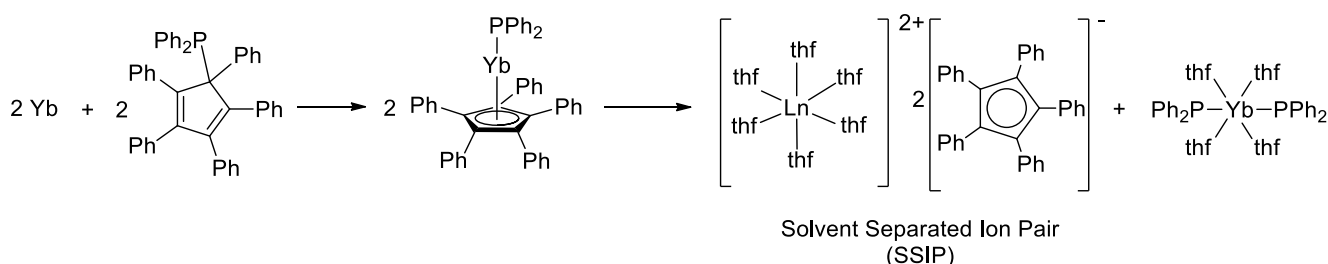
Initially, two plausible routes were postulated: a) a single electron transfer from the metal onto the cyclopentadiene moiety, subsequently leading to homolytic C-P bond cleavage, yielding the C_5Ph_5 anion and the formation of a $\text{PPh}_2\cdot$ radical, or b) by oxidative insertion of the lanthanoid metal into the C-P bond, followed by ligand redistribution to yield the sandwich complex. The radical pathway was thought to be the most likely, as the formation of the $\text{PPh}_2\cdot$ radical explains the formation of the $\text{Ph}_2\text{P-PPh}_2$ co-product as a result of radical self-coupling. The observed formation of PPh_2H also supported the proposed radical pathway, forming as a result of the $\text{PPh}_2\cdot$ abstracting a proton from surrounding solvent. Reactions were undertaken with ytterbium metal, **3.2**, and activated with iodine and sonicated for 18 hours as per the established method.

In order to assess the proposed radical pathway, a radical trapping experiment was trialled with 2,2,6,6-tetramethylpiperidine 1-oxyl radical (TEMPO) in an effort to form and isolate a diphenylphosphine radical coupled adduct. Using the above reaction conditions, alongside one molar equivalent of TEMPO, the solution was sonicated for 18 hours. Analysis of the reaction

mixture by ^{31}P NMR spectroscopy displayed no inhibition of reaction progress, and no resonance corresponding to a diphenylphosphine TEMPO adduct. Complete consumption of **3.2** was still achieved, and only the coupled diphosphine $\text{Ph}_2\text{P}-\text{PPh}_2$ was observed. After workup, the ytterbium sandwich was isolated with a yield of 67%, suggesting no inhibition of the reaction progress.

Secondly, the reaction was again attempted with the standard reaction conditions of ytterbium metal (activated with iodine) with **3.2** in $\text{thf}-d_8$, to see if the $\text{PPh}_2\cdot$ radical would instead abstract deuterium from the solvent to yield PPh_2D , which could be easily detected by ^{31}P NMR spectroscopy as a triplet rather than a doublet. After sonicating for 18 hours, an aliquot was removed and the ^{31}P NMR spectrum was collected, showing only a broad singlet at -2.49 ppm, and an absence of $\text{Ph}_2\text{P}-\text{PPh}_2$ and both PPh_2H and PPh_2D . The broad singlet was identified as $[\text{Yb}(\text{PPh}_2)_2(\text{thf})_4]$, a reported ytterbium phosphide species.^[26]

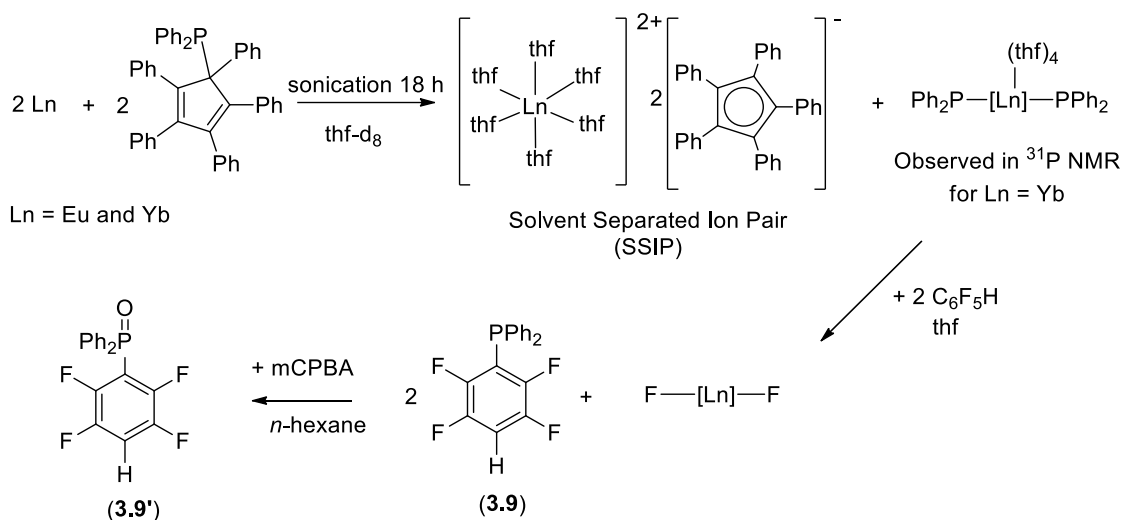
The detection of this ytterbium phosphide species supported the second postulated mechanism, whereby the ytterbium metal oxidises and inserts into the C-P bond. This would yield an $[\text{Yb}(\text{C}_5\text{Ph}_5)(\text{PPh}_2)]$ intermediate, which could undergo redistribution resulting in the detected $[\text{Yb}(\text{PPh}_2)_2(\text{thf})_4]$ and the SSIP (Scheme 3.17).



Scheme 3.17 – Proposed oxidative insertion mechanism of Yb with **3.2** yielding the detected $[\text{Yb}(\text{PPh}_2)_2(\text{thf})_4]$ species.

Owing to the basic nature of the PPh_2^- anionic ligands, the formation of PPh_2H was instead attributed to small amounts of unreacted $\text{C}_5\text{Ph}_5\text{H}$ present in the starting material (**3.2**), that would readily undergo protolysis with the $[\text{Yb}(\text{PPh}_2)_2(\text{thf})_4]$ complex, forming another equivalent of the SSIP, and PPh_2H . However, the formation of the $\text{Ph}_2\text{P}-\text{PPh}_2$ product was still not clear and remains under investigation. A radical process for this step has not been entirely discounted, as precedents of E-E bond formation (E = N, P, As) have been reported from similar bismuth complexes.^[27]

While the reaction progress for the ytterbium analogues could easily be followed by ^{31}P NMR, this method is not possible for the paramagnetic europium species. As such, to confirm the mechanism for the europium analogues, an alternative confirmation of the $[\text{Ln}(\text{PPh}_2)_2(\text{thf})_x]$ species had to be performed. A trapping reaction was developed using the ytterbium reaction with **3.2** to set a precedent which could be extended to the europium reaction with **3.2**, utilising pentafluorobenzene ($\text{C}_6\text{F}_5\text{H}$). Addition of $\text{C}_6\text{F}_5\text{H}$ to the reaction mixture containing $[\text{Yb}(\text{PPh}_2)_2(\text{thf})_4]$ immediately formed a precipitate $[\text{YbF}_2(\text{thf})_x]$ and *p*-tetrafluorophenyl diphenylphosphine ($\text{PPh}_2(\text{C}_6\text{F}_4\text{H})$) (**3.9**). This compound was found to be air and/or moisture sensitive, so it was subsequently oxidised with mCPBA to form the air stable phosphine oxide ($\text{O}=\text{PPh}_2(\text{C}_6\text{F}_4\text{H})$) (**3.9'**) (Scheme 3.18) for further characterisation by mass spectrometry. Extension of this trapping procedure to the analogous europium reaction also provided both **3.9** and **3.9'**, confirming the formation of $[\text{Eu}(\text{PPh}_2)_2(\text{thf})_x]$, and thus the same mechanism.



Scheme 3.18 – Trapping reaction of $[\text{Ln}(\text{PPh}_2)_2(\text{thf})_x]$ (Ln = Yb and Eu) with $\text{C}_6\text{F}_5\text{H}$.

The identities of **3.9** and **3.9'** were confirmed by ^1H , ^{19}F and ^{31}P NMR spectroscopy, alongside mass spectrometry (Figure 3.11).

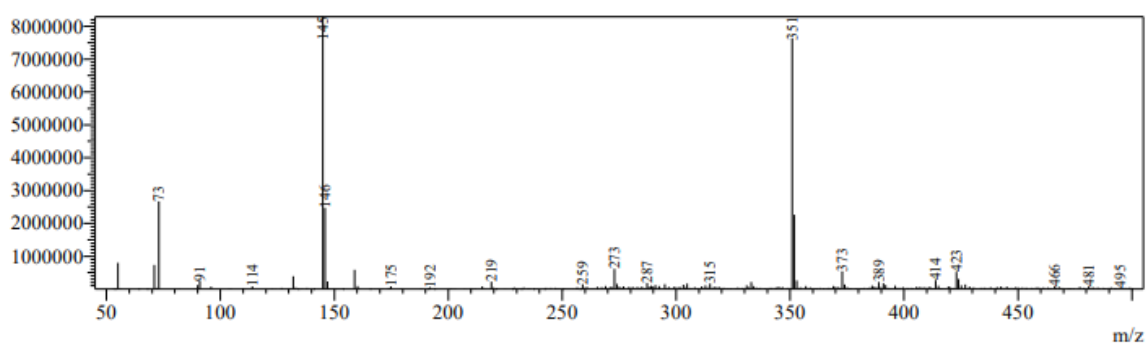


Figure 3.11 – Mass spectrum of $\text{O}=\text{PPh}_2(\text{C}_6\text{F}_4\text{H})$ (**3.9'**) showing M+1 peak of **3.9'** at 351 m/z.

3.3 Conclusion

A new synthetic method has been developed to afford divalent lanthanoid sandwich complexes with bulky tetra- and penta-phenylcyclopentadienyl ligands. Two new tetra- and penta-phenylcyclopentadienyldiphenylphosphine pro-ligands, **3.1** and **3.2** respectively, have been synthesised, which are capable of undergoing selective carbon-phosphorus bond cleavage when treated with a range of lanthanoid or group 2 metals. This carbon-phosphorus bond cleavage of **3.1** was employed to synthesise three known tetraphenylcyclopentadienyl sandwich complexes of Eu (**3.3**), Sm (**3.4**) and Yb (**3.5**). The heteroleptic ytterbium iodide half-sandwich species (**3.5'**) was also isolated when additional iodine was added during the synthesis of **3.5**. This synthetic route was further extended to the carbon-phosphorus bond cleavage of **3.2**, yielding the pentaphenylcyclopentadienyl sandwich complexes of Sm (**3.6**), Eu (**3.7**) and Yb (**3.8**). Single crystal X-ray diffraction studies of **3.7** and **3.8** showed that they differed from previous reports, in that they bear lattice solvent, whilst prior reports are free from lattice solvent. Group 2 metals, and other lanthanoid metals were shown to cleave the carbon-phosphorus bond of **3.2**, however no complexes of these metals were able to be isolated. The mechanism of the carbon-phosphorus bond cleavage of **3.2** was also studied by ^{31}P NMR spectroscopy, and further trapping reactions with pentafluorobenzene. When **3.2** was treated with Yb metal in thf- d_8 , the ytterbium phosphide species $[\text{Yb}(\text{PPh}_2)_2(\text{thf})_4]$ was detected, suggesting that the ytterbium metal undergoes oxidative insertion into the long C-P bond of **3.2** before undergoing redistribution to yield theSSIP and $[\text{Yb}(\text{PPh}_2)(\text{thf})_4]$. Furthermore, treatment of the $[\text{Yb}(\text{PPh}_2)_2(\text{thf})_4]$ with pentafluorobenzene yielded the substituted $\text{PPh}_2(\text{C}_6\text{F}_4\text{H})$ species (**3.9**), which could be oxidised with mCPBA to yield the air stable phosphine oxide derivative $\text{O}=\text{PPh}_2(\text{C}_6\text{F}_4\text{H})$ (**3.9'**). Owing to the paramagnetic nature of europium complexes, NMR studies could not be used to gain insight into the mechanism, and as such, this same trapping study was used to determine that an $[\text{Eu}(\text{PPh}_2)(\text{thf})_x]$ species was

forming, as treatment of the reaction mixture of Eu and **3.2** with pentafluorobenzene also yielded **3.9**. The C-P activation pathway has proven to be an effective means of accessing divalent polyarylcyclopentadienyl complexes of lanthanoid metals, however, there is still opportunity for extension of the synthetic route to be refined and applied to the synthesis of group 2 metallocenes, the formation of trivalent lanthanoid cyclopentadienyl complexes, alongside furthering the scope to include other ligand subsets which can utilise a C-P cleavage pathway to access their corresponding complexes.

3.4 Experimental

For materials and general procedures, see Appendix One.

3.4.1 Syntheses

Tetraphenylcyclopentadienyldiphenylphosphine ($C_5Ph_4HPPh_2$) (**3.1**)

A Schlenk flask equipped with a magnetic stirrer bar was charged with tetraphenylcyclopentadiene (0.50 g, 1.35 mmol) in anhydrous diethyl ether (5 mL). *n*BuLi (2.5 M in hexanes) (0.76 mL, 1.9 mmol, 1.4 equivalents) was added slowly, and stirred overnight. To the resulting suspension was added PPh_2Cl (0.36 mL, 1.9 mmol, 1.4 equivalents) and stirred for four hours. The solvent was then removed under reduced pressure, and the residue taken up into toluene (5 mL) before isolating the supernatant solution by filter cannula. The solvent was again removed under reduced pressure, and the solid washed with hexane (2 x 5 mL) yielding an off-white powder (0.64 g, 1.15 mmol, 85%) Colourless crystals of **3.1** were grown from anhydrous diethyl ether. *Anal.* Calc. for $C_{41}H_{31}P$: C, 88.77; H, 5.63. Found: C, 88.84; H, 5.60%. 1H NMR (300 MHz, C_6D_6 , 25 °C): δ 7.48 (m, 4H, ArH), 7.29 (m, 4H, ArH), 7.04-6.88, (m, 20H, ArH), 6.87-6.81 (m, 2H, ArH), 5.36 (d, $J = 0.41$ Hz, 1H, CpH). ^{13}C NMR (101 MHz, C_6D_6 , 25 °C) δ 144.69 (s), 142.99 (s), 136.85 (s), 135.95 (s), 134.24 (d, $J = 21.6$ Hz), 133.53 (d, $J = 22.0$ Hz), 130.01 (s), 129.65 (s), 128.49 (s), 126.39 (d, $J = 24.7$ Hz). 57.02 (d, $J = 32.8$ Hz). ^{31}P (162 MHz, C_6D_6 , 25 °C): δ 13.36 (s). IR (Nujol, cm^{-1}): 2727 w, 1573 w, 1538 w, 1304 m, 1260 s, 1157 m, 1090 m, 1070 m, 1025 s, 919 w, 836 vs, 798s, 777 w, 756 m, 695 s.

Pentaphenylcyclopentadienyldiphenylphosphine ($C_5Ph_5PPh_2$) (**3.2**)

A Schlenk flask equipped with a magnetic stirrer bar was charged with pentaphenylcyclopentadiene (1.0 g, 2.24 mmol) and suspended in diethyl ether (10 mL). *n*BuLi (2.0 M in hexanes) (1.35 mL, 2.70 mmol, 1.2 equivalents) was added slowly and the mixture

was stirred overnight. To this suspension was added PPh_2Cl (0.5 mL, 2.70 mmol, 1.2 equivalents) and stirred overnight. The off-white suspension was allowed to settle, and the supernatant solution was removed by filter cannula. The solids were dried under reduced pressure, washed with anhydrous hexane (2 x 5 mL), and then taken up into anhydrous toluene (10 mL). The resulting suspension was heated until a deep purple solution had formed, and then the solution was separated from the remaining solid by filter cannula. The solvent was evaporated under reduced pressure, yielding a pale purple solid, which was washed with anhydrous hexanes (2 x 5 mL) yielding a pale yellow solid (1.30 g, 2.06 mmol, 92%). Colourless crystals of **3.2** were grown from the slow cooling of a hot toluene solution. *Anal.* Calc. for $\text{C}_{47}\text{H}_{35}\text{P}$: C, 89.50; H, 5.59. Found: C, 89.52; H, 5.716%. ^1H NMR (300 MHz, C_6D_6 , 25 °C): δ 8.23 (br d, $J = 5.81$, 2H, ArH), 7.72 (tt, 4H, ArH), 7.22-7.16 (m, 6H, ArH), 6.99-6.80 (m, 17H, ArH), 6.73-6.70 (m, 6H, ArH). ^{13}C NMR (101 MHz, C_6D_6 , 25 °C) δ 150.36 (s), 145.92 (s), 140.40 (d, $J = 14.4$ Hz), 137.33 (d, $J = 16.9$ Hz), 135.90 (d, $J = 20.9$ Hz), 134.92 (d, $J = 20.9$ Hz), 131.64 (s), 131.27 (s), 130.36 (d, $J = 17.2$ Hz), 129.52 (s), 129.36 (d, $J = 2.4$ Hz), 127.99 (s), 127.28 (d, $J = 27.1$ Hz). ^{31}P NMR (162 MHz, C_6D_6 , 25 °C) δ 9.75 (s). IR (Nujol, cm^{-1}): 2332 w, 1946 m, 1884 m, 1811 m, 1757 w, 1595 s, 1571 s, 1459 s, 1377 m, 1340 w, 1276 w, 1260 w, 1178 m, 1162 w, 1152 w, 1095 m, 1027 s, 1009 w, 919 m, 849 m, 802 s, 778 w, 760 m, 691 m, 617 m, 587 m, 562 m.

[Eu(C₅Ph₄H)₂(dme)]·1.5dme (3.3)

Freshly filed europium metal (0.100 g, 0.658 mmol) was added to a Schlenk flask containing $\text{C}_5\text{Ph}_4\text{HPPH}_2$ (**3.1**) (0.055 g, 0.10 mmol). Anhydrous thf (5 mL) and a crystal of iodine, to activate the metal, were added, and the suspension sonicated for 18 hours. The resulting suspension was left to settle, and the solution removed by filter cannula and evaporated to dryness under reduced pressure, yielding an orange solid. The solid was washed with

Chapter Three

anhydrous hexane (2 x 5 mL), yielding **3.3** as a bright orange powder (0.042 g, 93%). Bright orange crystals of **3.3** were grown from a dme solution at 4 °C, confirming the unit cell.^[5] *Anal.* Calc. for C₆₈H₆₇O₅Eu: C, 73.17; H, 6.05. Found: C, 72.65; H, 6.00%. IR (Nujol, cm⁻¹): 3057 w, 2355 w, 2311 w, 1962 w, 1594 s, 1578 m, 1534 m, 1506 w, 1495 w, 1305 m, 1260 vs, 1203 m, 1154 w, 1097 vs, 1078 m, 1069 s, 1046 vs, 1020 vs, 934 m, 916 m, 848 m, 799 vs, 757 s, 731 s, 700 s. Spectroscopic data were in agreement with those reported.^[5]

[Sm(C₅Ph₄H)₂(thf)₂] (**3.4**)

Prepared as per the synthesis of **3.3** but using Sm metal filings (0.100 g, 0.667 mmol) in place of Eu metal, yielding a dark red solid (0.037 g, 84%). ¹H NMR (300 MHz, C₆D₆, 25 °C): δ 20.53 (8H, s, ArH), 14.02 (8H, s, ArH), 11.15 (4H, s, ArH), 8.90 (8H, s), 7.55 (8H, s, ArH), 7.36 (4H, s, ArH), 4.90 (22H, m, thf CH₂), 0.81 (22H, m, thf CH₂), -6.55 (2H, s, CpH). IR (Nujol, cm⁻¹): 1595 m, 1508 m, 1306 w, 1261 w, 1166 w, 1072 w, 1026 w, 914 w, 790 w, 759 m, 737 m, 723 m, 696 s. Spectroscopic data were in agreement with those reported.^[5]

[Yb(C₅Ph₄H)₂(thf)] (**3.5**)

Freshly filed ytterbium metal (0.100 g, 0.578 mmol) was added to a Schlenk flask containing C₅Ph₄HPPH₂ (**3.1**) (0.055 g, 0.10 mmol). Anhydrous thf (5 mL) and a crystal of iodine, to activate the metal, were added, and the suspension sonicated for 18 hours. The resulting suspension was left to settle, and the solution removed by filter cannula and evaporated to a paste, but not to dryness. Anhydrous toluene (5 mL) was added and the solid precipitated at 4 °C. The supernatant solution was then removed. Owing to the susceptibility of **3.5** to decomposition when desolvated, the solid was not dried under reduced pressure, and thus an accurate yield could not be recorded. ¹H NMR (300 MHz, C₆D₆, 25 °C): δ 7.52 (4H, d, *J* = 7.5 Hz, ArH), 7.36 (2H, s, ArH), 7.30 (4H, d *J* = 7.7 Hz, ArH), 7.06 (24H, d, *J* = 7.1 Hz, ArH), 6.96 (6H, s, ArH), 6.72 (2H, s, CpH). IR (Nujol, cm⁻¹): 1596 m, 1509 w, 1307 w, 1260 w, 1132

m, 1071 m, 1025 m, 916 w, 790 w, 760 s, 723 s, 696 s. Spectroscopic data were in agreement with those reported, with slight chemical shift deviations due to influence of excess solvent.^[14]

[Yb(C₅Ph₄H)I(thf)₂]₂·2 C₆D₆ (3.5')

As per synthesis of **3.5** but using ca. 5 mg of I₂ (25 mol%), a small crop of crystals of **3.5'** were isolated from the mixture. Owing to the limited yield, only an X-ray crystal structure was obtained.

[Sm(C₅Ph₅)₂]₂·2 PhMe (3.6)

Freshly filed samarium (0.100 g, 0.667 mmol) was added to a Schlenk flask containing C₅Ph₅PPh₂ (**3.2**) (0.063 g, 0.10 mmol). To this Schlenk flask, 5 mL of anhydrous thf, and a crystal of iodine, to activate the metal were added, and the suspension sonicated for 18 hours. The resulting suspension was left to settle before isolating the supernatant liquid by a filtration cannula. The resulting filtrate was evaporated to dryness under reduced pressure, yielding a dark brown solid, and then taken up into anhydrous toluene (5 mL) to form **3.6** as an insoluble dark brown solid. The supernatant solution was concentrated to 2 mL, before removing by filter cannula, and drying the solid under reduced pressure. Dark red crystals of **3.6** were grown from a hot toluene solution (0.035g, 67%). ¹H NMR (300 MHz, C₆D₆, 25 °C): δ 11.46 (br s, 20H, ArH), 9.78 br s, 10H, ArH). IR (Nujol, cm⁻¹): 1594 m, 1501 m, 1309 w, 1261 w, 1154 w, 1076 m, 1026 m, 915 w, 840 w, 802 m, 778 m, 738 m, 700 s. Spectroscopic data were in agreement with those reported.^[5]

[Eu(C₅Ph₅)₂]₂·2 PhMe (3.7)

Method 1: Prepared as per the synthesis of **3.6** but using europium metal filings (0.100 g, 0.658 mmol) in place of samarium, and C₅Ph₅PPh₂ (**3.2**) (0.063 g, 0.10 mmol). Bright orange crystals of **3.7** were grown from a hot toluene solution (0.045 g, 85%). IR (Nujol, cm⁻¹): 1594 m, 1574

w, 1501 m, 1261 m, 1179 w, 1154 w, 1143 w, 1076 m, 1025 m, 914 m, 012 m, 778 m, 736 m, 702 s, 679 w. Spectroscopic data were in agreement with those reported.^[5]

Method 2: As per *Method 1*, however without addition of I₂. The reaction mixture was sonicated for 96 hours before complete consumption of **3.2** was observed by ³¹P NMR spectroscopy. Yielded **3.7** as a bright orange solid (0.042 g, 79%).

[Yb(C₅Ph₅)₂]·2.5 C₆D₆ (3.8**)**

Method 1: Freshly filed ytterbium metal (0.100 g, 0.578 mmol) was added to a Schlenk flask containing C₅Ph₅PPh₂ (**3.2**) (0.030 g, 0.048 mmol). To this Schlenk flask, 5mL of anhydrous thf, and a crystal of iodine, to activate the metal were added, and the suspension sonicated for 18 hours. The resulting suspension was left to settle before separating the supernatant liquid by a filtration cannula. The resulting filtrate was evaporated to dryness under reduced pressure, yielding a dark brown solid, which was then taken up into anhydrous toluene (5 mL) to form the desired sandwich as an insoluble dark green solid. The solvent was then removed under reduced pressure, and the solid washed with anhydrous hexane (2 x 5 mL) (0.018g, 71%). Dark green crystals of **3.8** were grown from a hot C₆D₆ solution. ¹H NMR (300 MHz, C₆D₆, 25 °C): δ 6.99 (m, 20H, ArH), 6.90 (m, 10H, ArH), 6.80 (m, 20H, ArH). IR (Nujol, cm⁻¹): 1594 m, 1574 w, 1501 m, 1307 w, 1155 w, 1075 m, 1026 m, 1013 m, 917 m, 862 m, 801 m, 776 m, 737 m, 722 m, 701 s, 678 w. Spectroscopic data were in agreement with those reported.^[4]

Method 2: As per *Method 1*, however without addition of I₂. The reaction mixture was sonicated for 96 hours before complete consumption of **3.2** was observed by ³¹P NMR spectroscopy. Yielded **3.8** as a dark brown solid (0.016 g, 65%).

3.4.2 Trapping reactions

Addition of C₆F₅H to [Ln(PPh₂)₂(thf)_x] to form PPh₂(C₆F₄H) (3.9**)**

To the crude reaction mixture (from treatment of Ln with **3.2**) containing [Yb(PPh₂)₂(thf)₄] (or [Eu(PPh₂)₂(thf)_x]) was added C₆F₅H (1 mL, excess). A precipitate of LnF₂ immediately formed. The resulting solution was isolated by a filter cannula, and the solvent and excess C₆F₅H removed under reduced pressure. The solid was analysed by ¹H, ¹⁹F and ³¹P NMR. ¹H NMR (400 MHz, C₆D₆, 25 °C) δ 7.41 (m, 5H, ArH), 7.02 (m, 5H, ArH), 6.20 (tt, 1H, C₆F₄H). ¹⁹F NMR (377 MHz, C₆D₆, 25 °C) δ -128.46 (m, 2F), -137.81 (m, 2F). ³¹P NMR (162 MHz, C₆D₆, 25 °C) δ -23.74 (tt).

Oxidation of PPh₂(C₆F₄H) to O=PPh₂(C₆F₄H) (3.9'**)**

The dried solid from the previous reaction was taken up into hexane (to remove it from [Ln(C₅Ph₅)₂]) and transferred into a Schlenk with excess mCPBA. The resulting solution was stirred overnight, and the crude reaction mixture analysed by ¹⁹F and ³¹P NMR. ¹⁹F NMR (377 MHz, C₆D₆, 25 °C) δ -128.74 (m, 2F), -136.19 (m, 2F). ³¹P NMR (162 MHz, C₆D₆, 25 °C) δ 22.08 (tt). MS (APCI) *m/z* Calc. for C₁₈H₁₁OF₄P (350.2 + 1). Found 351 (M⁺ + 1).

3.5 Crystal and refinement data

Tetraphenylcyclopentadienyldiphenylphosphine (C₅Ph₄HPPh₂) (3.1)

C₄₁H₃₁P (*M* = 554.63 g/mol): triclinic, space group $P\bar{1}$ (no. 2), *a* = 6.0760(12) Å, *b* = 12.198(2) Å, *c* = 19.747(4) Å, α = 92.67(3)°, β = 92.54(3)°, γ = 90.16(3)°, *V* = 1460.5(5) Å³, *Z* = 2, *T* = 100(2) K, μ (Synchrotron) = 0.123 mm⁻¹, *D*_{calc} = 1.261 g/cm³, 18649 reflections measured (3.342° ≤ 2 Θ ≤ 49.994°), 4789 unique (*R*_{int} = 0.1401, *R*_{sigma} = 0.1142) which were used in all calculations. The final *R*₁ was 0.0699 (*I* > 2 σ (*I*)) and *wR*₂ was 0.1903 (all data).

Pentaphenylcyclopentadienyldiphenylphosphine (C₅Ph₅PPh₂) (3.2)

C₄₇H₃₅P (*M* = 630.72 g/mol): triclinic, space group $P\bar{1}$ (no. 2), *a* = 9.1150(18) Å, *b* = 10.483(2) Å, *c* = 19.585(4) Å, α = 96.14(3)°, β = 90.06(3)°, γ = 115.02(3)°, *V* = 1683.8(7) Å³, *Z* = 2, *T* = 100(2) K, μ (Synchrotron) = 0.115 mm⁻¹, *D*_{calc} = 1.244 g/cm³, 49067 reflections measured (2.094° ≤ 2 Θ ≤ 51.358°), 6286 unique (*R*_{int} = 0.0473, *R*_{sigma} = 0.0208) which were used in all calculations. The final *R*₁ was 0.0443 (*I* > 2 σ (*I*)) and *wR*₂ was 0.1224 (all data).

[Yb(C₅Ph₄H)I(thf)₂]₂·2 C₆D₆ (3.5')

C₉₈H₈₆D₁₂I₂O₄Yb₂ (*M* = 1951.64 g/mol): triclinic, space group $P\bar{1}$ (no. 2), *a* = 11.9588(2) Å, *b* = 12.29030(10) Å, *c* = 14.33660(10) Å, α = 88.2270(10)°, β = 80.3900(10)°, γ = 82.4170(10)°, *V* = 2059.33(4) Å³, *Z* = 1, *T* = 123(2) K, μ (CuK α) = 10.367 mm⁻¹, *D*_{calc} = 1.564 g/cm³, 41407 reflections measured (7.256° ≤ 2 Θ ≤ 140.064°), 7811 unique (*R*_{int} = 0.0722, *R*_{sigma} = 0.0447) which were used in all calculations. The final *R*₁ was 0.0340 (*I* > 2 σ (*I*)) and *wR*₂ was 0.0868 (all data).

[Sm(C₅Ph₅)₂]·PhMe (3.6)

C₈₄H₆₆Sm (*M* = 1225.71 g/mol): monoclinic, space group *P*2₁/*c* (no. 14), *a* = 10.481(2) Å, *b* = 17.845(4) Å, *c* = 16.322(3) Å, *β* = 95.03(3)°, *V* = 3041.0(11) Å³, *Z* = 2, *T* = 100(2) K, *μ*(Synchrotron) = 1.013 mm⁻¹, *D*_{calc} = 1.339 g/cm³, 31042 reflections measured (3.388° ≤ 2 Θ ≤ 50.07°), 5119 unique (*R*_{int} = 0.2739, *R*_{sigma} = 0.1712) which were used in all calculations. The final *R*₁ was 0.1207 (*I* > 2 σ (*I*)) and *wR*₂ was 0.3250 (all data).

[Eu(C₅Ph₅)₂]·PhMe (3.7)

C₈₄H₆₆Eu (*M* = 1227.32 g/mol): monoclinic, space group *P*2₁/*c* (no. 14), *a* = 10.480(2) Å, *b* = 17.830(4) Å, *c* = 16.380(3) Å, *β* = 94.90(3)°, *V* = 3049.6(11) Å³, *Z* = 2, *T* = 100(2) K, *μ*(Synchrotron) = 1.076 mm⁻¹, *D*_{calc} = 1.337 g/cm³, 55676 reflections measured (3.384° ≤ 2 Θ ≤ 57.148°), 6700 unique (*R*_{int} = 0.0387, *R*_{sigma} = 0.0208) which were used in all calculations. The final *R*₁ was 0.0538 (*I* > 2 σ (*I*)) and *wR*₂ was 0.1493 (all data).

[Yb(C₅Ph₅)₂]·2.5 C₆D₆ (3.8)

C₉₇H₅₂D₁₅Yb (*M* = 1430.62 g/mol): triclinic, space group *P*1̄ (no. 2), *a* = 12.870(3) Å, *b* = 13.490(3) Å, *c* = 21.010(4) Å, *α* = 83.15(3)°, *β* = 87.83(3)°, *γ* = 79.75(3)°, *V* = 3563.4(13) Å³, *Z* = 2, *T* = 100(2) K, *μ*(Synchrotron) = 1.362 mm⁻¹, *D*_{calc} = 1.319 g/cm³, 61483 reflections measured (1.952° ≤ 2 Θ ≤ 50.696°), 12701 unique (*R*_{int} = 0.0264, *R*_{sigma} = 0.0205) which were used in all calculations. The final *R*₁ was 0.0361 (*I* > 2 σ (*I*)) and *wR*₂ was 0.0972 (all data).

3.6 References

- [1] P. S. Tanner, T. P. Hanusa, *Polyhedron* **1994**, *13*, 2417–2420.
- [2] H. M. Nicholas, D. P. Mills, *Encycl. Inorg. Bioinorg. Chem.* **2017**, 1–10.
- [3] C. M. Forsyth, G. B. Deacon, L. D. Field, C. Jones, P. C. Junk, D. L. Kay, A. F. Masters, A. F. Richards, *Chem. Commun.* **2006**, 1003–1005.
- [4] G. B. Deacon, C. M. Forsyth, F. Jaroschik, P. C. Junk, D. L. Kay, T. Maschmeyer, A. F. Masters, J. Wang, L. D. Field, *Organometallics* **2008**, *27*, 4772–4778.
- [5] R. P. Kelly, T. D. M. Bell, R. P. Cox, D. P. Daniels, G. B. Deacon, F. Jaroschik, P. C. Junk, X. F. Le Goff, G. Lemercier, A. Martinez, J. Wang, D. Werner, *Organometallics* **2015**, *34*, 5624–5636.
- [6] C. Ruspic, J. R. Moss, M. Schürmann, S. Harder, *Angew. Chem. Int. Ed.* **2008**, *47*, 2121–2126.
- [7] S. Harder, D. Naglav, C. Ruspic, C. Wickleder, M. Adlung, W. Hermes, M. Eul, R. Pöttgen, D. B. Rego, F. Poineau, K. R. Czerwinski, R. H. Herber, I. Nowik, *Chem. Eur. J.* **2013**, *19*, 12272–12280.
- [8] N. J. C. Van Velzen, S. Harder, *Organometallics* **2018**, *37*, 2263–2271.
- [9] M. P. Castellani, J. M. Wright, S. J. Geib, A. L. Rheingold, W. C. Trogler, *Organometallics* **1986**, *5*, 1116–1122.
- [10] M. P. Castellani, S. J. Geib, A. L. Rheingold, W. C. Trogler, *Organometallics* **1987**, *6*, 1703–1712.
- [11] M. P. Castellani, S. J. Geib, A. L. Rheingold, W. C. Trogler, *Organometallics* **1987**, *6*,

- 2524–2531.
- [12] D. P. Daniels, Substituted Cyclopentadienyl Chemistry of the Alkaline Earth and Rare Earth Elements, PhD Thesis, Monash University, **2011**.
- [13] G. B. Deacon, F. Jaroschik, P. C. Junk, R. P. Kelly, *Organometallics* **2015**, *34*, 2369–2377.
- [14] G. B. Deacon, F. Jaroschik, P. C. Junk, R. P. Kelly, *Chem. Commun.* **2014**, *50*, 10655–10657.
- [15] F. Alonso, I. P. Beletskaya, M. Yus, *Chem. Rev.* **2002**, *102*, 4009–4091.
- [16] Y. Taniguchi, N. Fujii, K. Takaki, Y. Fujiwara, *J. Organomet. Chem.* **1995**, *491*, 173–179.
- [17] K. Takaki, Y. Itono, A. Nagafuji, Y. Naito, T. Shishido, K. Takehira, Y. Makioka, Y. Taniguchi, Y. Fujiwara, *J. Org. Chem.* **2000**, *65*, 475–481.
- [18] E. Lu, Y. Chen, J. Zhou, X. Leng, *Organometallics* **2012**, *31*, 4574–4578.
- [19] G. B. Deacon, C. M. Forsyth, B. M. Gatehouse, A. Philosofof, B. W. Skelton, A. H. White, P. A. White, *Aust. J. Chem.* **1997**, *50*, 959–970.
- [20] Y. Schulte, H. Weinert, C. Wölper, S. Schulz, *Organometallics* **2020**, *39*, 206–216.
- [21] C. Lichtenberg, M. Elfferding, L. Finger, J. Sundermeyer, *J. Organomet. Chem.* **2010**, *695*, 2000–2006.
- [22] Y. Schulte, C. Stienen, C. Wölper, S. Schulz, *Organometallics* **2019**, *38*, 2381–2390.
- [23] N. A. Pushkarevsky, I. Y. Ilyin, P. A. Petrov, D. G. Samsonenko, M. R. Ryzhikov, P.

Chapter Three

- W. Roesky, S. N. Konchenko, *Organometallics* **2017**, *36*, 1287–1295.
- [24] V. D. Romanenko, V. I. Tovstenko, L. N. Markovski, *Synth.* **1980**, *1980*, 823–825.
- [25] W. T. Gong, G. L. Ning, X. C. Li, L. Wang, Y. Lin, *J. Org. Chem.* **2005**, *70*, 5768–5770.
- [26] G. W. Rabe, G. P. A. Yap, A. L. Rheingold, *Inorg. Chem.* **1995**, *34*, 4521–4522.
- [27] K. Oberdorf, A. Hanft, J. Ramler, I. Krummenacher, F. M. Bickelhaupt, J. Poater, C. Lichtenberg, *Angew. Chem. Int. Ed.* **2021**, *60*, 6441–6445.

Chapter 4: Synthesis of alkaline earth and lanthanoid octaphenyl *ansa* metallocene complexes by reductive dimerisation

4.1 Introduction

As described earlier (Chapter 1 and 3), the cyclopentadienyl ligand is very versatile, and has been subject to many modifications, since the discovery of ferrocene, to alter its electronic and steric properties, and the coordination environment once coordinated to a metal centre. Many of these modifications involve substitution of different functional groups or moieties onto the cyclopentadienyl ring, although one popular modification involves introduction of a linking group, or interannular bridge, connecting two cyclopentadiene rings. Sandwich complexes bearing this tethering moiety are referred to as *ansa* metallocenes (Figure 4.1), *ansa* being the Latin prefix meaning “bent handle”, a term introduced by Brintzinger,^[1] who played a key role in the early work of *ansa* metallocenes. This tethering group greatly influences the structure and reactivity of the complexes compared to their untethered counterparts.

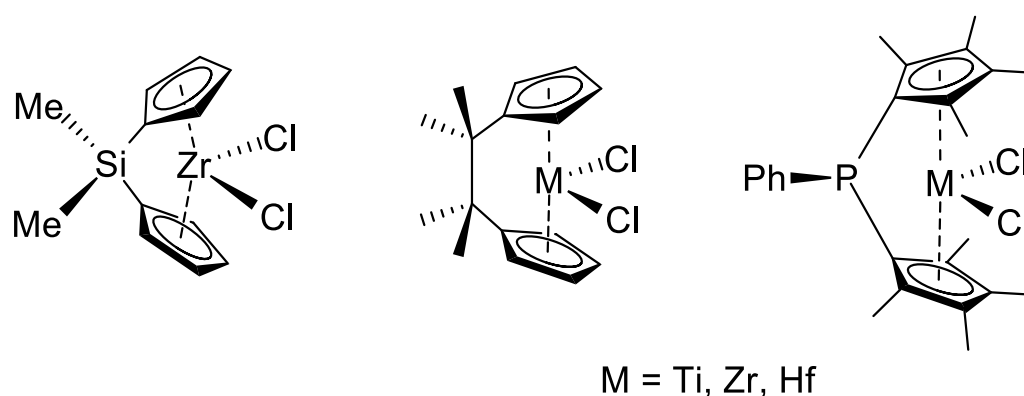


Figure 4.1 – Some examples of *ansa* metallocenes with different interannular bridges.^[2]

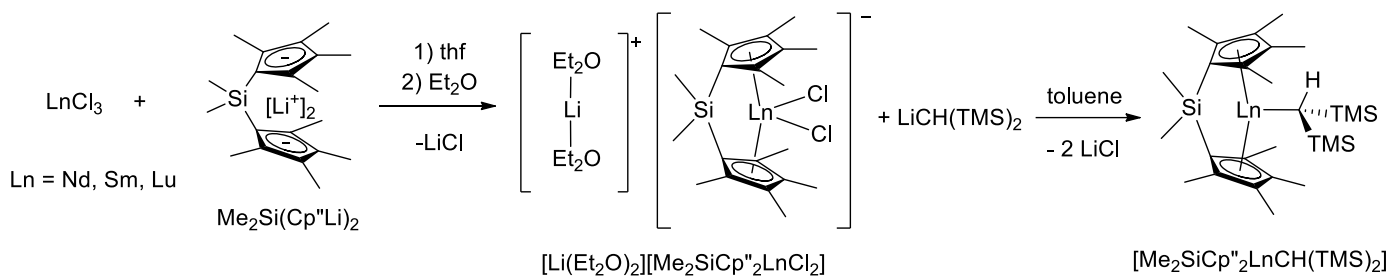
There are three major categories of linking groups: C_n bridges, Si_n bridges, and heteroatom bridges. C_n bridges have been reported with single carbon atoms, and up to as many as five

carbon atoms,^[3] however, three atom and longer bridges are scarce in the literature owing to their low rigidity, offering less stereochemical control in their application as polymerisation catalysts. Despite the huge diversity in tethering moieties amongst *ansa* metallocene complexes, this chapter focusses primarily on C₂ bridged complexes.

Whilst *ansa* metallocene complexes of transition metals are the most widely reported, a range of rare earth *ansa* metallocene complexes have been synthesised, with more attention being drawn to them in recent years as they have shown to be effective alkene polymerisation catalysts,^[4–10] as well as catalysts for asymmetric synthetic organic transformations.^[11] Alkaline earth *ansa* metallocene complexes, particularly of magnesium and calcium, also represent a large portion of the reported complexes, whilst those of strontium and barium are very limited.^[12]

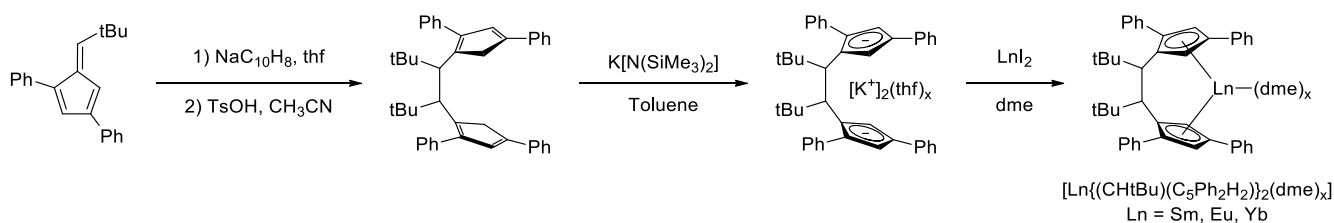
4.1.1 Rare earth *ansa* metallocene complexes

The first structurally characterised rare earth *ansa* metallocene complexes were synthesised in 1985 by the Marks group, utilising an Si(CH₃)₂ bridged bis-tetramethylcyclopentadienyl ligand system (Me₂SiCp''₂).^[13] Salt elimination metathesis reactions were carried out with the corresponding lithium salt of Me₂SiCp''₂ and lanthanoid chlorides of neodymium, samarium and lutetium, yielding the halide and alkali metal included products [Li(Et₂O)₂][Me₂SiCp''₂LnCl₂] (Scheme 4.1).^[13] Further treatment of these ionic complexes with bis(trimethylsilyl)methyl lithium (LiCH(TMS)₂) yielded the organolanthanoid complexes of the general form [Me₂SiCp''₂LnCH(TMS)₂] (Scheme 4.1).^[13] Since then, numerous Si₁ bridged *ansa* metallocene complexes of rare earth metals have been synthesised, but the number of structurally characterised C₂ *ansa* metallocene complexes remains relatively low.



Scheme 4.1 – Synthesis of the first structurally characterised rare earth *ansa* metallocene complexes by a series of salt elimination metathesis reactions.^[13]

Similarly, Balaich developed a facile, three step synthetic pathway enabling access to C_2 bridged divalent lanthanoid *ansa* metallocene complexes of samarium, europium, and ytterbium. This involved use of the bulky 1,3-diphenyl-6-*tert*-butyl fulvene starting material, firstly coupling two fulvenes together with sodium naphthalenide, followed by forming the potassium salt of the bridged dicyclopentadiene, and then treatment with divalent LnI_2 reagents to form the desired *ansa* metallocene complexes by salt metathesis (Scheme 4.2).^[14]

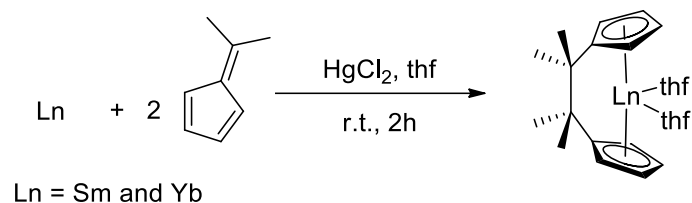


Scheme 4.2 - Three step synthesis of lanthanoid *ansa* metallocene complexes avoiding radical side reactions.^[14]

Balaich's route offered the distinct advantage of avoiding halide and alkali metal inclusion into the resulting *ansa* metallocene complex and allowed for the synthesis of the divalent C_2 complexes.

Alternatively, direct reductive dimerisation of fulvenes by treatment with lanthanoid metals (Sm and Yb) presents a convenient and efficient method of accessing lanthanoid *ansa* metallocene complexes. Reductive dimerisation with free lanthanoid metals was first utilised

by the Edelman group, who treated 6,6-dimethylfulvene with activated lanthanoid metals (Sm and Yb), and the corresponding *ansa* metallocene complexes were isolated (Scheme 4.3).^[15]

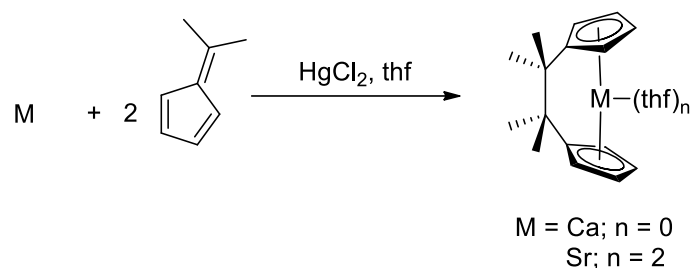


Scheme 4.3 – Synthesis of lanthanoid *ansa* metallocene complexes by reductive dimerisation mediated by the free metal.^[15]

Despite the convenience of reductive dimerisation, it has not gained traction as a popular synthetic method for the synthesis of lanthanoid *ansa* metallocene complexes, with only very few examples being synthesised by this route.^[15,16]

4.1.2 Alkaline earth *ansa* metallocene complexes

Group 2 *ansa* metallocene complexes are dominated by both magnesium and calcium species, with very few examples of barium, and even fewer of strontium, with none of the latter being structurally characterised.^[2] Despite the prominence of group 2 *ansa* metallocene complexes, C₂ based complexes of alkaline earth metals, excluding the commonly used calcium, are quite scarce. The first example was synthesised by the Edelmann group in 1993, again, utilising reductive dimerisation of 6,6'-dimethylfulvene and the activated metal (calcium and strontium) (Scheme 4.4).^[17]



Scheme 4.4 – Synthesis of alkaline earth *ansa* metallocene complexes by reductive dimerisation mediated by the free metal.^[17]

Since then, the reductive dimerisation of fulvenes has proven to be a hugely popular synthetic approach to C₂ calcium *ansa* metallocene complexes with varying substituents,^[18–23] whilst the only structurally characterised C₂ magnesium *ansa* metallocene complexes have been synthesised by protolysis between dibutylmagnesium and the corresponding bridged indene or cyclopentadiene ligand.^[24]

4.2 Current study

Much like bulky cyclopentadienyl complexes of the rare and alkaline earth metals, bulky polyaryl *ansa* metallocene complexes have not been studied extensively. With this in mind, it was of great interest to synthesise a series of octaphenyl *ansa* metallocene complexes which resembled their non-tethered octaphenyl metallocene counterparts described in Chapter 3, to gain insight into the effect of the tether on their structure, reactivity, and physical properties. This was aimed to be achieved by reductive dimerisation of 1,2,3,4-tetraphenylfulvene by the free alkaline earth and lanthanoid metals, offering a synthetic pathway with a high atom economy, and a simple one pot procedure.

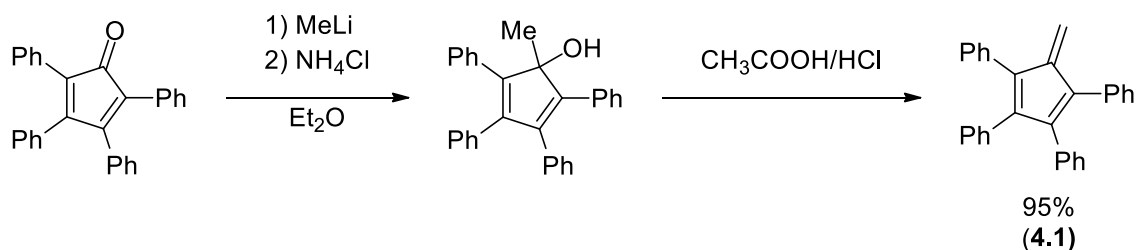
The 1,2,3,4-tetraphenylfulvene starting material (**4.1**) was synthesised by a two-step process, starting from 2,3,4,5-tetraphenylcyclopentadienone. The ketone was treated with excess methyl lithium, yielding the cyclopentadienol upon acidic workup, which could undergo dehydration when heated in the presence of glacial acetic acid and hydrochloric acid, yielding the fulvene (**4.1**) in very good yields. Treatment of the fulvene with calcium, magnesium, strontium or barium metal filings, with a crystal of iodine for activation, in thf for three days led to isolation of the *ansa* metallocene complexes $[\text{Ca}(\text{C}_5\text{Ph}_4\text{CH}_2)_2(\text{thf})]$ (**4.2**), $[\text{Mg}(\text{C}_5\text{Ph}_4\text{CH}_2)_2]$ (**4.3**), $[\text{Sr}(\text{C}_5\text{Ph}_4\text{CH}_2)_2(\text{thf})_2] \cdot 3\text{thf}$ (**4.4**) and $[\text{Ba}(\text{C}_5\text{Ph}_4\text{CH}_2)_2(\text{thf})_2] \cdot 3\text{thf}$ (**4.5**) in moderate yields. Similarly, treatment with samarium, europium, and ytterbium metal filings led to the divalent $[\text{Sm}(\text{C}_5\text{Ph}_4\text{CH}_2)_2(\text{thf})_2] \cdot 3\text{thf}$ (**4.6**), $[\text{Eu}(\text{C}_5\text{Ph}_4\text{CH}_2)_2(\text{thf})_2] \cdot 3\text{thf}$ (**4.7**), and $[\text{Yb}(\text{C}_5\text{Ph}_4\text{CH}_2)_2(\text{thf})] \cdot 2.5\text{thf}$ (**4.8**) *ansa* metallocene complexes. Across all five structurally characterised examples (**4.4 - 4.8**), the effect of the ionic radius of the metal centre is exhibited by a significant change in the planar angles of the two cyclopentadienyl rings, that is, an increase in ionic radius results in a reduced planar angle, opening up access to the metal centre. Similar to its untethered octaphenyl europocene counterpart, the europium *ansa* metallocene

complex (4.7) displayed interesting luminescence properties, with longer luminescence lifetime and a red shifted emission.

4.3 Results and discussion

4.3.1 Synthesis and characterisation of 1,2,3,4-tetraphenylfulvene

The first report of 1,2,3,4-tetraphenylfulvene was made in 1940, whereby the synthesis involved treating 2,3,4,5-tetraphenylcyclopenta-2,4-dienone with methyl magnesium bromide, followed by a subsequent dehydration in a mixture of hydrochloric and acetic acids.^[25] A modified synthesis has been used here, involving treatment of 2,3,4,5-tetraphenylcyclopenta-2,4-dienone with excess methyl lithium and heating to reflux, quenching with saturated ammonium chloride and extracting the resultant cyclopentadienol compound, followed by heating in acetic and hydrochloric acid at reflux. The organic materials were extracted with toluene, and then the solvent removed under reduced pressure, and orange solids washed with hexanes to yield the dehydrated 1,2,3,4-tetraphenylfulvene product (**4.1**) in good yields (Scheme 4.5). Crystals of **4.1** could be grown from the slow evaporation of a dichloromethane solution.



Scheme 4.5 – Synthesis of 1,2,3,4-tetraphenylfulvene from 2,3,4,5-tetraphenylcyclopenta-2,4-dieneone.

The fulvene (**4.1**) was characterised by ^1H and ^{13}C NMR spectroscopy. The exocyclic CH_2 group produces a distinct resonance at 6.03 ppm in the ^1H NMR spectrum, whilst the overlapping phenyl proton signals are difficult to assign between 6.85 and 7.35 ppm. Single crystal X-ray diffraction studies were performed on crystals of **4.1** (Figure 4.2).

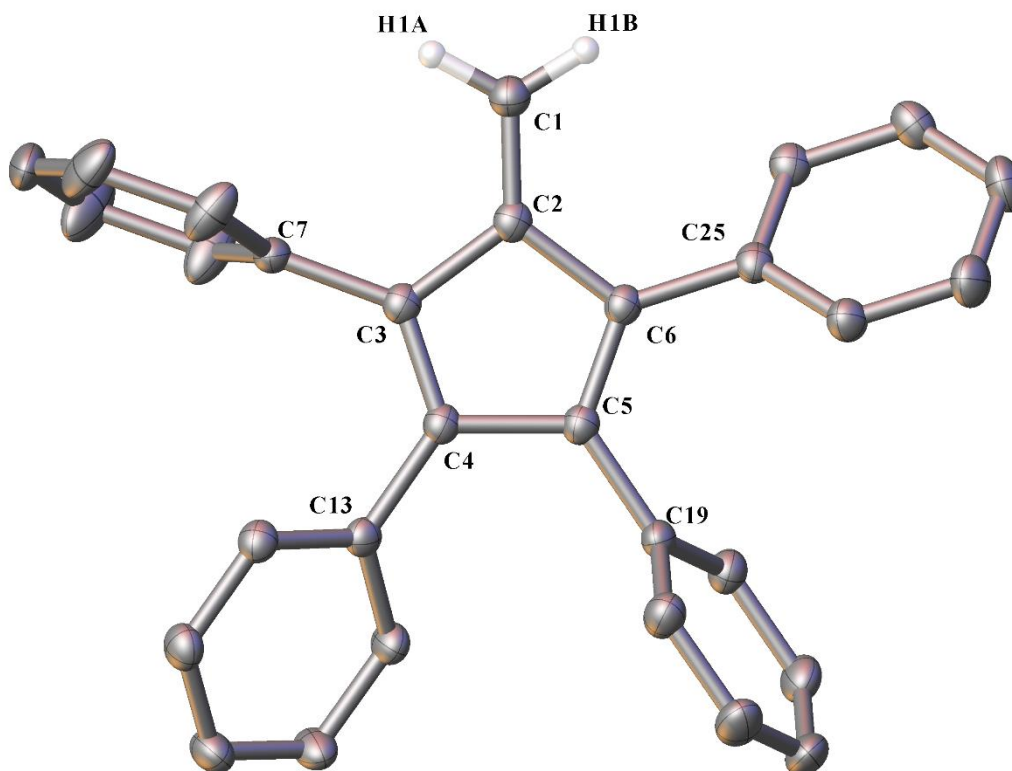


Figure 4.2 – ORTEP diagram of **4.1** showing atom numbering scheme for relevant atoms. Thermal ellipsoids are drawn at the 50% probability level. Phenyl hydrogen atoms have been removed for clarity.

The fulvene (**4.1**) crystallised in the monoclinic space group $P2/c$, with one molecule in the asymmetric unit. Compound **4.1** shows bond lengths and angles comparable to the analogous 6,6-dicyano-2,3,4,5-tetraphenylfulvene.^[26] The exocyclic C(1)-C(2) double bond of **4.1** is 1.3396(16) Å, compared to the longer C-C double bond of the 6,6-cyano analogue (1.3660(16) Å). The C(3)-C(2)-C(6) angle of **4.1** is 106.40(9)°, similar to that of the 6,6-cyano analogue of 107.05(9)°. In the case of the 6,6-cyano analogue, the phenyl moieties adjacent to the exocyclic C-C double bond exhibit some $\pi - \pi$ interactions, with the planes aligning with the C-N triple bonds. These interactions are absent in **4.1**, however, the phenyl rings in both fulvenes exhibit a propeller formation. Interestingly, the packing of **4.1** shows a distance between the two

centroids of the fulvene rings of 5.9127(1) Å, and the exocyclic C-C double bonds aligned, allowing for facile reductive dimerisation (Figure 4.3).

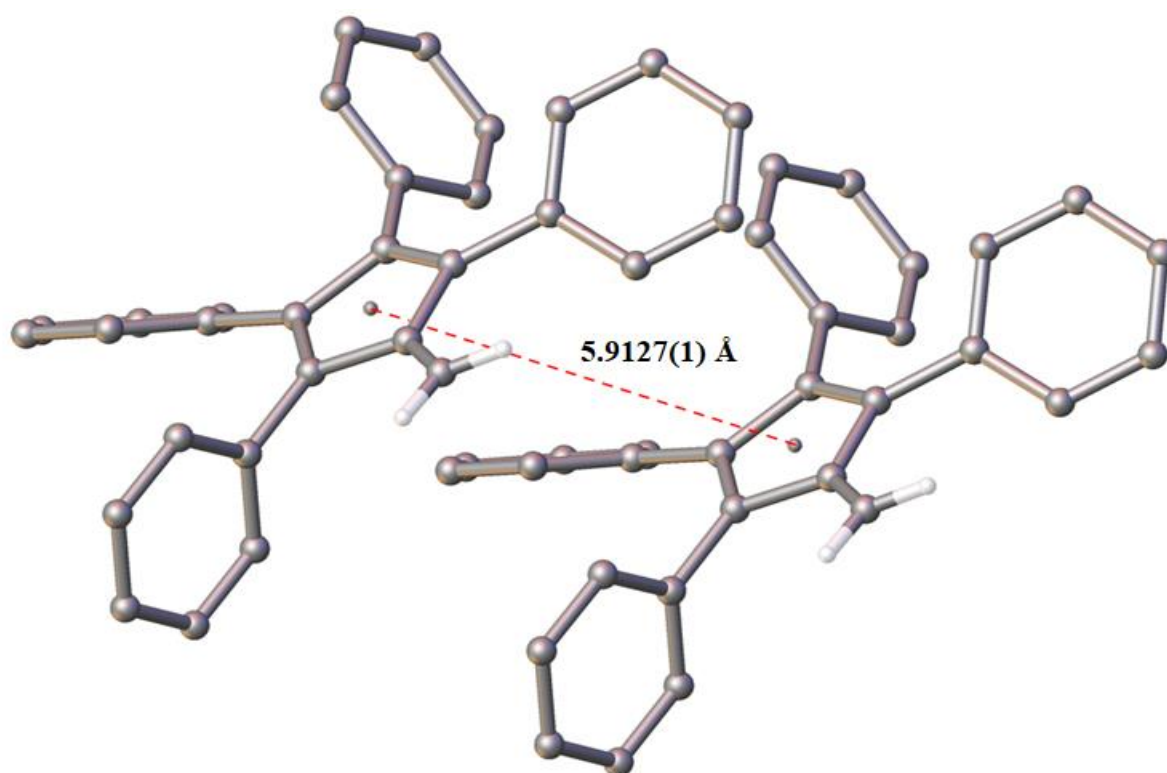
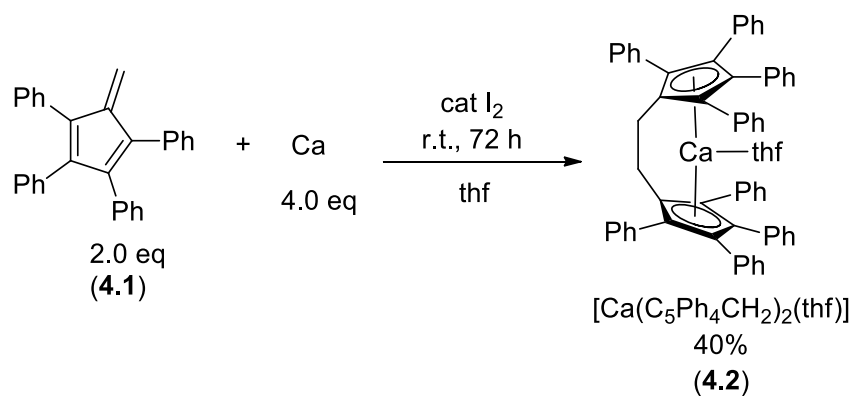


Figure 4.3 – Packing diagram of **4.1** in the crystalline state, showing interplanar distance of the two centroids.

4.3.2 Synthesis and characterisation of alkaline earth *ansa* metallocene complexes

Reports of reductive dimerisation of fulvenes with alkaline earth and lanthanoid metals have utilised a range of different stoichiometric ratios of fulvene to metal.^[15,18–23] Whilst a 2:1 ratio of fulvene:metal seems most logical, there is no clear consensus on the optimal conditions, and perhaps it is indeed dependent on the metal and type of fulvene utilised. Previous attempts to synthesise the octaphenyl *ansa* metallocene complex of calcium within the Junk group proved successful utilising this 2:1 ratio of fulvene:calcium metal. A typical reaction involved combination of the fulvene **4.1** (2 equivalents), calcium metal (1 equivalent), anhydrous thf,

and a crystal of iodine to activate the metal, in a Schlenk flask equipped with a magnetic stirrer bar and stirred for 48 hours. The solids were allowed to settle, and the supernatant solution isolated by cannula filtration, and the complex precipitated by layering with hexane. Attempts to reproduce this were unsuccessful, yielding poor, or no conversion of **4.1** as evidenced by the ^1H NMR spectra, showing the resonance of the exocyclic CH_2 protons at 6.03 ppm. Subsequent attempts were made with an excess of calcium metal, with the best results observed when using a four-fold excess and increasing the reaction duration to 72 hours (Scheme 4.6). Notably, a large amount of precipitate was observed in all cases, which was unable to be characterised by NMR spectroscopy. The supernatant solution could be easily isolated by cannula filtration, and $[\text{Ca}(\text{C}_5\text{Ph}_4\text{CH}_2)_2(\text{thf})]$ (**4.2**) was isolated as an orange-red powder. Attempts to crystallise **4.2** from thf, C_6D_6 and toluene were unsuccessful.

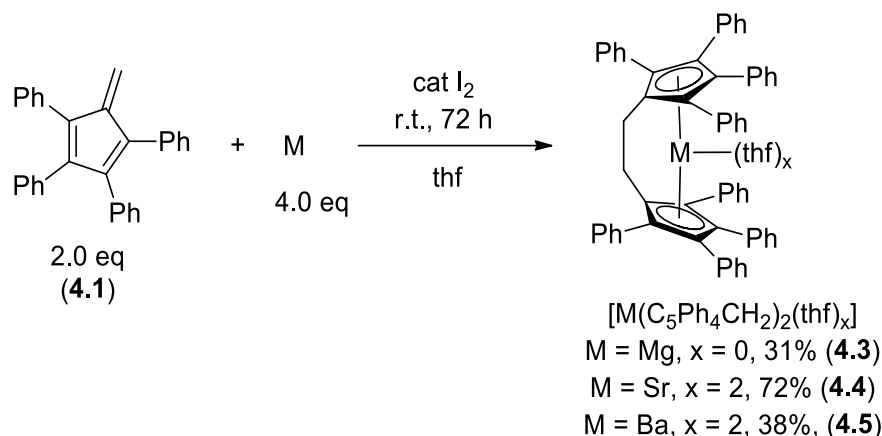


Scheme 4.6 – Synthesis of **4.2** by reductive dimerisation of **4.1** with activated Ca metal.

Complex **4.2** was analysed by ^1H and ^{13}C NMR spectroscopy. The ^1H NMR spectrum of **4.2** in C_6D_6 shows the phenyl protons in the expected region of 7.13 – 6.74 ppm, and the $\text{CH}_2\text{-CH}_2$ tether at 3.44 ppm, partially overlapping with one of the signals of the coordinated thf molecule. The $\text{CH}_2\text{-CH}_2$ tether is also distinct in the ^{13}C NMR spectrum, appearing as a singlet at 27.87 ppm.

As mentioned, the vast majority of alkaline earth cyclopentadienyl complexes are magnesium and calcium based, whilst strontium and barium complexes are far less common,^[12] and there have been no reports of a structurally characterised strontium *ansa* metallocene complex, with any type of interannular bridge.^[17] This methodology was applied to the other alkaline earth metals (magnesium, strontium and barium) in a similar fashion, in an attempt to extend the synthetic pathway of reductive dimerisation of **4.1** to access other alkaline earth metal *ansa* metallocene complexes.

Utilising the same reaction conditions that proved successful for the synthesis of **4.2**, the analogous reactions were undertaken with magnesium strips and strontium and barium metal filings (Scheme 4.7), and the reaction mixtures stirred for 72 hours before isolating the supernatant solutions. In the case of magnesium, the supernatant solution was found only to contain unreacted fulvene (**4.1**), with a significant amount of pale green precipitate formed over the course of the reaction. A small amount of the pale green solid was dissolved in hot C₆D₆, changing colour to a deep yellow solution. The ¹H NMR spectrum indicated that the green precipitate was indeed the pure magnesium *ansa* metallocene complex [Mg(C₅Ph₄CH₂)₂] (**4.3**). Interestingly, once dissolved, even upon cooling, it remained soluble. The remainder of the green precipitate was dissolved in hot toluene, isolated by filtration, and dried under reduced pressure to yield **4.3**. Crystals of **4.3** were not obtained, whilst crystals of **4.4** and **4.5** were grown from concentrated thf solutions at room temperature.



Scheme 4.7 – Synthesis of magnesium (**4.3**), strontium (**4.4**) and barium (**4.5**) *ansa* metallocene complexes by reductive dimerisation of **4.1**.

The ^1H and ^{13}C NMR spectra of **4.3** remain consistent with the calcium analogue (**4.2**), displaying quite clearly the $\text{CH}_2\text{-CH}_2$ bridge at 3.22 and 27.46 ppm respectively. Most notably, the spectra show total absence of coordinated thf, however with one molecule of hexane observed. Elemental analysis was undertaken and agreed with the obtained ^1H NMR spectral data, after accounting for one molecule of hexane retained after drying. Despite the absence of structural characterisation, complex **4.3** shows the highest degree of variation when compared to the series of synthesised alkaline earth *ansa* metallocene complexes, owing to the lack of coordinated thf. This is similar to that of the reported octaphenyl magnesocene,^[27] which is also devoid of coordinated solvent, and allows for the parallel coplanar arrangement of the Cp moieties about the metal centre. However, without structural characterisation it remains unknown whether **4.3** also exhibits this parallel arrangement of the Cp moieties.

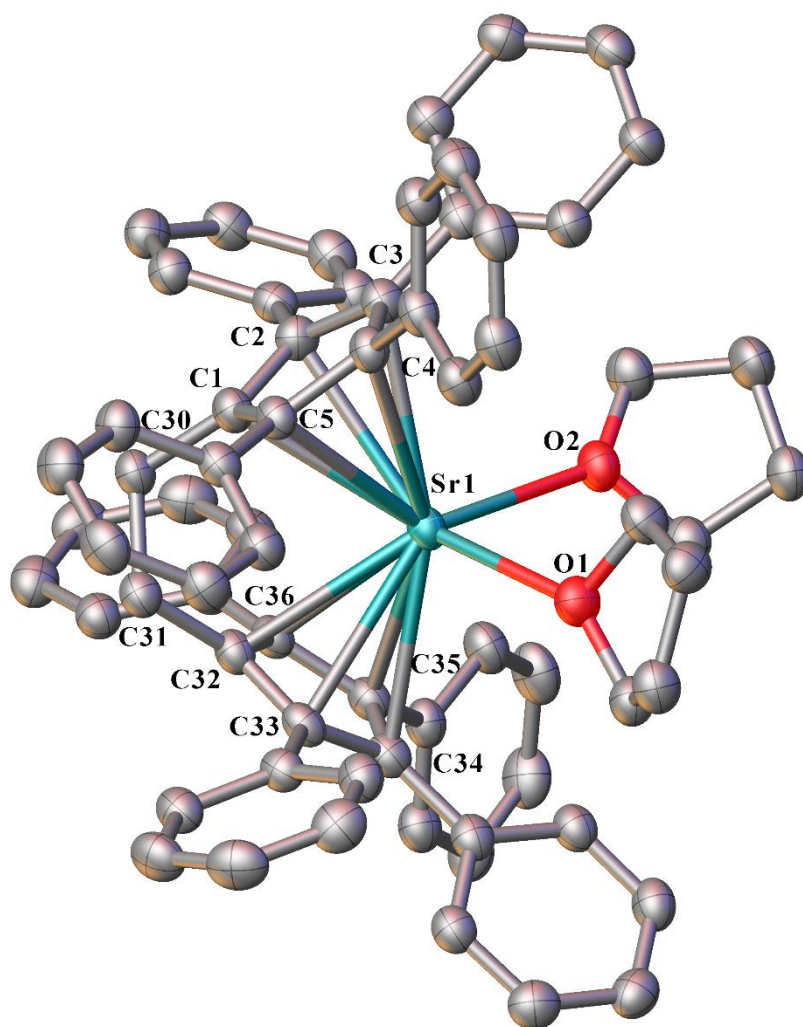


Figure 4.4 - ORTEP diagram of complex **4.4** showing atom-numbering scheme for relevant atoms. Thermal ellipsoids are drawn at the 50% probability level. Hydrogen atoms and lattice solvent are omitted for clarity. Selected bond lengths of **4.4** (Å): Sr(1)-Cn(1) 2.6459(19), Sr(1)-Cn(2) 2.6433(18), Sr(1)-O(1) 2.607(3), Sr(1)-O(2) 2.584(3).

Complex **4.4** crystallised in the monoclinic space group $P2_1$ (Figure 4.4), with three thf molecules in the lattice. The complex is composed of a strontium centre, with two bent cyclopentadienyl rings about the metal core, again, tethered by a $\text{CH}_2\text{-CH}_2$ bridge, and two coordinated thf molecules. As observed in **4.2**, the phenyl groups of the cyclopentadienyl rings are not arranged in a propellor formation. Despite several examples of strontium *ansa* metallocene complexes described in the literature, none have been structurally characterised

by single crystal X-ray diffraction studies.^[17] Complex **4.4** represents the first structurally characterised strontium *ansa* metallocene complex, and as such, there is limited comparison to be made (as even comparable octa- and deca-phenyl strontocenes are yet to be structurally characterised). However, the ionic radius of Sr²⁺ is very similar to that of Eu²⁺ (1.26 vs 1.25 Å respectively for eight-coordinate cations),^[28] and expectedly, analogous complexes of Sr and Eu show very similar structural properties. The strontium to centroid bond distances are Sr(1)-Cn(1) 2.6459(19) and Sr(1)-Cn(2) 2.6433(18) Å, which are in close agreement to those of the analogous europium species (**4.7** - discussed in further on in this chapter), with Eu to centroid bond distances of Eu(1)-Cn(1) 2.616(2) and Eu(1)-Cn(2) 2.6246(18) Å.

The ¹H and ¹³C NMR spectra of **4.4** are consistent with those of **4.2**, again, distinctly showing the CH₂-CH₂ interannular bridge at 3.49 and 27.60 ppm respectively. The ¹H NMR spectrum also shows presence of three molecules of thf, despite the X-ray crystal structure only showing two coordinated thf molecules, suggesting an excess of solvent. Attempts to remove excess solvent under reduced pressure led to decomposition of the complex.

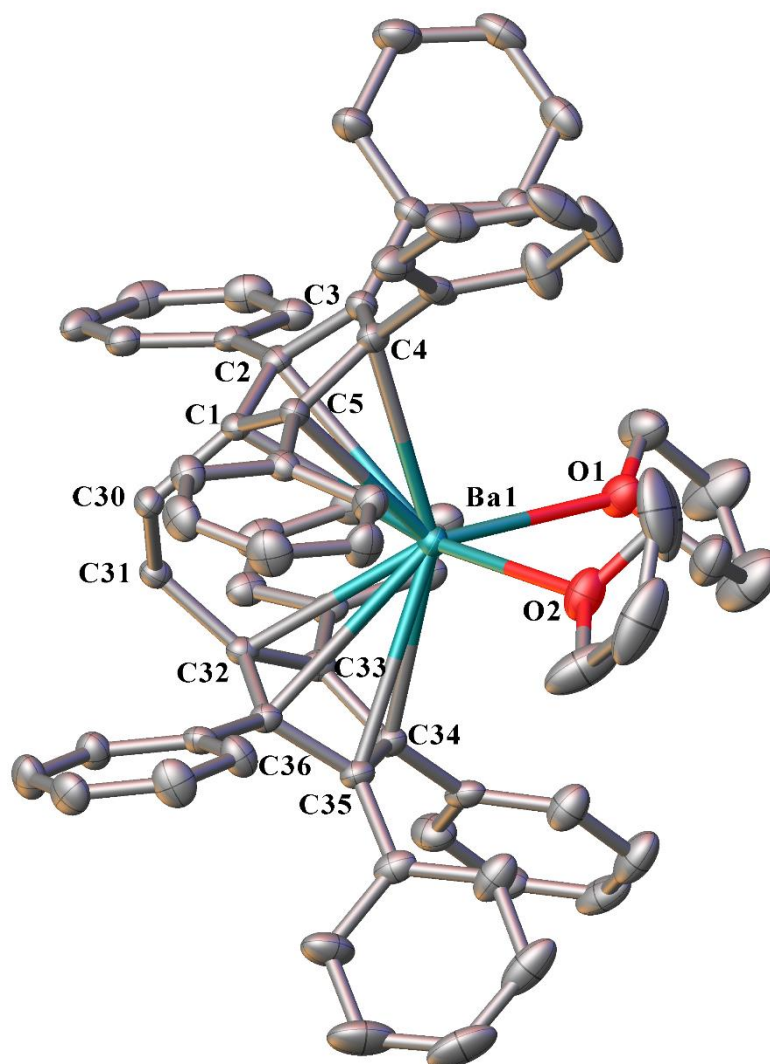


Figure 4.5 – ORTEP diagram of **4.5** showing atom-numbering scheme for relevant atoms. Thermal ellipsoids are drawn at the 50% probability level. Hydrogen atoms and lattice thf are omitted for clarity. Selected bond lengths of **4.5** (Å): Ba(1)-Cn(1) 2.8250(14), Ba(1)-Cn(2) 2.8128(14), Ba(1)-O(1) 2.828(3), Ba(1)-O(2) 2.809(3).

Complex **4.5** crystallised in the monoclinic space group $P2_1$ (Figure 4.5) with three thf molecules in the lattice. Consistent with **4.2**, the barium complex consists of two tetraphenylcyclopentadienyl rings coordinated to the barium centre and tethered by a $\text{CH}_2\text{-CH}_2$ interannular bridge. The barium centre is also ligated by two thf molecules. The planes of the two cyclopentadienyl rings exhibit an $111.65(4)^\circ$ angle with respect to the barium centre (i.e.,

Cn(1)-Ba(1)-Cn(2)), which is considerably smaller than that of **4.2**, owing to the reduced ionic radius of calcium(II).

Both octa- and deca-phenyl barocenes have been reported, however, no X-ray crystal structure has been obtained of the more representative octaphenyl barocene.^[29] Complex **4.5** exhibits barium to centroid distances of 2.8128(14) and 2.8250(14) Å, considerably longer than that of the decaphenyl barocene (2.670 Å), however, this elongation is common among barocene species that do not display a parallel, planar Cp arrangement.^[30,31]

¹H and ¹³C NMR spectra of **4.5** are in agreement with those of **4.2** – **4.4**, with the CH₂-CH₂ interannular bridge easily distinguished as a sharp singlet at 3.43 ppm in the ¹H NMR spectrum, distinct from the coordinated thf resonance, and at 27.20 ppm in the ¹³C NMR spectrum. A satisfactory elemental analysis was obtained from the crystals of **4.5**, accounting for loss of one lattice thf molecule after drying under reduced pressure.

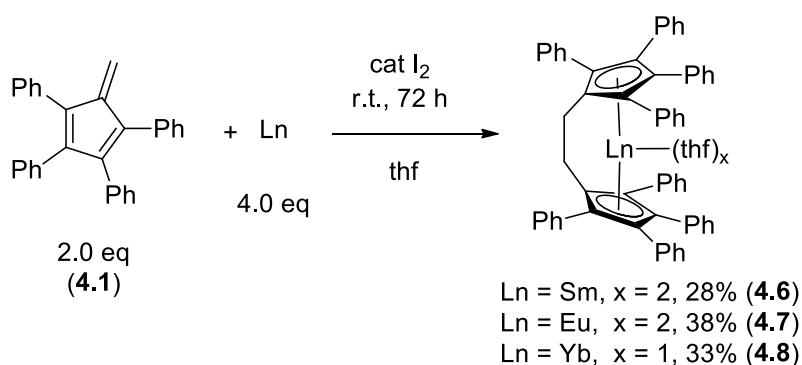
Selected bond lengths and angles for **4.4** and **4.5** have been summarised in Table 4.1. The angle of Cn(1)-M-Cn(2) (γ) represents the angle between the vectors from the metal to the ring centroids, whilst the angle of Cn(1)-Cn(2) (β) represents the angle between the vectors normal to the ring centroids. These parameters are particularly useful, as the difference between these parameters (i.e. $\gamma - \beta$) reflects the amount of slippage of the metal from a standard η^5 mode of coordination to each ring.^[2] The large ionic radius of the Ba²⁺ cation, when compared to the smaller Sr²⁺ cation, dramatically decreases the planar angle of the Cp moieties about the metal centre (γ) and the angle of the two vectors normal to the Cp planes (β). The degree of slippage is also affected by this change in ionic radius, as the barium *ansa* metallocene complex (**4.5**) observes a much larger deviation from a standard η^5 -coordination mode than that of the strontium analogue (**4.4**).

Table 4.1 – Selected bond lengths (Å), angles (°) and slippage (°) of complexes **4.4** and **4.5**

Parameter	4.4	4.5
M-Cn(1)	2.6459(19)	2.852(14)
M-Cn(2)	2.6433(18)	2.8128(14)
M-O(1)	2.584(3)	2.809(3)
M-O(2)	-	2.828(3)
Cn(1)-M-Cn(2) (γ)	115.20(6)	111.65(4)
Cn(1)-Cn(2) (β)	111.49(16)	106.48(13)
Slippage	3.71	5.17

4.3.3 Synthesis and characterisation of rare earth *ansa* metallocene complexes

Divalent lanthanoid complexes can exhibit both structural and synthetic similarities to their alkaline earth counterparts, owing to the similar ionic radii of given pairs of alkaline earth and lanthanoid metals (e.g., calcium and ytterbium, and strontium and europium).^[28] Therefore, it was of interest to synthesise the analogous divalent lanthanoid *ansa* metallocene complexes of samarium, europium, and ytterbium to compare with the alkaline earth *ansa* metallocene complexes. Using the same conditions as those used to synthesise the alkaline earth complexes, the lanthanoid species (**4.6-4.8**) were isolated as crystals grown from thf solutions (Scheme 4.8). Reactions with lanthanoid metals also produced an unidentifiable, insoluble material over the course of the reaction.



Scheme 4.8 – Synthesis of samarium (**4.6**), europium (**4.7**) and ytterbium (**4.8**) *ansa* metallocene complexes by reductive dimerisation of **4.1**.

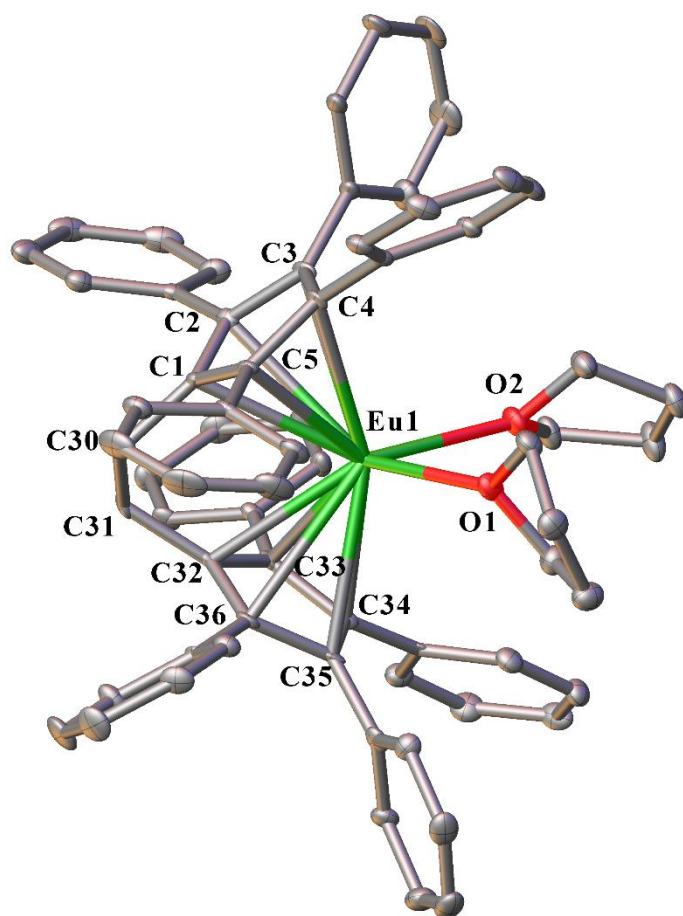


Figure 4.6 – ORTEP diagram of complex **4.7** (also representative of **4.6**) showing atom-numbering scheme for relevant atoms. Thermal ellipsoids are drawn at the 50% probability level. Hydrogen atoms and lattice thf are omitted for clarity. Selected bond lengths of **4.7** (with data for **4.6** in square brackets) (Å): Ln(1)-Cn(1) 2.616(2) [2.6265(2)], Ln(1)-Cn(2) 2.6246(18) [2.627(3)], Ln(1)-O(1) 2.605(3) [2.646(4)], Ln(1)-O(2) 2.628(3) [2.613(4)].

Complexes **4.6** and **4.7** are isomorphous (Figure 4.6), both crystallising in the monoclinic space group $P2_1$ and bearing similarity to the larger barium complex **4.5**, whereby two thf molecules are coordinated to the metal centre. The cyclopentadienyl rings of **4.6** and **4.7** display similar centroid-metal-centroid bond angles of $115.83(7)^\circ$ and $115.78(9)^\circ$ respectively, owing to their similar ionic radii. Both complexes exhibit longer metal to centroid bond lengths than those observed for their octaphenyl counterparts (**4.6**: Sm-Cn = 2.625(2) and 2.672(3) compared to

octaphenyl samarocene [$\text{Sm}(\text{C}_5\text{Ph}_4\text{H})_2(\text{thf})$]: Sm-Cn = 2.573 and 2.564 Å, and **4.7**: Eu-Cn = 2.616(2) and 2.6246(18) compared to octaphenyl europocene [$\text{Eu}(\text{C}_5\text{Ph}_4\text{H})_2(\text{thf})$]: Eu-Cn = 2.576(2) and 2.562(3) Å (described in Chapter 5)). The planar angle of the Cp rings about the Sm metal centre in complex **4.6** (115.83(7)°) is much smaller than that observed for octaphenyl samarocene (151.47(6)°),^[32] again demonstrating the influence of the tether on the planar angle. These bond parameters have been summarised in Table 4.2.

The paramagnetic Sm complex **4.6** was analysed by ^1H and ^{13}C NMR spectroscopy. Owing to the paramagnetism of the Sm^{2+} centre, the chemical shifts of observed resonances in the ^1H spectrum fall between +25 and -5 ppm and were broadened considerably. Notably, the protons from the $\text{CH}_2\text{-CH}_2$ tether are distinct at -2.50 ppm, in a similar region to that observed for the CpH protons of octaphenyl samarocene (-6.55 ppm).^[32] In the ^{13}C NMR spectrum signals were observed from +180 to -50 ppm.

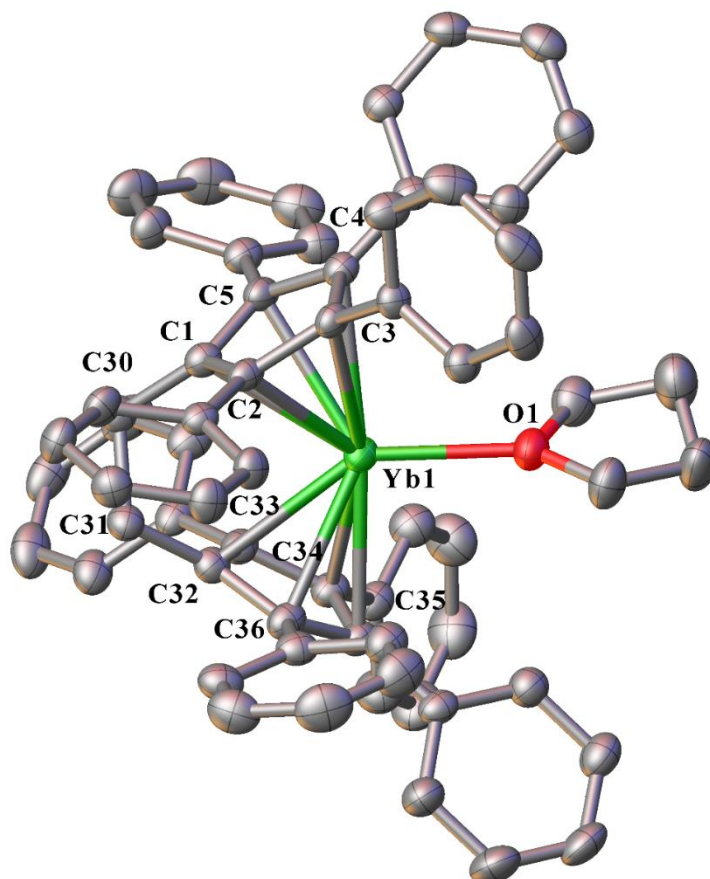


Figure 4.7 – ORTEP diagram of complex **4.8** showing atom-numbering scheme for relevant atoms. Thermal ellipsoids are drawn at the 50% probability level. Hydrogen atoms and lattice thf are omitted for clarity. Selected bond lengths of **4.8** (Å): Yb(1)-Cn(1) 2.4105(14), Yb(1)-Cn(2) 2.4151(14), Yb(1)-O(1) 2.389(2).

Complex **4.8** crystallised in the monoclinic $C2/c$ space group (Figure 4.7) whereby the Yb centre is coordinated to the two cyclopentadienyl rings, and one molecule of thf. The planar angle between the two cyclopentadienyl rings with respect to the ytterbium centre is $124.61(5)^\circ$, much smaller than the corresponding angle of octaphenyl ytterbocene ($150.84(9)^\circ$),^[33] which demonstrates the strong influence of the $\text{CH}_2\text{-CH}_2$ tether on the planar angle. The Yb-Cn bond lengths observed for **4.8** are consistent with those reported for the analogous octaphenyl ytterbocene (Yb-Cn = 2.440(3) and 2.448(3) Å) (summarised in Table 4.2), and slightly longer

than that of decaphenyl ytterbocene (Yb-Cn = 2.3710(12) and 2.3814(13) Å for the ytterbocene with lattice C₆D₆ (**3.8**) reported in Chapter 3) and 2.3711(10) Å for the solvent free ytterbocene),^[34] as observed with the barium analogues. Both **4.8** and octaphenyl ytterbocene have only one molecule of thf coordinated to the metal centre, whereas **4.6** and **4.7** both have two coordinated thf molecules, compared to the one molecule of thf coordinated in their octaphenyl metallocene counterparts.^[32]

Complexes **4.6** – **4.8** demonstrate the effect of the ionic radius on the planar angle of the Cp rings about the metal centres, as an increase in ionic radius from Yb to Sm leads to a decrease in the planar angle. The size of the metal centre also influences the degree of slippage, with a smaller metal centre exhibiting greater deviation from a standard η^5 -coordination mode, opposing the trend exhibited by the group 2 metals (Table 4.1), where the larger Ba centre displayed the largest deviation. This is likely owing to the dramatic increase in ionic radius from eight-coordinate Sm(II) (1.27 Å) to the significantly larger eight-coordinate Ba(II) (1.42 Å),^[28] hugely influencing the structure and causing the observed discrepancy in the slippage.

Table 4.2 – Selected bond lengths (Å), angles (°) and slippage (°) of complexes **4.6** - **4.8** and comparisons with their untethered octaphenyl counterparts.

Parameter	4.6	Sm(C ₅ Ph ₄ H) ₂ (thf)	4.7	Eu(C ₅ Ph ₄ H) ₂ (thf)	4.8	Yb(C ₅ Ph ₄ H) ₂ (thf)
M-Cn(1)	2.625(2)	2.5733(19)	2.616(2)	2.576(2)	2.4105(14)	2.448(3)
M-Cn(2)	2.627(3)	2.5642(18)	2.6246(18)	2.562(3)	2.4151(14)	2.440(3)
M-O(1)	2.646(4)	2.488(3)	2.605(3)	2.484(5)	2.389(2)	2.369(5)
M-O(2)	2.613(4)	-	2.628(3)	-	-	-
Cn(1)-M-Cn(2) (γ)	115.78(9)	151.47(6)	115.83(7)	151.34(9)	124.61(5)	150.84(9)
Cn(1)-Cn(2) (β)	112.0(2)	-	111.72(19)	-	120.48(13)	-
Slippage	3.78	-	4.11	-	4.13	-

Satisfactory elemental analyses were obtained for complexes **4.6** – **4.8**, whereby variable loss of lattice thf was observed. **4.6** and **4.7** retained all of their lattice solvent, whilst **4.8** lost one half of a lattice thf molecule.

In line with other polyaryl europocene complexes,^[5,32] the Eu *ansa* metallocene complex (**4.7**) exhibits luminescence properties, with a considerably long lifetime. Luminescence of complex **4.7** was measured in the solid state, with an excitation wavelength (λ_{exc}) of 532 nm and emission wavelength (λ_{em}) of 680 nm, with a luminescence lifetime of 2.15 μs . Alternatively, when measured in solution (thf) the λ_{exc} shifted to 359 nm, and λ_{em} shifted to 720 nm. Both excitation and emission wavelengths, and the luminescence lifetime vary considerably from that of the untethered octaphenyl europocene ($\lambda_{\text{exc}} = 490$ nm, $\lambda_{\text{em}} = 645$ nm and 1.270 μs),^[32]

again, demonstrating the influence of the interannular bridge on the physical properties of the complex.

4.4 Conclusion

1,2,3,4-Tetraphenylfulvene (**4.1**) was synthesised by treatment of 2,3,4,5-tetraphenylcyclopenta-2,4-dienone with methyllithium, and then subsequent dehydration in glacial acetic and hydrochloric acids. The fulvene (**4.1**) could be treated with a range of alkaline earth metals to synthesise alkaline earth *ansa* metallocene complexes by reductive dimerisation. *Ansa* metallocene complexes of Ca (**4.2**), Mg (**4.3**), Sr (**4.4**), and Ba (**4.5**) were synthesised by treatment of the iodine activated metal with the fulvene (**4.1**) in a 2:1 ratio. Complexes **4.4** and **4.5** were structurally characterised by single crystal X-ray studies, representing the first C₂ *ansa* metallocene complexes of Sr and Ba. This methodology was extended to the synthesis of divalent lanthanoid *ansa* metallocene complexes of Sm (**4.6**), Eu (**4.7**), and Yb (**4.8**), which clearly displayed the influence of the ionic radius of the metal centre on the structure, as an increase in ionic radius resulted in a decrease in the planar angle of the Cp rings, increasing the exposure of the metal centre. The luminescence of the Eu *ansa* metallocene complex (**4.7**) was studied and exhibited an increased luminescence lifetime compared to the untethered europocenes, with a considerable red shift. Reductive dimerisation of 1,2,3,4-tetraphenylfulvene by lanthanoid and group 2 metals has shown to be an effective means of synthesising these divalent species, however, extension to both trivalent complexes, and potentially actinide complexes is still to be assessed.

4.5 Experimental

For materials and general procedures, see Appendix One.

Synthesis of 1,2,3,4-tetraphenylfulvene (**4.1**)

MeLi (20 mL, 1.6 M in Et₂O, 32 mmol) was added to a two-necked round bottom flask equipped with a condenser containing 2,3,4,5-tetraphenylcyclopentadienone (2.0 g, 5.2 mmol). The suspension was heated to 40 °C for 40 minutes, before quenching with dilute HCl, then extracted with ethyl acetate (2 x 20 mL). The organic fractions were combined and stirred over MgSO₄, filtered, and the solvent removed under reduced pressure to yield the desired alcohol as a yellow solid. The yellow solid was dissolved in glacial acetic acid (40 mL) and heated to 140 °C before concentrated HCl (37% aqueous solution, 1.8 mL) was added. The mixture was heated to reflux for two hours then extracted with toluene (2 x 25 mL). The organic fractions were combined and stirred over MgSO₄, filtered, and then solvent removed under reduced pressure. The dark orange solid was then washed with hexanes, and filtered, yielding the fulvene (**4.1**) as a bright orange powder (1.82g, 4.76 mmol, 95%). Crystals of **4.1** could be grown from the slow evaporation of a dichloromethane solution. ¹H NMR (CDCl₃, 400 MHz, 25 °C): δ 7.30-6.88 (m, 20H, ArH), 6.04 (s, 2H, CH₂). ¹³C NMR (CDCl₃, 101 MHz, 25 °C): δ 152.44 (s), 143.56 (s), 135.06 (s), 133.05 (s), 130.96 (s), 130.29 (s), 127.93 (s), 127.44 (s), 126.63 (s), 126.53 (s), 123.83 (s). IR (ATR, cm⁻¹): 3051 m, 1963 w, 1882 m, 1669 m, 1596 s, 1573 m, 1553 w, 1485 s, 1438 s, 1394 m, 1340 m, 1260 w, 1179 m, 1156 m, 1106 m, 1074 m, 1027 s, 939 m, 907 s, 845 w, 794 m, 767 m, 748 s, 730 s, 693 s, 654 w, 640 w, 618 w, 589 w, 555 w, 542 s, 516 s, 497 m, 476 m, 456 m.

Synthesis of [Ca(C₅Ph₄CH₂)₂(thf)] (4.2)

A Schlenk flask was charged with 1,2,3,4-tetraphenylfulvene (0.220 g, 0.576 mmol), freshly filed calcium metal (0.040 g, 1.00 mmol) and a catalytic amount of iodine. Anhydrous thf (5 mL) was added, and the reaction mixture stirred for 72 hours. The resulting suspension was allowed to settle, and the supernatant solution isolated by cannula filtration. The solvent was concentrated under reduced pressure, and left to stand, affording **4.2** as an orange-red precipitate (0.105 g, 40 %). ¹H NMR (C₆D₆, 500 MHz, 25 °C): δ 7.13-6.74 (m, 40H, ArH), 3.43 (s, 4H, CH₂) ¹³C NMR (C₆D₆, 500 MHz, 25 °C): δ 134.17 (s), 131.52 (s), 131.33 (s), 128.60 (s), 128.40 (s), 128.15 (s), 126.99 (s), 126.61 (s), 126.52 (s), 123.98 (s), 27.87 (s). IR (Nujol, cm⁻¹): 1936 w, 1794 w, 1594 m, 1574 s, 1492 w, 1329 w, 1307w, 1260 w, 1174 w, 1155 w, 1099 w, 1071 m, 1026 m, 1015 m, 902 w, 863 w, 839 w, 796 w, 787 w, 750 m, 696 m.

Synthesis of [Mg(C₅Ph₄CH₂)₂] (4.3)

A Schlenk flask was charged with 1,2,3,4-tetraphenylfulvene (**4.1**) (0.200 g, 0.524 mmol), magnesium metal strips (0.050 g, 2.1 mmol) and a catalytic amount of iodine. Anhydrous thf (5 mL) was added, and the reaction mixture stirred for 72 hours. A pale green precipitate had formed, with a dark orange supernatant solution. The supernatant solution was removed by filtration, and the solids dried under reduced pressure. The solids were then taken up into toluene (5 mL) and warmed gently to dissolve the material. The resulting solution was separated from unreacted magnesium strips by filtration, dried under reduced pressure, and washed with anhydrous hexane (5 mL) yielding **4.3** as a beige solid (0.065 g, 31%). *Anal. Calc.* for C₆₆H₅₈Mg (875.47 g.mol⁻¹): C, 90.55; H, 6.68. Found: C, 91.37; H, 6.97 %. ¹H NMR (400 MHz, C₆D₆): δ 7.09-7.00 (m, 25H, ArH), 6.89-6.79 (m, 15H, ArH), 3.22 (s, 4H, CH₂), 1.04 (m, 8H, hexane), 0.69 (t, 6H, hexane). ¹³C NMR (101 MHz, C₆D₆): δ 138.40 (s), 137.99 (s), 132.14

(s), 131.71 (s), 127.37 (s), 125.61 (s), 125.01 (s), 124.53 (s), 121.72 (s), 117.38 (s), 31.96 (s), 27.46 (s), 23.05 (s), 14.34 (s). IR (Nujol, cm^{-1}): 1948 m, 1879 m, 1804 m, 1752 m, 1671 w, 1596 s, 1575 w, 1310 w, 1261 m, 1176 m, 1155 m, 1096 m, 1071 s, 1027 m, 1006 m, 910 m, 858 m, 839 m, 788 m, 769 w, 747 m, 697 s.

Synthesis of $[\text{Sr}(\text{C}_5\text{Ph}_4\text{CH}_2)_2(\text{thf})_2] \cdot 3\text{thf}$ (**4.4**)

The synthesis of **4.3** was carried out in the same way as that of **4.2**, but with strontium metal filings (0.100 g, 1.15 mmol) in place of magnesium metal. After 72 hours, the solid material was allowed to settle, and the supernatant solution isolated by filtration, and dried under reduced pressure, affording **4.4** as a gold powder (0.16 g, 72 %). Colourless crystals of **4.4** were grown from the thf solution. *Anal.* Calc. for $\text{C}_{72}\text{H}_{68}\text{O}_3\text{Sr}$ (1068.93 $\text{g}\cdot\text{mol}^{-1}$ after loss of two lattice thf): C, 80.90; H, 6.41. Found: C, 80.96; H, 6.52 %. ^1H NMR (400 MHz, C_6D_6): δ 7.09-6.99 (m, 25H, ArH), 6.89-6.76 (m, 15H, ArH), 3.60 (br s, 12H, thf), 3.49 (s, 4H, CH_2), 1.36 (br s, 12H, thf). ^{13}C NMR (101 MHz, C_6D_6): δ 139.74 (s), 138.93 (s), 131.99 (s), 130.46 (s), 128.69 (s), 127.29 (s), 126.18 (s), 125.51 (s), 124.78 (s), 124.63 (s), 68.93 (s, thf) 27.60 (s), 25.53 (s, thf). IR (Nujol, cm^{-1}): 1941 w, 1876 w, 1806 w, 1593 s, 1574 m, 1259 w, 1177 m, 1154 m, 1122 w, 1099 w, 1071 m, 1026 s, 907 m, 870 m, 789 m, 770 m, 743 s, 696 s, 616 w, 557 w.

Synthesis of $[\text{Ba}(\text{C}_5\text{Ph}_4\text{CH}_2)_2(\text{thf})_2] \cdot 3\text{thf}$ (**4.5**)

The synthesis of **4.5** was carried out in the same way as that of **4.4**, but with barium metal filings (0.137 g, 1.00 mmol) in place of strontium metal. After filtration the solution was concentrated to ~2 mL and allowed to stand at room temperature, yielding large colourless crystals of **4.5** (0.105 g, 38 %). *Anal.* Calc. for $\text{C}_{68}\text{H}_{60}\text{O}_2\text{Ba}$ (1046.53 $\text{g}\cdot\text{mol}^{-1}$ after loss of 1 lattice thf): C, 78.041; H, 5.78. Found: C, 78.88; H, 6.096 %. ^1H NMR (400 MHz, C_6D_6): δ 7.08 – 6.99 (m, 26H, ArH), 6.83 (tt, 9H, ArH), 6.76 (tt, 5H, ArH), 3.48 (br s, 16H, thf), 3.43

(s, 4H, CH₂), 1.35 (br s, 16H, thf). ¹³C NMR (101 MHz, C₆D₆): δ 139.86 (s), 139.50 (s), 131.79 (s), 130.80 (s), 128.56 (s), 127.33 (s), 127.27 (s), 125.77 (s), 124.75 (s), 124.33 (s), 68.03 (s), 27.20 (s), 25.51 (s). IR (Nujol, cm⁻¹): 1958 m, 1883 m, 1805 m, 1743 m, 1596 s, 1575 w, 1328 w, 1308 w, 1257 w, 1180 m, 1155 w, 1125 w, 1068 m, 1028 m, 909 m, 790 m, 771 w, 744 m, 695 m.

Synthesis of [Sm(C₅Ph₄CH₂)₂(thf)₂]₂·3thf (4.6)

A Schlenk flask was charged with 1,2,3,4-tetraphenylfulvene (**4.1**) (0.076 g, 0.20 mmol), freshly filed samarium metal (0.15 g, 1.0 mmol) and a catalytic amount of iodine. Anhydrous thf (5 mL) was added, and the reaction mixture stirred for 72 hours. The solid material was allowed to settle, and the supernatant solution isolated by cannula filtration. The solution was concentrated to ~1 mL and allowed to stand at room temperature, yielding dark brown crystals of **4.6** (0.035g, 28%). *Anal.* Calc. for C₈₀H₈₄O₅Sm (1275.88 g.mol⁻¹): C, 75.31; H, 6.64. Found: C, 75.32; H, 5.929 %. ¹H NMR (400 MHz, C₆D₆) δ 17.47 (s, 6H), 13.21 (s, 4H, ArH), 5.22 (s, 6H, ArH), 4.92 (s, 10H, ArH), 2.54 (s, 30H, thf), -0.45 (s, 30H, thf), -4.11 (s, 4H, CH₂). ¹³C NMR (126 MHz, C₆D₆) δ 175.18 (s), 151.15 (s), 136.70 (s), 131.79 (s), 131.40 (s), 126.58 (s), 123.21 (s), 86.98 (s), 67.91 (s), 25.38 (s), -1.56 (s), -29.84 (s), -46.69 (s). IR (Nujol, cm⁻¹): 1593 m, 1305 w, 1260 m, 1154 w, 1072 w, 1025 m, 789 w, 771 w, 723 m, 696 m.

Synthesis of [Eu(C₅Ph₄CH₂)₂(thf)₂]₂·3thf (4.7)

The synthesis of complex **4.7** was carried out in the same way as that described for complex **4.6**, but with 1,2,3,4-tetraphenylfulvene (**4.1**) (0.200 g, 0.524 mmol) and europium filings (0.230 g, 1.51 mmol) were used in place of samarium. Amber crystals of **4.7** were grown from ~2 mL of thf at room temperature (0.120 g, 38%). *Anal.* Calc. for C₈₀H₈₄O₅Eu (1277.48 g.mol⁻¹): C, 75.21; H, 6.63. Found: C, 75.25; H, 6.65%. IR (Nujol, cm⁻¹): 1593 m, 1574 w, 1308 w,

Chapter Four

1260 m, 1176 w, 1153 w, 1096 w, 1069 w, 1020 m, 907 w, 869 m, 789 m, 771 w, 744 m, 695 m, 661 w, 616 w.

Synthesis of $[\text{Yb}(\text{C}_5\text{Ph}_4\text{CH}_2)_2(\text{thf})] \cdot 2.5\text{thf}$ (**4.8**)

The synthesis of complex **4.8** was carried out in the same way as that described for complex **4.7**, but with ytterbium filings (0.270 g, 1.52 mmol) used in place of europium. Green-brown crystals of **4.8** were grown from ~2 mL of thf at room temperature (0.095 g, 33%). *Anal.* Calc. for $\text{C}_{72}\text{H}_{68}\text{O}_3\text{Yb}$ (1154.35 $\text{g}\cdot\text{mol}^{-1}$ after loss of one half of a lattice thf): C, 74.91; H, 5.94. Found: C, 74.30; H, 5.518%. IR (Nujol, cm^{-1}): 1944 w, 1882 w, 1802 w, 1595 m, 1574 w, 1342 w, 1261 m, 1176 w, 1155 w, 1100 m, 1071 m, 1027 m, 939 w, 911 m, 865 w, 838 w, 795 w, 788 w, 249 m, 696 s, 628 w, 616 w.

4.6 Crystal and refinement data

1,2,3,4-tetraphenylfulvene (4.1)

$C_{30}H_{22}$ ($M=382.47$ g/mol): monoclinic, space group $P2/c$ (no. 13), $a = 12.09250(10)$ Å, $b = 5.91270(10)$ Å, $c = 29.4925(3)$ Å, $\beta = 98.6750(10)^\circ$, $V = 2084.57(4)$ Å³, $Z = 4$, $T = 123.00(10)$ K, $\mu(\text{Cu K}\alpha) = 0.520$ mm⁻¹, $D_{\text{calc}} = 1.219$ g/cm³, 21996 reflections measured ($7.396^\circ \leq 2\Theta \leq 159.166^\circ$), 4463 unique ($R_{\text{int}} = 0.0336$, $R_{\text{sigma}} = 0.0267$) which were used in all calculations. The final R_1 was 0.0417 ($I > 2\sigma(I)$) and wR_2 was 0.1073 (all data).

[Sr(C₅Ph₄CH₂)₂(thf)]·3 thf (4.4)

$C_{80}H_{84}O_5\text{Sr}$ ($M=1213.09$ g/mol): monoclinic, space group $P2_1$ (no. 4), $a = 12.920(3)$ Å, $b = 18.590(4)$ Å, $c = 13.900(3)$ Å, $\beta = 108.83(3)^\circ$, $V = 3159.8(12)$ Å³, $Z = 2$, $T = 100(2)$ K, $\mu(\text{Synchrotron}) = 0.907$ mm⁻¹, $D_{\text{calc}} = 1.275$ g/cm³, 56524 reflections measured ($3.096^\circ \leq 2\Theta \leq 51.362^\circ$), 11830 unique ($R_{\text{int}} = 0.0369$, $R_{\text{sigma}} = 0.0266$) which were used in all calculations. The final R_1 was 0.0396 ($I > 2\sigma(I)$) and wR_2 was 0.1064 (all data).

[Ba(C₅Ph₄CH₂)(thf)₂]·2 thf (4.5)

$C_{76}H_{76}\text{BaO}_4$ ($M=1190.70$ g/mol): monoclinic, space group $P2_1$ (no. 4), $a = 11.2111(2)$ Å, $b = 16.1916(2)$ Å, $c = 16.8585(3)$ Å, $\beta = 104.361(2)^\circ$, $V = 2964.62(9)$ Å³, $Z = 2$, $T = 123.01(10)$ K, $\mu(\text{Mo K}\alpha) = 0.722$ mm⁻¹, $D_{\text{calc}} = 1.334$ g/cm³, 81991 reflections measured ($6.948^\circ \leq 2\Theta \leq 64.566^\circ$), 18149 unique ($R_{\text{int}} = 0.0589$, $R_{\text{sigma}} = 0.0543$) which were used in all calculations. The final R_1 was 0.0354 ($I > 2\sigma(I)$) and wR_2 was 0.0731 (all data).

[Sm(C₅Ph₄CH₂)₂(thf)₂]·3thf (4.6)

C₈₀H₈₄O₅Sm ($M=1275.82$ g/mol): monoclinic, space group $P2_1$ (no. 4), $a = 12.9260(2)$ Å, $b = 18.6121(3)$ Å, $c = 13.8914(2)$ Å, $\beta = 108.6490(10)^\circ$, $V = 3166.52(9)$ Å³, $Z = 2$, $T = 123.00(10)$ K, $\mu(\text{Cu K}\alpha) = 7.375$ mm⁻¹, $D_{\text{calc}} = 1.338$ g/cm³, 31650 reflections measured ($7.218^\circ \leq 2\Theta \leq 159.744^\circ$), 10970 unique ($R_{\text{int}} = 0.0867$, $R_{\text{sigma}} = 0.0932$) which were used in all calculations. The final R_1 was 0.0386 ($I > 2\sigma(I)$) and wR_2 was 0.0956 (all data).

[Eu(C₅Ph₄CH₂)₂(thf)₂]·3thf (4.7)

C₈₀H₈₄EuO₅ ($M=1277.43$ g/mol): monoclinic, space group $P2_1$ (no. 4), $a = 12.94120(10)$ Å, $b = 18.59470(10)$ Å, $c = 13.89350(10)$ Å, $\beta = 108.6760(10)^\circ$, $V = 3167.26(4)$ Å³, $Z = 2$, $T = 123.00(10)$ K, $\mu(\text{Cu K}\alpha) = 7.500$ mm⁻¹, $D_{\text{calc}} = 1.339$ g/cm³, 65080 reflections measured ($7.21^\circ \leq 2\Theta \leq 159.576^\circ$), 13084 unique ($R_{\text{int}} = 0.0502$, $R_{\text{sigma}} = 0.0349$) which were used in all calculations. The final R_1 was 0.0399 ($I > 2\sigma(I)$) and wR_2 was 0.1058 (all data).

[Yb(C₅Ph₄CH₂)₂(thf)]·2.5thf (4.8)

C₇₄H₇₂O_{3.5}Yb ($M=1190.35$ g/mol): monoclinic, space group $C2/c$ (no. 15), $a = 43.6591(4)$ Å, $b = 12.38390(10)$ Å, $c = 20.9409(2)$ Å, $\beta = 93.6440(10)^\circ$, $V = 11299.22(18)$ Å³, $Z = 8$, $T = 123.00(10)$ K, $\mu(\text{Cu K}\alpha) = 3.453$ mm⁻¹, $D_{\text{calc}} = 1.399$ g/cm³, 59008 reflections measured ($7.422^\circ \leq 2\Theta \leq 159.564^\circ$), 12031 unique ($R_{\text{int}} = 0.0624$, $R_{\text{sigma}} = 0.0445$) which were used in all calculations. The final R_1 was 0.0434 ($I > 2\sigma(I)$) and wR_2 was 0.1112 (all data).

4.7 References

- [1] J. A. Smith, J. von Seyerl, G. Huttner, H. H. Brintzinger, *J. Organomet. Chem.* **1979**, *173*, 175–185.
- [2] P. J. Shapiro, *Coord. Chem. Rev.* **2002**, *231*, 67–81.
- [3] C. Qian, J. Guo, C. Ye, J. Sun, P. Zheng, *J. Chem. Soc. Dalton Trans.* **1993**, 3441–3445.
- [4] W. Kaminsky, *J. Chem. Soc. Dalton Trans.* **1998**, 1413–1418.
- [5] C. Ruspic, J. R. Moss, M. Schürmann, S. Harder, *Angew. Chem. Int. Ed.* **2008**, *47*, 2121–2126.
- [6] H. H. Brintzinger, D. Fischer, R. Mülhaupt, B. Rieger, R. M. Waymouth, *Angew. Chem., Int. Ed. Engl.* **1995**, *34*, 1143–1170.
- [7] G. G. Hlatky, *Coord. Chem. Rev.* **1999**, *181*, 243–296.
- [8] N. Schneider, M. E. Huttenloch, U. Stehling, R. Kirsten, F. Schaper, H. H. Brintzinger, *Organometallics* **1997**, *16*, 3413–3420.
- [9] M. E. Huttenloch, B. Dorer, U. Rief, M. H. Prosenc, K. Schmidt, H. H. Brintzinger, *J. Organomet. Chem.* **1997**, *541*, 219–232.
- [10] H. L. Lentzner, W. E. Watts, *Tetrahedron* **1971**, *27*, 4343–4351.
- [11] A. H. Hoveyda, *Catalytic Enantioselective Alkylation of Alkenes by Chiral Metallocenes*, Wiley-VCH/GmbH, Verlag/Weinheim, **2005**.
- [12] S. Baguli, S. Mondal, C. Mandal, S. Goswami, *Chem. Asian J.* **2022**, *17*, e202100962.

- [13] G. Jeske, Laurel E. Schock, P. N. Swepston, H. Schumann, T. J. Marks, *J. Am. Chem. Soc.* **1985**, *107*, 665.
- [14] S. K. Adas, G. J. Balaich, *J. Organomet. Chem.* **2018**, *857*, 200–206.
- [15] A. Recknagel, F. T. Edelmann, *Angew. Chem., Int. Ed. Engl.* **1991**, *30*, 693–694.
- [16] I. L. Fedushkin, S. Dechert, H. Schumann, *Angew. Chem. Int. Ed.* **2001**, *40*, 561.
- [17] M. Rieckhoff, U. Pieper, D. Stalke, F. T. Edelmann, *Angew. Chem. Int. Ed. Engl.* **1993**, *32*, 1079–1081.
- [18] G. J. Matare, K. M. Kane, P. J. Shapiro, A. Vij, *J. Chem. Crystallogr.* **1998**, *28*, 731–734.
- [19] P.-J. Sinnema, B. Twamley, P. J. Shapiro, *Acta Crystallogr. Sect. E Struct. Reports Online* **2001**, *57*, m438–m440.
- [20] B. Twamley, G. J. Matare, P. J. Shapiro, A. Vij, *Acta Crystallogr. Sect. E Struct. Reports Online* **2001**, *57*, m402–m403.
- [21] K. M. Kane, P. J. Shapiro, A. Vij, R. Cubbon, A. L. Rheingold, *Organometallics* **1997**, *16*, 4567–4571.
- [22] P. J. Shapiro, K. M. Kane, A. Vij, D. Stelck, G. J. Matare, R. L. Hubbard, B. Caron, *Organometallics* **1999**, *18*, 3468–3473.
- [23] P.-J. Sinnema, P. J. Shapiro, B. Höhn, B. Twamley, *J. Organomet. Chem.* **2003**, *676*, 73–79.
- [24] H. R. H. Damrau, A. Geyer, M. H. Prosenc, A. Weeber, F. Schaper, H. H. Brintzinger, *J. Organomet. Chem.* **1998**, *553*, 331–343.

- [25] W. Diltthey, P. Huchtemann, *J. Prakt. Chem.* **1940**, *154*, 238–265.
- [26] T. L. Andrew, J. R. Cox, T. M. Swager, *Org. Lett.* **2010**, *12*, 5302–5305.
- [27] G. B. Deacon, F. Jaroschik, P. C. Junk, R. P. Kelly, *Organometallics* **2015**, *34*, 2369–2377.
- [28] R. D. Shannon, *Acta Crystallogr. Sect. A* **1976**, *32*, 751–767.
- [29] P. S. Tanner, T. P. Hanusa, *Polyhedron* **1994**, *13*, 2417–2420.
- [30] M. J. Harvey, K. T. Quisenberry, T. P. Hanusa, V. G. Young, *Eur. J. Inorg. Chem.* **2003**, 3383–3390.
- [31] R. A. Williams, K. F. Tesh, T. P. Hanusa, *J. Am. Chem. Soc.* **1991**, *113*, 4843–4851.
- [32] R. P. Kelly, T. D. M. Bell, R. P. Cox, D. P. Daniels, G. B. Deacon, F. Jaroschik, P. C. Junk, X. F. Le Goff, G. Lemercier, A. Martinez, J. Wang, D. Werner, *Organometallics* **2015**, *34*, 5624–5636.
- [33] G. B. Deacon, F. Jaroschik, P. C. Junk, R. P. Kelly, *Chem. Commun.* **2014**, *50*, 10655–10657.
- [34] G. B. Deacon, C. M. Forsyth, F. Jaroschik, P. C. Junk, D. L. Kay, T. Maschmeyer, A. F. Masters, J. Wang, L. D. Field, *Organometallics* **2008**, *27*, 4772–4778.

Chapter 5: Carbon-fluorine bond activation of pentafluorobenzene by lanthanoid metals and applications in organolanthanoid synthesis

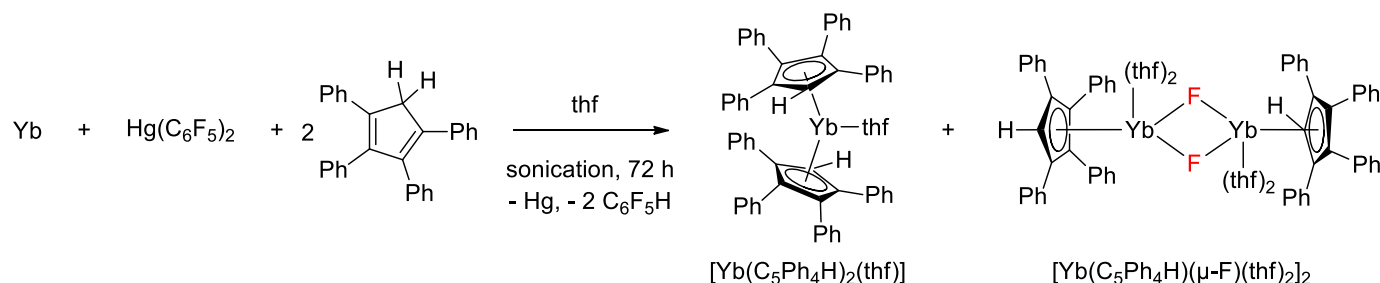
5.1 Introduction

As mentioned in Chapter 1, carbon-fluorine bonds represent the strongest carbon-element bonds in chemistry, a result of the small size and high electronegativity of the fluorine atom, and thus the activation of these bonds poses a great challenge. Owing to the high fluorophilicity of rare earth metals, these elements, and complexes of these elements, offer unique pathways to activate C-F bonds. Whilst extensive work has been undertaken on a range of fluorinated molecules with a range of metals, this introduction will focus on the C-F activation of fluorinated aromatic species by rare earth metals and their complexes. Largely, these C-F activation processes are a result of redox transmetallation/protolysis (RTP) reactions utilising $\text{Hg}(\text{C}_6\text{F}_5)_2$, $\text{Ag}(\text{C}_6\text{F}_5)$ and $\text{Bi}(\text{C}_6\text{F}_5)_3$,^[1-3] producing $\text{C}_6\text{F}_5\text{H}$ as a co-product, or through the formation of some $\text{Ln}(\text{C}_6\text{F}_5)_x$ species.

5.1.1 Redox transmetallation/protolysis based C-F activation of aromatic fluorides

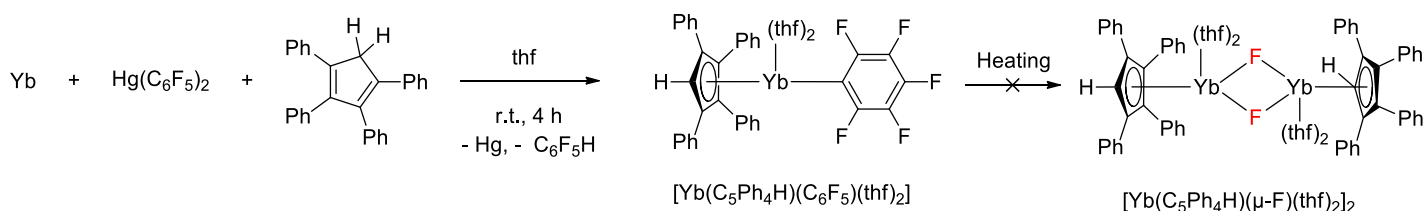
Many C-F activation reactions with rare earth metals have involved pentafluorobenzene ($\text{C}_6\text{F}_5\text{H}$), formed as a co-product from RTP reactions using $\text{Hg}(\text{C}_6\text{F}_5)_2$, $\text{Ag}(\text{C}_6\text{F}_5)$ and $\text{Bi}(\text{C}_6\text{F}_5)_3$ (as described in Chapter 1), or intermediates/precursors formed during the RTP reactions with a general $\text{Ln}(\text{C}_6\text{F}_5)_x$ motif. Whilst typically the formation of $\text{C}_6\text{F}_5\text{H}$ does not interfere with the course of the reaction, several examples of C-F activation are reported, with isolated complexes and organic compounds, exhibiting fluoride inclusion.

One of the major investigations into this phenomenon was undertaken by the Deacon group in 2014, when attempting to synthesise octaphenyl ytterbocene by RTP with $\text{Hg}(\text{C}_6\text{F}_5)_2$ the fluoride bridged half-sandwich was isolated alongside the metallocene (Scheme 5.1).^[4]



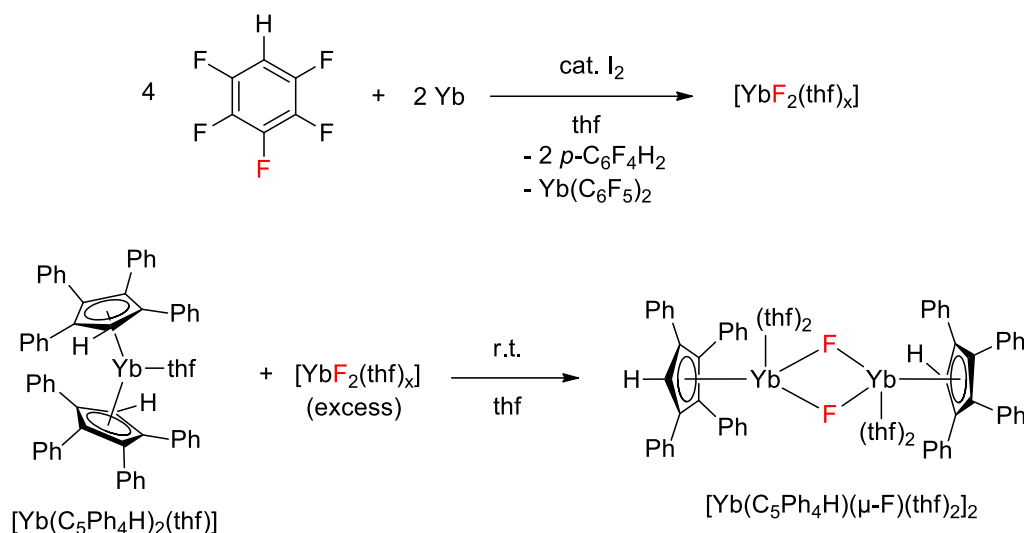
Scheme 5.1 – Synthesis of $[\text{Yb}(\text{C}_5\text{Ph}_4\text{H})_2(\text{thf})]$ and isolation of C-F activation product $[\text{Yb}(\text{C}_5\text{Ph}_4\text{H})(\mu\text{-F})(\text{thf})_2]_2$.^[4]

Isolation of the fluoride included product $[\text{Yb}(\text{C}_5\text{Ph}_4\text{H})(\mu\text{-F})(\text{thf})_2]_2$ sparked investigation into the C-F activation process, with the initial precursor thought to be $[\text{Yb}(\text{C}_5\text{Ph}_4\text{H})(\text{C}_6\text{F}_5)(\text{thf})_2]$, which upon heating/sonication, could form $[\text{Yb}(\text{C}_5\text{Ph}_4\text{H})(\mu\text{-F})(\text{thf})_2]_2$. In order to assess this, the precursor, $[\text{Yb}(\text{C}_5\text{Ph}_4\text{H})(\text{C}_6\text{F}_5)(\text{thf})_2]$, was synthesised by using one equivalent of Yb, $\text{Hg}(\text{C}_6\text{F}_5)_2$ and $\text{C}_5\text{Ph}_4\text{H}_2$ and stirring at room temperature in thf. Further heating of this $[\text{Yb}(\text{C}_5\text{Ph}_4\text{H})(\text{C}_6\text{F}_5)(\text{thf})_2]$ precursor did not result in the fluoride bridged half sandwich (Scheme 5.2).



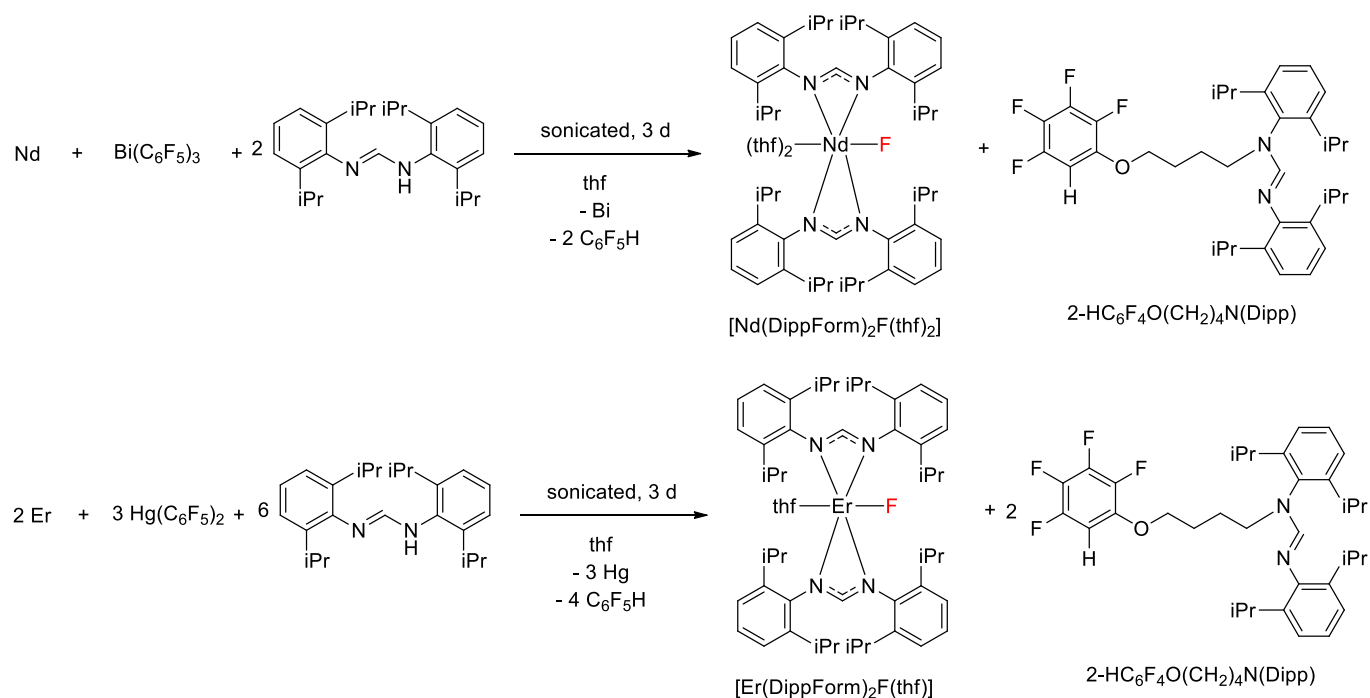
Scheme 5.2 – Attempted synthesis of $[\text{Yb}(\text{C}_5\text{Ph}_4\text{H})(\mu\text{-F})(\text{thf})_2]_2$ via the $[\text{Yb}(\text{C}_5\text{Ph}_4\text{H})(\text{C}_6\text{F}_5)(\text{thf})_2]$ precursor.^[4]

Having ruled out the $[\text{Yb}(\text{C}_5\text{Ph}_4\text{H})(\text{C}_6\text{F}_5)(\text{thf})_2]$ precursor, attention was then turned towards $\text{C}_6\text{F}_5\text{H}$ as the fluoride source. The RTP reaction described in Scheme 5.1 utilised an excess of ytterbium metal, which was thought to react with the produced $\text{C}_6\text{F}_5\text{H}$, producing $[\text{YbF}_2(\text{thf})_x]$, which could then undergo a redistribution with one equivalent of $[\text{Yb}(\text{C}_5\text{Ph}_4\text{H})_2(\text{thf})]$ to form $[\text{Yb}(\text{C}_5\text{Ph}_4\text{H})(\mu\text{-F})(\text{thf})_2]_2$. This proposed pathway was supported by several key observations: a) $p\text{-C}_6\text{F}_4\text{H}_2$ was detected in the reaction mixture by ^{19}F NMR spectroscopy and gas chromatography/mass spectrometry (GC/MS) studies, confirming fluoride abstraction from $\text{C}_6\text{F}_5\text{H}$; b) monitoring the RTP reaction by ^{19}F NMR spectroscopy showed gradual consumption of $\text{C}_6\text{F}_5\text{H}$ over time, with a proportional increase in $p\text{-C}_6\text{F}_4\text{H}_2$; c) performing the analogous RTP reaction with the fluorine-free $\text{Hg}(\text{Ph}_2)$, with subsequent addition of $\text{C}_6\text{F}_5\text{H}$ to the reaction mixture, led to some formation of $[\text{Yb}(\text{C}_5\text{Ph}_4\text{H})(\mu\text{-F})(\text{thf})_2]_2$; d) after completion of a stoichiometric reaction of Yb , $\text{Hg}(\text{C}_6\text{F}_5)_2$ and two equivalents of $\text{C}_5\text{Ph}_4\text{H}_2$, addition of excess Yb metal led to the formation of $[\text{Yb}(\text{C}_5\text{Ph}_4\text{H})(\mu\text{-F})(\text{thf})_2]_2$; and e) direct treatment of iodine activated Yb metal with $\text{C}_6\text{F}_5\text{H}$ led to the formation of $p\text{-C}_6\text{F}_4\text{H}_2$, $[\text{Yb}(\text{C}_6\text{F}_5)_2]$ and insoluble $[\text{YbF}_2(\text{thf})_x]$. The formation of $[\text{YbF}_2(\text{thf})_x]$ was confirmed by isolating the solid, and treating it with $[\text{Yb}(\text{C}_5\text{Ph}_4\text{H})_2(\text{thf})]$, which readily formed $[\text{Yb}(\text{C}_5\text{Ph}_4\text{H})(\mu\text{-F})(\text{thf})_2]_2$ (Scheme 5.3).^[4]



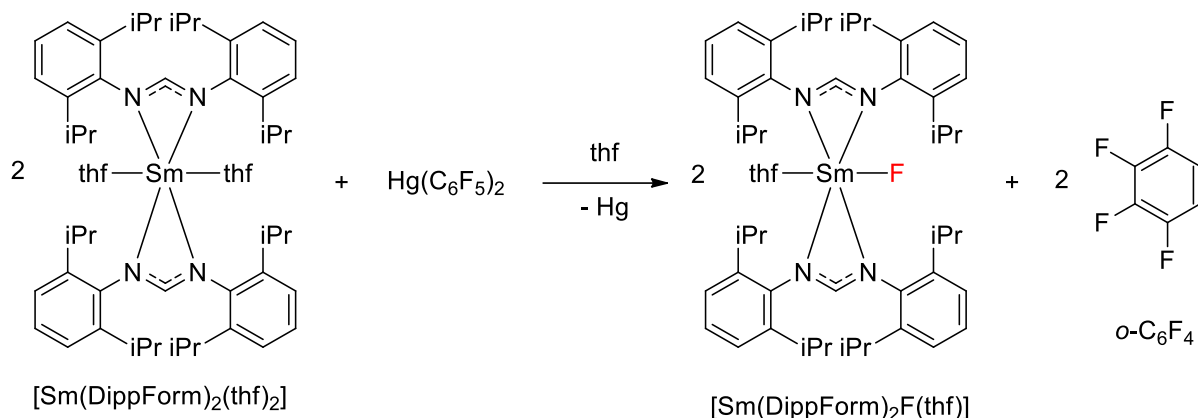
Scheme 5.3 – Proposed formation of [YbF₂(thf)_x] by C-F activation of C₆F₅H, and subsequent treatment with [Yb(C₅Ph₄H)₂(thf)] to yield [Yb(C₅Ph₄H)(μ-F)(thf)₂]₂ from redistribution.^[4]

Similarly, C-F activation has been observed in the synthesis of lanthanoid formamidinate complexes when synthesised by RTP, with both Bi(C₆F₅)₃ and Hg(C₆F₅)₂. Reactions were undertaken with N,N'-bis(2,6-diisopropylphenyl)formamidine (DippFormH), and either Nd metal with Bi(C₆F₅)₃ or Er metal with Hg(C₆F₅)₂. Both reactions saw inclusion of a fluoride ion into the formed trivalent complex, and isolation of the organic compound 2-HC₆F₄O(CH₂)₄N(Dipp), comprised of a ring-opened thf with *o*-C₆F₄H and DippForm moieties (Scheme 5.4).^[2]



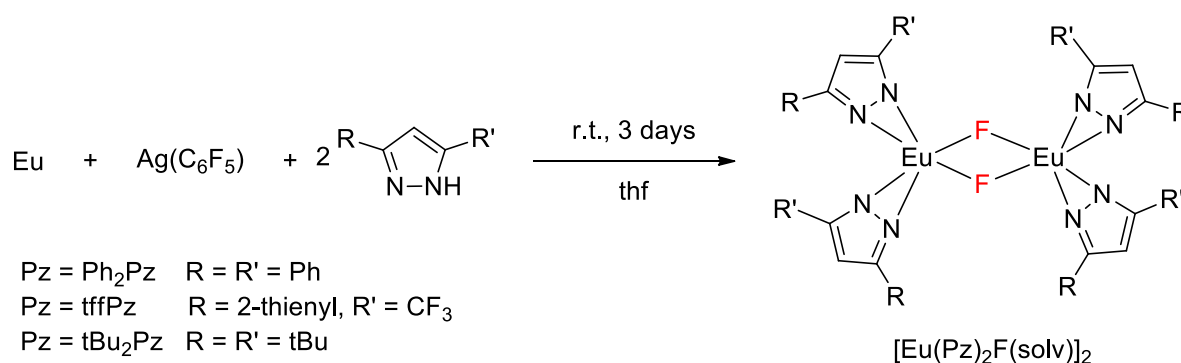
Scheme 5.4 – RTP reactions of Nd and Er metals, DippFormH and $\text{Bi}(\text{C}_6\text{F}_5)_3$ and $\text{Hg}(\text{C}_6\text{F}_5)_2$ respectively, yielding the fluoride included products $[\text{Nd}(\text{DippForm})_2\text{F}(\text{thf})_2]$ and $[\text{Er}(\text{DippForm})_2\text{F}(\text{thf})]$, alongside $2\text{-HC}_6\text{F}_4\text{O}(\text{CH}_2)_4\text{N}(\text{Dipp})$.^[2]

Whilst seemingly similar to the C-F activation observed when synthesising $[\text{Yb}(\text{C}_5\text{Ph}_4\text{H})(\mu\text{-F})(\text{thf})_2]_2$, the trivalent complexes in Scheme 5.4 are thought to be a result of the bulky DippFormH ligands inhibiting the third and final protolysis step of the RTP reaction, generating precursors of the general form $[\text{LnL}_2(\text{C}_6\text{F}_5)]$.^[5] Alternatively, incomplete protolysis of the generated $[\text{Ln}(\text{C}_6\text{F}_5)_3]$ species can also yield such precursors.^[5] In both cases, short metal-fluoride interactions facilitate C-F activation. This was confirmed in the case of samarium, where the divalent samarium complex $[\text{Sm}(\text{DippForm})_2(\text{thf})_2]$ could be further treated with $\text{Hg}(\text{C}_6\text{F}_5)_2$ to form $[\text{Sm}(\text{DippForm})_2\text{F}(\text{thf})]$ alongside *o*-tetrafluorobenzene (*o*- C_6F_4) (Scheme 5.5), proceeding by an $[\text{Sm}(\text{DippForm})_2(\text{C}_6\text{F}_5)]$ intermediate.^[6]



Scheme 5.5 – Conversion of [Sm(DippForm)₂(thf)₂] to the homoleptic, trivalent fluoride complex [Sm(DippForm)₂F(thf)].^[6]

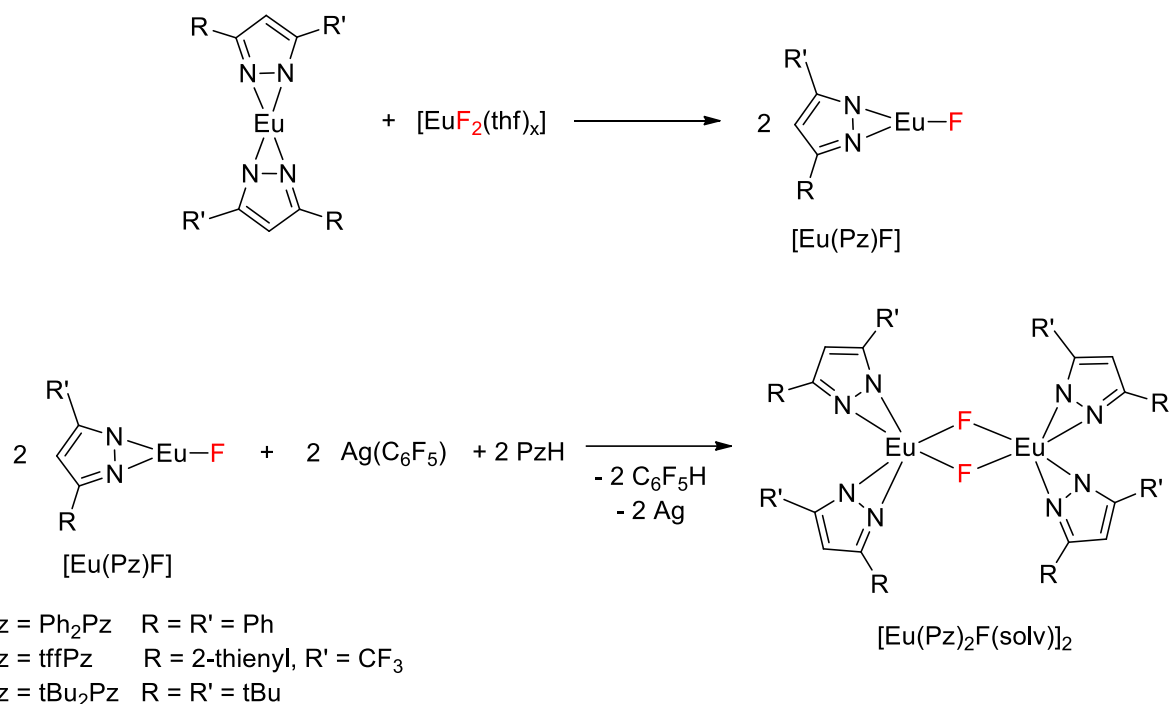
Similarly, europium pyrazolate complexes synthesised *via* RTP utilising Ag(C₆F₅) have also exhibited fluoride inclusion as a result of C-F activation. Treatment of Eu metal with Ag(C₆F₅) and a range of pyrazole ligands in thf resulted in fluoride bridged dinuclear complexes (Scheme 5.6).^[7]



Scheme 5.6 – C-F activation when synthesising europium pyrazolates by RTP with Ag(C₆F₅) resulting in [Eu(Pz)₂F(solv)]₂ (solvent omitted for clarity).^[7]

The fluoride inclusion as thought to proceed *via* firstly, formation of [EuF₂(thf)_x] analogous to the [YbF₂(thf)_x] formation described in Scheme 5.3, followed by redistribution with the synthesised [Eu(Pz)₂] complex to form the divalent, heteroleptic [Eu(Pz)₂F] species. This

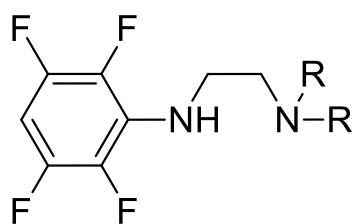
divalent species can undergo further redox transmetalation by a further equivalent of $\text{Ag}(\text{C}_6\text{F}_5)$, followed by protolysis to yield $[\text{Eu}(\text{Pz})_2\text{F}]_2$ (Scheme 5.7).^[7]



Scheme 5.7 – Proposed formation of trivalent $[\text{Eu}(\text{Pz})_2\text{F}(\text{solv})]_2$ complexes by redistribution and subsequent redox transmetalation/protolysis (solvent omitted for clarity).^[7]

5.1.2 Other examples of C-F bond activation of aromatic fluorides

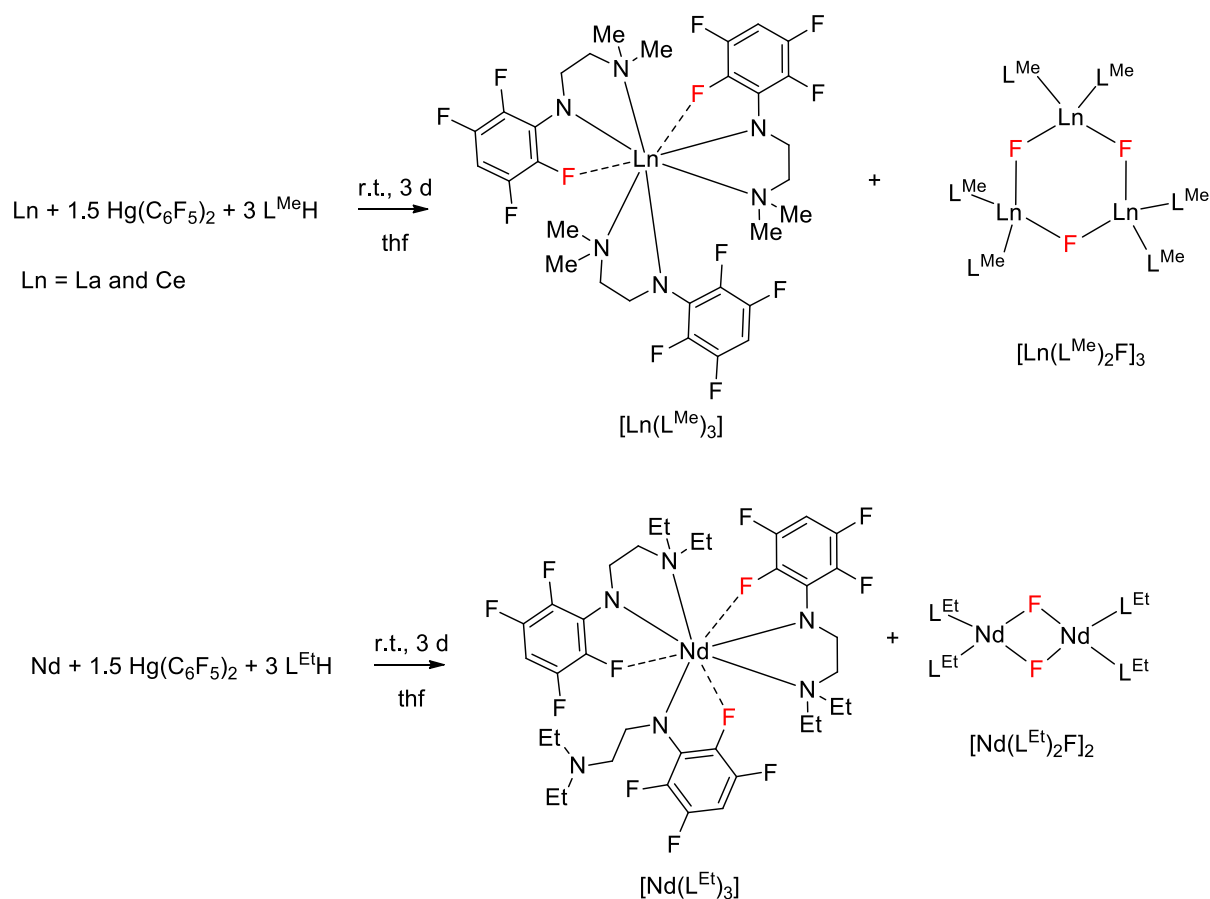
Whilst RTP reactions present lanthanoid metals with ample conditions for C-F activation, owing to short Ln-F interactions in $\text{Ln}(\text{C}_6\text{F}_5)_x$ containing species, and producing $\text{C}_6\text{F}_5\text{H}$ in the presence of highly active metals over the course of the reaction, these conditions can be induced by ligands that bear aromatic fluoride moieties that, once coordinated to the metal, promote intramolecular Ln-F coordination. These interactions have been readily observed by the Deacon group with N,N-dialkyl-N'-2,3,5,6-tetrafluorophenylethane-1,2-diamine (L^{RH}) ligands (Figure 5.1).^[8,9]



$L^R\text{H}$, R = Me or Et

Figure 5.1 – Molecular structure of N,N-dialkyl-N'-2,3,5,6-tetrafluorophenylethane-1,2-diamine ($L^R\text{H}$).^[8,9]

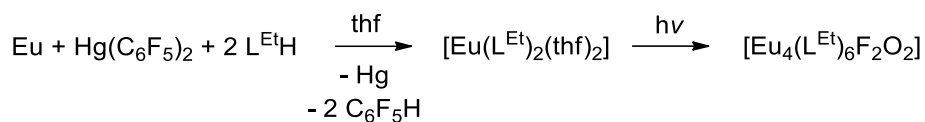
RTP reactions of La, Ce and Nd metals with $\text{Hg}(\text{C}_6\text{F}_5)_2$ and $L^{\text{Me/Et}}\text{H}$ in thf produced complexes of the general form $[\text{Ln}(L^{\text{Me/Et}})_3]$ (Ln = La, Ce and Nd), alongside low yields of $[\text{Ln}(L^{\text{Me}})_2\text{F}]_3$ (Ln = La and Ce) or $[\text{Nd}(L^{\text{Et}})_2\text{F}]_2$ (Scheme 5.8).^[8]



Scheme 5.8 – Synthesis of $[\text{Ln}(\text{L}^{\text{R}})_3]$ and $[\text{Ln}(\text{L}^{\text{Me}})_2\text{F}]_3$ (Ln = La and Ce) and $[\text{Nd}(\text{L}^{\text{Et}})_2\text{F}]_2$ complexes *via* C-F activation.^[8]

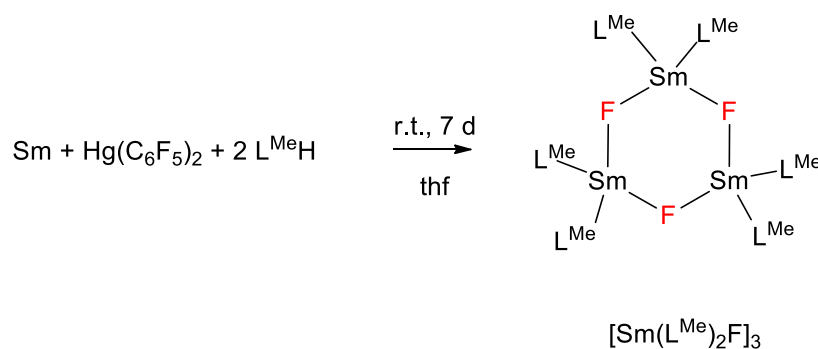
Close C-F interactions are harboured in the three synthesised complexes of the general form $[\text{Ln}(\text{L}^{\text{R}})_3]$, facilitating C-F activation. In these examples, the fluoride source was confirmed to be from the fluorinated ligands, and not $\text{C}_6\text{F}_5\text{H}$, as GC/MS studies of hydrolysed samples indicated defluorination of the L^{R} moieties.^[8]

Further examples of C-F activation have been observed with the same diaminate ligands with Eu and Sm metals.^[9] The divalent europium complex $[\text{Eu}(\text{L}^{\text{Et}})_2(\text{thf})_2]$ was synthesised by RTP *via* treatment of Eu metal with $\text{Hg}(\text{C}_6\text{F}_5)_2$ and $\text{L}^{\text{Et}}\text{H}$, however, after exposure of the complex to light, the trivalent mixed fluoride/oxide cluster $[\text{Eu}_4(\text{L}^{\text{Et}})_6\text{F}_2\text{O}_2]$ was isolated (Scheme 5.9).^[9]



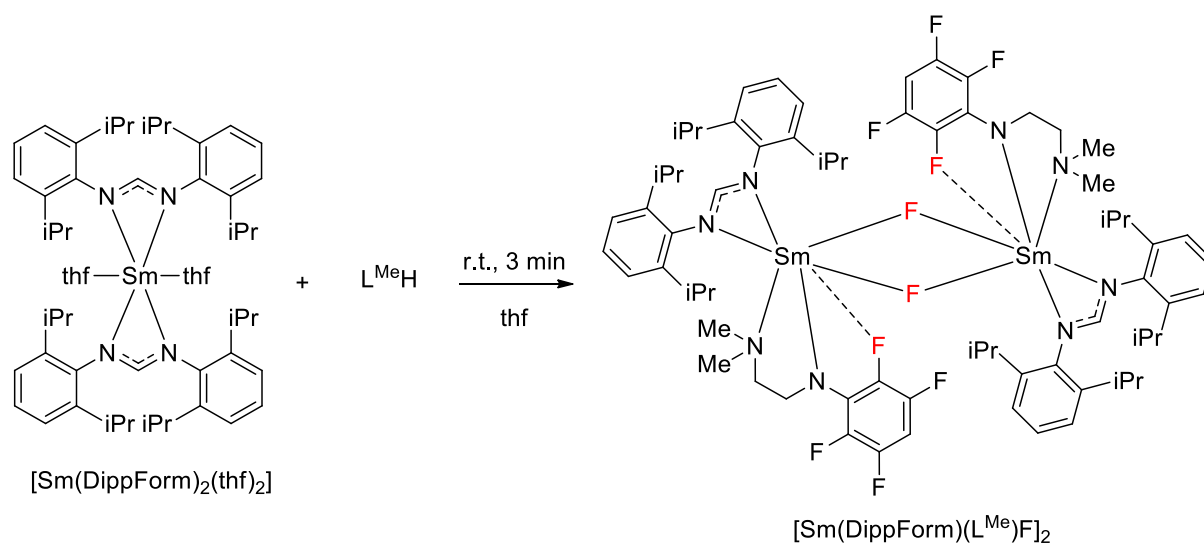
Scheme 5.9 – Synthesis of $[\text{Eu}(\text{L}^{\text{Et}})_2(\text{thf})_2]$ and subsequent light induced C-F activation to form the mixed fluoride/oxide cluster $[\text{Eu}_4(\text{L}^{\text{Et}})_6\text{F}_2\text{O}_2]$.^[9]

The analogous reaction with samarium metal and $\text{L}^{\text{Me}}\text{H}$ with $\text{Hg}(\text{C}_6\text{F}_5)_2$ produced small amounts of the heteroleptic complex $[\text{Sm}(\text{L}^{\text{Me}})_2\text{F}]_3$ (Scheme 5.10),^[9] analogous to the cerium and lanthanum complexes described in Scheme 5.8.



Scheme 5.10 – Synthesis of $[\text{Sm}(\text{L}^{\text{Me}})_2\text{F}]_3$ from an RTP reaction.^[9]

The Deacon group, again, confirmed the source of the fluoride to be from the $\text{L}^{\text{Me}}\text{H}$ ligand by performing a protolysis reaction between $[\text{Sm}(\text{DippForm})_2(\text{thf})_2]$ with $\text{L}^{\text{Me}}\text{H}$, readily undergoing protolysis, but also C-F activation, isolating the mixed ligand samarium fluoride species $[\text{Sm}(\text{DippForm})(\text{L}^{\text{Me}})\text{F}]_2$ (Scheme 5.11).^[9]

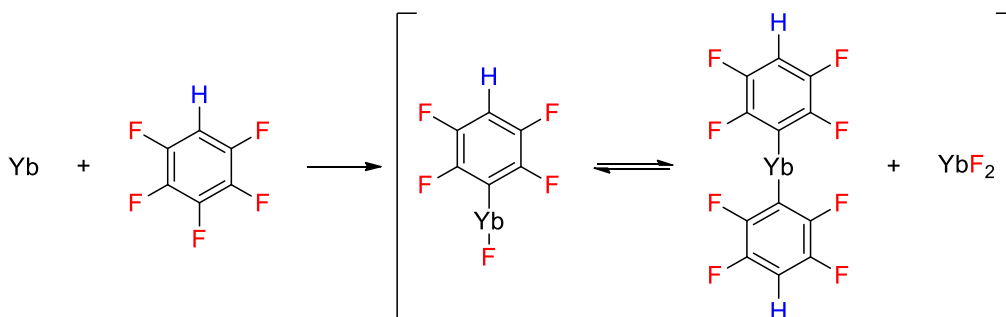


Scheme 5.11 – Protolysis reaction of $[\text{Sm}(\text{DippForm})_2(\text{thf})_2]$ with $\text{L}^{\text{Me}}\text{H}$ to yield the C-F activation product $[\text{Sm}(\text{DippForm})(\text{L}^{\text{Me}})\text{F}]_2$.^[9]

5.2 Results and discussion

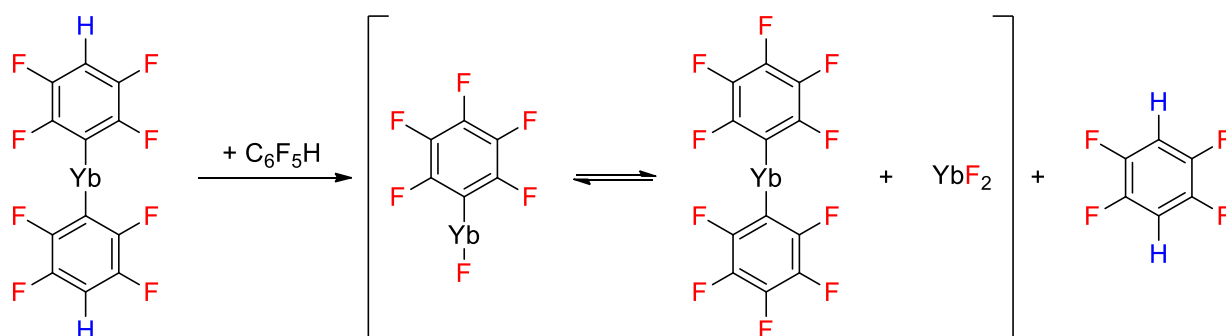
5.2.1 C-F activation studies of pentafluorobenzene by lanthanoid metals

Based on the initial qualitative findings of the Deacon group on the C-F activation of pentafluorobenzene by ytterbium metal, further experiments were undertaken to gain a quantitative understanding of this process, again with ytterbium metal, and extended to europium and samarium metals. As reported, treatment of iodine activated ytterbium metal with pentafluorobenzene led to the formation of *p*-C₆F₄H₂, some [Yb(C₆F₅)₂] and [YbF₂(thf)_x].^[4] Initially proposed to proceed by the radical mechanism outlined in the introduction, the formation of the detected [Yb(C₆F₅)₂] could not be explained. Instead, it is now proposed that the reaction proceeds by the initial formation of a pseudo-Grignard reagent, [Yb(C₆F₄H)F] (Scheme 5.12). This pseudo-Grignard reagent can readily undergo redistribution to yield [Yb(*p*-C₆F₄H)₂] and [YbF₂(thf)_x].



Scheme 5.12 – Proposed pseudo-Grignard mechanism for the C-F activation of C₆F₅H by Yb metal.

Owing to the very slow nature of the C-F activation, large amounts of unreacted C₆F₅H remain in solution as small amounts of the [Yb(*p*-C₆F₄H)F] pseudo-Grignard reagent forms, and the very basic *p*-C₆F₄H⁻ ligands of this pseudo-Grignard reagent can readily deprotonate C₆F₅H, yielding [Yb(C₆F₅)₂] and *p*-C₆F₄H₂ (Scheme 5.13).

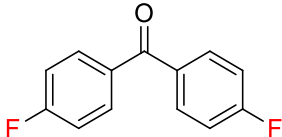
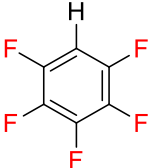
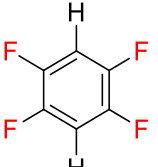
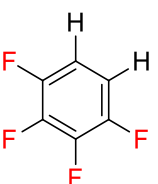
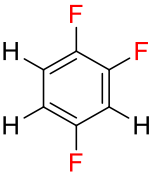


Scheme 5.13 – Protolysis reaction of $[\text{Yb}(p\text{-C}_6\text{F}_4\text{H})_2]$ with $\text{C}_6\text{F}_5\text{H}$ to form $[\text{Yb}(\text{C}_6\text{F}_5)_2]$ and *p*- $\text{C}_6\text{F}_4\text{H}_2$.

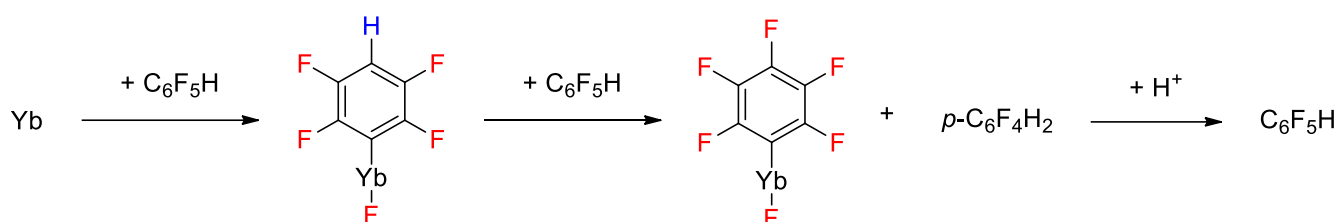
To support this proposed mechanism, reactions were undertaken involving two equivalents of ytterbium metal, one equivalent of pentafluorobenzene, and a crystal of iodine in thf, and stirring the suspension for 72 hours. After this duration, the reaction was cooled to $0\text{ }^\circ\text{C}$ in an ice bath (to avoid evaporation of the volatile polyfluoroaromatic compounds), and quenched with distilled water, and the organic materials extracted with diethyl ether. During this process, an internal standard of 4,4'-difluorobenzophenone was added, to aid in quantification of the products, and recovered pentafluorobenzene. The ^{19}F NMR spectrum of the ethereal solution was then analysed, and the integrations of relevant signals compared to the 4,4'-difluorobenzophenone internal standard in order to quantify the products formed.

A summary of the products formed, with their relevant chemical shifts, and yields are summarised in Table 5.1.

Table 5.1 – Summary of the products formed (and recovered C₆F₅H) from the reactions of C₆F₅H with Yb metal after 72 hours with their respective ¹⁹F NMR chemical shifts, and ratios (expressed as percentages).

Compound	Chemical shifts (ppm) and number of fluorine atoms	Yield (%)
4,4'-difluorobenzophenone (internal standard)	 -106.9 (2F)	-
C ₆ F ₅ H	 -139.5 (2F), -155.0 (1F), -163.0 (2F)	79%
<i>p</i> -C ₆ F ₄ H ₂	 -139.9 (4F)	14%
<i>o</i> -C ₆ F ₄ H ₂	 -140.1 (2F), -157.2 (2F)	6%
1,2,4-C ₆ F ₃ H ₃	 -116.0 (1F), -137.1 (1F), -140.4 (1F)	< 1%

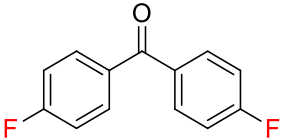
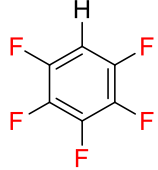
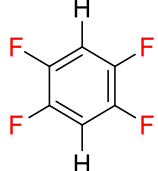
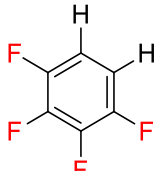
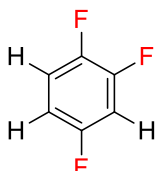
Whilst multiple C-F activation products were observed, most notably, p -C₆F₄H₂ is observed even before quenching the reaction mixture with water. This supports the pseudo-Grignard mechanism outlined above, as if two equivalents of C₆F₅H are used, this allows the formation of one equivalent of [Yb(p -C₆F₄H)F] which can deprotonate a further equivalent of C₆F₅H, yielding one equivalent of p -C₆F₄H₂, and one equivalent of [Yb(C₆F₅)F]. Quenching the reaction mixture with water then provides a proton for the regeneration of the C₆F₅H starting material (Scheme 5.14). Whilst the primary products observed for both metals were p -C₆F₄H₂, there was also evidence of further C-F activation yielding traces of 1,2,4-trifluorobenzene.



Scheme 5.14 – Simplified justification of product formation for the reaction of Yb metal with C₆F₅H (ignoring Schlenk equilibria products, and subsequent C-F activation of p -C₆F₄H₂ for simplicity).

Whilst the Jaroschik group had performed extensive qualitative studies with ytterbium metal, europium and samarium metals had yet to be analysed. In the same fashion, C-F activation studies with these two metals were undertaken, involving treatment of one equivalent of C₆F₅H with two equivalents of Ln metal (Ln = Eu or Sm), and a crystal of iodine in thf, and stirred for 72 hours before quenching, adding the internal standard, and extracting. The crude mixtures were again analysed by ¹⁹F NMR spectroscopy. The products of these reactions are summarised in Tables 5.2 and 5.3 respectively.

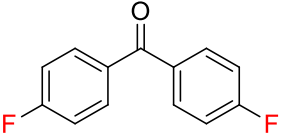
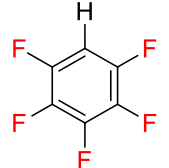
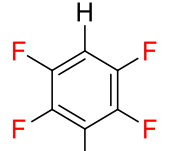
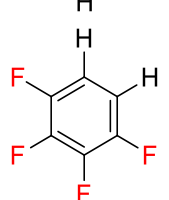
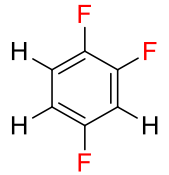
Table 5.2 – Summary of the products formed (and recovered C_6F_5H) from the reactions of C_6F_5H with Eu metal after 72 hours with their respective ^{19}F NMR chemical shifts, and ratios (expressed as percentages).

Compound		Chemical shifts (ppm) and number of fluorine atoms	Yield (%)
4,4'-difluorobenzophenone (internal standard)		-106.9 (2F)	-
C_6F_5H (recovered)		-139.5 (2F), -155.0 (1F), -163.0 (2F)	92%
<i>p</i> - $C_6F_4H_2$		-139.9 (4F)	6%
<i>o</i> - $C_6F_4H_2$		-140.1 (2F), -157.2 (2F)	2%
1,2,4- $C_6F_3H_3$		-116.0 (1F), -137.1 (1F), -140.4 (1F)	< 1%

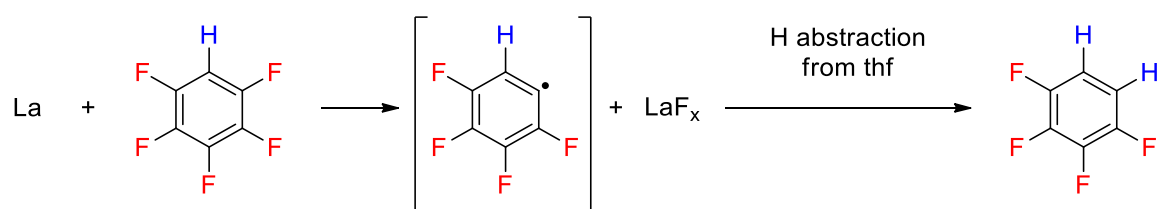
Chapter Five

The C-F activation of pentafluorobenzene by europium metal behaves very similarly to that of ytterbium metal, however with considerably lower activity, resulting in the same products: *p*-C₆F₄H₂ (major), *o*-C₆F₄H₂ (minor) and 1,2,4-trifluorobenzene (trace).

Table 5.3 – Summary of the products formed (and recovered C₆F₅H) from the reactions of C₆F₅H with Sm metal after 72 hours with their respective ¹⁹F NMR chemical shifts, and ratios (expressed as percentages).

Compound		Chemical shifts (ppm) and number of fluorine atoms	Yield (%)
4,4'-difluorobenzophenone (internal standard)		-106.9 (2F)	-
C ₆ F ₅ H		-139.5 (2F), -155.0 (1F), -163.0 (2F)	79%
<i>p</i> -C ₆ F ₄ H ₂		-139.9 (4F)	3%
<i>o</i> -C ₆ F ₄ H ₂		-140.1 (2F), -157.2 (2F)	18%
1,2,4-C ₆ F ₃ H ₃		-116.0 (1F), -137.1 (1F), -140.4 (1F)	< 1 %

Like both ytterbium and europium, the C-F activation by samarium metal, after quenching, led to formation of *p*-C₆F₄H₂, however, in much smaller quantities than ytterbium and europium, and signals in the ¹⁹F NMR spectrum corresponding to the *ortho* activated *o*-C₆F₄H₂ were also observed in much higher quantities. This suggested that the C-F activation by samarium metal proceeded by either two competing mechanisms, or an entirely different mechanism altogether. Initially it was proposed that, owing to the tendency for samarium metal to readily occupy either the divalent or trivalent states, a trivalent species could be responsible for this *ortho* activation. To assess this, a qualitative C-F activation reaction was performed with lanthanum metal in place of samarium, as lanthanum preferentially forms trivalent species, with a duration of 24 hours to determine if the same *ortho* activation would occur. ¹⁹F NMR spectroscopic analysis of the crude extract showed one prominent pair of signals, corresponding to *o*-C₆F₄H₂, with no *para* activated *p*-C₆F₄H₂ observed. Extension of the reaction duration to 96 hours led to complete consumption of C₆F₅H, which also suggested that no pseudo-Grignard species was forming, as quenching did not lead to recovery of C₆F₅H. Work from the Jaroschik group had shown that when the reaction was performed in thf-*d*₈, deuterium incorporation into the *ortho* tetrafluorobenzene (i.e., *o*-C₆F₄HD) was observed, confirmed by GC/MS, suggesting a radical pathway with proton (or deuterium) abstraction from thf (Scheme 5.14).



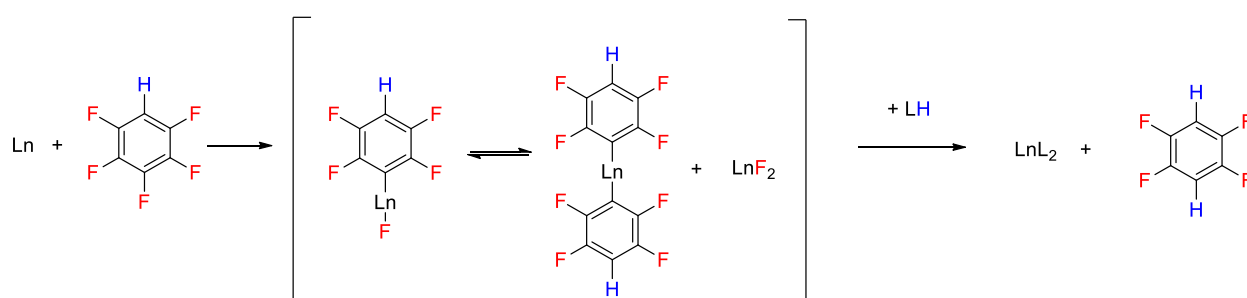
Scheme 5.14 – Proposed reaction mechanism of La metal induced C-F activation of pentafluorobenzene yielding 1,2,3,4-tetrafluorobenzene.

Because the formation and stabilisation of La(II) species is very difficult, the preference for the La(III) formation is likely responsible for the sole isolation of *o*-C₆F₄H₂, whereas the strongly

reducing Sm(II), which can readily oxidise to Sm(III), results in a mixture of both *p*- and *o*-C₆F₄H₂. This rationale can also be used to justify the formation of trace amounts of *o*-C₆F₄H₂ in the cases of Yb and Eu, which can also oxidise to form Ln(III) species, although much less preferentially than Sm.

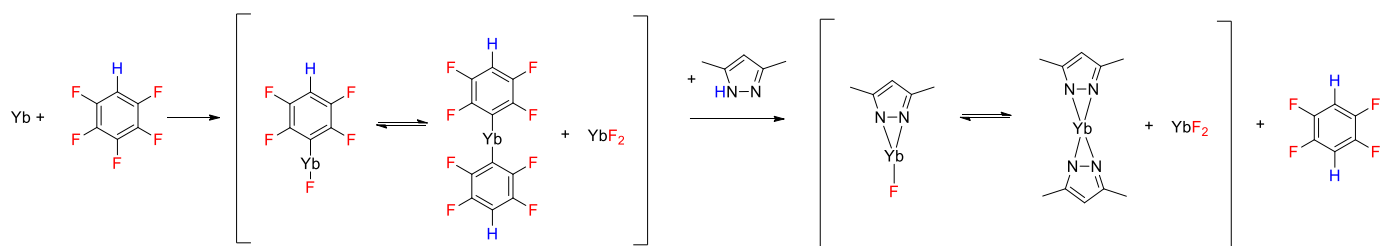
5.2.2 Synthesis of divalent cyclopentadienyl lanthanoid complexes by C-F activation/protolysis from Ln metal and pentafluorobenzene

Owing to the preferential formation of pseudo-Grignard reagents with europium and ytterbium metals, the C-F activation of C₆F₅H with europium and ytterbium metals was performed in the presence of protic ligands in an attempt to harness these *in situ* generated protolysis reagents to synthesise known, divalent organolanthanoid complexes. As described in Chapter 1, protolysis reactions are an effective means of synthesising rare earth complexes, however, as many lanthanoid protolysis reagents are derived from lanthanoid halide species, these reactions can suffer from “ate” complex formation, or halide inclusion. Whilst the C-F activation of C₆F₅H would seemingly offer the same drawbacks, as an [Ln(Ar)F] species is generated *in situ*, the extremely low solubility of [LnF₂(thf)_x] may be sufficient to avoid undesired fluoride inclusion into the final product (Scheme 5.15).



Scheme 5.15 – Proposed reaction scheme for the synthesis of organolanthanoid complexes by C-F activation/protolysis, where LH represents a protic reagent.

Like that of the redox transmetalation/protolysis reaction with $\text{Hg}(\text{C}_6\text{F}_5)_2$ that was described in Chapter 1 and 2, one of the major conditions is that the pK_a of the protic ligand used (LH) is lower than that of $\text{C}_6\text{F}_5\text{H}$, to ensure that LH is preferentially deprotonated by the generated $[\text{Ln}(p\text{-C}_6\text{F}_4\text{H})_2]$ species over any unreacted $\text{C}_6\text{F}_5\text{H}$. To determine the viability of this synthetic route, a pilot reaction was undertaken with Yb metal, $\text{C}_6\text{F}_5\text{H}$, with a catalytic amount of iodine in thf, and one equivalent of 3,5-dimethylpyrazole as the protic reagent (Scheme 5.16). The low steric bulk pyrazole, whilst difficult to isolate complexes of, has a pK_a value of approximately 20, being around one thousand times more acidic than $\text{C}_6\text{F}_5\text{H}$, and thus appropriate for a trial reaction.

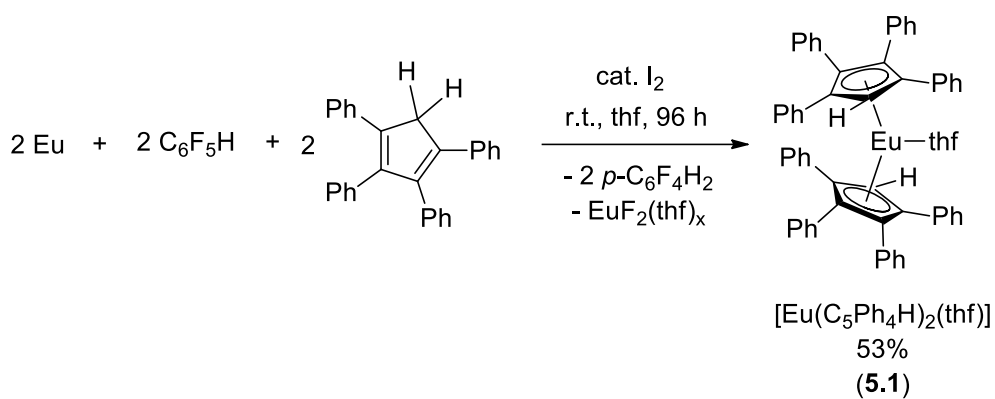


Scheme 5.16 – Pilot reaction of C-F activation/protolysis using 3,5-dimethylpyrazole as a protic reagent.

The reaction was followed by ^{19}F NMR spectroscopy, with the indication of a successful protolysis reaction being the complete consumption of $\text{C}_6\text{F}_5\text{H}$, and, upon quenching, no recovery of $\text{C}_6\text{F}_5\text{H}$, as no $[\text{Yb}(\text{C}_6\text{F}_5)\text{F}]$ or $[\text{Yb}(\text{C}_6\text{F}_5)_2]$ species should form in the presence of a protic ligand with a lower pK_a than $\text{C}_6\text{F}_5\text{H}$. After stirring for 72 hours, the ^{19}F NMR spectrum showed complete consumption of $\text{C}_6\text{F}_5\text{H}$, and upon quenching an aliquot, no $\text{C}_6\text{F}_5\text{H}$ was recovered, inferring that no $[\text{Yb}(\text{C}_6\text{F}_5)\text{F}]$ or $[\text{Yb}(\text{C}_6\text{F}_5)_2]$ remained. Notably, small quantities of the *meta* C-F activation product, 1,2,3,5-tetrafluorobenzene were also present, which have otherwise not been observed in detectable quantities in the ligand-free reactions with Yb or Eu metal under the same conditions. The presence of this product suggests the possibility of some

complex-induced C-F activation, owing to the effect of the ligand. Attempts were made to isolate the ytterbium pyrazolate complex, however, owing to the reactive nature of 3,5-dimethylpyrazolate complexes,^[10] these attempts were unsuccessful. With the success of the one pot C-F activation/protolysis reaction with ytterbium metal and 3,5-dimethylpyrazole, this methodology was extended to try and synthesise known, isolable complexes, such as lanthanoid polyarylcyclopentadienyl complexes.^[11,12]

Analogous to the pilot reaction with 3,5-dimethylpyrazole, a reaction was undertaken with europium metal and 1,2,3,4-tetraphenylcyclopenta-2,4-diene ($C_5Ph_4H_2$), in thf alongside C_6F_5H , and a crystal of I_2 . Whilst the pilot study was performed successfully with ytterbium metal, europium was selected initially, as the formation of an $[Eu(C_5Ph_4H)_2(solv)]$ species could be easily confirmed qualitatively by luminescence, as exciting with a blue laser (~ 405 nm) would emit red light upon formation of the sandwich complex. Utilising an excess of europium metal, one equivalent of C_6F_5H , one equivalent of $C_5Ph_4H_2$, and a crystal of iodine, the reagents were combined and anhydrous thf added, and the reaction was allowed to stir for 96 hours before the ^{19}F NMR spectrum showed complete consumption of C_6F_5H . At this point, the black suspension exhibited red luminescence from excitation with a blue laser (~ 405 nm), consistent with reports of $[Eu(C_5Ph_4H)_2(dme)]$.^[11] The solid materials were allowed to settle, and a dark yellow solution was isolated by filtration. Removing the solvent under reduced pressure and washing with *n*-pentane provided solvated the sandwich complex $[Eu(C_5Ph_4H)_2(thf)]$ (**5.1**) in moderate yields as a bright orange powder (Scheme 5.17). Crystals of **5.1** were grown from the slow cooling of a hot toluene solution.



Scheme 5.17 – C-F activation/protolysis reaction of Eu metal with C₆F₅H and C₅Ph₄H₂ to yield [Eu(C₅Ph₄H)₂(thf)₂] (**5.1**).

Whilst the yield was lower than those reported from the RTP reaction,^[11] and C-P cleavage route previously outlined in Chapter 3, this facile one pot synthesis with only one air sensitive reagent, no mercury reagents, and no prior pro-ligand synthesis required, demonstrates an effective and straightforward means of accessing these divalent lanthanocenes.

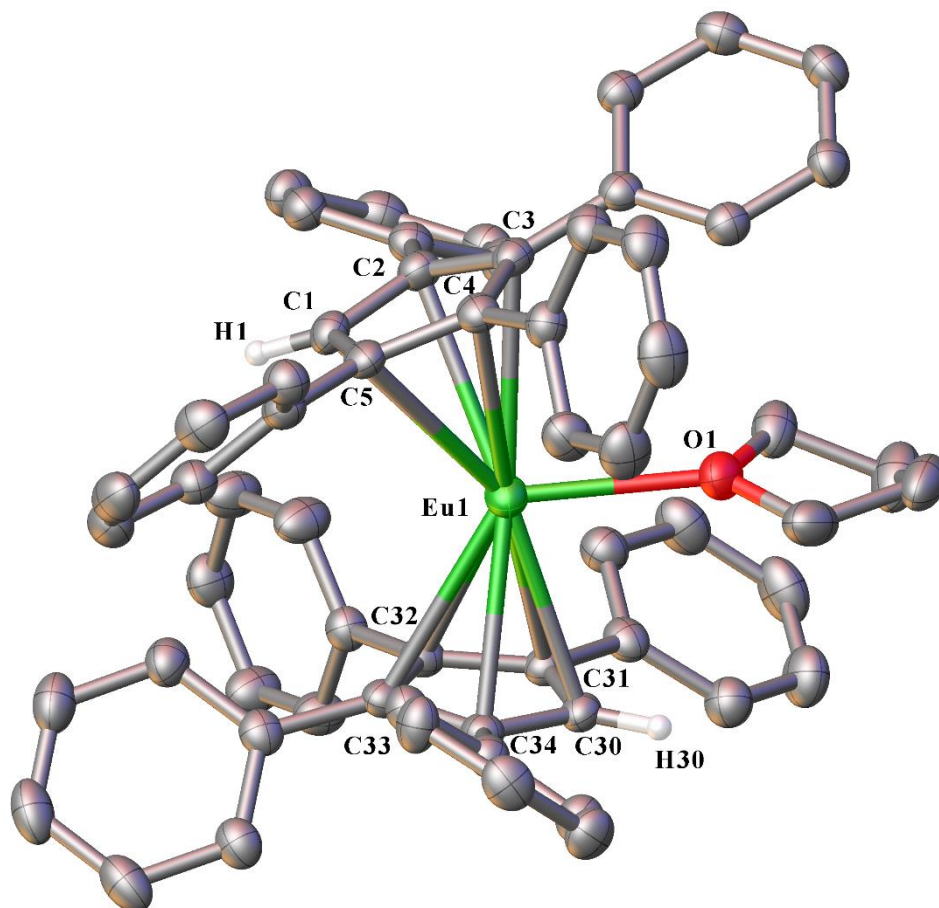
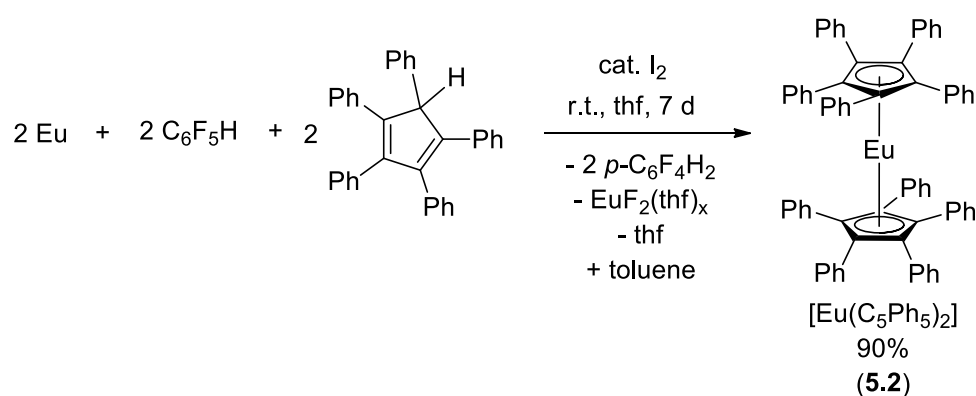


Figure 5.2 – ORTEP diagram of complex **5.1** showing atom-numbering scheme for relevant atoms. Thermal ellipsoids are drawn at the 30% probability level. Phenyl hydrogen atoms are omitted for clarity. Selected bond lengths of **5.1** (Å): Eu(1)-Cn(1) 2.576(2), Eu(1)-Cn(2) 2.562(3), Eu(1)-O(1) 2.484(5).

Complex **5.1** (Figure 5.2) crystallises in the monoclinic space group $P2_1/n$. It is isomorphous with both the reported octaphenyl samarocene $[\text{Sm}(\text{C}_5\text{Ph}_4)_2(\text{thf})]^{[11]}$ and octaphenyl ytterbocene $[\text{Yb}(\text{C}_5\text{Ph}_4\text{H})_2(\text{thf})]^{[4]}$. Previously, only the dme adduct had been reported, whereby one dme coordinated to the Eu centre,^[11] whereas **5.1** bears one thf molecule in place of the coordinated dme, which adversely affects the geometry of the complex. Compared to the dme adduct $[\text{Eu}(\text{C}_5\text{Ph}_4\text{H})_2(\text{dme})]$, **5.1** has shorter metal to centroid bond lengths ($[\text{Eu}(\text{C}_5\text{Ph}_4\text{H})_2(\text{dme})]$ Eu(1)-Cn(1) = 2.6044(12) and Eu(1)-Cn(2) = 2.6082(11)), owing to the

steric bulk about the coordinated dme when compared to a molecule of thf. The reduced steric bulk of the coordinated thf also influences the planar angle of the two Cp moieties about the metal, with **5.1** exhibiting a Cn(1)-Eu(1)-Cn(2) angle of $151.34(9)^\circ$, compared to $128.34(4)^\circ$.^[11]

The C-F activation/protolysis reaction was aimed to be extended by attempting the same reaction with europium metal and 1,2,3,4,5-pentaphenylcyclopentadiene (C_5Ph_5H). The reaction with C_5Ph_5H was undertaken in the same way as that described for the synthesis of **5.1**, however, after stirring for 24 hours, additional Eu metal and I_2 were added to ensure the reaction had initiated, as no major colour change was observed during this time. The ^{19}F NMR spectrum showed complete consumption of C_6F_5H after 7 days, at which point the reaction was stopped, and the solids allowed to settle before isolating the supernatant solution by filtration. As discussed in Chapter 3, divalent lanthanoid complexes of $C_5Ph_5^-$ readily form solvent separated ion pairs (SSIPs) in thf. Thus, the thf was removed under reduced pressure, and the sandwich complex $[Eu(C_5Ph_5)_2]$ (**5.2**) was precipitated from toluene in very good yields (Scheme 5.18). Crystals of **5.2** were grown from a thf: C_6D_6 (2:1) solution in an NMR tube.



Scheme 5.18 - C-F activation/protolysis reaction of Eu metal with C_6F_5H and C_5Ph_5H to yield $[Eu(C_5Ph_5)_2]$ (**5.2**).

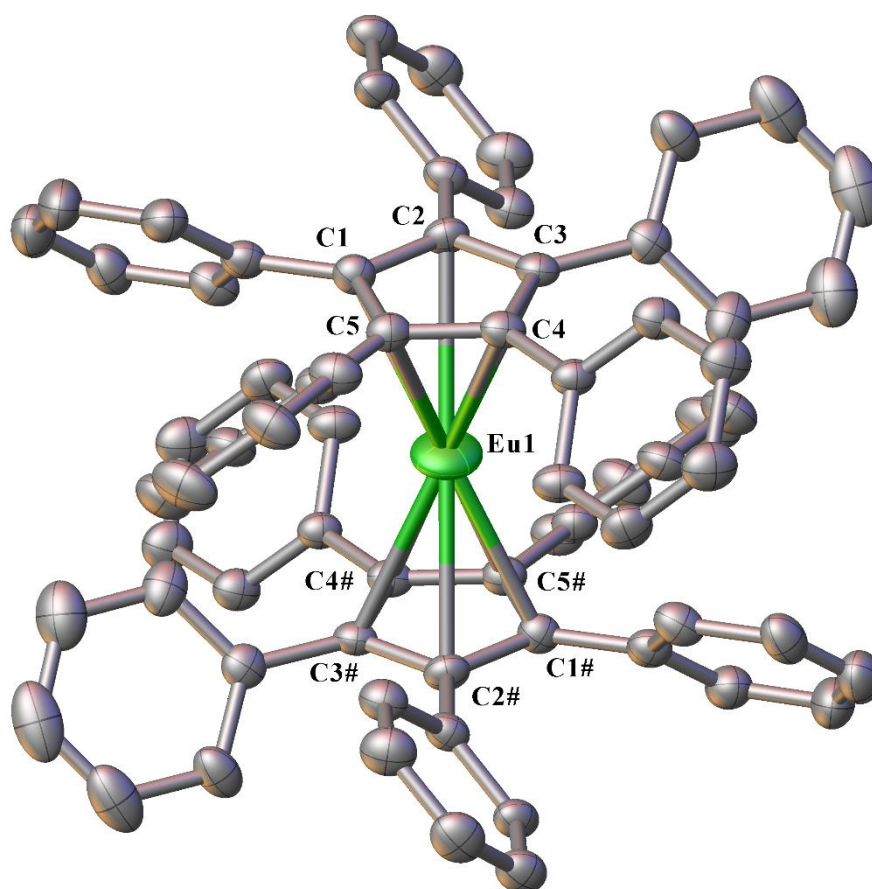


Figure 5.3 – ORTEP diagram of **5.2** showing atom-numbering scheme for relevant atoms. Thermal ellipsoids are drawn at the 40% probability level. Hydrogen atoms and lattice C_6D_6 are omitted for clarity. # Generated by symmetry (symmetry operation used 2-X, 1-Y, 2-Z).

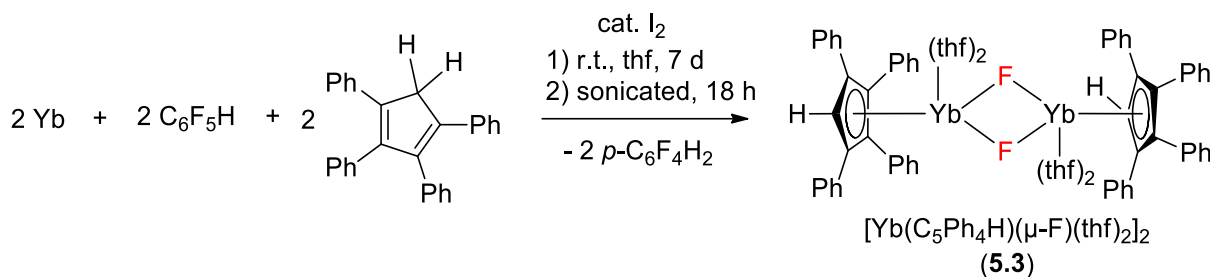
Complex **5.2** (Figure 5.3) crystallises in the triclinic space group $P\bar{1}$, bearing two half molecules in the asymmetric unit. There are 2.5 molecules of C_6D_6 in the lattice. Complex **5.2** is isomorphous with $[Yb(C_5Ph_5)_2] \cdot 2.5C_6D_6$ (**3.8**) reported in Chapter 3. The bond parameters are consistent with those reported for the Eu complex $[Eu(C_5Ph_5)_2] \cdot PhMe$ (**3.7**), and the same planar parallel Cp arrangement is observed. The phenyl rings are also in the same propellor formation as the previously reported decaphenyl lanthanocenes.^[11,12]

Interestingly, no formation of $[\text{Eu}(\text{C}_5\text{Ph}_5)(\mu\text{-F})(\text{thf})_2]_2$ was observed, as reported by the Deacon group when performing the RTP reaction with $\text{Hg}(\text{C}_6\text{F}_5)_2$ and $\text{C}_5\text{Ph}_5\text{H}$ with europium metal and sonicating.^[13] It was reported that small amounts of $[\text{Eu}(\text{C}_5\text{Ph}_5)(\mu\text{-F})(\text{thf})_2]_2$ crystallised alongside the desired $[\text{Eu}(\text{C}_5\text{Ph}_5)_2]$, thought to be a result of redistribution with $[\text{EuF}_2(\text{thf})_x]$ formation from the C-F activation of the $\text{C}_6\text{F}_5\text{H}$ by-product. $[\text{Eu}(\text{C}_5\text{Ph}_5)(\mu\text{-F})(\text{thf})_2]_2$ formation was avoided by either removing the fluoride source by using HgPh_2 in place of $\text{Hg}(\text{C}_6\text{F}_5)_2$, or by performing the reaction at room temperature with stirring instead of sonication. As the C-F activation/protolysis reactions were performed at room temperature with stirring, this was likely sufficient to avoid the fluoride incorporation that resulted in formation of the lanthanoid fluoride half sandwich complex observed by the Deacon group.

Having shown promising results for the synthesis of europium sandwich complexes with the C-F activation/protolysis route, and as the C-F activation of $\text{C}_6\text{F}_5\text{H}$ by europium and ytterbium metals both proceed by the same pseudo-Grignard mechanism, two further reactions were attempted with ytterbium metal to yield the analogous ytterbium sandwich complexes.

Excess ytterbium metal was treated with one equivalent of $\text{C}_6\text{F}_5\text{H}$, one equivalent of $\text{C}_5\text{Ph}_4\text{H}_2$, and a crystal of I_2 in thf , and stirred for several days, monitoring the reaction progress by ^{19}F NMR spectroscopy. After 48 hours, analysis by ^{19}F NMR spectroscopy showed partial conversion of $\text{C}_6\text{F}_5\text{H}$ to *p*- $\text{C}_6\text{F}_4\text{H}_2$, however, when compared to the analogous reaction with Eu metal and $\text{C}_5\text{Ph}_4\text{H}_2$, the progress was much slower. An additional stoichiometric equivalent of Yb metal and crystal of I_2 were added, and the reaction continued to stir for a further 48 hours. After 96 hours, the ^{19}F NMR spectrum showed approximately 33% conversion of $\text{C}_6\text{F}_5\text{H}$ to *p*- $\text{C}_6\text{F}_4\text{H}_2$, and like the Eu reactions, small amounts of *m*- $\text{C}_6\text{F}_4\text{H}_2$. Most notably, two other signals appeared much further downfield than typical polyfluoroaromatic resonances: two singlets at -57.7 and -81.9 ppm, each flanked by two satellites ($J = 450$ Hz). The resonance at -57.7 ppm

was not able to be assigned, however the singlet at -81.9 ppm corresponds directly to the reported Yb-F signal of $[\text{Yb}(\text{C}_5\text{Ph}_4\text{H})(\mu\text{-F})(\text{thf})_2]_2$,^[4] with the resultant satellites due to ^{171}Yb - ^{19}F coupling. Formation of $[\text{Yb}(\text{C}_5\text{Ph}_4\text{H})(\mu\text{-F})(\text{thf})_2]_2$ (**5.3**) suggests that the formed octaphenyl ytterbocene undergoes redistribution with $[\text{YbF}_2(\text{thf})_x]$, yielding the ytterbium fluoride half sandwich complex **5.3** (Scheme 5.19).

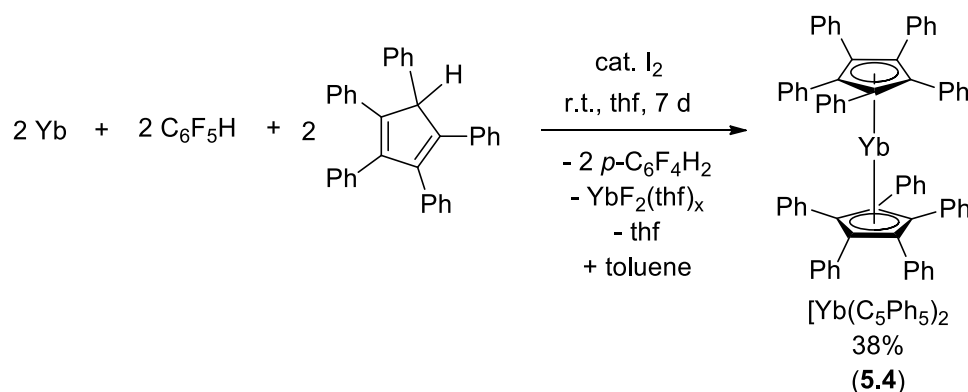


Scheme 5.19 - C-F activation/protolysis reaction of Yb metal with $\text{C}_6\text{F}_5\text{H}$ and $\text{C}_5\text{Ph}_4\text{H}_2$ to yield $[\text{Yb}(\text{C}_5\text{Ph}_4\text{H})(\mu\text{-F})(\text{thf})_2]_2$ (**5.3**).

As only partial conversion of the $\text{C}_6\text{F}_5\text{H}$ was observed after 4 days, the reaction was continued for a total of 7 days, until the $\text{C}_6\text{F}_5\text{H}$ was totally consumed. As more $\text{C}_6\text{F}_5\text{H}$ was consumed, and thus more $[\text{YbF}_2(\text{thf})_x]$ produced, the $[\text{Yb}(\text{C}_5\text{Ph}_4\text{H})(\mu\text{-F})(\text{thf})_2]_2$ (**5.3**) signal at -81.9 ppm increased, although not proportionally, as an expected ratio of $p\text{-C}_6\text{F}_4\text{H}_2$: Yb-F of 4 : 1 would be achieved given total conversion, whereas instead a 4 : 0.95 ratio was observed. The unassigned signal at -57.7 ppm did not increase during this time. The reaction was stopped, and the solids allowed to settle, and the dark red supernatant solution isolated by filter cannula. Attempts to grow crystals of **5.3** were unsuccessful, and isolation of the solid material by removing solvent under reduced pressure led to decomposition, and loss of the Yb-F signal in the ^{19}F NMR spectrum. As such, a yield, and further characterisation were not obtained.

The analogous reaction was prepared with one equivalent of $\text{C}_5\text{Ph}_5\text{H}$, one equivalent of $\text{C}_6\text{F}_5\text{H}$, excess Yb metal, and a crystal of I_2 in thf , and stirred for 4 days. After this time the ^{19}F NMR

spectrum of the crude reaction mixture showed 35% conversion of C_6F_5H to $p-C_6F_4H_2$, and so another equivalent of Yb metal and I_2 were added and stirred for 3 days further (7 days total), at which point all of the C_6F_5H had been consumed. The crude 1H NMR spectrum also showed complete consumption of the C_5Ph_5H starting material (4.99 ppm). Compared to the analogous reaction with $C_5Ph_4H_2$, no clear Yb-F signal had developed, suggesting solely formation of the ytterbium SSIP, and that no fluoride inclusion had occurred. The reaction was stopped, the supernatant solution isolated by filtration, and the thf and volatile polyfluoroaromatics removed under reduced pressure before precipitating the ytterbium sandwich complex $[Yb(C_5Ph_5)_2]$ (**5.4**) from toluene (Scheme 5.20). Crystals of **5.4** were grown from a C_6D_6 solution, and the identity confirmed by 1H NMR and IR spectroscopy, alongside single crystal X-ray diffraction studies.^[12]



Scheme 5.20 - C-F activation/protolysis reaction of Yb metal with C_6F_5H and C_5Ph_5H to yield $[Yb(C_5Ph_5)_2]$ (**5.4**).

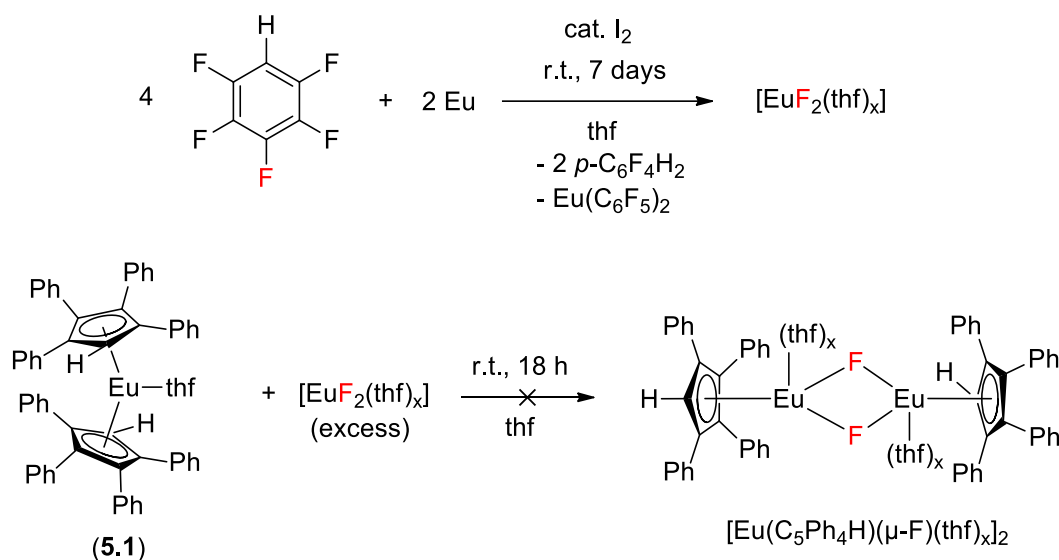
Attempts to synthesise the samarium analogues by C-F activation/protolysis were undertaken with the same conditions as outlined for europium and ytterbium, however, poor conversion of C_6F_5H was observed, even with reaction durations of over 10 days, and only the ligands could be recovered.

5.2.3 Synthesis of lanthanoid fluoride half sandwich complexes by redistribution with $[\text{LnF}_2(\text{thf})_x]$

Of the four sandwich complexes synthesised by the C-F activation/protolysis route with Ln metals and $\text{C}_6\text{F}_5\text{H}$, formation of only one lanthanoid fluoride half sandwich was observed in the form of $[\text{Yb}(\text{C}_5\text{Ph}_4\text{H})(\mu\text{-F})(\text{thf})_2]_2$ (**5.3**). This synthetic route had otherwise proven to be an effective means of synthesising divalent octaphenyl europocene, and decaphenyl europocene and ytterbocene, however, it was of interest to determine if the lanthanoid fluoride half sandwich complexes could be intentionally synthesised. A range of lanthanoid half sandwich complexes incorporating chlorides, bromides and iodides have been directly synthesised by treatment of the respective sandwich complex with the corresponding lanthanoid halide.^[11] Comparatively, the synthesis of fluoride half sandwich complexes in this regard has proven difficult, owing to the limited solubility of lanthanoid fluoride species, with only one example reported in $[\text{Yb}(\text{C}_5\text{Ph}_4\text{H})(\mu\text{-F})(\text{thf})_2]_2$.^[4] Therefore, investigation into treating the lanthanoid metallocenes with their corresponding lanthanoid fluorides formed *in situ* through C-F activation of $\text{C}_6\text{F}_5\text{H}$, was undertaken to assess the viability of synthesising these lanthanoid fluoride half sandwich complexes.

Initial attempts were made with **5.1** owing to its luminescence when excited with a blue laser (~405 nm), potentially allowing for the qualitative confirmation of its consumption. The proposed reaction involved firstly synthesising $[\text{EuF}_2(\text{thf})_x]$ by C-F activation of $\text{C}_6\text{F}_5\text{H}$. Treating an excess of $\text{C}_6\text{F}_5\text{H}$ with one equivalent of Eu metal, activated by I_2 , in thf, and stirring for 7 days led to formation of a black suspension. The solids were allowed to settle, and the supernatant solution (containing polyfluoroaromatics, and $[\text{Eu}(\text{C}_6\text{F}_5)_2]$) was removed by filtration, and the solids dried under reduced pressure yielding $[\text{EuF}_2(\text{thf})_x]$ and any unreacted

Eu metal. A solution of **5.1** in thf was then added to the solid and stirred overnight (Scheme 5.21).



Scheme 5.21 – Proposed reaction scheme for the synthesis of [EuF₂(thf)_x] and subsequent treatment with **5.1** to yield [Eu(C₅Ph₄H)(μ-F)(thf)_x]₂.

Upon addition of the bright orange solution of **5.1** to [EuF₂(thf)_x], a bright yellow solution was immediately produced, and pink luminescence was observed when the suspension was excited with a blue laser (~405 nm). The suspension was stirred overnight at room temperature to ensure the reaction progressed to completion before isolating the dark yellow/brown supernatant solution by filtration, removing the solvent under reduced pressure, and then dissolving in hot toluene and allowing to stand. An orange precipitate was recovered, confirmed to be unreacted **5.1**, alongside small colourless crystals, found to be 2,2',2'',3,3',3'',5,5',5'',6,6',6''-dodecafluoro-1,1':4',1''-terphenyl (Figure 5.4).

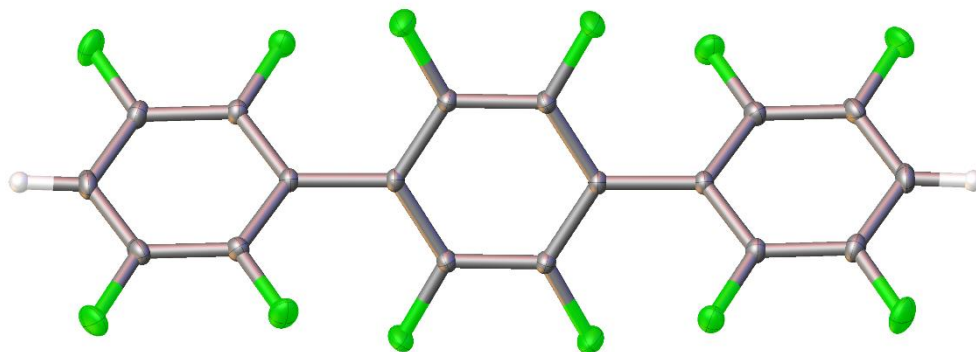
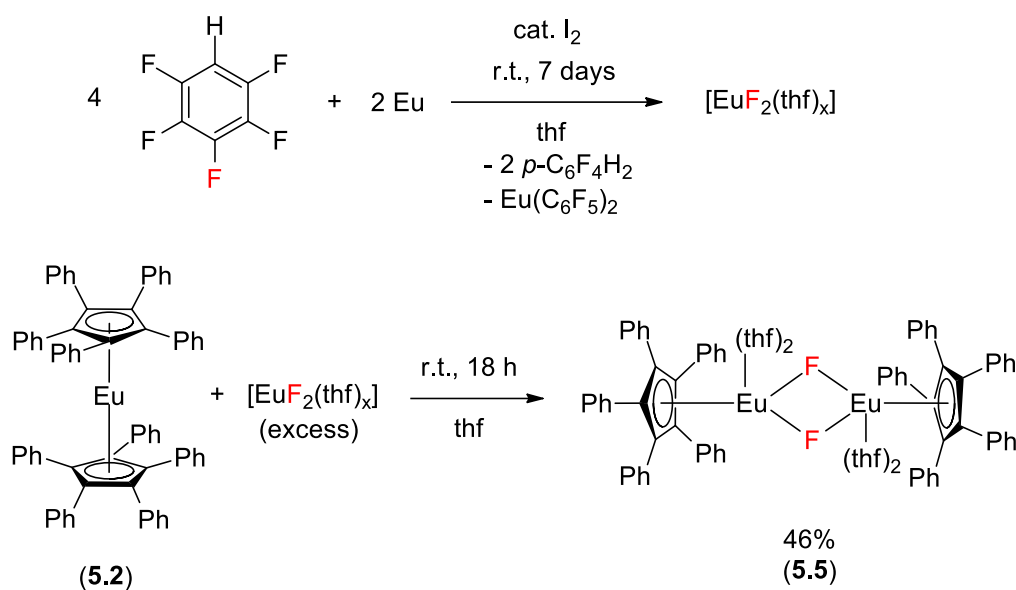


Figure 5.4 – ORTEP diagram of 2,2',2'',3,3',3'',5,5',5'',6,6',6''-dodecafluoro-1,1':4,1''-terphenyl recovered from attempted synthesis of $[\text{Eu}(\text{C}_5\text{Ph}_4\text{H})(\mu\text{-F})(\text{thf})_x]_2$.

The terphenyl was thought to arise from Wurtz coupling of two $\text{C}_6\text{F}_4\text{H}^-$ moieties after formation of the pseudo-Grignard $[\text{Eu}(\text{C}_6\text{F}_4\text{H})_2]$ species to form 2,2',3,3',5,5',6,6'-octafluorobiphenyl, followed by C-H activation and further coupling to form the above terphenyl species.

An analogous attempt was made using **5.2** to synthesise the pentaphenylcyclopentadienyl europium fluoride half sandwich $[\text{Eu}(\text{C}_5\text{Ph}_5)(\mu\text{-F})(\text{thf})_2]_2$ (**5.5**) (Scheme 5.22), which proved to be successful.



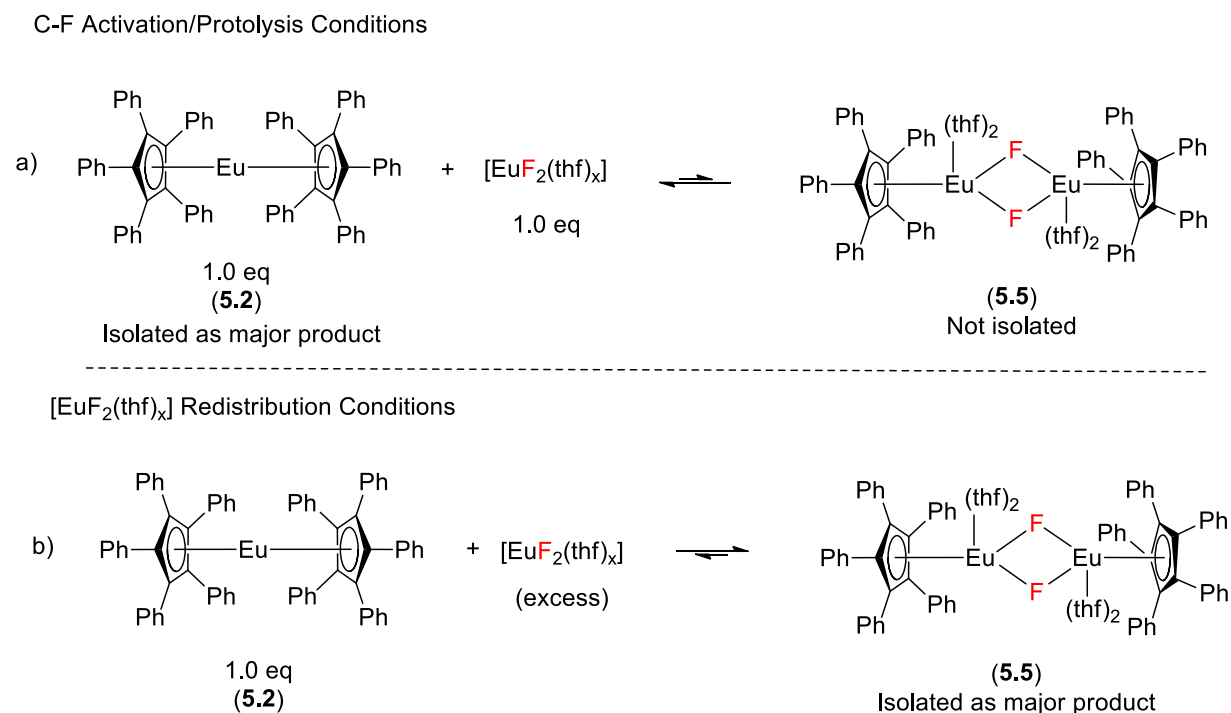
Scheme 5.22 – Reaction scheme for the synthesis of [EuF₂(thf)_x] and subsequent treatment with **5.2** to yield [Eu(C₅Ph₅)(μ-F)(thf)₂]₂ (**5.5**).

The solution of **5.5** and the isolated solid material matched the description of that described by past Deacon group member, Dr. Rory Kelly.^[13] Owing to the paramagnetic nature of **5.5**, no satisfactory NMR spectra could be obtained, however, IR spectroscopy, and microanalysis returned results in agreement with the crystal structure reported by Dr. Rory Kelly (Figure 5.5).^[13]

Complex **5.5** represents the first divalent europium fluoride species to be structurally characterised, and the intentional synthesis of this complex by redistribution sets an exciting precedent for the formation of fluoride bridged half sandwich complexes.

Despite the lack of formation of the europium fluoride half sandwich complexes observed by the C-F activation/protolysis reactions performed at room temperature with stirring, introduction of an excess of [EuF₂(thf)_x] proved to be an effective means of isolating the interesting, new pentaphenyl half sandwich complex. As the redistribution reaction is a result of the Schlenk equilibrium, a possible explanation for the preferential formation of **5.5** when

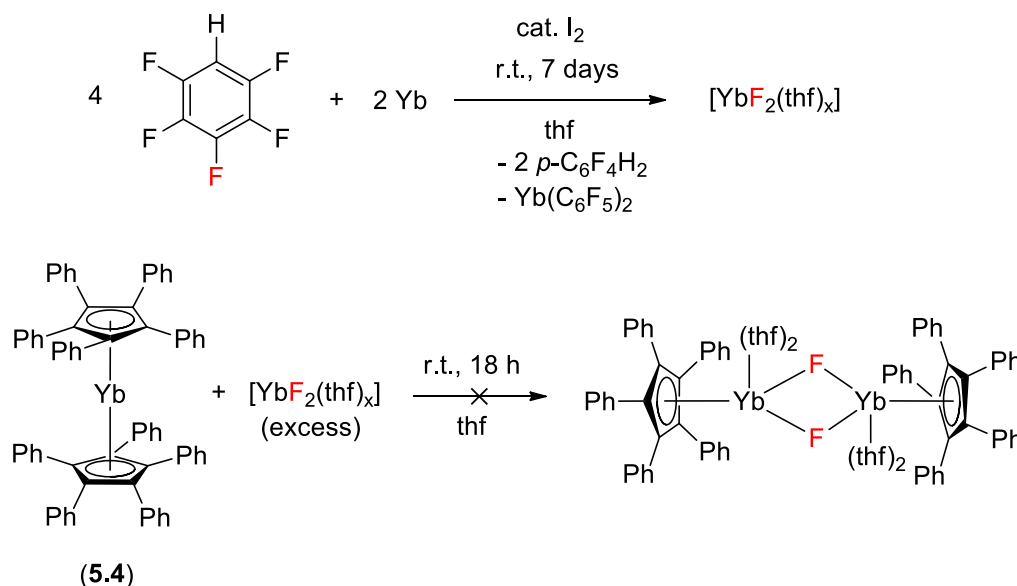
exposed to excess $[\text{EuF}_2(\text{thf})_x]$ has been proposed: as previously described, the solubility of lanthanoid fluorides was thought to be sufficiently low to avoid influencing the Schlenk equilibrium in favour of the lanthanoid fluoride half sandwiches, however, when a huge excess of lanthanoid fluoride is used, despite its poor solubility, the equilibrium can be influenced to favour the formation of the lanthanoid fluoride half sandwich complex (Scheme 5.23).



Scheme 5.23 – Schlenk equilibrium between **5.2** and **5.5** in the presence of $[\text{EuF}_2(\text{thf})_x]$ under a) C-F activation/protolysis conditions, and b) $[\text{EuF}_2(\text{thf})_x]$ redistribution conditions.

The redistribution reaction of **5.2**, and lack thereof of redistribution of **5.1**, is possibly attributed to the stability of the two compounds when dissolved in thf. The octaphenyl europocene (**5.1**) in thf results in a stable, isolable complex, whereas the decaphenyl europocene **5.2** forms the less stable, non-isolable, solvent-separated ion pair (SSIP) $[\text{Eu}(\text{thf})_x][\text{C}_5\text{Ph}_5]_2$, which may result in its increased propensity to react.

This approach was further extended to decaphenyl ytterbocene, being treated with $[\text{YbF}_2(\text{thf})_x]$ (generated by the same route as $[\text{EuF}_2(\text{thf})_x]$), in order to synthesise $[\text{Yb}(\text{C}_5\text{Ph}_5)(\mu\text{-F})(\text{thf})_2]_2$ (Scheme 5.24).



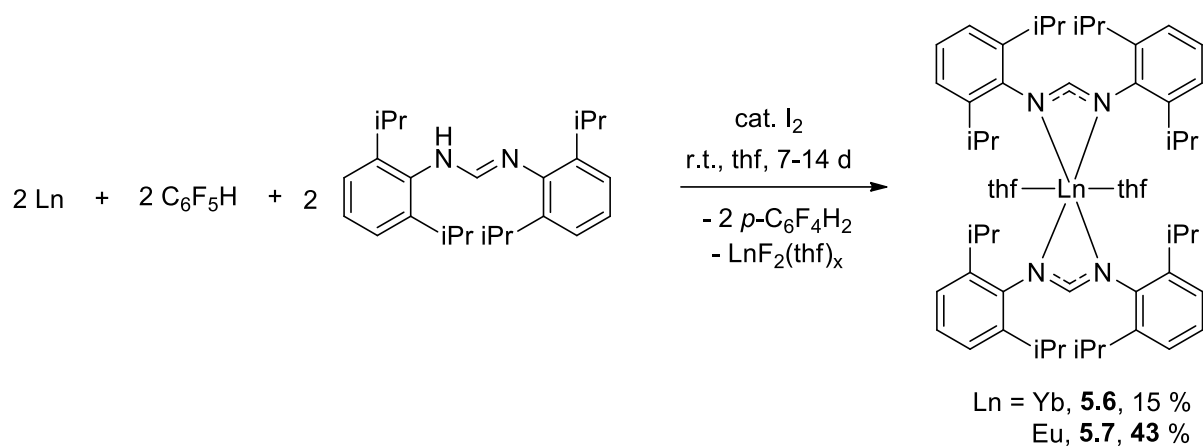
Scheme 5.24 - Reaction scheme for the attempted synthesis of $[\text{YbF}_2(\text{thf})_x]$ and subsequent treatment with **5.4** to yield $[\text{Yb}(\text{C}_5\text{Ph}_5)(\mu\text{-F})(\text{thf})_2]_2$.

After 18 hours of stirring, the reaction mixture produced a dark black suspension, and allowing this to settle resulted in a near colourless solution. ^{19}F NMR spectroscopy showed no Yb-F signals, suggesting instead that the complex had decomposed. The lack of reactivity for **5.4** towards $\text{YbF}_2(\text{thf})_x$ may also be attributed to the stability of the $[\text{Yb}(\text{thf})_6][\text{C}_5\text{Ph}_5]_2$ SSIP formed when **5.4** is dissolved in thf.^[12] The ytterbium SSIP has been successfully isolated, and thus this stability may decrease the reactivity of **5.4** towards redistribution to form the half sandwich complex.

5.2.4 Synthesis of other divalent lanthanoid complexes

Whilst the synthesis of europium and ytterbium sandwich complexes by C-F activation/protolysis proved to be both an efficient alternative to redox transmetallation/protolysis, the versatility of the system had yet to be shown towards other protic ligands. A selection of common ligands (in our laboratory) were trialled under analogous conditions to those already described, in order to assess the scope of the C-F activation/protolysis route for accessing other divalent lanthanoid complexes.

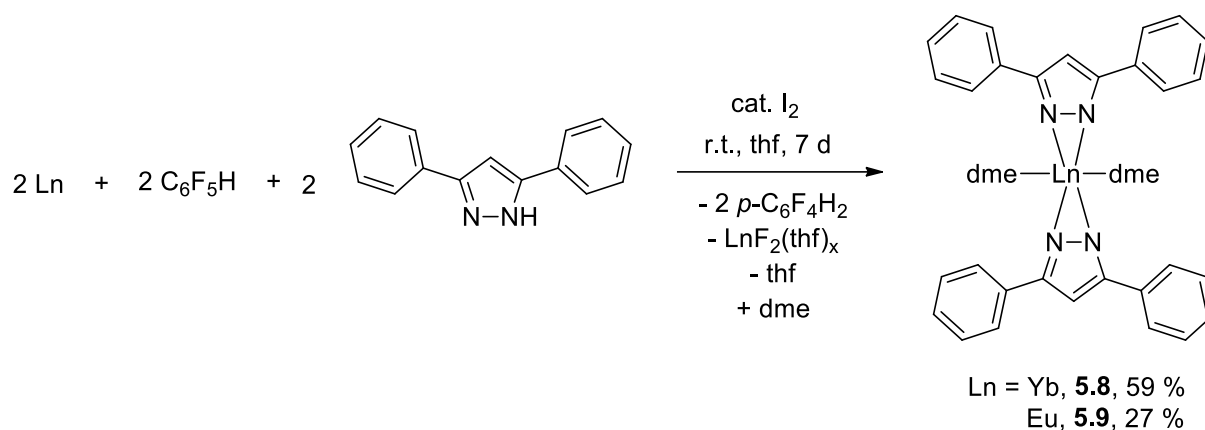
Formamidinate ligands represent a subclass of amidinate ligands, which have been well studied within the Junk group, and thus an appropriate target. Whilst many formamidine pro-ligands have been synthesised for use in lanthanoid chemistry, only N,N'-bis(2,6-diisopropylphenyl)formamidine (DippFormH) has been used in these studies as a representative formamidine ligand. Utilising the same conditions as for the synthesis of lanthanocenes, reactions with ytterbium and europium metals were undertaken with pentafluorobenzene and DippFormH, and the reaction progress followed by ^{19}F NMR spectroscopy. Complete consumption of $\text{C}_6\text{F}_5\text{H}$ was observed after 14 days in the case of ytterbium, and 7 days in the case of europium. The reactions were ceased, and the supernatant solutions isolated by filtration, and concentrated under reduced pressure, and left to stand, affording crystals of the formamidinate complexes $[\text{Ln}(\text{DippForm})_2(\text{thf})_2] \cdot 2\text{thf}$ ($\text{Ln} = \text{Yb}$ (**5.6**) and Eu (**5.7**)) (Scheme 5.25).



Scheme 5.25 – Synthesis of divalent lanthanoid formamidinate complexes by C-F activation/protolysis.

Crystals of **5.6** were analysed by ^1H NMR and IR spectroscopy, and found to be consistent with the reported spectral data.^[14] Owing to the paramagnetic nature of Eu^{2+} complexes, ^1H NMR spectroscopy could not be used to confirm the identity of **5.7**. Instead, IR spectroscopy and single crystal X-ray diffraction studies were undertaken, and again, found to be consistent with reported data.^[14]

Similarly, pyrazolates are a well-studied ligand system within the Junk group. 3,5-Diphenylpyrazole (Ph_2PzH) was selected as a representative pyrazolate ligand for these reactions, which were undertaken analogously to those already described. After 7 days, both Yb and Eu reactions showed complete consumption of $\text{C}_6\text{F}_5\text{H}$ as per the ^{19}F NMR spectra, and the supernatant solutions were isolated, thf removed under reduced pressure, and solids redissolved in dme and left to stand, affording crystals of $[\text{Ln}(\text{Ph}_2\text{Pz})(\text{dme})_2]$ (Ln = Yb (**5.8**) and Eu (**5.9**)) (Scheme 5.26).



Scheme 5.26 – Synthesis of divalent lanthanoid pyrazolate complexes by C-F activation/protolysis.

The identity of complex **5.8** was confirmed by IR and ^1H NMR spectroscopy (^{19}F NMR spectroscopy showed no sign of fluoride inclusion), and complex **5.9** was confirmed by IR spectroscopy, showing a mixture of both the *cisoid* and *transoid* isomers, alongside confirmation of the unit cell for both isomers.^[15]

For both ligand subsets, no fluoride inclusion was observed, however, the C-F activation/protolysis route still proved to be an efficient, mercury free method for accessing these divalent complexes.

5.3 Conclusion

The C-F activation of C₆F₅H by lanthanoid metals has been observed extensively in RTP reactions that employ Hg(C₆F₅)₂, and to gain insight into the process, a study has been undertaken. Direct reactions of C₆F₅H with iodine activated Eu and Yb metal were found to selectively activate the C-F bond *para* to the hydrogen, by oxidative insertion of the Ln metal into the C-F bond. This resulted in a pseudo-Grignard species of the general form [Ln(*p*-C₆F₄H)F] which could actively redistribute to [Ln(*p*-C₆F₄H)₂] and [LnF₂(thf)_x]. This pseudo-Grignard species was able to deprotonate any unreacted C₆F₅H to yield [Ln(*p*-C₆F₅)F]/[Ln(C₆F₅)₂] and *p*-C₆F₄H₂ as products. Small amounts of the *ortho* activated product *o*-C₆F₄H₂ were also observed with these metals.

Alternatively, Sm metal was found to behave differently, producing both *p*-C₆F₄H₂ and *o*-C₆F₄H₂ as products, suggesting two competing mechanisms were at play. An analogous reaction was undertaken with La metal, producing purely *o*-C₆F₄H₂, suggesting the ready access to the trivalent state resulted in the different C-F activation. A radical mechanism was proposed for the formation of the *o*-C₆F₄H₂, owing to deuterium incorporation being observed when the reaction was performed in thf-*d*₈.

The formation of pseudo-Grignard reagents by C-F activation was exploited as a synthetic pathway for the synthesis of divalent lanthanoid cyclopentadienyl complexes of Eu and Yb. Complexes [Eu(C₅Ph₄H)₂(thf)] (**5.1**), [Eu(C₅Ph₅)₂]·2.5C₆D₆ (**5.2**), [Yb(C₅Ph₄H)(μ-F)(thf)₂]₂ (**5.3**), and [Yb(C₅Ph₅)₂]·2.5C₆D₆ (**5.4**) were synthesised in one pot reactions of Ln metal activated with I₂, in the presence of C₆F₅H and the corresponding CpH pro-ligand (C₅Ph₄H₂ or C₅Ph₅H). Most notably, fluoride inclusion was observed for **5.3**, but no other complexes. The [EuF₂(thf)_x] species from the C-F activation was also found to be useful in synthesising the lanthanoid fluoride half sandwich complex [Eu(C₅Ph₅)(μ-F)(thf)₂]₂ (**5.5**) when treated with

[Eu(C₅Ph₅)₂] (**5.2**). The versatility of the C-F activation/protolysis synthetic route was established by broadening the synthesis to other common divalent lanthanoid complexes. The formamidinate and pyrazolate complexes of N,N'-bis(2,6-diisopropylphenyl)formamidine (DippFormH) and 3,5-diphenylpyrazole (Ph₂PzH) were also synthesised, yielding [Yb(DippForm)₂(thf)₂] (**5.6**), [Eu(DippFormH)₂(thf)₂] (**5.7**), [Yb(Ph₂Pz)₂(dme)₂] (**5.8**) and [Eu(Ph₂Pz)₂(dme)₂] (**5.9**). No further examples of fluoride inclusion were observed with the use of these ligand systems. The organolanthanoid complexes formed by the C-F activation of pentafluorobenzene by lanthanoid metals have proven to be effective synthetic precursors for a range of divalent lanthanoid complexes and shown to be versatile towards a range of protic ligands. Whilst only two lanthanoid fluoride complexes have been synthesised by this method, the use of lanthanoid fluorides as synthetic reagents which can instigate redistribution to yield heteroleptic fluoride species sets an exciting precedent for future directions of organolanthanoid chemistry.

5.4 Experimental

For materials and general procedures, see Appendix One.

5.4.1 Typical procedure for the C-F activation of pentafluorobenzene with quantification

A Schlenk flask equipped with a magnetic stirrer bar was charged with Ln metal (Ln = Sm, Eu or Yb) (2.00 mmol), C₆F₅H (0.11 mL, 1.00 mmol), anhydrous thf (2 mL), and a crystal of I₂. The reaction mixture was stirred for 72 hours before cooling to 0 °C in an ice bath and quenching with 2 mL of distilled water. The organic materials were then extracted with diethyl ether (2 mL), and the crude organic layer analysed by ¹⁹F NMR spectroscopy (with a drop of CDCl₃).

5.4.2 Syntheses

[Eu(C₅Ph₄H)₂(thf)] (5.1)

A Schlenk flask equipped with a magnetic stirrer bar was charged with Eu metal filings (0.30 g, 2.00 mmol), C₅Ph₄H₂ (0.325 g, 0.88 mmol), C₆F₅H (0.10 mL, 0.88 mmol), anhydrous thf (3 mL) and a crystal of iodine. The reaction mixture was stirred for 96 hours, until the ¹⁹F NMR spectrum showed complete consumption of C₆F₅H. The solid material was allowed to settle, and the supernatant solution isolated by filter cannula. The dark yellow-brown solution was evaporated to dryness, washed with *n*-pentane, and then dried under reduced pressure, yielding **5.1** as a bright orange solid (0.210 g, 53%). Crystals of **5.1** were grown from the slow cooling of a hot toluene solution and the structure confirmed by X-ray crystallography.

[Eu(C₅Ph₅)₂]·2.5C₆D₆ (5.2)

A Schlenk flask equipped with a magnetic stirrer bar was charged with Eu metal filings (0.152 g, 1.00 mmol), C₅Ph₅H (0.220 g, 0.50 mmol), C₆F₅H (0.06 mL, 0.5 mmol), anhydrous thf (3

mL) and a crystal of iodine. The reaction mixture was stirred for 24 hours, and then a second amount of Eu metal (0.152 g, 1.00 mmol) and iodine were added, and stirring continued for 6 days further until the ^{19}F NMR spectrum showed complete consumption of $\text{C}_6\text{F}_5\text{H}$. The solid material was allowed to settle, and the supernatant solution isolated by filter cannula. The dark orange solution was then dried under reduced pressure and then washed with toluene to precipitate the sandwich complex **5.2** as an orange powder (0.235 g, 90 %). Crystals of **5.2** were grown from a solution of thf: C_6D_6 (2:1), and the structure confirmed by X-ray crystallography.

[Yb(C₅Ph₄H)(μ -F)(thf)₂]₂ (5.3)

The synthesis of **5.3** was carried out in the same way as **5.1** however, using Yb metal (0.50 g, 2.8 mmol) in place of Eu metal, with $\text{C}_5\text{Ph}_4\text{H}_2$ (0.500 g, 1.35 mmol) and $\text{C}_6\text{F}_5\text{H}$ (0.15 mL, 1.35 mmol). A second addition of Yb metal (0.25 g, 1.38 mmol) and I_2 was performed after stirring for 4 days, at which point the reaction mixture was a khaki green suspension. The reaction was stirred for 6 days total, until the ^{19}F NMR spectrum showed complete consumption of $\text{C}_6\text{F}_5\text{H}$. The reaction was stopped, the solids were allowed to settle, and the dark red supernatant solution isolated by filter cannula. Attempted isolation of the complex by drying under reduced pressure led to decomposition, and thus further characterisation was not obtained. ^{19}F NMR (C_6D_6 , 282.4 MHz, 303K): δ -81.9 (s, 2F; ^{171}Yb satellites at -81.3 and -82.5 ppm, $^1J_{\text{Yb,F}} = 447$ Hz).

[Yb(C₅Ph₅)₂] \cdot 2.5C₆D₆ (5.4)

The synthesis of **5.4** was carried out in the same way as **5.2**, however using Yb metal (0.26 g, 1.5 mmol) in place of Eu metal. The reaction mixture was stirred for 24 hours before adding another equivalent of Yb metal and I_2 and stirred for 6 days further. The solids were allowed to settle, and the supernatant solution isolated by filter cannula. The solvent was removed under

reduced pressure and washed with toluene to precipitate **5.4** as a green solid (0.110 g, 38%). Crystals of **5.4** were grown from a C₆D₆ solution, and the structure confirmed by X-ray crystallography. ¹H NMR (300 MHz, C₆D₆, 25 °C): δ 6.99 (m, 20H, ArH), 6.90 (m, 10H, ArH), 6.80 (m, 20H, ArH). IR (Nujol, cm⁻¹): 1594 m, 1574 w, 1501 m, 1307 w, 1155 w, 1075 m, 1026 m, 1013 m, 917 m, 862 m, 801 m, 776 m, 737 m, 722 m, 701 s, 678 w. Spectroscopic data were in agreement with those reported.^[12]

[Eu(C₅Ph₅)(μ-F)(thf)₂]₂ (5.5)

A Schlenk flask equipped with a magnetic stirrer bar was charged with Eu metal (0.300 g, 2.0 mmol), C₆F₅H (1.1 mL, 10 mmol), anhydrous thf (4 mL), and a crystal of iodine for metal activation, and stirred for 5 days. The suspension was allowed to settle, and the supernatant solution removed by filter cannula, and the solid dried under reduced pressure leaving unreacted Eu and [EuF₂(thf)_x]. A solution of [Eu(C₅Ph₅)₂] (0.042 g, 0.047 mmol) in anhydrous thf (5 mL) was transferred onto the [EuF₂(thf)_x] (excess) and the resulting suspension was stirred overnight, yielding a bright yellow solution. The solids were allowed to settle, and the resulting solution isolated by filter cannula. The solvent was then removed under reduced pressure, yielding **5.5** as a pale brown solid (0.033 g, 46 %). *Anal.* Calc. for C₈₆H₈₂F₂O₄Eu₂ (1521.5 g.mol⁻¹): C, 67.89; H, 5.43. Found C, 67.85; H, 4.752 %. IR (Nujol, cm⁻¹): 1594 m, 1500 m, 1261 w, 1155 w, 1071 w, 1029 m, 908 w, 802 m, 769 m, 737 w, 697 m.

[Yb(DippForm)₂(thf)] (5.6)

A Schlenk flask equipped with a magnetic stirrer bar was charged with Yb metal filings (0.345 g, 2.0 mmol), DippFormH (0.364 g, 1.0 mmol), C₆F₅H (0.11 mL, 1.0 mmol), anhydrous thf (4 mL) and a crystal of I₂ for metal activation. The reaction mixture was stirred for 24 hours before adding a second equivalent of Yb filings and I₂. The suspension was stirred for 14 days total before showing complete consumption of C₆F₅H by ¹⁹F NMR analysis. The solids were

allowed to settle, and the supernatant solution isolated by filtration cannula, concentrated under reduced pressure, and left to stand, affording orange block crystals of **5.6** (0.10 g, 19 %). ^1H NMR (300 MHz, C_6D_6 , 25 °C): δ 8.24 (s, 2H, NC(*H*)N; Yb 171 satellites, $^3J(^1\text{H}, ^{171}\text{Yb}) = 50$ Hz, 7.14 - 7.06 (m, 12H, ArH), 3.61 (br s, 16H, thf), 3.51 (m, 8H, CH(CH $_3$) $_3$), 1.38 (br s, 16H, thf), 1.17 (d, 48H, CH(CH $_3$) $_3$). IR (Nujol, cm^{-1}): 1666 s, 1589 w, 1529 m, 1314 w, 1288 m, 1235 m, 1182 m, 1098 w, 1073 m, 1037 m, 935 w, 878 w, 821 w, 800 m, 767 m, 754 m, 722 m. Spectroscopic data were in agreement with those reported.^[14]

[Eu(DippForm) $_2$ (thf) $_2$] (5.7)

The synthesis of **5.7** was carried out in the same way as **5.6**, however using Eu metal filings (0.30 g, 2.0 mmol) in place of Yb. The reaction mixture was stirred for 7 days total before showing complete consumption of $\text{C}_6\text{F}_5\text{H}$ by ^{19}F NMR analysis. The dark yellow supernatant solution was isolated by filtration, concentrated under reduced pressure, and left to stand, affording yellow crystals of **5.7** (0.220 g, 43 %). IR (Nujol, cm^{-1}): 1856 w, 1792 w, 1667 m, 1593 m, 1525 m, 1359 w, 1306 m, 1255 w, 1237 w, 1180 m, 1157 w, 1105 m, 1053 w, 1035 m, 1014 w, 960 w, 932 m, 877 m, 822 w, 799 s, 765 w, 751 w, 721 m 668 w. Unit cell and spectroscopic data were in agreement with those reported.^[14]

[Yb(Ph $_2$ Pz) $_2$ (dme) $_2$] (5.8)

A Schlenk flask equipped with a magnetic stirrer bar was charged with Yb metal filings (0.345 g, 2.0 mmol), Ph $_2$ PzH (0.220 g, 1.0 mmol), $\text{C}_6\text{F}_5\text{H}$ (0.11 mL, 1.0 mmol), anhydrous thf (4 mL) and a crystal of I_2 for metal activation. The reaction mixture was stirred for 24 hours before adding a second equivalent of Yb filings and I_2 . The suspension was stirred for 10 days total before showing complete consumption of $\text{C}_6\text{F}_5\text{H}$ by ^{19}F NMR analysis. The dark maroon supernatant solution was isolated by filtration, the solvent removed under reduced pressure, and dissolved in hot dme and left to stand at room temperature, affording **5.8** as a brown

precipitate (0.232 g, 59%). ^1H NMR (300 MHz, C_6D_6 , 25 °C): δ 7.93 (d, 8H, ArH), 7.23 (t, 8H, ArH), 7.10-7.00 (m, 6H, ArH and NC(*H*)N). IR (Nujol, cm^{-1}): 1602 m, 1192 m, 1155 w, 1114 m, 1058 w, 1027 m, 969 m, 940 w, 859 m, 802 m 754 s, 723 s, 695 s, 685 m. Unit cell and spectroscopic data were in agreement with those reported.^[16]

[Eu(Ph₂Pz)₂(dme)₂] (5.9)

The synthesis of **5.9** was carried out in the same way as **5.8**, however using Eu metal filings (0.30 g, 2.0 mmol) in place of Yb. The reaction mixture was stirred for 7 days total before showing complete consumption of $\text{C}_6\text{F}_5\text{H}$ by ^{19}F NMR analysis. The dark blue supernatant solution was isolated by filtration, the solvent under reduced pressure, and dissolved dme and left to stand at room temperature, affording yellow crystals of **5.9** (0.105 g, 27 %). IR (Nujol, cm^{-1}): 1601 m, 1510 w, 1299 w, 1284 w, 1256 w, 1213 w, 1193 w, 1175 w, 1155 w, 1115 w, 1095 w, 1069 w, 1058 w, 1024 w, 1015 w, 979 w, 967 m, 906 w, 851 s, 833 w, 770 w, 749 w, 723 w, 696 m, 679 m. Unit cell and spectroscopic data were in agreement with those reported.^[15]

Attempted synthesis of [Eu(C₅Ph₄H)(μ -F)(thf)_x]₂

A Schlenk flask was charged with Eu metal (0.30 g, 2.0 mmol), $\text{C}_6\text{F}_5\text{H}$ (1.1 mL, 10 mmol) anhydrous thf (4 mL) and a crystal of iodine for metal activation and stirred for 7 days. The suspension was allowed to settle, and the supernatant solution removed by filter cannula, and the solid dried under reduced pressure, leaving unreacted Eu and $[\text{EuF}_2(\text{thf})_x]$. A solution of $[\text{Eu}(\text{C}_5\text{Ph}_4\text{H})_2(\text{thf})]$ (**5.1**) (0.104 g, 0.11 mmol) in thf (5 mL) was transferred onto the $[\text{EuF}_2(\text{thf})_x]$ (excess) and the resulting suspension was stirred overnight. The solids were allowed to settle, and the dark yellow/brown supernatant solution was isolated by filter cannula. The solvent was then removed under reduced pressure, and the brown solids dissolved in hot

toluene, and filtered from the brown, insoluble materials, and left to slowly cool. **5.1** was recovered as an orange powder.

Attempted synthesis of [Yb(C₅Ph₅)(μ-F)(thf)_x]₂

The synthesis of [Yb(C₅Ph₅)(μ-F)(thf)_x]₂ was carried out in the same way as that of [Eu(C₅Ph₄H)(μ-F)(thf)_x]₂, however Yb metal (0.35 g, 2.0 mmol) was used in place of Eu metal, and [Yb(C₅Ph₅)₂] (0.100 g, 1.05 mmol) used in place of [Eu(C₅Ph₅)₂]. After stirring for 18 hours, the supernatant solution had lost all colour, and only C₅Ph₅H was recovered.

Attempted synthesis of [Sm(C₅Ph₄H)₂(thf)]

The attempted synthesis of [Sm(C₅Ph₄H)₂(thf)] was carried out in the same way as **5.1**, however using Sm metal filings (0.300 g, 2.00 mmol) in place of Eu metal. The reaction mixture was stirred for 24 hours before adding another equivalent of Sm metal filings and I₂, then stirred for 48 hours further. The brown solution was isolated by filtration and concentrated under reduced pressure. Only crystals of unreacted C₅Ph₄H₂ were recovered.

Attempted synthesis of [Sm(C₅Ph₅)₂]

The attempted synthesis of [Sm(C₅Ph₅)₂] was carried out in the same way as **5.2**, however using Sm metal filings (0.150 g, 1.00 mmol) in place of Eu metal, C₅Ph₅H (0.160 g, 0.36 mmol), and C₆F₅H (0.04 mL, 0.36 mmol). The reaction mixture was stirred for 2 days before adding another equivalent of Sm metal filings and I₂, then stirred for 8 days further. After 10 days total, the ¹⁹F NMR spectrum showed large amounts of C₆F₅H remained, however, the supernatant solution was dark red in colour, representative of the samarium SSIP. The supernatant was removed from the solid by filtration, the thf removed under reduced pressure, and dissolved in toluene in an attempt to precipitate the decaphenyl samarocene, however, only a white precipitate was observed, confirmed to be unreacted C₅Ph₅H by ¹H NMR spectroscopy.

5.5 Crystal and refinement data

[Eu(C₅Ph₄H)₂(thf)] (5.1)

C₆₂H₅₀EuO (*M* = 962.98 g/mol): monoclinic, space group *P*2₁/*n* (no. 14), *a* = 10.36976(16) Å, *b* = 40.8727(5) Å, *c* = 11.1439(2) Å, *β* = 105.1813(18)°, *V* = 4558.39(13) Å³, *Z* = 4, *T* = 173.00(10) K, *μ*(Mo Kα) = 1.420 mm⁻¹, *D*_{calc} = 1.403 g/cm³, 72400 reflections measured (4.826° ≤ 2 Θ ≤ 52.992°), 9400 unique (*R*_{int} = 0.0628, *R*_{sigma} = 0.0293) which were used in all calculations. The final *R*₁ was 0.0679 (*I* > 2 σ (*I*)) and *wR*₂ was 0.1654 (all data).

5.6 References

- [1] Z. Guo, R. Huo, Y. Q. Tan, V. Blair, G. B. Deacon, P. C. Junk, *Coord. Chem. Rev.* **2020**, *415*, 213232.
- [2] Z. Guo, V. L. Blair, G. B. Deacon, P. C. Junk, *Dalton Trans.* **2020**, *49*, 13588–13600.
- [3] G. B. Deacon, C. M. Forsyth, S. Nickel, *J. Organomet. Chem.* **2002**, *647*, 50–60.
- [4] G. B. Deacon, F. Jaroschik, P. C. Junk, R. P. Kelly, *Chem. Commun.* **2014**, *50*, 10655–10657.
- [5] M. L. Cole, G. B. Deacon, C. M. Forsyth, P. C. Junk, K. Konstas, J. Wang, *Chem. Eur. J.* **2007**, *13*, 8092–8110.
- [6] M. L. Cole, P. C. Junk, *Chem. Commun.* **2005**, 2695–2697.
- [7] Z. Guo, V. L. Blair, G. B. Deacon, P. C. Junk, *Chem. Eur. J.* **2022**, *28*, e202103865.
- [8] G. B. Deacon, C. M. Forsyth, P. C. Junk, R. P. Kelly, A. Urbatsch, J. Wang, *Dalton Trans.* **2012**, *41*, 8624–8634.
- [9] G. B. Deacon, P. C. Junk, R. P. Kelly, J. Wang, *Dalton Trans.* **2016**, *45*, 1422–1435.
- [10] N. Eslamirad, Synthesis of Rare Earth Complexes Involving Pyrazolate Ligands, PhD Thesis, James Cook University, **2018**.
- [11] R. P. Kelly, T. D. M. Bell, R. P. Cox, D. P. Daniels, G. B. Deacon, F. Jaroschik, P. C. Junk, X. F. Le Goff, G. Lemercier, A. Martinez, J. Wang, D. Werner, *Organometallics* **2015**, *34*, 5624–5636.
- [12] G. B. Deacon, C. M. Forsyth, F. Jaroschik, P. C. Junk, D. L. Kay, T. Maschmeyer, A.

- F. Masters, J. Wang, L. D. Field, *Organometallics* **2008**, *27*, 4772–4778.
- [13] R. P. Kelly, *Advances in the Organometallic and Organoamidometallic Chemistry of the Lanthanoids and Alkaline Earths*, PhD Thesis, Monash University, **2013**.
- [14] M. L. Cole, G. B. Deacon, C. M. Forsyth, P. C. Junk, K. Konstas, J. Wang, H. Bittig, D. Werner, *Chem. Eur. J.* **2013**, *19*, 1410–1420.
- [15] G. B. Deacon, E. E. Delbridge, B. W. Skelton, A. H. White, *Eur. J. Inorg. Chem.* **1999**, 751–761.
- [16] G. B. Deacon, E. E. Delbridge, B. W. Skelton, A. H. White, *Eur. J. Inorg. Chem.* **1998**, 543–545.

Appendix One

Materials and general procedures

All manipulations were performed under nitrogen, using standard Schlenk techniques. Lanthanoid metals were from Santoku/Molycorp/Eutectix. Large chunks were filed in the drybox before use. Solvents (thf, toluene C_6D_6) were distilled over sodium or sodium benzophenone ketyl before being stored under an atmosphere of nitrogen over 3 Å molecular sieves, and hexane and diethyl ether were purified by an SPS and stored over 5 Å molecular sieves before use. 2,2'-Methylene-bis(6-*tert*-butyl-4-methylphenol), trimethylaluminium, *rac*-lactide, chlorodiphenylphosphine, anhydrous *n*-pentane, anhydrous pentafluorobenzene and 3,5-dimethylpyrazole were commercially available, and used without further purification. Bis(pentafluorophenyl)mercury^[1], 1,2,3,4-tetraphenylcyclopentadiene,^[2] pentaphenylcyclopentadiene,^[3] *N,N'*-bis(2,6-diisopropylphenyl)formamidine,^[4] and 3,5-diphenylpyrazole^[5] were prepared by the literature methods. In all RTP reactions, a drop of Hg metal was added to form a reactive lanthanoid-mercury amalgam to promote reactivity. In all reactions utilising I_2 , ca. 1 mg of I_2 (5 mol%) was used to activate the metal. Metal analyses were determined by Na_2H_2edta titration with a Xylenol Orange indicator and hexamethylenetetramine buffer, after decomposition of complexes with dilute HCl. For the Y-Al heterobimetallic complex (**2.9**), aluminium was masked in this process by addition of 5% sulfosalicylic acid solution.^[6] Infrared spectra ($4000-400\text{ cm}^{-1}$) were obtained as Nujol mulls between NaCl plates with a Nicolet-Nexus FT-IR spectrometer. 1H , ^{13}C , ^{19}F , and ^{31}P NMR spectra were recorded on a Bruker 400 MHz spectrometer. 1H and ^{13}C NMR spectra were referenced against residual solvent peaks, and ^{19}F and ^{31}P NMR spectra were referenced externally against 85% H_3PO_4 ($\delta = 0$) and CCl_3F ($\delta = 0$) respectively. The chemical shifts are expressed in parts per million (ppm). No interpretable NMR spectra could be collected for the

Appendix One

highly paramagnetic complexes **2.2-2.6**, **2.10**, **3.3**, **3.6**, **4.7**, **5.1**, **5.2**, **5.5** and **5.6**. Microanalyses were determined by the Elemental Analysis Service, London Metropolitan University, and the Elemental Analysis Service, Macquarie University, and all the samples were sealed in tubes under nitrogen before transport. Molecular weights and molecular weight distributions of polymers from ROP reactions in Chapter 2 were determined against polystyrene standards by gel permeation chromatography (GPC) on a 1260 Infinity II Multi-Detector GPC (Agilent Technologies) equipped with an ultraviolet (UV) absorbance and refractive index detector. The two PLgel 5 μ L MIXED-C columns (300 x 7.5 mm) (Agilent Technologies) were calibrated using polystyrene narrow standards in thf at 35 °C and using thf (HPLC grade) as an eluent with a flow rate of 1.0 mL/min at 35 °C. Mass spectra were obtained with a Shimadzu LCMS-2020.

X-ray crystallography

Single crystals were covered with viscous hydrocarbon oil were mounted on a glass fibre. Data for complexes **2.1-2.11**, **3.1**, **3.2**, **3.6-3.8**, and **4.4** were obtained at -173 °C (100 K) on the MX1: Macromolecular Crystallography beamline at the Australian Synchrotron, Victoria, Australia. Data collection and integration on the MX1: Macromolecular Crystallography beamline was accomplished using Blu-Ice.^[7] Data for complex **3.3** and **5.1** were collected using a Bruker X8 APEX II diffractometer equipped with graphite monochromated Mo K α radiation ($\lambda = 0.71013$ Å). Data were initially processed with the SAINT program.^[8] Data for complexes **4.1**, **4.5**, and **4.6-4.8** were obtained at -150 °C (123 K) and were measured on a Rigaku SynergyS diffractometer. The SynergyS operated using microsource Mo-K α radiation ($\lambda = 0.71073$ Å) and Cu-K α radiation ($\lambda = 1.54184$ Å). Data processing was conducted using CrysAlisPro.55 software suite.^[9] All structures were solved using SHELXS7 and refined by full-matrix least-squares on all F² data using SHELX2014^[10] in conjunction with the X-Seed

graphical user interface.^[11] All hydrogen atoms were placed in calculated positions using the riding model.

References

- [1] G. B. Deacon, J. E. Cosgriff, E. T. Lawrenz, C. M. Forsyth, D. L. Wilkinson, *Herrmann-Brauer, Synthetic Methods of Organometallic and Inorganic Chemistry*, Thieme, Stuttgart, **1997**.
- [2] M. P. Castellani, J. M. Wright, S. J. Geib, A. L. Rheingold, W. C. Trogler, *Organometallics* **1986**, *5*, 1116–1122.
- [3] B. Martín-Matute, M. Edin, K. Bogár, F. B. Kaynak, J. E. Bäckvall, *J. Am. Chem. Soc.* **2005**, *127*, 8817–8825.
- [4] R. M. Roberts, *J. Am. Chem. Soc.* **1949**, *71*, 3848–3849.
- [5] G. B. Deacon, E. E. Delbridge, B. W. Skelton, A. H. White, *Eur. J. Inorg. Chem.* **1999**, 751–761.
- [6] J. J. Lingane, *Complexometric Titrations*, Methuen, London, **1958**.
- [7] T. M. McPhillips, S. E. McPhillips, H. J. Chiu, A. E. Cohen, A. M. Deacon, P. J. Ellis, E. Garman, A. Gonzalez, N. K. Sauter, R. P. Phizackerley, S. M. Soltis, P. Kuhn, *J. Synchrotron Radiat.* **2002**, *9*, 401–406.
- [8] Bruker AXS Ltd. Apex II Program Suite, **2005**.
- [9] CrysAlisPRO v.55. Agilent Technologies Ltd., Yarnton, Oxfordshire, England.
- [10] G. M. Sheldrick, *Acta Crystallogr. Sect. C Struct. Chem.* **2015**, *71*, 3–8.
- [11] L. J. Barbour, *J. Supramol. Chem.* **2001**, *1*, 189–191.

Appendix Two

List of publications

1. A. C. G. Shephard, S. H. Ali, J. Wang, Z. Guo, M. S. Davies, G. B. Deacon and P. C. Junk, *Dalton Trans.* **2021**, 50, 14653-14661.
2. S. H. Ali, A. C. G. Shephard, J. Wang, Z. Guo, M. S. Davies, G. B. Deacon, P. C. Junk, *Chem. Asian J.* **2022**, e202101328.
3. A. C. G. Shephard, A. Delon, R. P. Kelly, Z. Guo, S. Chevreux, G. Lemerrier, G. B. Deacon, G. A. Dushenko, F. Jaroschik, P. C. Junk, *Aust. J. Chem.* **2022**, DOI: 10.1071/CH21324.
4. A. C. G. Shephard, D. P. Daniels, G. B. Deacon, Z. Guo, F. Jaroschik, P. C. Junk, *Chem. Commun.* **2022**, 58, 4344-4347.